GRS

2D/3D Program
Work Summary
Report

GRS

2D/3D Program
Work Summary Report

Prepared Jointly by:
- Japan Atomic Energy
  Research Institute
- Gesellschaft für Anlagen-
  und Reaktorsicherheit
  (GRS) mbH
- Siemens AG, UB KWU
- U.S. Nuclear Regulatory
  Commission
- Los Alamos National
  Laboratory
- MPR Associates, Inc.

Edited by:
Paul S. Damerell and
John W. Simons
MPR Associates, Inc.

December 1992

N O T I C E:

This Report was prepared as an account of work prepared in the international 2D/3D Program which was jointly conducted by the German Federal Minister for Research and Technology (BMFT), the Japan Atomic Energy Research Institute (JAERI) and the United States Nuclear Regulatory Commission (USNRC). The Responsibility for the content of this report rests with the authors.

The Authors make no warranty or assume any legal liability for the correctness, completeness or applicability of information compiled in this report.

ZUSAMMENFASSUNG

Das 2D/3D-Programm wurde von Deutschland, Japan und den Vereinigten Staaten von Amerika durchgeführt, um die Thermohydraulik von Kühlmittelverluststörfällen mit großen Brüchen der druckführenden Umschließung von Druckwasserreaktoren zu erforschen. Es wurde eine Durchführungsform gewählt, in der jedes Land einen beträchtlichen Beitrag zum Gesamtprogramm leistete und alle drei Länder gleichermaßen teil hatten an den erzielten Ergebnissen. Deutschland baute und betrieb die Großversuchsanlage Upper Plenum Test Facility (UPTF), während Japan Bau und Betrieb der Versuchsanlagen Cylindrical Core Test Facility (CCTF) und Slab Core Test Facility (SCTF) beitrug. Der Beitrag der USA bestand aus der Bereitstellung fortschrittlicher Instumentierung für die drei Versuchsanlagen sowie aus der Überprüfung des Rechenprogramms TRAC anhand der Versuchsergebnisse. Versuchsauswertungen wurden in allen drei Ländern durchgeführt. Der vorliegende Bericht faßt das 2D/3D-Programm zusammen, in dem die beigesteuerten Leistungen der drei beteiligten Länder beschrieben werden.

ABSTRACT

The 2D/3D Program was carried out by Germany, Japan and the United States to investigate the thermal-hydraulics of a PWR large-break LOCA. A contributory approach was utilized in which each country contributed significant effort to the program and all three countries shared the research results. Germany constructed and operated the Upper Plenum Test Facility (UPTF), and Japan constructed and operated the Cylindrical Core Test Facility (CCTF) and the Slab Core Test Facility (SCTF). The US contribution consisted of provision of advanced instrumentation to each of the three test facilities, and assessment of the TRAC computer code against the test results. Evaluations of the test results were carried out in all three countries. This report summarizes the 2D/3D Program in terms of the contributing efforts of the participants.

TABLE OF CONTENTS

TABLE OF CONTENTS (Continued)

LIST OF FIGURES

LIST OF TABLES

ACKNOWLEDGEMENTS

Section 1

INTRODUCTION

BACKGROUND

The thermal-hydraulic response of a PWR primary coolant system to a Loss-of-Coolant Accident (LOCA) and the performance of the Emergency Core Cooling System (ECCS) have been areas of research interest for two decades. The primary objective of LOCA/ECCS research has been to improve the understanding and modeling of the phenomena so that safety margins can be better quantified and more realistic evaluation approaches can be utilized. Initially, the focus of the research was the depressurization (blowdown) transient. Later, the focus shifted to include the post-blowdown phases (refill and reflood).

The 2D/3D Program was the major program on PWR end-of-blowdown and post-blowdown phenomena for the countries of Germany, Japan and the United States. The formal program name is "The International Program on the Thermal-Hydraulic Behavior of ECC during the Refill and Reflood Phases of a LOCA in a PWR." The common name became "2D/3D Program" because phenomena during end-of-blowdown, refill and reflood are strongly influenced by multidimensional (2D and 3D) effects.

PARTICIPANTS IN 2D/3D PROGRAM

The participants in the 2D/3D Program were the governments of the Federal Republic of Germany (FRG), Japan, and the United States of America (US) as represented by the following agencies:

- The Federal Ministry for Research and Technology (BMFT) in the FRG.
- The Japan Atomic Energy Research Institute (JAERI) in Japan.
- The US Nuclear Regulatory Commission (USNRC) in the US.

The 2D/3D Program used a "contributory" approach. Each of the three participants contributed significant effort to the program and all three countries shared the research results. There was no exchange of funds between the participants. This approach fostered technical cooperation among the three countries.

1-1

Several organizations in the three countries were involved in carrying out the work in the 2D/3D Program. Figure 1-1 summarizes the key organizations.

SCOPE OF 2D/3D PROGRAM

In general terms, the scope of the 2D/3D Program was PWR LOCA end-of-blowdown and post-blowdown phenomena. Sections 2.1 and 2.2 present a more detailed discussion of the specific objectives and approach of the program. The major facilities in the 2D/3D Program constituted some of the largest and most sophisticated thermal-hydraulic facilities ever employed. This is reflected in the combined financial commitment of the three participants which exceeded the equivalent of US $500,000,000.

PURPOSE AND SCOPE OF THIS REPORT

This report presents a summary of the 2D/3D Program in terms of the contributing efforts of the participants. Each of the major sub-programs is discussed individually:

- Cylindrical Core Test Facility and Slab Core Test Facility (Section 3)
- Upper Plenum Test Facility (Section 4)
- TRAC Code Analysis (Section 5)
- Advanced Instrumentation (Section 6)

This report is a companion to another report entitled "Reactor Safety Issues Resolved by the 2D/3D Program," which summarizes the program in terms of the reactor safety issues investigated.

AVAILABILITY OF RESULTS FROM 2D/3D PROGRAM

Numerous reports document the detailed results from the 2D/3D Program; many are cited in this report. Most of these reports have a restricted availability per the 2D/3D Program International Agreement. The detailed reports have been made available to users in the three host countries for the purposes of improving reactor safety.
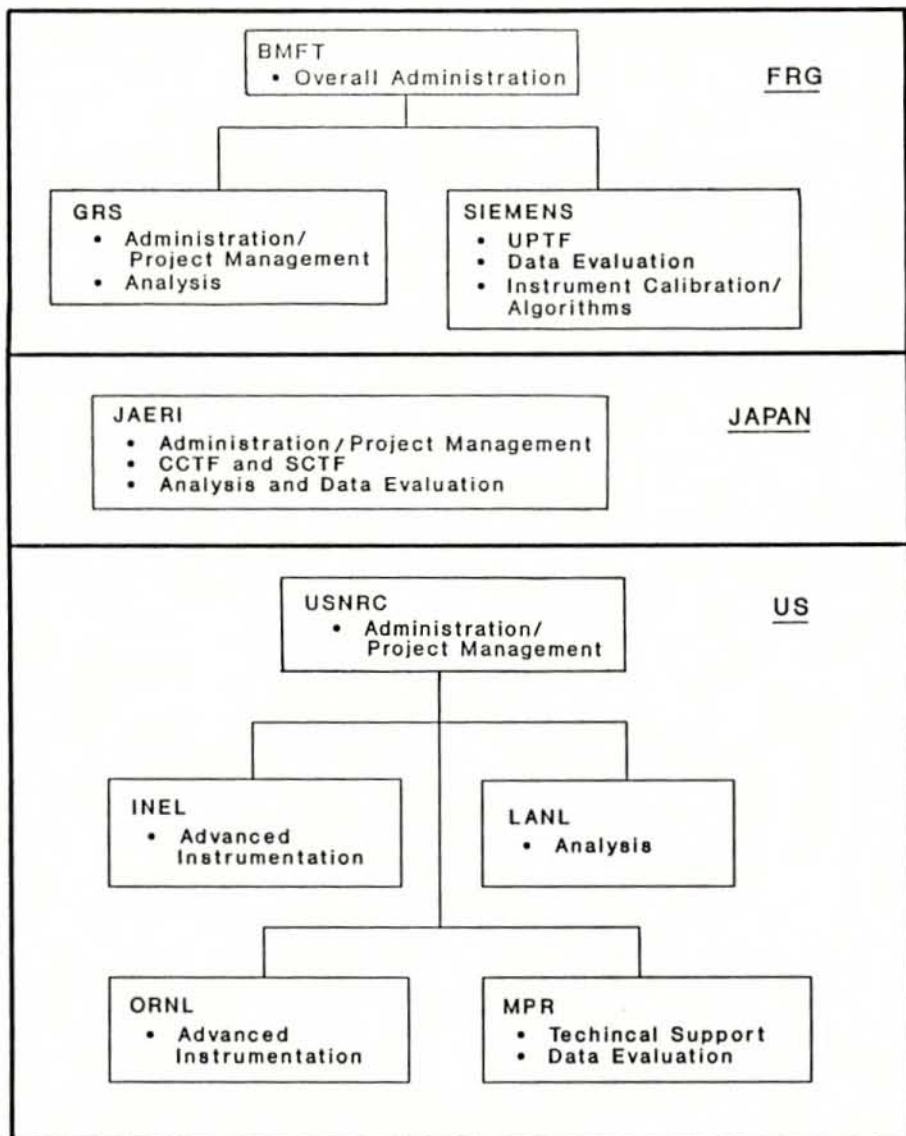
MAJOR ORGANIZATIONS IN 2D/3D PROGRAM
FIGURE 1-1

Section 2

2D/3D PROGRAM OVERVIEW

2.1 OBJECTIVES OF PROGRAM

The overall objective of the 2D/3D Program was to study the end-of-blowdown and post-blowdown phases of a PWR LOCA, and to provide improved experimental data and analysis tools for this transient. The detailed objectives of the 2D/3D Program are summarized as follows:

1. Study the effectiveness of several types of ECC systems (including cold leg injection, combined injection, upper plenum injection and downcomer injection) during the end-of-blowdown and refill phases of a large-break LOCA by evaluating:

    •   Penetration of ECC to the lower plenum during the end-of-blowdown.

    •   Condensation of steam by ECC including the effect of dissolved nitrogen in ECC.

    •   Liquid storage in cold legs, downcomer, upper plenum and hot legs.

    •   The liquid flow pattern through the core (for hot leg and upper plenum injection) and resultant core cooling.

2. Study the effectiveness of several types of ECC systems during the reflood phase of a large break LOCA by evaluating:

    •   Entrainment, storage and transport of liquid water in the upper core, upper plenum, hot legs and steam generators.

    •   Vaporization of entrained water in steam generators.

    •   Steam condensation by ECC.

    •   Steam/ECC interaction and flow patterns, particularly in regions between the ECC injectors and the core.

2-1

- Water delivery to the core.

- Fluid dynamics and heat transfer in the core.

- Downcomer driving head and loop pressure drop.

- The influence of nitrogen discharge from accumulators.

3. Study selected phenomena from other transients; e.g., hot leg steam/water countercurrent flow during a small break LOCA (SBLOCA), fluid/fluid mixing during a pressurized thermal shock event, and high pressure ECC injection into the hot legs during an SBLOCA.

2.2 APPROACH OF RESEARCH

The objectives of the 2D/3D Program were addressed using a combined experimental/analytical approach. Three major facilities were designed, fabricated, and operated within the 2D/3D Program.

- Cylindrical Core Test Facility (CCTF) in Japan

- Slab Core Test Facility (SCTF) in Japan

- Upper Plenum Test Facility (UPTF) in the FRG

The design of each facility involved input from all three countries. Advanced instruments were designed and fabricated by the US for use in all three facilities.

Evaluations of the experimental data were carried out in all three countries. A major analysis program involving the development, assessment and use of a best-estimate computer code was carried out in the US. The computer code is the Transient Reactor Analysis Code (TRAC). TRAC analyses of PWRs and selected tests were also performed by Japan and Germany.

2.3 AREAS OF INVESTIGATION AND RELATIONSHIP TO PWRs

The areas of investigation and their relationship to PWRs are summarized in Figure 2-1. The 2D/3D Program included both separate effects tests which were designed to isolate and study individual areas as well as integral tests which were designed to simulate the combined phenomena. The areas of investigation are discussed individually in a companion report entitled "Reactor Safety Issues Resolved by the 2D/3D Program."
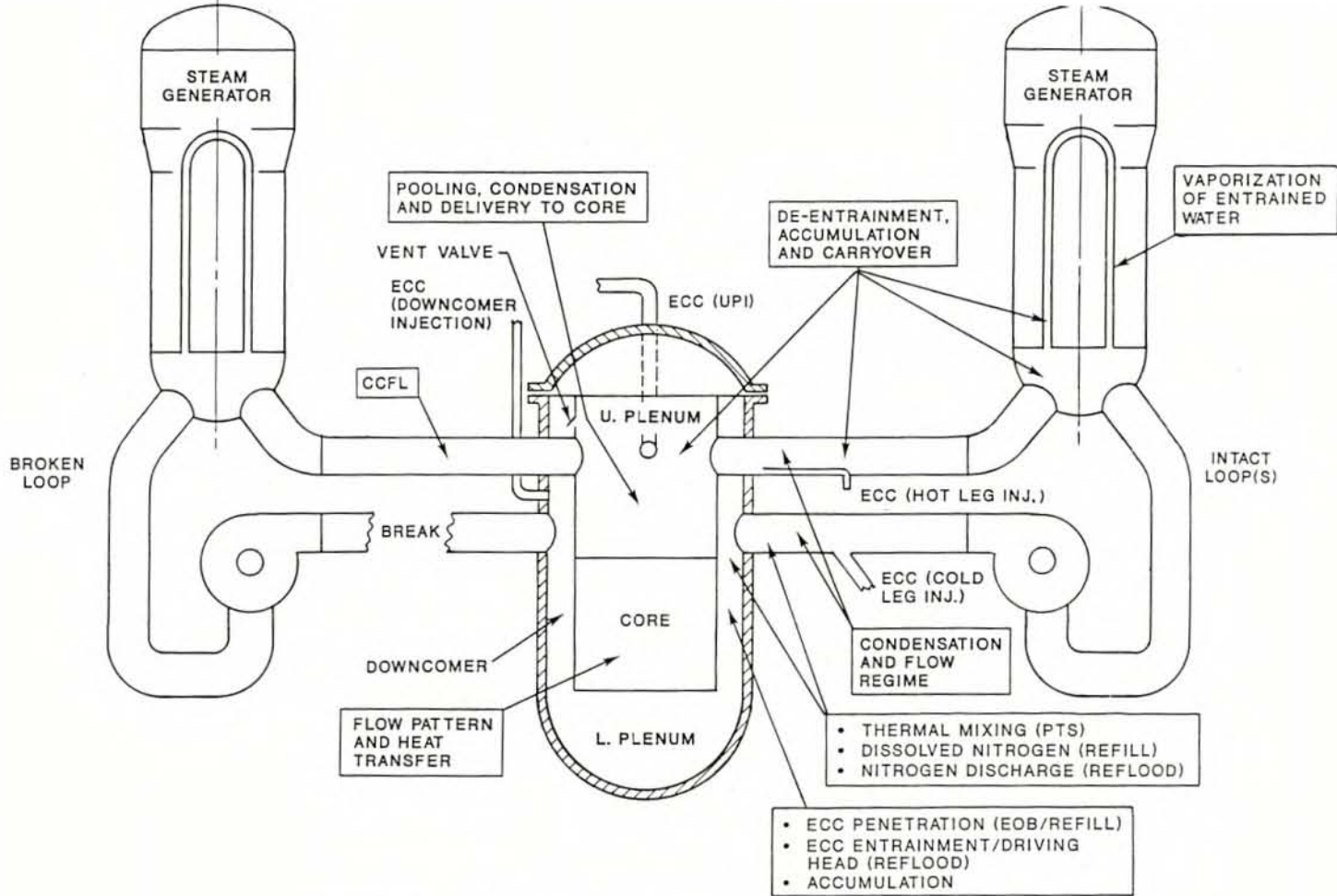
MAJOR AREAS INVESTIGATED BY 2D/3D PROGRAM

FIGURE 2-1

Section 3

CCTF AND SCTF TESTS

3.1 DESCRIPTION OF FACILITIES AND TEST CONDITIONS

3.1.1 Cylindrical Core Test Facility (CCTF)

CCTF was a full-height, 1/21-scale model of the primary coolant system of an 1,100 MWe four-loop PWR. The facility simulated the overall primary system response, as well as the in-core behavior, during the refill and reflood phases of a large cold leg break LOCA. Figure 3.1-1 depicts the major components in the facility. They included a pressure vessel, four primary piping loops (three intact and one broken), two steam generators, four pump simulators, and two tanks attached to the ends of the broken loop to simulate containment. Each of the two steam generator vessels was shared by two loops (a vertical plate divided each steam generator in half) so each loop essentially had its own steam generator. Vertical dimensions and locations of system components were as close as practicable to the corresponding dimensions and locations in the reference reactor.

The following is a brief description of the CCTF components and instrumentation. This discussion also addresses the differences in facility configuration for the two test series run at CCTF (CCTF-I and CCTF-II). The JAERI data reports for each test contain more detailed facility descriptions.

Pressure Vessel and Internals
Figure 3.1-2 shows the CCTF pressure vessel. The full-height pressure vessel housed a downcomer, lower plenum, core, and upper plenum. Pressure vessel flow areas were scaled at a ratio of 1/21.4 as compared to an 1,100 MWe PWR, except that the downcomer annulus was somewhat larger to avoid excessive hot wall effects which would lead to an unrealistically low effective downcomer driving head. To simulate the effective downcomer driving head more realistically, the baffle area of a PWR was included in the downcomer. The design pressure of the pressure vessel and the entire primary system was 600 kPa. Electrical resistance heaters in the wall of the pressure vessel were used to preheat the wall before a test, to accurately simulate the release of stored heat which would occur during a LOCA in a PWR. The CCTF-II vessel was the same as that used in CCTF-I, except for the addition of an upper ring containing an upper plenum injection header and additional instrumentation nozzles. The CCTF core contained 32, 8 x 8 bundles (Figure 3.1-3), each containing

3.1-1

57 electrically-heated rods and 7 nonheated rods (total of 1,824 heated rods and 224 nonheated rods). The nonheated rods simulated the guide thimble tubes and instrument thimble tubes in PWR fuel assemblies. All heated rods were Inconel-clad and had an outer diameter of 10.5 mm and heated length of 3.66 m. The heat capacity of the heated rods was approximately 30% larger than that of actual fuel rods.

Figure 3.1-3 shows the three (high, medium, and low) power zones of the electrically heated core, and identifies the bundle numbering scheme used throughout this report. The radial power distribution of the core was controlled by setting the power supplied to each zone. In CCTF-I, each bundle included rods with three different power densities. In CCTF-II, all heated rods in each bundle were provided with the same power. The axial power profile in all rods was a chopped cosine with an axial peaking factor (ratio of maximum to average power) of 1.49 for CCTF-I and 1.40 for CCTF-II.

As shown in Figure 3.1-2, the core/upper plenum boundary included an upper core support plate and end box tie plate. These plates were perforated plates with appropriately scaled flow areas.

CCTF upper plenum internals modeled those used in the reference Westinghouse plant; in particular, control rod drive structures and support columns. Although the CCTF upper plenum internals were full height, the horizontal dimensions were 8/15 of those of the Westinghouse plant to allow individual upper plenum internal structures to be placed over the individual 8 x 8 heated rod bundles in the CCTF core. This approach gave a more uniform and realistic flow distribution than using reactor-typical, larger size structures. The arrangement of upper plenum structures is shown in Figure 3.1-3.

In CCTF-II, four vent valves, located in the barrel between the upper plenum and downcomer annulus, simulated the vent valves in Babcock & Wilcox (B&W) reactor vessels. For CCTF-II tests simulating B&W reactors, these vent valves were free to open; for all other tests the valves were locked shut.

Primary Loops and Containment Tanks
Four full-length primary loops were connected to the central pressure vessel (Figure 3.1-1). Three of the loops were intact; that is, they allowed flow from the reactor vessel upper plenum, through the hot leg, steam generator, pump simulator, and cold leg to the reactor vessel downcomer. The fourth loop simulated a full-size, double-ended, offset cold leg break about two meters from the vessel wall. Quick-opening break valves were located at the two ends of the cold leg break. The inside diameter of the loop piping was 0.15 m. The pipe area was scaled from the PWR by the ratio of core flow areas. An orifice plate in the pump simulator in each loop simulated the resistance of a locked-rotor pump.

The steam generator simulators were vertical, U-tube and shell type heat exchangers. During a test, the steam generator secondary sides contained saturated water at 540 K and 5300 kPa. These conditions corresponded to those on the secondary side of the steam generator in a PWR during the reflood portion of a LOCA. There was no flow on the secondary side of the steam generators during the tests.

Two interconnected tanks, one attached to each of the two ends of the cold leg break, simulated the PWR containment (Figure 3.1-1). On the tank connected to the hot leg side of the break, a pressure control system maintained pressure at a preselected value by venting steam, as needed, to the atmosphere. On the tank connected to the vessel side of the break, an internal steam/water separator and a liquid level meter together allowed for measurement of broken cold leg phase flow rates.

Emergency Core Cooling System (ECCS)

In CCTF-I, the ECCS included two water supply tanks: the pressurized accumulator (ACC) tank, capable of providing water at a high flow rate for a short duration, and the low pressure coolant injection (LPCI) tank, which provided water at a lower flow rate for a longer duration through LPCI pumps. Each tank could supply water to either the lower plenum or to the cold legs. In CCTF-II a second pressurized tank was added, with ECCS piping to the upper plenum injection header, the downcomer, and the hot legs. The upper plenum, downcomer, and hot leg injection nozzles were also newly installed in CCTF-II.

Instrumentation

CCTF instrumentation consisted of over 1,600 sensors, including both conventional devices (e.g., pressure transducers and thermocouples) provided by JAERI, and advanced two-phase flow instrumentation developed by the USNRC and their contractors for the 2D/3D Program. Advanced instrumentation provided by USNRC, which primarily monitored local two-phase fluid conditions, is described in Section 6.

3.1.2 Slab Core Test Facility (SCTF)

SCTF was a full-height, full-radius 1/21-scale model of a sector of an 1,100 MWe, four-loop PWR. The objective of the SCTF test program was to study two-dimensional thermal-hydraulic behavior within the reactor vessel during the refill and reflood phases of a large break LOCA in a PWR. While the pressure vessel was simulated in detail, only a crude loop simulation was used (Figure 3.1-4). The most significant feature of SCTF was that it contained a full-height heated core with realistic rod diameters and spacing, and a core lateral extent of over 1.8 m (the core radius of the largest PWRs). This large core lateral extent provided the capability to examine multidimensional effects.

Figure 3.1-4 depicts the major components in the facility. They included a pressure vessel, a hot leg, a steam/water separator, an intact loop with a pump simulator, a broken cold leg, and two tanks attached to the ends of the broken loop to simulate containment.

The following is a brief description of the SCTF components and instrumentation. This discussion also addresses the differences in facility configuration among the three test series run at SCTF (SCTF-I, SCTF-II, and SCTF-III). Detailed facility descriptions are contained in References J-481, J-521, J-551, and also in the JAERI data reports for each test.

Pressure Vessel and Internals
Figure 3.1-5 shows the SCTF pressure vessel. The vessel housed a downcomer, lower plenum, core, and upper plenum. The vessel simulated a radial slice of a PWR from the center (Bundle 1 in Figure 3.1-5) to the periphery (downcomer). Heights of components within the pressure vessel were about the same as those in the reference reactor.

The core consisted of eight simulated fuel bundles arranged in a row (i.e., a slab geometry). Each bundle contained 234 electrically-heated rods and 22 nonheated rods arranged in a 16 x 16 array. Power to each bundle was individually adjustable to permit simulation of a radial power distribution. In SCTF-I only, two of the fuel bundles (Bundles 3 and 4) contained flow blockage sleeves to simulate the effect of ballooned fuel cladding.

Honeycomb insulator panels surrounded the core. In SCTF-I, the surface next to the core was discontinuous as there were numerous panels. In SCTF-II and SCTF-III, the panels were covered by a continuous plate to provide a smooth surface facing the core and upper plenum.

Located above the core were the end boxes and the upper core support plate. Appropriate hydraulic resistance simulators were included to model the cross-flow resistance of the fuel rod tips at the top of the core and the axial flow resistance of the control rods when they are inserted.

A full-height core baffle region simulated the volume between the core and the core barrel in the reference reactor (Figure 3.1-5). In SCTF-II and III, the flow paths at the bottom and the side of the core baffle region were blocked to prevent water from flowing into the core baffle region.

Flow area in the full-height downcomer was adjustable (using a filler) to simulate the flow area for different reactor designs (e.g., US/Japanese or German). Provisions were made for blocking the bottom of the downcomer to conduct forced flooding

tests. In addition, a U-shaped pipe connected the downcomer directly to the upper plenum to allow simulation of B&W PWRs with vent valves.

The lower and upper plena of the pressure vessel were volume-scaled from the reference PWR, using the powered-rod ratio as a scale factor. This approach resulted in a realistic-height upper plenum and slightly shorter lower plenum (Figure 3.1-5). The upper plenum internals consisted of control rod guide tubes, support columns, orifice plates, and open holes. As in CCTF, the radius of each internal was scaled down from that of the reference reactor by a factor of 8/15, to give a more realistic flow path simulation.

Hot leg and cold leg nozzles were located at elevations that match the nozzle elevations in the reference reactor as closely as possible. However, because of space restrictions, the broken cold leg and the intact cold leg nozzles were located slightly below the hot leg penetration to avoid interference between the nozzles and the hot leg penetration in the downcomer (Figure 3.1-4).

For SCTF-III, several changes were made to the components in the pressure vessel to better simulate the German Siemens/KWU PWR, which was the focus of SCTF-III. The significant changes were the following:

- In the downcomer, the filler used in Core-I and Core-II was removed to simulate the larger downcomer flow area in the German PWR (GPWR).

- The baffle region was isolated from the core.

- Although the total number of rods remained the same, the number of heated rods was increased slightly from 234 to 236. The nonheated rod arrangement was changed to better simulate German fuel bundles.

- The Core-III components comprising the core/upper plenum interface (end boxes and upper core support plate) were representative of those in the GPWR.

- In the Core-III upper plenum, internal structures simulated the GPWR at full-scale. The support columns of Core-III were split and mounted in a staggered arrangement to achieve the desired flow simulation.

- An ECC injection nozzle was installed in the Core-III upper plenum to simulate ECC injection into the hot leg.

Primary Loops and Containment Tanks
The primary flow loops were simulated using a simplified system consisting of a single hot leg, a steam/water separator, an intact cold leg, and a broken cold leg.

The hot leg connected the upper plenum to the steam/water separator. Hot leg flow area was scaled from the total flow area of four PWR hot legs. The cross-section of the hot leg was an elongated circle of full height.

A steam/water separator located in the hot leg provided a measurement of the amount of water entrained in the steam flow out of the upper plenum and through the hot leg (Figure 3.1-4). Although the separator did not simulate an actual steam generator, it was designed to obtain a realistic two-phase flow pattern at its inlet.

The intact cold leg connected the steam/water separator with the upper portion of the downcomer. The flow area was scaled from the flow area for three PWR cold legs. A pump simulator and a loop seal were provided in the intact cold leg. An orifice plate was used to obtain flow resistance in the pump simulator.

The broken cold leg was simulated with two pipes: one pipe connected the downcomer to a containment tank, and the second pipe connected the steam/water separator to the other containment tank. The two containment tanks were the same tanks used for CCTF (see discussion above).

Emergency Core Cooling System (ECCS)
The SCTF ECCS consisted of an accumulator and a low pressure injection system. The injection ports for these systems were located in the lower plenum, downcomer, broken cold leg, hot leg, and intact cold leg between pump simulator and pressure vessel. Additionally, injection and extraction systems provided and/or removed ECC using special nozzles located just above the upper core support plate.

Instrumentation
SCTF was instrumented with over 1,500 sensors which included both conventional devices (e.g., pressure transducers, thermocouples) provided by JAERI and advanced two-phase flow instrumentation provided by the USNRC. The advanced instrumentation is described in Section 6.

3.1.3 Test Series

Table 3.1-1 lists the CCTF and SCTF tests, classified first by the injection configuration being simulated (cold leg injection, combined injection, downcomer injection, or upper plenum injection) and then further classified by test objective. Within each of those categories, the tests are listed by facility and test series in the following order: CCTF-I, CCTF-II, SCTF-I, SCTF-II, and SCTF-III. The JAERI data, quick look, and evaluation reports are listed in the bibliography (Section 8) by test series. The bibliography also lists evaluation reports prepared by the US which summarize the results of each test series.

3.1.4 Test Procedure

Essentially all CCTF and SCTF tests used the same basic test procedure, with some differences according to the test objective. Accordingly, the discussion below first describes, in some detail, the test procedure for a typical test (cold leg injection, reflood test in CCTF), and then describes variations from that basic procedure for other tests in CCTF and for SCTF tests.

CCTF Cold Leg Injection Reflood Test
The accumulator tank, LPCI tank, and the secondary sides of the steam generators were filled with water. All instruments were zeroed and the calibration checked. Specified primary system fluid temperature and pressure, containment pressure, steam generator secondary side pressure and temperature, ACC tank water temperature, and vessel and piping wall temperatures for the test were also established. In reflood tests, the pressures of the vessel and the containment tanks were the same (typically about 200 kPa). Nitrogen gas was injected into the space above the water in the accumulator tank to obtain a preselected pressure. Electric power was supplied to heaters on the pressure vessel to attain and maintain a preselected temperature of the vessel wall. A specified level of saturated water was established in the lower plenum. In reflood tests, this level was about 0.9 m above the bottom of the vessel, which corresponds to about 1.2 m below the bottom of the core.

When initial conditions had stabilized, rod heat-up was started by supplying continuous electric power to the heated rods at a constant level. ACC injection was initiated when the peak rod surface temperature had reached a preselected value. This value was chosen so as to attain a specified peak cladding temperature at the time when the water in the lower plenum reached the bottom of the core (bottom reflood initiation), considering the rod heat-up rate and the lower plenum fill rate. Note that in the PWRs modeled in CCTF-II, the accumulator injection was either into the cold legs, the downcomer, or into both the hot and cold legs. However, in reflood tests in CCTF-II involving cold leg or downcomer injection, accumulator water was initially injected into the lower plenum to avoid atypical condensation oscillations which could occur if subcooled ECC injection flow were injected into the primary piping or downcomer at a time when the facility was stagnant and no steam was being generated in the core. This method is acceptable for reflood tests as this lower plenum fill is considered part of the pretest preparation and the test is considered to start at bottom reflood initiation.

When water was estimated to have reached the bottom of the core (reflood initiation) a programmed decay of the heating power to the core was initiated to simulate nuclear fission product decay heat.

At a predetermined time after reflood initiation (usually a few seconds), the accumulator injection location was changed from the lower plenum to the three intact cold leg ECC ports. After another specified time delay, the accumulator injection stopped and low pressure coolant injection began. The time delay chosen simulated the time required to empty a typical accumulator.

Throughout the tests, steam was vented from Containment Tank II to maintain the containment pressure at the preselected value. The test was stopped after all instrumented heated rods in the core had quenched, typically around 600 seconds after test initiation.

CCTF Refill Tests
The test procedure was similar to that for reflood tests, with the following differences:

- Initially, the vessel pressure was about 600 kPa and the containment pressure was 200 kPa; this pressure difference was maintained by closing blowdown valves in each of the broken loop lines to the containment tanks. At a preselected time after the start of core heat-up, the two blowdown valves were opened to simulate the pressure decay during the last part of refill.

- For refill tests, the period when the lower plenum was filling was part of the test, so initial accumulator injection was into the three intact cold legs rather than the lower plenum.

CCTF Alternative ECCS Tests
For alternative ECCS tests (combined injection, downcomer injection, and upper plenum injection) the test procedure was similar to that for cold leg injection except for the injection location. In two downcomer injection tests which simulated B&W PWRs, the vent valves were free to open.

SCTF Tests
For SCTF cold leg injection reflood tests, the test procedure was similar to that for CCTF, with the following significant differences:

- Locations of accumulator and low pressure coolant injection depended on the type of test being run: forced flood, or gravity flood. In forced flood tests, the ECC water was injected into the lower plenum only by isolating the downcomer from the lower plenum; i.e., ECC water was forced to flow into the core. These tests investigated two-dimensional core cooling behavior based on clearly specified boundary conditions at the core inlet. The gravity flood tests included the effect of downcomer water head on the two-dimensional core cooling behavior.

- In some of the tests, accumulator injection was spread out over a longer period of time (to avoid hydraulic oscillations) and in these cases the power decay was delayed slightly.

This basic test procedure was used in SCTF refill tests which simulated depressurization of the pressure vessel during end-of-blowdown and refill. The SCTF alternative ECCS tests also used the basic test procedure, with the significant difference being the injection location.

Table 3.1-1

CCTF AND SCTF TESTS

Page 1 of 7

Group	Test Objective	Test/Run Number[1]	Description [2]	Comments
Cold Leg Injection Parameter Effects	Base Case	C1-5/14	CCTF-I Base Case	
		C2-SH1/53	CCTF-II Base Case	Same as CCTF-I EM test (C1-19)
		C2-4/62[3]	CCTF-II Base Case/ Repeatability	
		S1-1/507	SCTF-I Forced Feed Base Case	
		S1-10/516[3]	SCTF-I Forced Feed Base Case/Repeatability	
		S1-12/518	SCTF-I Gravity Feed Base Case	Lower plenum injection
		S1-14/520	SCTF-I Gravity Feed Base Case	Cold leg injection
		S2-10/615	SCTF-II Forced Feed Base Case	
		S2-SH1/604	SCTF-II Gravity Feed Base Case	Cold leg injection
	Effect of Pressure	C1-10/19	Low pressure	Compare to C1-5
		C1-12/21	High Pressure	Compare to C1-5
		C2-8/67	Low Pressure	Compare to C2-4
		C2-1/55	High Pressure	Compare to C2-4
		S1-2/508	Forced Feed, Low Pressure	Compare to S1-1
		S1-SH2/506	Forced Feed, High Pressure	Compare to S1-1
		S2-2/607	Gravity Feed, Low Pressure	Compare to S2-SH1
		S2-1/606[3]	Gravity Feed, High Pressure, Steep Q, Steep T	Compare to S2-6
	Effect of Core Power	C2-SH2/54	Low Power	Initial Power = 7.9 MW; compare to C2-4
		C2-5/63	Low Power	Initial Power = 7.1 MW; compare to C2-4
		S1-6/512	Forced Feed, High Power	Compare to S1-1
	Effect of Initial Cladding Temperature	C1-7/16	High Cladding Temperature	Maximum cladding temperature = 973 K at beginning of core recovery; compare to C1-5
		C1-14/23	High Cladding Temperature	Maximum cladding temperature = 1073 K at beginning of core recovery; compare to C1-5
		C2-AC1/52	Low Cladding Temperature	Compare to C2-4
		S2-AC3/603[3]	Gravity Feed, BE, Low Cladding Temperature	Compare to S2-9 for effect of cladding temperature at BE conditions

Table 3.1-1

CCTF AND SCTF TESTS

Page 2 of 7

Group	Test Objective	Test/Run Number[1]	Description [2]	Comments
Cold Leg Injection Parameter Effects (Continued)	Effect of Power/ Temperature Distribution	C2-5/63 C2-6/64	Steep Q Flat Q	
		S1-7/513	Forced Feed, Flat Q	Test terminated due to computer failure; repeated as S1-11
		S1-11/517 S1-8/514	Forced Feed, Flat Q Forced Feed, Steep Q	Repeat of S1-7
		S2-17/622 S2-16/621	Forced Feed, Flat Q, Flat T Forced Feed, Steep Q, Steep T	
		S2-SH2/605 S2-1/606[3]	Gravity Feed, Flat Q, Flat T Gravity Feed, High Pressure, Steep Q, Steep T	
		S2-6/611	Gravity Feed, Steep Q, Steep T	
		S2-7/612[3]	Radial Power Distribution Like CCTF Test C2-5	
		S3-14/718 S3-15/719 S3-16/720	Flat Q Slant Q Steep Q	
	Combined Effects of Power/ Temperature Distribution and UCSP Liquid Level Distribution	S2-14/619[3]	Forced Feed, Flat Q, Flat T, Flat Liquid Level	Counterpart to CCTF-II Test C2-6; Compare to S2-17 for liquid level distribution
		S2-12/617	Forced Feed, Steep Q, Steep T, Flat Liquid Level	Compare to S2-16 for liquid level distribution
		S2-15/620	Forced Feed, Steep Q, Flat T, Flat Liquid Level	
		S2-21/626	Forced Feed, Flat Q, Steep T, Flat Liquid Level	
	Effect of ECC Flow Rate	C1-2/11[3]	Low ACC Flow Rate/No Upper Plenum Guide Tube Internals	Compare to C1-5
		C1-11/20	Low ACC Flow Rate/ Repeatability	Compare to C1-5
		C1-6/15 C1-9/18 C1-13/22	High LPCI Flow Rate Low LPCI Flow Rate Short ACC Flow Duration	Compare to C1-5 Compare to C1-5 Comapre to C1-5
		C2-9/68	High LPCI Flow Rate	Compare to C2-SH2
		S1-SH1/505 S1-5/511	Forced Feed, High Flow Rate Forced Feed, Low LPCI Flow Rate	
		S1-9/515	Forced Feed, High ACC and LPCI Flow Rate	
		S1-16/522	Gravity Feed, Low ACC Flow Rate	
		S1-17/523	Gravity Feed, Low ACC and LPCI Flow Rates	
		S1-21/531	Gravity Feed, Low LPCI Flow Rate	
		S1-22/532	Gravity Feed, No ACC Injection, Low LPCI Flow Rate	

Table 3.1-1

CCTF AND SCTF TESTS

Page 3 of 7

Group	Test Objective	Test/Run Number[1]	Description [2]	Comments
Cold Leg Injection Parameter Effects (Continued)	Effect of ECC Flow Rate (Continued)	S2-11/616	Forced Feed, High ACC Flow Rate	Compare to S2-10
		S2-19/624	Forced Feed, High LPCI Flow Rate	Compare to S2-10
		S2-AC1/601	Gravity Feed, High ACC Flow Rate	Compare to S2-SH1
		S2-AC2/602	Gravity Feed, Short ACC Flow Duration	Compare to S2-SH1
		S2-AC3/603[3]	Gravity Feed, Low and Long ACC Flow Rate	Compare to S2-SH1
	Effect of ECC Temperature	S1-4/510	Forced Feed, Low ECC Temperature	Compare to S1-1
		S1-15/521	Gravity Feed, High ACC Temperature (Saturated)	Compare to S1-14
		S1-18/542[3]	Refill, High ACC Temperature (Saturated)	Compare to S1-19
		S2-8/613	Gravity Feed, Low ECC Temperature	Compare to S1-SH1
	Effect of Downcomer Wall Temperature	C1-2/11[3]	High Downcomer Wall Temperature	
		C1-3/12	Low Downcomer Wall Temperature	
	Effect of Loop Flow Resistance	C1-SH4/8	High Loop Flow Resistance, High ECC Temperature	Cold leg injection scoping test; compare to C1-2
		C1-1/10	High Loop Flow Resistance, Low ECC Temperature	Compare to C1-2
	Effect of Downcomer Water Accumulation Rate	C2-3/61	High Rate of Downcomer Water Accumulation	Compare to C2-4
	Effect of UCSP Liquid Level	S1-3/509	Low UCSP Liquid Level	Compare to S1-1
Cold Leg Injection Special Purpose Tests	Evaluation Model (EM) Tests	C1-19/38	Evaluation Model	Same as CCTF-II base case (C2-SH1); compare to C1-5
		S3-9/713	Evaluation Model Integral Test	Compare to S3-10

Table 3.1-1

CCTF AND SCTF TESTS

Page 4 of 7

Group	Test Objective	Test/Run Number[1]	Description [2]	Comments
Cold Leg Injection Special Purpose Tests (Continued)	Best Estimate (BE) Tests	C2-12/71	Best Estimate	Compare to C2-4
		S2-9/614	Gravity Feed, Best Estimate	Compare to S2-SH1
		S3-10/714	Best Estimate Integral Test	Compare to S3-9
	Refill Tests	C1-SH1/5 C1-4/13 C1-15/24	Refill, No Core Power Refill/Reflood Refill/Reflood Nitrogen Injection	
		C2-2/56 C2-14/74 C2-17/77 C2-11/70	Refill Refill/Reflood Refill/Reflood, Steam Injection Refill, Blocked Loops	No reflood simulation
		S1-19/525 S1-18/524[3]	Refill Refill, High ACC Temperature (Saturated)	
	Effect of Asymmetric Power/Temperature Distribution	C1-17/36 C1-20/39	Asymmetric Core Power Asymmetric Core Temperature	Compare to C1-5
	Effect of Water in Loop Seal	C1-8/17	Loop Seal Filling	Test terminated early due to high cladding temperature; repeated as C1-18.
		C1-18/37	Loop Seal Filling	Repeat of C1-8; compare to C1-5
	Effect of Forced vs. Gravity Feed	S1-12/518	Gravity Feed, Lower Plenum Injection	Compare to S1-14
	Evaluation of SCTF Gravity Feed Oscillations	S1-23/536 S1-24/537	Low ACC Flow Rate, Long ACC Duration Gradual Reduction from ACC Flow Rate to LPCI Flow Rate	
	Facility Coupling Tests	C1-16/25 C1-21/40 C1-22/41	Counterpart to FLECHT-SET Test 3105B Counterpart to FLECHT-SET Test 2714B Counterpart to FLECHT-SET Test 3420B	

Table 3.1-1

CCTF AND SCTF TESTS

Page 5 of 7

Group	Test Objective	Test/Run Number[1]	Description [2]	Comments
Cold Leg Injection Special Purpose Test (Continued)	Facility Coupling Tests (Continued)	C2-AC2/52	Counterpart to FLECHT-SET Test 2714B and CCTF-I Test C1-21	
		C2-15/75	Counterpart to FLECHT-SET Test 2714B	
		S1-13/519	Counterpart of FLECHT-SEASET Test 43716C	
		S2-7/612[3]	Radial Power Distribution Like CCTF Test C2-5	Cold leg injection
		S2-14/619[3]	Forced Feed, Flat Q, Flat T, Flat Liquid Level; Counterpart to CCTF-II Test C2-6.	
		S2-18/623	Counterpart to CCTF-II Test C2-5	Forced feed
Other Cold Leg Injection Tests	Repeatability Tests	C1-11/20[3]	Low ACC Flow Rate/Repeatability	
		C2-4/62[3]	CCTF-II Base Case/Repeatability	Compare to C2-SH1
		S1-10/516[3]	SCTF-I Forced Feed Base Case/Repeatability	Compare to S1-1
		S2-13/618	SCTF-I/II Repeatability	Compare to S1-1
	Miscellaneous	C1-SH2/6	Low Power, Flat Power Profile, High Pressure, LP Injection	Low power and LP injection scoping test
		C1-SH3/7	Low Power, Non-Flat Power Profile, High Pressure, LP Injection	Steep Q and LP injection scoping test
		S1-20/530	Effect of Closed Vent Valve Line	Vent valve line was inadvertently left open on previous SCTF-I tests (S1-14/520 to S1-17/523)
		S1-14/520[3]	Effect of Open Vent Line	
Combined Injection Separate Effects Tests	CCFL Evaluation	S2-3/608	Steam Injection, Saturated ECC, No Core Power	Water injected into upper plenum
		S2-4/609	Steam Injection, Saturated ECC, Core Power On	Water injected into upper plenum
		S2-5/610	Steam Injection, Subcooled ECC, Core Power On	Water injected into upper plenum
		S3-3/707	Uniform Subcooled Water	
		S3-4/708	Local Subcooled Water	
		S3-5/709	Distributed Subcooled Water	

Table 3.1-1

CCTF AND SCTF TESTS

Page 6 of 7

Group	Test Objective	Test/Run Number[1]	Description [2]	Comments
Combined Injection Separate Effects Tests (Continued)	Core Cooling Evaluation	S3-SH1/703 S3-1/705 S3-2/706 S3-6/710 S3-7/711 S3-8/712 S3-12/716 S3-AC2/702	Core Cooling Base Case Lower Plenum Water Level Effect Subcooling Effect Power Distribution Effect ECC Location Effect ECC Location Changing Effect High Power, High Cladding Temperature Core Cooling BE	
Combined Injection Integral Tests	Effect of Injection Configuration	C2-21/81	7/8 Injection (4 Hot Legs, 3 Cold Legs)	Compare to C2-19 (5/8 injection: 2HL, 3CL) for effect of ECC flow rate to hot legs
		S3-13/717[3] S3-20/724 S3-22/726	Continuous UP Injection Intermittent UP Injection Alternate UP Injection	
	Effect of ECC Temperature	S1-SH3/528 S1-SH4/529	Saturated ECC Subcooled ECC	
		S3-18/722	High Injection Temperature	Compare to S3-13
	Effect of Core Power and Cladding Temperature	S3-19/723 S3-21/725	Low Pressure, High Power, High Cladding Temperature Low Pressure, High Power, High Injection Temperature	Failed test Compare to S3-13
	Evaluation Model (EM) Tests	C2-19/79	5/8 Injection (2 Hot Legs, 3 Cold Legs)	
		S3-SH2/704 S3-13/717[3]	EM Orientation EM	Compare to S3-11
	Best Estimate (BE) Tests	C2-20/80 [3]	BE	Compare to C2-19
		S3-AC1/701 S3-11/715	BE Orientation BE	Compare to S3-13
Combined Injection Special Purpose Tests	Facility Coupling Tests	C1-SH5/9	Counterpart to PKL Test K7A	
		C2-20/80 [3]	Counterpart to PKL	
Upper Plenum Injection Tests	Base Case	C2-16/76	Asymmetric (One Port) Injection	
	Parameter Effects	C2-AS1/59 C2-13/72 C2-AA1/57 C2-18/78	Symmetric (Two Port) Injection Symmetric (Two Port) Injection, High UPI Flow Rate Symmetric (Two Port) Injection, High Power, Very High HPI Flow Rate UPI Best Estimate/Refill	

Table 3.1-1

CCTF AND SCTF TESTS   Page 7 of 7

Group	Test Objective	Test/Run Number[1]	Description [2]	Comments
Downcomer Injection Tests	Parameter Effects	C2-AA2/58 C2-AS2/60 C2-10/69	Vent Valves Closed Vent Valves Open Vent Valves Open, Loops Blocked	
		S3-17/721	Vent Valve Test	
Mass Balance Calibration Test	Verification of Mass Flow Measurements	C2-7/65	Mass Balance Calibration	

NOTES:

1.   Test number identifies facility and test series:

C1 = CCTF Core-I
C2 = CCTF Core-II
S1 = SCTF Core-I
S2 = SCTF Core-II
S3 = SCTF Core-III

2.   The following abbreviations are used in the test descriptions:

BE = Best estimate
EM = Evaluation model
IT = Integral test
Flat Q = Flat power profile
Slant Q = Slant power profile
Steep Q = Steep power profile
Flat T = Flat initial clad temperature profile
Steep T = Steep initial clad temperature profile
ACC = Accumulator
ECC = Emergency core coolant

3.   Test is listed twice in the table because it can be used to evaluate more than one effect.

Pressure
Regulation
Valve

Exhaust
Line

Pressure
Vessel

ECC
Port

Steam
Generator

Pump
Simulator

Containment
Tank-2

Containment
Tank-1
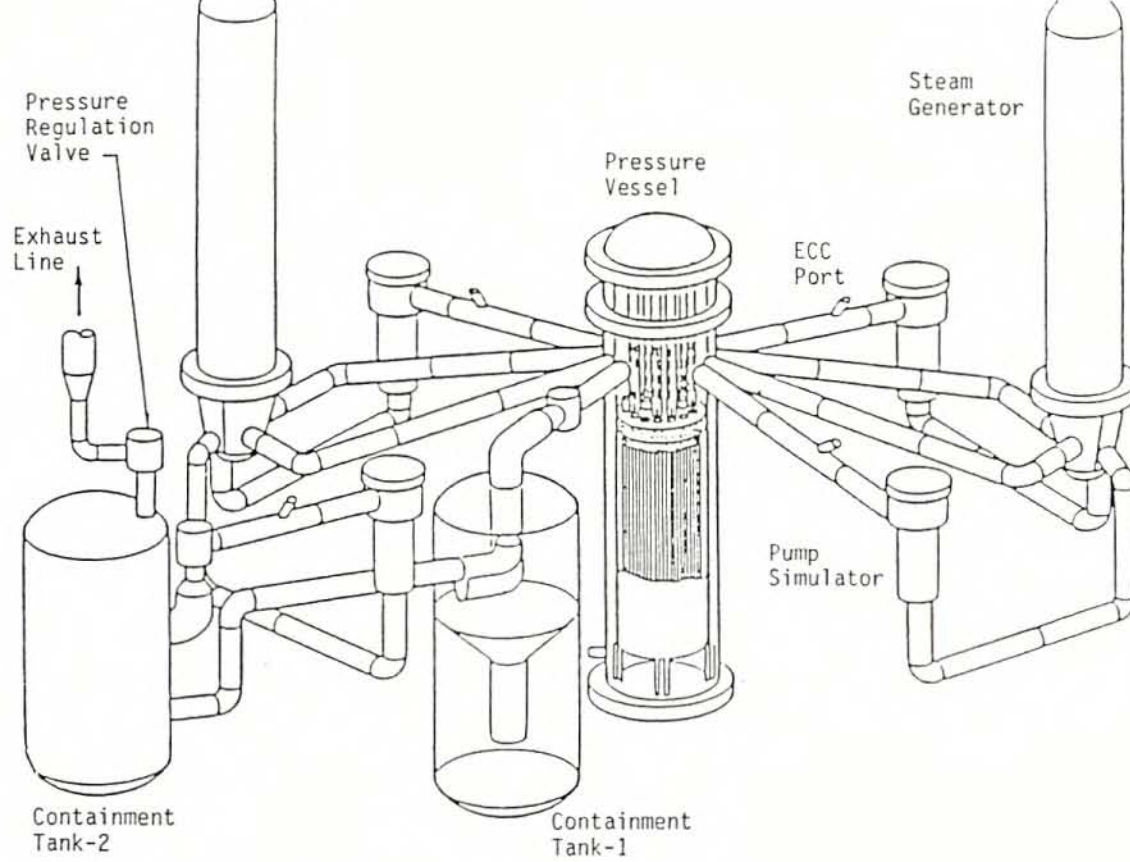
CYLINDRICAL CORE TEST FACILITY
(CCTF)

FIGURE 3.1-1

Upper Head

Upper Support Plate

Upper Ring
(Core II Only)

Vent Valve

Core Flooding
Nozzle

Upper Core
Support Plate

Downcomer

Core

Baffle Region

Barrel

Lower Core
Support Plate

Lower Grid

Bottom Plate

542 R

1264 ⌀

1084 ⌀

961 ⌀

929 ⌀

780

1620

970

297

8647

3660

1160

890

Bottom of
Support Plate

Loop Nozzle
Center

Bottom of
Core Plate

Top of Heated
Section

Bottom of
Heated Section

Top of Core
Plate

Bottom of
Grid

Unit : mm

CCTF CORE-II
PRESSURE VESSEL
FIGURE 3.1-2

PN

Guide Tube
Support Column
Open Hole

Hot Leg   Hot Leg

Downcomer
Injection Nozzle
(Core II only)

Cold Leg   Cold Leg

Cold Leg   Broken Cold Leg

Downcomer
Injection Nozzle
(Core II only)

Hot Leg   Broken
                 Hot Leg

UPPER PLENUM

Plant North

Hot Leg 2   Hot Leg 1   High Power Zone
                                    (4 Assemblies)

                                    Medium Power Zone
                                    (12 Assemblies)

Cold Leg 2   Cold Leg 1

                                    Low Power Zone
                                    (16 Assemblies)

                                    Pressure
                                    Vessel

Cold Leg 3   Broken
                                    Cold Leg 4

                                    Downcomer

Note: Barrel

Primary loop nozzles are   Hot Leg 3   Broken
at the upper plenum   Hot Leg 4
elevation, but are shown
on the core cross-section   CORE (See Note)
for reference.

CCTF PRESSURE VESSEL CROSS SECTIONS

FIGURE 3.1-3

Downcomer

Steam
Water
Separator

Broken Cold Leg

Upper
Plenum

Pressure
Vessel

Hot Leg

ECC Inj. Port

Intact Loop

To Containment
Tank - II

Broken Cold Leg

Honeycomb

Simulated
Fuel Assembly

ECC Inj. Ports

Pump
Simulator

Reinforcement

To Containment
Tank - I

Lower Plenum

Saturated
Water Supply

ECC Inj. Port
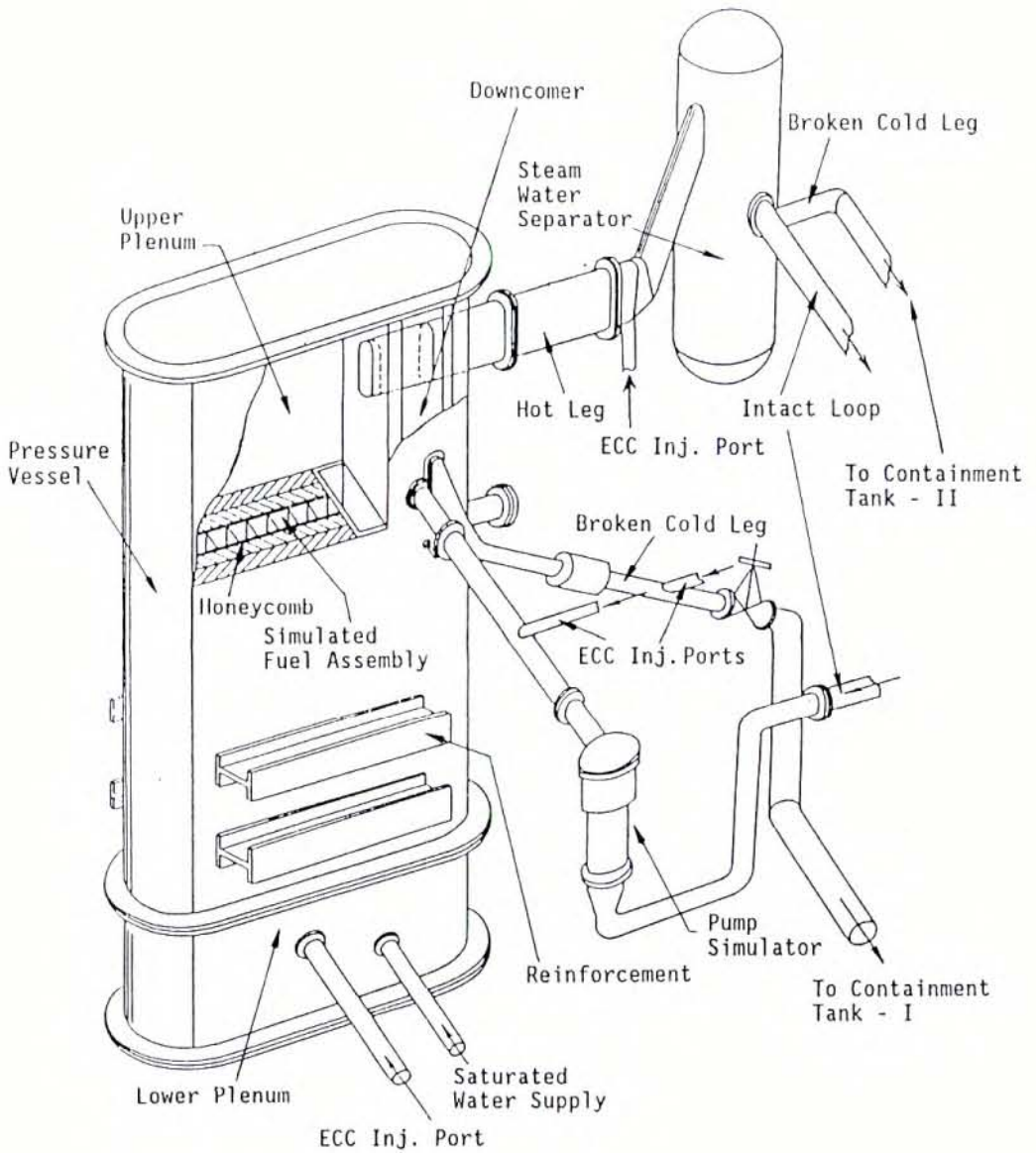
OVERVIEW OF SLAB CORE TEST FACILITY
FIGURE 3.1-4

Upper head

Upper plenum

Hot leg

Intact cold leg
Broken cold leg

Filler

Core

Honey—
comb

Downcomer

8657

Baffle region

Bundle no.
1 2 3 4 5 6 7 8

Lower plenum

247

460

2301

3121
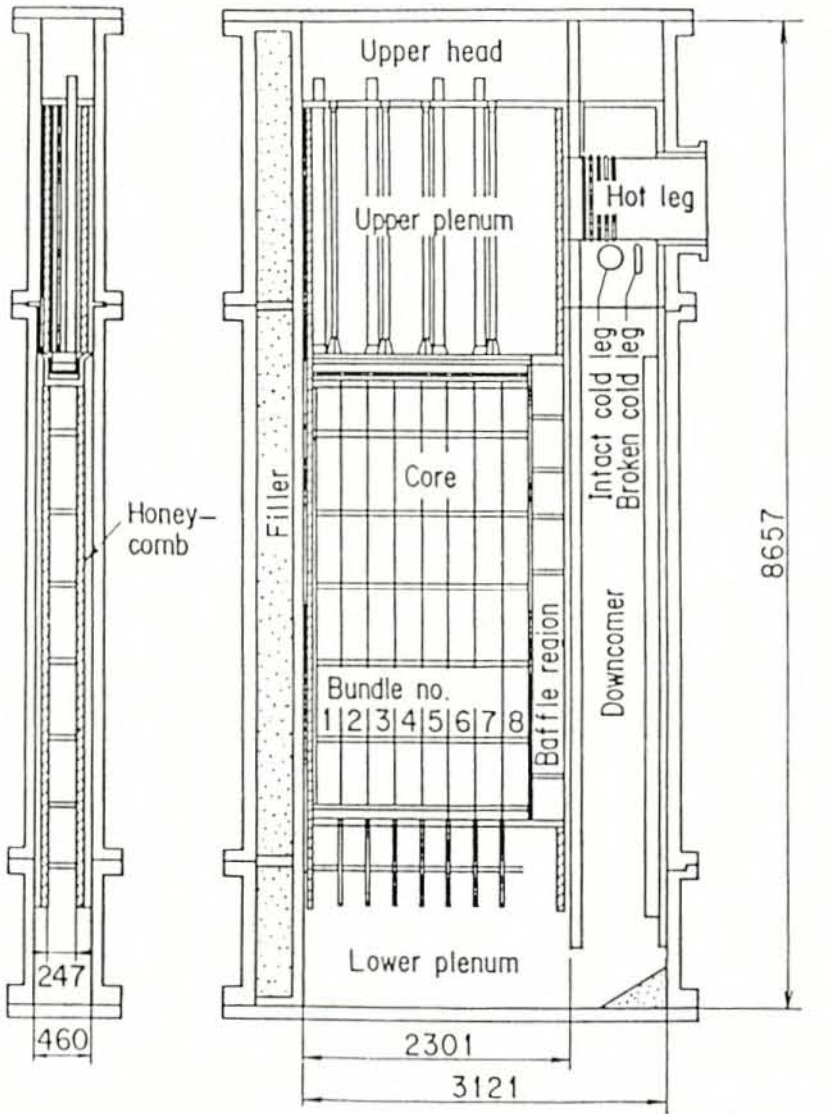
Unit: mm

VERTICAL CROSS-SECTION
OF SCTF CORE-II PRESSURE VESSEL

FIGURE 3.1-5

3.2 COLD LEG ECC INJECTION TESTS

3.2.1 Overall Transient

The overall large break LOCA (LBLOCA) transient for cold leg injection is described below based on the results of tests at both CCTF and SCTF. The description of the end-of-blowdown/refill portion of an LBLOCA is based on special tests which simulated the refill portion of an LBLOCA. The description of the reflood portion of an LBLOCA is based on CCTF and SCTF base case tests, which were carried out with EM conditions (single LPCI pump failure; decay heat 20% higher than 1971 ANS standard; high initial core temperature; locked rotor flow resistance). Figures 3.2-1 through 3.2-4 are schematics which depict system behavior at different times in the transient. Data plots of overall system response for Test C2-4 are provided in Figure 3.2-5.

End-of-Blowdown/Refill (see Figures 3.2-1 and 3.2-2)
After initiation of the break, the primary system pressure decreased as fluid was discharged through the break. The fluid in the pressure vessel was vented to containment by flowing up the downcomer to the broken cold leg. The downcomer upflow was a two-phase mixture of steam with entrained water. When this upflow was high, ECC injected into the cold legs was carried over to the broken cold leg (i.e., ECC bypass). Therefore, ECC injected during this period did not contribute to core cooling.

The two-phase flow in the downcomer decreased with time. When the two-phase upflow in the downcomer was low enough, ECC flowed down to the lower plenum, initiating refill. Most ECC injected during this period accumulated in the lower plenum and the downcomer with little ECC bypass. The water level in the lower plenum reached the bottom of the core (i.e., reflood initiation) shortly after blowdown was complete.

During end-of-blowdown and refill, water was not present in the core. Consequently, core cooling was negligible and the cladding temperature increased almost adiabatically.

Reflood -- Accumulator Injection (see Figures 3.2-3 and 3.2-5)
In the early portion of reflood, the downcomer water level increased rapidly due to the high ECC flow from the accumulators. This increase in downcomer level forced water into the core. Steam generation in the core initiated first at the bottom of the core as water entered the core from the lower plenum. Within a few seconds, water carried by the steam flow was present throughout the core. This increase in liquid fraction enhanced core cooling above the quench front. The steam generated in the core was vented to containment via the upper plenum and reactor coolant loops.

Early in the transient the core flooding rate was high and the collapsed water level in the core increased rapidly. The core flooding rate decreased quickly when the downcomer water level stabilized near the cold leg elevation and some of the ECC spilled out the broken cold leg. Although the core flooding rate decreased, the core steam generation rate remained essentially constant, indicating almost no degradation of core cooling.

Some of the water in the core flowed out of the core with the steam flow. The water was either de-entrained in the upper plenum, or carried over with the steam to the reactor coolant loops. In the upper plenum, the de-entrained water was either accumulated as a two-phase mixture, re-entrained, or fell back to the core. The water carried over to the loops was de-entrained and accumulated in the hot legs and steam generator inlet plena. Typically, entrained water did not reach the steam generator tube regions during the accumulator injection portion of reflood. The steam flow through the loops created a pressure differential between the upper plenum and downcomer which reduced the core flooding rate (i.e., the steam binding effect).

In the intact loops, the steam flow toward the downcomer was completely condensed by the subcooled ECC. Due to the high ECC flows, the condensation resulted in the formation of water plugs in the cold legs which oscillated upstream and downstream from the injection nozzle location. The period of these oscillations was typically a few seconds. The water plugs reversed direction before reaching the pump simulators; hence, loop seals were not formed in the pump seal (or crossover) piping.

Reflood -- LPCI (see Figures 3.2-4 and 3.2-5)
When accumulator injection terminated, ECC flow decreased to the low pressure coolant injection (LPCI) flow. Due to the reduced ECC flow, only a portion of the steam flow was condensed in the intact cold legs. The uncondensed steam flowed to containment via the downcomer and broken cold leg. This steam flow around the downcomer reduced the downcomer water level slightly below the nozzle elevation by entraining water out the break.

The reduced ECC flow also resulted in an increase in the temperature of ECC delivered to the downcomer to near saturation. As saturated water replaced subcooled water in the downcomer, heat release from the vessel wall resulted in steam generation. This steam generation (i.e., voiding) contributed to the reduction of the collapsed water level in the downcomer.

Core flooding rate, which decreased quickly after the downcomer filled to the cold leg nozzles (see previous discussion), remained nearly constant. The collapsed water level in the core continued to increase, but at a reduced rate. Water flow out the top of the core also decreased due to the reduced flooding rate. However, late in reflood as the quench front reached the upper regions of the core, water flow out the top of the core increased.

The collapsed liquid level in the upper plenum typically increased with time as the water flow out of the core increased. In Test C2-4, the upper plenum water level was about 0.3 m when the quench front was at the mid-plane of the core.

Shortly after termination of accumulator injection, entrained water reached the steam generator tube regions. In CCTF, which had active steam generators, essentially all of the water carried over to the tube regions was vaporized by heat transferred from the hot water on the secondary side of the steam generator. Consequently, the flow at the steam generator exit was single-phase, superheated steam flow. Single-phase, superheated steam flow through the pump flow resistance contributed to steam binding.

3.2.2 System Behavior

The major findings from the CCTF and SCTF tests regarding system behavior during reflood are discussed below. The discussion is based on the base case tests for each of the test series. The discussion is organized by region. Behavior in the core is discussed in Section 3.2.3.

Downcomer

- Water accumulation and flow in the downcomer were essentially one-dimensional.

- During the LPCI portion of reflood, the collapsed water level in the downcomer was below the cold leg elevation due to voiding from heat release from the vessel and entrainment by steam flow around the downcomer.

- The ECC flow entering the downcomer was subcooled during accumulator injection and saturated during LPCI flow. Since there was little axial mixing, the water in the downcomer was thermally stratified. The water flow out of the bottom of the downcomer into the core was initially subcooled but gradually increased to near saturation. As saturated water replaced subcooled water in the downcomer, voiding by wall steam generation became more significant.

- Only a part of ECC water flow into the downcomer entered the core and contributed to core cooling; excess ECC water flowed out the break.

Lower Plenum

- Most of the lower plenum acted as a dead space. Specifically, most of the water in the lower plenum did not enter the core or mix with the flow from the downcomer to the core inlet.

- Since most of the volume of the lower plenum acted as dead space, the temperature of water entering the core reflected the water temperature in the bottom of the downcomer. Specifically, the water entering the core was subcooled during the accumulator injection period and gradually increased to near saturation during the LPCI period.

Upper Plenum, Hot Legs and Steam Generators

- Water de-entrainment and accumulation upstream of the steam generator tubes (i.e., upper plenum, hot legs, and steam generator inlet plena) reduced water carryover to the steam generator tubes and reduced the pressure drop for flow through the loops.

- Essentially all the water entrained to the steam generator tubes was vaporized by heat transfer from the secondary side. For some conditions with high water flow (best-estimate test), partial vaporization occurred. Vaporization increases the volumetric flow, and therefore pressure drop, in the reactor coolant loops.

Intact Cold Legs

During the accumulator injection portion of reflood, water plugs formed in the intact cold legs as the steam flow in the loops was completely condensed by the high flow of subcooled ECC. However, during the LPCI portion of reflood when the ECC flow was considerably lower, only a portion of the steam flow was condensed and the flow regime in the cold legs was stratified (i.e., steam flow over a layer of water). Condensation efficiency was close to 100% during this period (i.e., water heated to saturation temperature).

Broken Loop

- During the accumulator injection portion of reflood after the downcomer filled with water, flow out of the broken cold leg was essentially single-phase water flow since the steam flow through the intact loops was completely condensed. However, a two-phase mixture of steam with entrained water flowed out the break during the LPCI portion of reflood.

- Steam flow in the broken hot leg was the same as in the intact hot legs during the accumulator injection portion of reflood when the steam flow through the intact loops was completely condensed. However, during the LPCI portion of reflood the steam flow through the broken hot leg was significantly greater than the flow in an intact loop due to the differential pressure for flow out the broken cold leg. This phenomenon helped reduce the impact of steam binding.

Intact Loops

Thermal-hydraulic behavior was nearly the same among the three intact loops. Oscillation among intact loops, which might be caused by parallel channel characteristics, was not observed.

3.2.3 Core Behavior

Core cooling by steam generation was initiated as water entered the core from the lower plenum. Differential pressure measurements at various elevations in the core indicate that water entrained by the boiling process was present throughout the core within a few seconds of reflood initiation (Figure 3.2-6). Similarly, water carryover from the core to the upper plenum initiated almost immediately after reflood initiation. The differential pressure measurements also showed that the water was evenly distributed across the core (i.e., in the horizontal or radial direction) even for tests with a non-uniform core power profile. Core cooling above the quench front was improved by the presence of water in the upper regions of the core, and by fallback of water which de-entrained in the upper plenum.

While the distribution of water in the core was one-dimensional, flow in the core exhibited multidimensionality. In tests at SCTF with a non-uniform power profile, a circulation flow between the high power and low power regions was observed. As shown in Figure 3.2-7, flow below the quench front was from the low power region to the high power region but flow above the quench front was from the high power region to low power region. As a result of this flow circulation, heat transfer was enhanced in the high power region and degraded in the low power region. However, since peak cladding temperature (PCT) occurred in the high power region, the net effect was a decrease in PCT.

The heat transfer coefficient was strongly related to void fraction as well as distance from the bottom quench front. As shown in Figure 3.2-8, the void fraction was well predicted with REFLA void fraction model developed based on JAERI's small-scale reflood tests by assuming complete mixing of fluid staying among subchannels. Also, the one-dimensional heat transfer coefficient was well predicted with the REFLA heat transfer model (Figure 3.2-9). References J-906, J-910 and J-984 describe the REFLA void fraction and heat transfer models, and the assessment of these models against CCTF data.

Other findings from the CCTF and SCTF tests regarding thermal-hydraulic behavior in the core are summarized below. The discussion includes the results of tests which varied the radial power profile in the core. Also, the results of tests at SCTF-I which investigated the effect of flow blockage due to ballooning of the fueled rods are discussed.

3.2-5

Radial Power Profile

- A non-uniform radial power profile created a multidimensional flow pattern which enhanced heat transfer in the high power region and degraded heat transfer in the low power region (see above discussion). The combination of heat transfer enhancement in the high power region and degradation in the low power region resulted in a nearly uniform quench front.

- The magnitude of the heat transfer enhancement in the high power region was primarily dependent on the bundle power ratio and the maximum bundle power rather than the shape of the radial power profile (Figure 3.2-10). These results applied to elevations where the PCT would be expected to occur and were insensitive to parameter variations (e.g., pressure).

- A large stepwise difference in bundle power ratio between adjacent bundles enhanced heat transfer locally on both sides of the power step.

Blockage Effect (60% blockage in two bundles)

- The flow blockage slightly affected heat transfer in the region just above (i.e., downstream) of the blockage. Specifically, quench time just above the blockage was delayed when accumulator injection rate was low and hastened when the accumulator injection rate was high.

- The effect of the flow blockage on heat transfer was limited to only 0.5m above the blockage; no effect was noted below the blockage. Overall, the effect of the flow blockage on PCT was negligible.

Grid Spacers without Vanes

The grid spacers affected heat transfer locally. Specifically, heat transfer above the spacer was slightly enhanced while heat transfer below the spacer was slightly degraded.

Non-heated Rods

Non-heated rods quenched earlier than adjacent heated rods and, in some cases, hastened quenching of adjacent heated rods (particularly in the upper region of the core). However, the overall effect of non-heated rods on PCT was negligible.

Configuration of Pressure Vessel

The configuration of the pressure vessel (e.g., location of hot leg, location and geometry of the upper plenum internals, configuration of core baffle region) influenced two-dimensional flow behavior; however, the effect of the two-dimensional flow behavior on PCT was negligibly small.

3.2.4 Parameter Effects

The initial and boundary conditions were varied parametrically to determine the effect of the different parameters on the reflood transient. The major results of these tests are summarized below.

System Pressure

- The major effect of changing system pressure was to change the density of steam. At higher pressures, the steam density increased resulting in a reduction of the steam binding effect and an increase in the core flooding rate. Also, since steam velocities were lower, more water was accumulated in the core (lower void fraction) and less water was entrained out of the vessel.

- Core cooling was improved at higher pressures due to the decrease in the void fraction above the quench front and the reduction in steam binding.

Core Power

- The primary effect of changing core power was increased steam generation and flow rate with increased core power. The increased steam generation was not noted until about 100 seconds after Bottom of Core Recovery (BOCREC). Apparently, heat transfer during the early portion of reflood is dominated by the initial stored energy and not core power.

- The core flooding rate was about the same for the high power and low power tests; i.e., flooding rate was essentially independent of power. However, for the high power case, more water was vaporized or carried over, leading to lower accumulation in the core.

- The thermal effect of increased core power was a higher cladding temperature rise and later core quench times. This effect of core power on temperature rise was small in the lower part of the core (consistent with heat transfer during early reflood being dominated by stored energy). In the upper half of the core, the temperature rise was significantly greater.

Initial Cladding Temperature

- Higher initial cladding temperatures resulted in increased steam generation in the core. The increase in steam generation occurred during the early portion of reflood when heat transfer was dominated by stored energy (see above discussion on core power).

- The effect of higher initial cladding temperature on cladding temperatures during reflood was an increase in PCT but a decrease in the cladding temperature rise.

Power/Temperature Distribution

- Overall system performance was essentially the same for tests with the same total core power and stored energy regardless of the power and initial temperature distribution.

- A non-uniform power profile affected core cooling locally (see Section 3.2.3).

ECC Flow Rate

- Higher LPCI flow resulted in stronger condensation of steam in the cold legs and hence lower system pressure. As discussed above, decreasing system pressure increased PCT. On the other hand, higher LPCI flow increased the subcooling of the water flow to the downcomer and reduced downcomer voiding as well as downcomer entrainment. These effects offset each other. The net effect of doubling LPCI flow (i.e., no LPCI pump failure vs. single LPCI pump failure) was a slight increase in PCT (about 5 K).

- An increase in the accumulator injection rate increased the core flooding rate, thereby increasing the initial steam generation rate and enhancing core cooling. This arrested core temperatures at all elevations essentially immediately. However, for a shorter duration of accumulator injection or a reduction of accumulator flow, the upper regions of the core heated up slightly before their temperatures were arrested.

- The effect on PCT of continued accumulator injection after the downcomer filled was essentially the same as an increase in the LPCI flow rate (see discussion above).

Downcomer Wall Temperature

- Lowering the initial downcomer wall temperature reduced heat transfer between ECC delivered to the downcomer and the downcomer walls. Consequently, voiding in the downcomer decreased and subcooling at the core inlet increased.

- The primary effect of lower initial wall temperatures in the downcomer on core cooling was a decrease in core steam generation due to the increase in subcooling at the core inlet. However, since this effect occurs during late reflood, the influence on PCT is small.

Loop Flow Resistance

- The effect of increasing the loop flow resistance was an increase in the pressure drop (i.e., back pressure) from flow through the loops. This increase in back pressure reduced the core flooding rate and thereby increased PCT.

- The increase in back pressure also increased the reactor vessel pressure. As described above, higher vessel pressure improves core cooling and reduces PCT. Apparently, the reduction in PCT due to the higher pressure was small in comparison to increase in PCT due to the reduced flooding rate.

3.2.5 Special Purpose Tests

At CCTF and SCTF, special tests were performed to investigate specific sets of conditions and phenomena. The major results of these tests are summarized below.

Reflood Behavior with BE Conditions (no LPCI failure; lower decay heat and initial core temperature)

- PCT and quench times were significantly lower for BE conditions than for EM conditions. Specifically, CCTF Test C2-12, a BE test, had a PCT of 648 K and a quench time of 120 seconds whereas typical CCTF-II tests (i.e., EM tests) had a PCT of 1132 K and a quench time of 571 seconds.

- System-wide hydraulic oscillations due to intermittent carryover to the SGs occurred at CCTF (Test C2-12). A brief core re-dryout with a small heatup prior to re-quench occurred during these oscillations.

Initial Loop Seal

- Water filled loop seals (i.e., blocked loops) resulted in pressurization of the upper plenum because the steam generated in the core could not vent to containment. However, a short time after BOCREC (40 seconds in Test C1-18), the increase in upper plenum pressure was sufficient to clear the loop seals.

- The initial increase in upper plenum pressure reduced the core flooding rate. Consequently, core cooling was significantly degraded until the loop seal cleared. After the loop seal cleared, good core cooling was achieved. The overall effect of loop seals was an increase in PCT of approximately 100 K in Test C1-18.

3.2-9

Nitrogen Discharge from the Accumulators

CCTF Test C1-15 injected nitrogen through the ECC piping to simulate discharge of nitrogen from the accumulators. The amount of nitrogen which reached the primary system was insufficient to adequately simulate the phenomena; however, the test did confirm that nitrogen discharge increases the differential pressure across the broken cold leg.
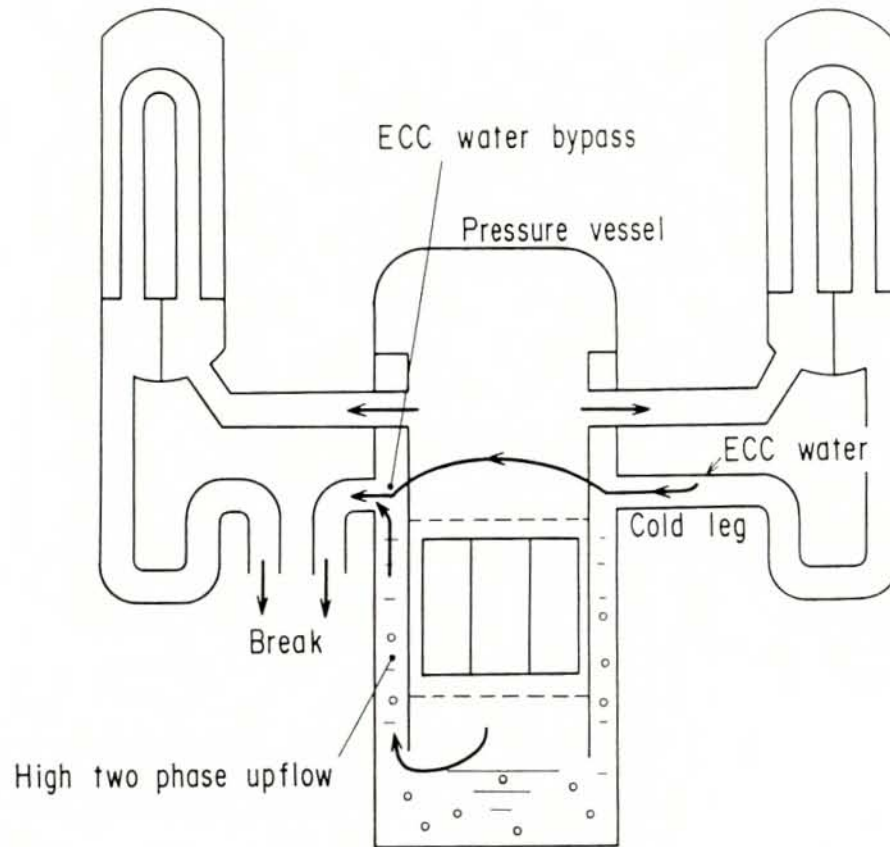
**OVERALL TRANSIENT FOR COLD LEG INJECTION TESTS:
END-OF-BLOWDOWN PHASE TO LOWER PLENUM REFILL
FIGURE 3.2-1**
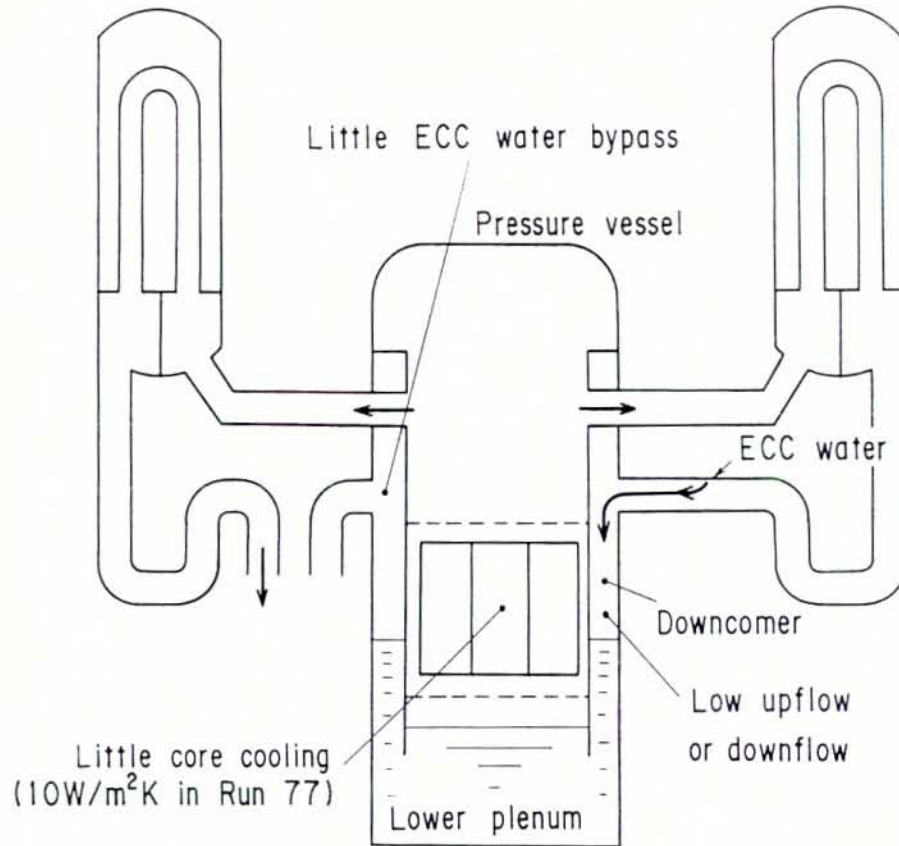
Little ECC water bypass

Pressure vessel

ECC water

Downcomer

Low upflow
or downflow

Little core cooling
($10W/m^2K$ in Run 77)

Lower plenum

OVERALL TRANSIENT FOR COLD LEG INJECTION TESTS:
LOWER PLENUM REFILL TO REFLOOD INITIATION
FIGURE 3.2-2

Water accumulation in upper plenum

Pressure vessel

Upper plenum

Hot leg

ECC water

No loop seal

Cold leg

Crossover leg

Water plug formation
Violent oscillation

Quick spreading of water to upper core

Downcomer

(Good cooling at entire core)

B   A

U tube type flow oscillation
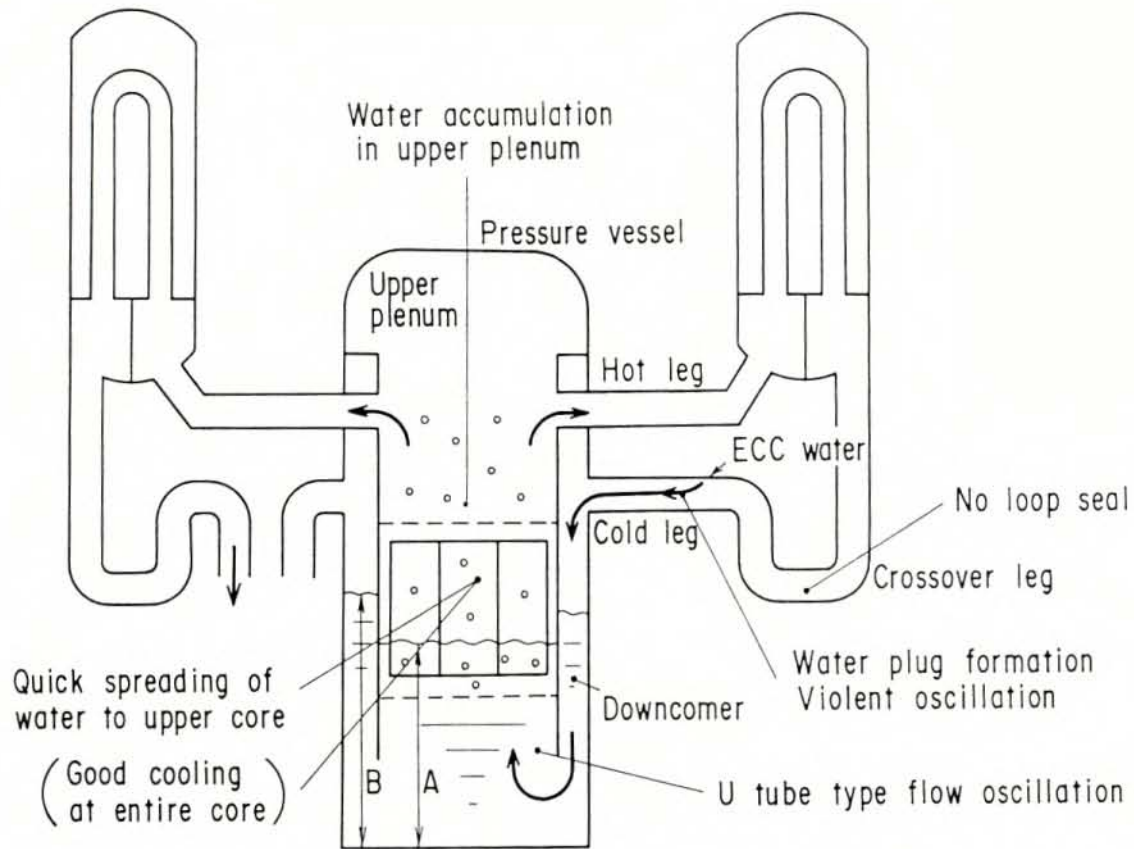
OVERALL TRANSIENT FOR COLD LEG INJECTION TESTS:
REFLOOD INITIATION TO ACC TERMINATION
FIGURE 3.2-3

Steam generator

Water accumulation

Upper plenum

Superheated steam

Broken loop

ECC water

Primary pump

Cold leg

Spill over of excessive water and steam

Two-phase mixture

Downcomer

Low core flooding rate (about 2 cm/s)

Turnaround and quench of rods
Bottom quench is dominant

Solid water
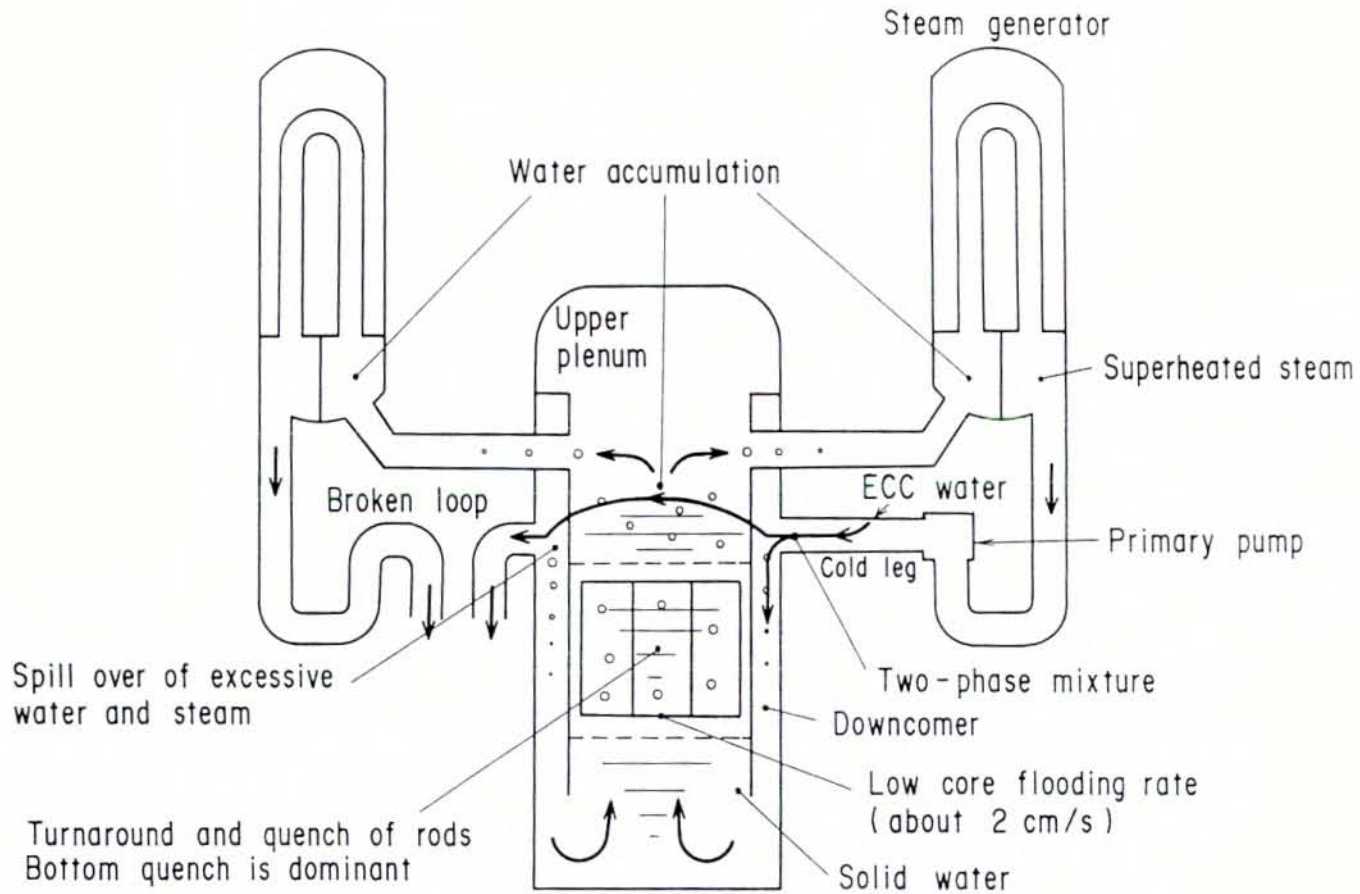
OVERALL TRANSIENT FOR COLD LEG INJECTION TESTS:
AFTER ACC INJECTION TERMINATION

FIGURE 3.2-4
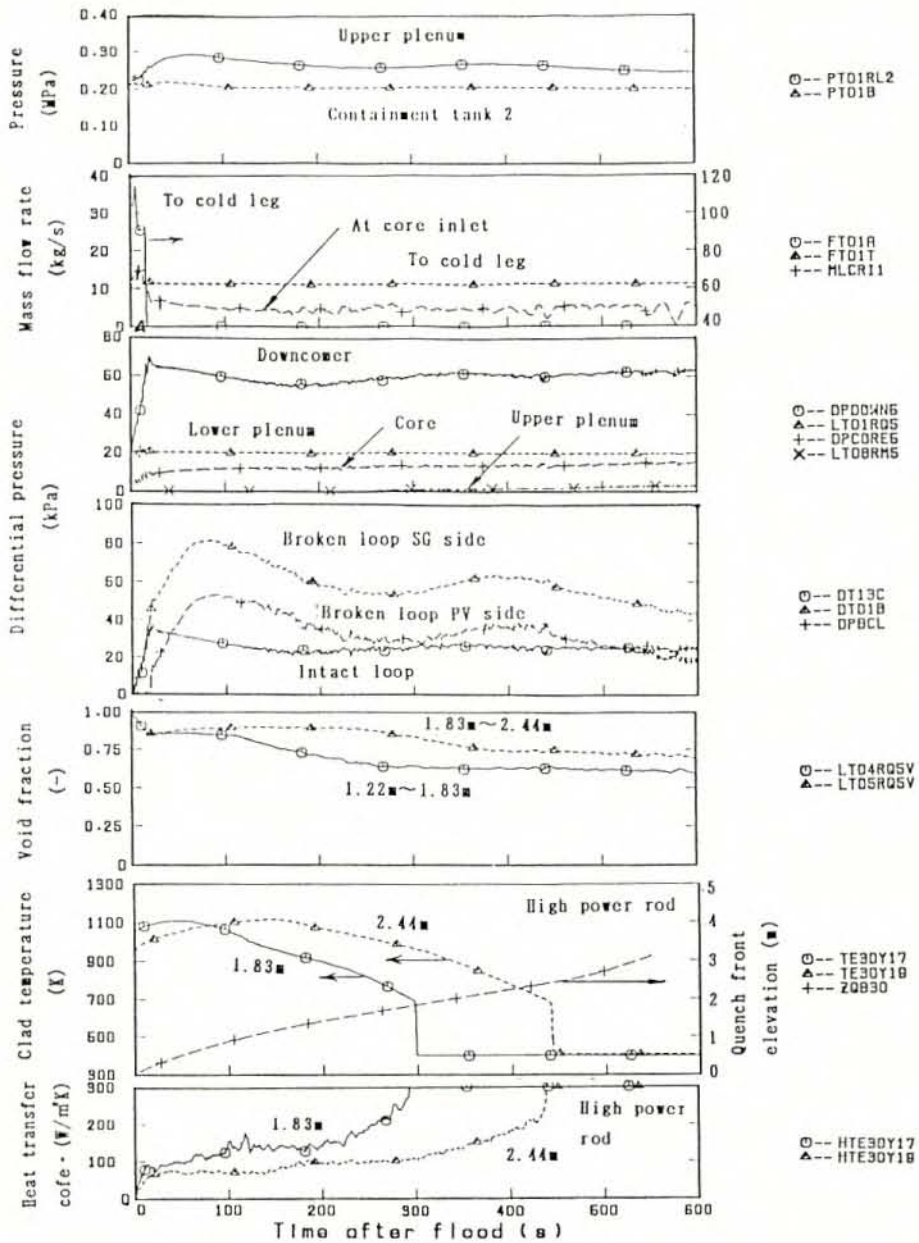
OVERALL SYSTEM RESPONSE WITH COLD LEG INJECTION
TEST C2-4
FIGURE 3.2-5
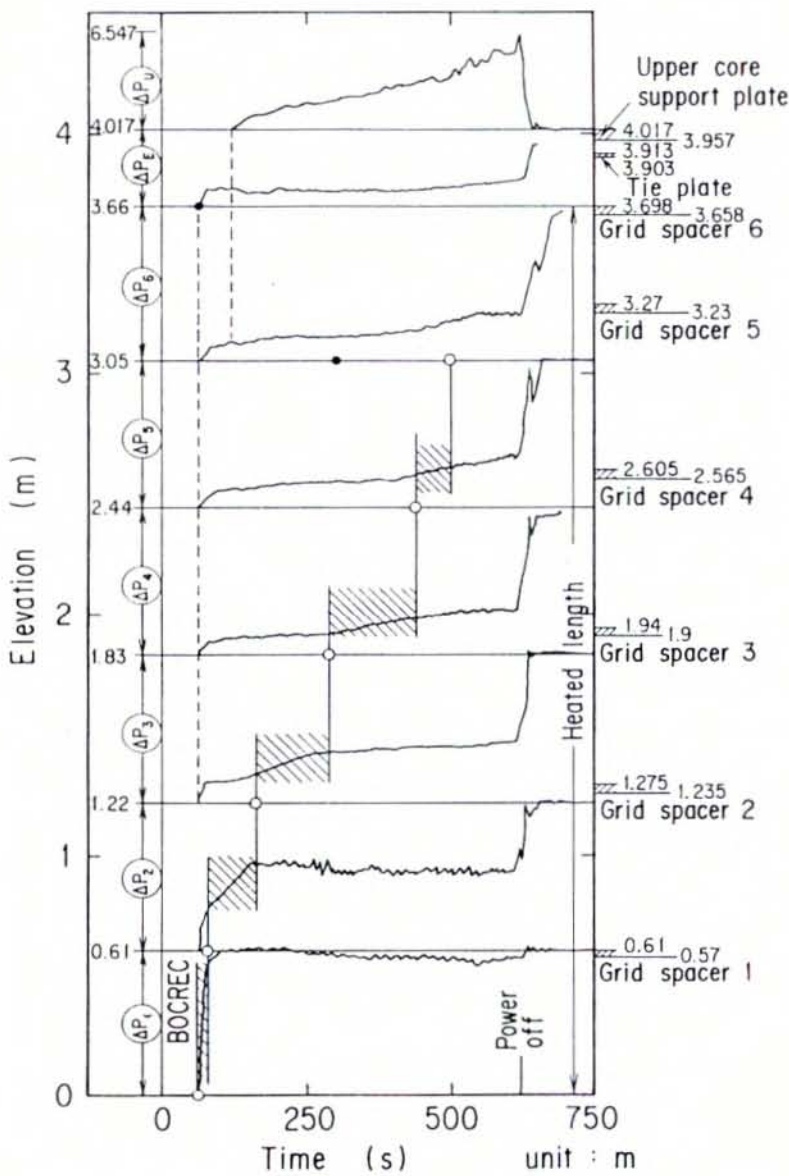
COMPARISON OF THE DIFFERENTIAL PRESSURES
AT DIFFERENT ELEVATIONS IN THE CORE AND UPPER PLENUM
FIGURE 3.2-6
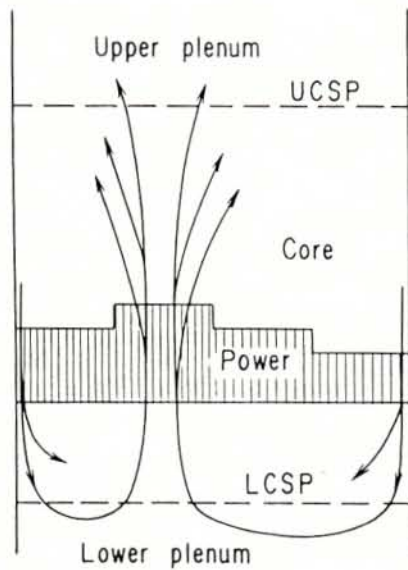
**MULTI-DIMENSIONAL BEHAVIOR IN CORE WITH A
NON-UNIFORM RADIAL POWER PROFILE**
FIGURE 3.2-7

Steep radial power test
$(F_p = 1.36)$

Experiment ———
Calculation —·—· No fluid mixing assumption
Calculation ----- Complete fluid mixing assumption

High power test
$(F_p = 1.36)$

Experiment ———
Calculation —·—· No fluid mixing assumption
Calculation ----- Complete fluid mixing assumption

Differential pressure (kPa)

Time after flood (s)
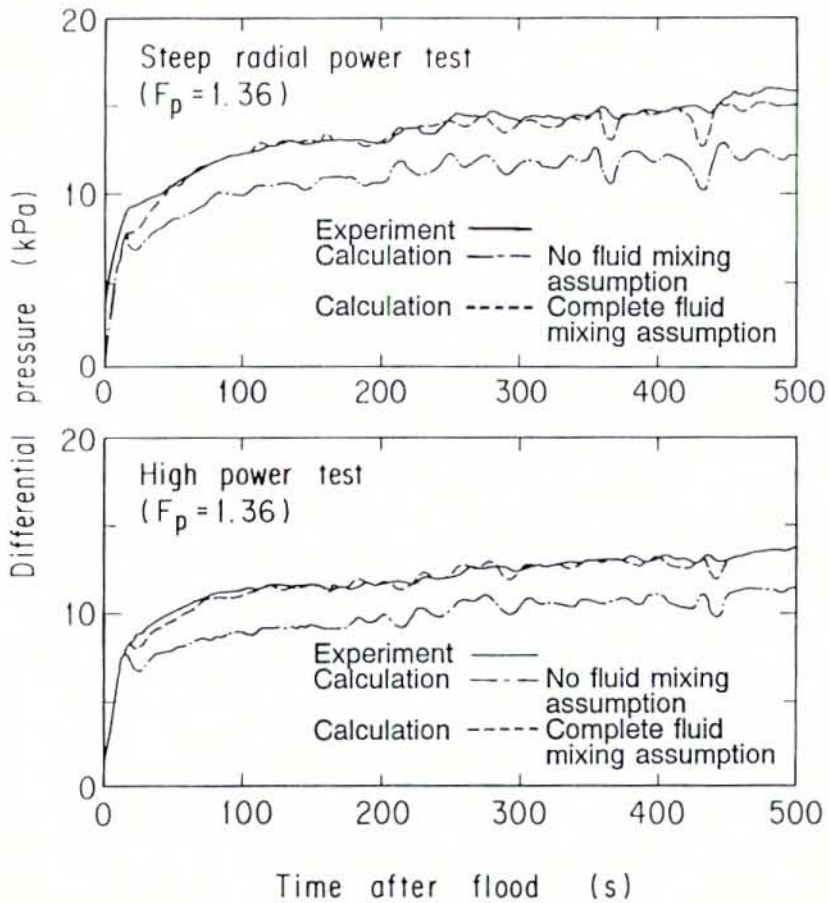
COMPARISON OF CORE DIFFERENTIAL PRESSURE
FROM A CCTF TEST WITH A REFLA CALCULATION
FIGURE 3.2-8
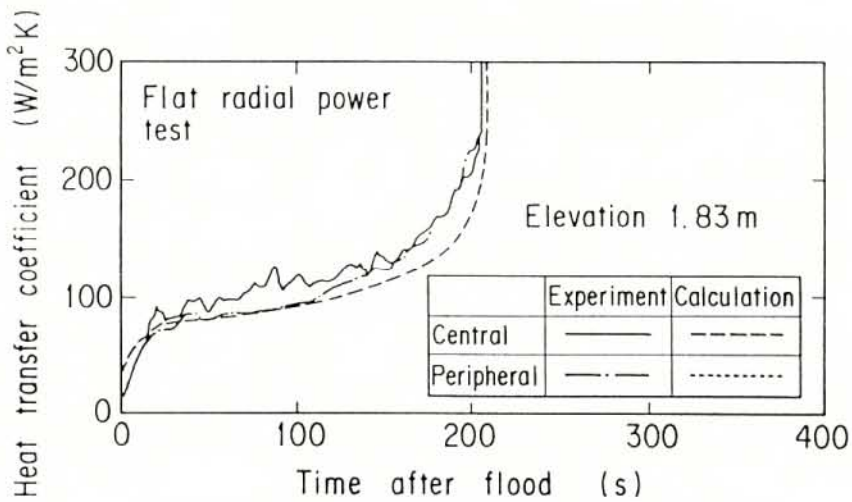
COMPARISON OF ONE-DIMENSIONAL HEAT TRANSFER
COEFFICIENT FROM A CCTF TEST WITH A REFLA CALCULATION
FIGURE 3.2-9
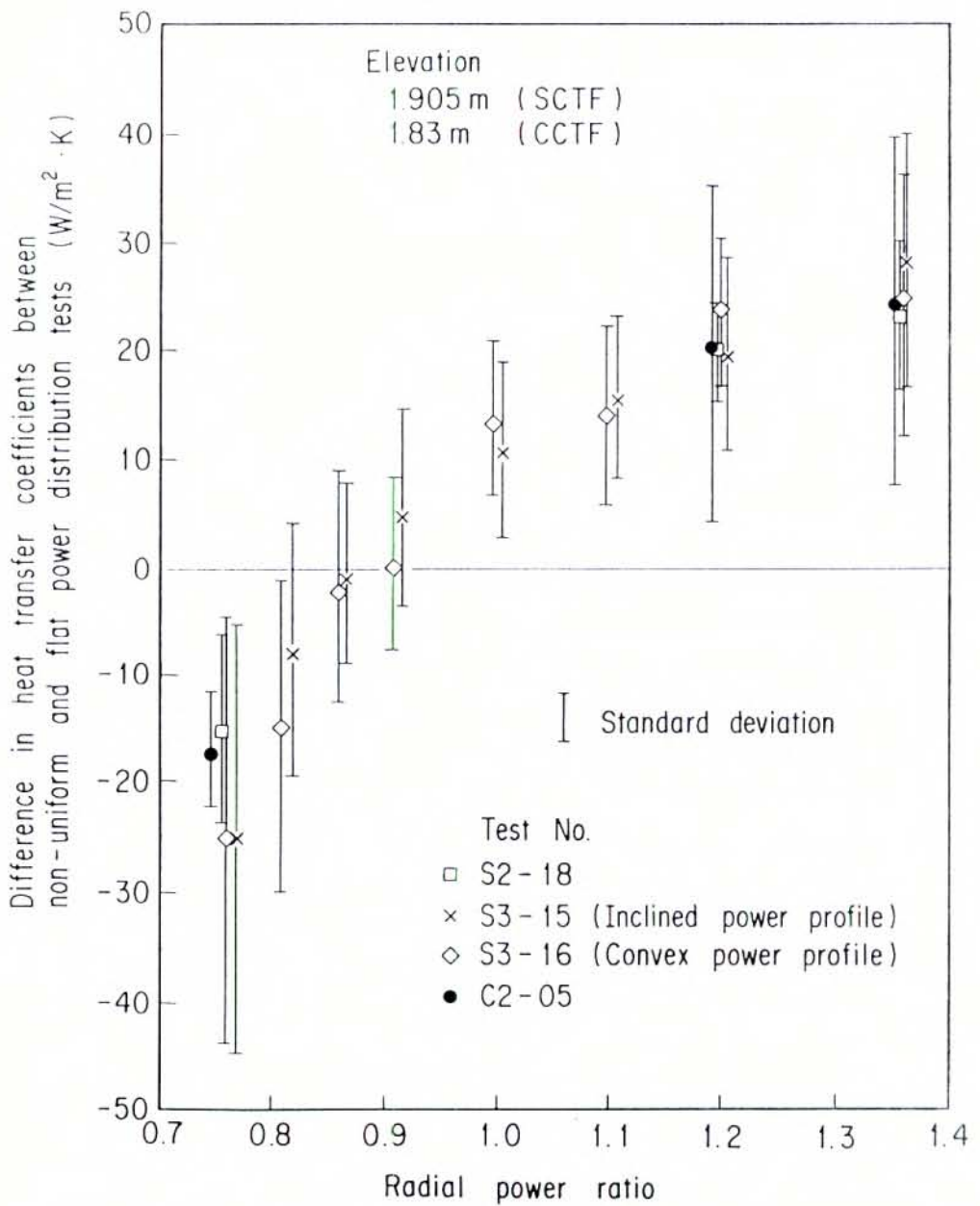
RELATIONSHIP BETWEEN HEAT TRANSFER ENHANCEMENT
AND POWER DISTRIBUTION
FIGURE 3.2-10

3.3 COMBINED INJECTION TESTS

3.3.1 Overall Transient

The overall large break LOCA (LBLOCA) transient for combined injection is described below based on the results of tests at both CCTF and SCTF. The description of the end-of-blowdown/refill portion of an LBLOCA is based on special tests which simulated the refill portion of an LBLOCA. The description of the reflood portion of an LBLOCA is based on tests carried out with EM conditions (single LPCI pump failure; decay heat 20% greater than 1971 ANS standard; high initial core temperature). Figures 3.3-1 through 3.3-3 are schematics which depict system behavior at different times in the transient. Data plots of overall system response for Tests S3-13 and C2-19 are provided in Figures 3.3-4 and 3.3-5, respectively.

End-of-Blowdown/Refill (Figures 3.3-1, 3.3-2 and 3.3-4)
After initiation of the break, pressure in the primary system decreased as fluid was discharged out the break. The fluid in the pressure vessel was vented to containment by flowing up the downcomer to the broken cold leg. This upflow in the downcomer was a two-phase mixture of steam and entrained water. When the two-phase upflow in the downcomer was high, ECC injected into the cold legs was carried out the broken cold leg. ECC injected in the hot legs entered the upper plenum and flowed downward through the tie plate and to the lower plenum. The ECC flow condensed steam in the pressure vessel which facilitated lower plenum refill. When the two-phase upflow in the downcomer was low enough, ECC injected in the cold legs flowed down the downcomer and contributed to refilling the lower plenum. Core reflood was initiated shortly after the end of depressurization when the water level reached the bottom of the core.

In SCTF tests, downflow of hot side ECC injection through the core occurred over local regions of the core. The water downflow initiated core cooling within the downflow region. The remainder of the core, however, heated up essentially adiabatically. In CCTF tests, clear separation between these two regions was not observed.

Reflood (Figures 3.3-3, 3.3-4 and 3.3-5)
Almost all ECC injected into the hot legs entered the upper plenum where the water either accumulated or penetrated through the tie plate to the core. Like refill, this downflow occurred over a localized region of the core. Hot leg ECC injection delivered to the lower plenum via the core either flowed up the downcomer to the break or back into the core from the bottom. This upflow occurred across the core exclusive of the water downflow region and resulted in bottom flooding behavior like that observed with cold leg ECC injection (see Section 3.2.3). Outside the water downflow region, steam generation initiated at the bottom of the core as water entered the core from the lower plenum. Water entrained by the boiling process was carried

to the upper regions of the core, initiating steam generation and therefore core cooling throughout the core.

Most of the steam generated in the core was condensed in the core, upper plenum and hot legs. Consequently, the steam flow through the loops was minimal, and steam binding was not important with this type of ECCS. The steam which did flow through the intact loops was condensed in the cold legs; hence, there was essentially no steam flow out the broken cold leg. Based on CCTF results, steam condensation in the hot legs created water plugs during the early reflood phase (high steam flow). Later in reflood when the steam flow was low, water overflow from the upper plenum filled the hot legs but did not reach the steam generator U-tubes. However, in the broken loop hot leg the water plugs oscillated between the upper plenum and steam generator U-tubes resulting in intermittent delivery of ECC to the upper plenum.

Stored energy and decay heat in the core were carried out of the pressure vessel by the steam flow through the loops and the water flow from the core to the break via the downcomer. Since the loop steam flows were very small, most of the energy was removed by the water flow up the downcomer. Hence, the contribution of ECC injected in the cold legs on core cooling was minimal.

3.3.2 System Behavior

The major observations from the CCTF and SCTF tests regarding system behavior with combined injection are summarized below. The discussion is organized by region. Behavior in the core is discussed in Section 3.3.3.

Downcomer

- During the initial portion of reflood the downcomer water level increased rapidly from both cold leg ECC injection and downflow of hot leg ECC injection through the core.

- In general, water flowed up the downcomer from the lower plenum to the cold leg because downflow of hot leg ECC injection exceeded the core flooding rate. Consequently, cold leg ECC injection flowed out the break.

- Typically the downcomer was filled to the cold leg elevation with subcooled water.

Lower Plenum

During reflood, the lower plenum was filled with subcooled water and the flow direction was generally from the core to the downcomer.

<u>Upper Plenum</u>

- As shown in Figure 3.3-6, the water accumulation in the upper plenum was divided into separate regions by fluid temperature. Specifically, the water was subcooled over a localized region and saturated over the remainder of the upper plenum. Water downflow to the core occurred predominantly beneath the subcooled region.

- Water downflow occurred where the fluid temperature above the tie plate was subcooled.

- Condensation efficiency in the upper plenum was governed by mixing behavior rather than by the condensation capacity of water.

<u>Intact Loops</u>

- Steam flow through the intact loops was small because most of the steam generated in the core was condensed in the upper plenum and the hot legs.

- The formation and behavior of water plugs in the hot legs was previously described in Section 3.3.1.

3.3.3 Core Behavior

The major observations regarding thermal-hydraulic behavior in the core are summarized below based on the results of SCTF tests.

A circulation flow path between the core and upper plenum was established during reflood. Specifically, the two-phase upflow (i.e., steam with entrained water) from the core to the upper plenum was returned to the core in the water downflow region. In the upper plenum, the condensation of the steam and de-entrainment of the water added to the inventory above the core. However, since the flow through the loops was minimal, the condensed steam and de-entrained water were returned to the lower plenum with the ECC downflow. Water delivered to the lower plenum flowed up the downcomer to the break or into the core.

In the core, separate regions for water downflow and two-phase upflow resulted in non-uniform thermal-hydraulic behavior in the horizontal direction. Figure 3.3-7 shows the fluid temperature profile across the core for several elevations at different times in an SCTF combined injection test. For the upper regions of the core (top two graphs), the temperature in the water downflow region (Bundles 7 and 8) was subcooled while that in the two-phase upflow region (Bundles 1-6) was saturated. This discontinuity indicates that mixing between the two regions was minimal.

Other findings from the SCTF tests regarding thermal-hydraulic behavior in the core with combined injection are summarized below.

Two-phase Upflow Region

- Shortly after initiation of reflood, water entrained by the boiling process was present axially throughout the core. Water entrainment initiated steam generation (and therefore core cooling) in the upper regions of the core.

- Quench propagation was mainly from the bottom up and not from the top down.

- Due to the flow circulation established in the reactor vessel, the core flooding rate and core inlet subcooling were higher than for cold leg injection.

- When water downflow was continuous, core cooling in the two-phase upflow region was uniform and essentially independent of the location of the downflow region and its movement. Core cooling was enhanced in the bundle directly adjacent to the downflow region.

- Void fraction and heat transfer coefficient were well predicted by the REFLA model (References J-970 and J-972).

Water Downflow Region

- The downflow region was filled with a two-phase mixture of steam and water early in reflood and single-phase, subcooled water for the remainder of reflood.

- In the early portion of reflood, before the downflow region was filled with subcooled water, downflow to the core was governed by countercurrent flow phenomena at the tie plate. This period ended with massive breakthrough at the tie plate which quenched the heated rods in the downflow regions, and filled the downflow region with subcooled water.

- During the middle and later portions of reflood, after the downflow region was filled with subcooled water, downflow was governed by the density difference between the water downflow and two-phase upflow regions.

3.3.4 Parameter Effects

The initial and boundary conditions were varied parametrically in order to determine the effect of different parameters on the transient. The major results of these tests are summarized below.

ECC Configuration

Intermittent and alternating water injection (or delivery to the upper plenum from the hot legs) did not affect core cooling relative to continuous delivery. When water delivery was intermittent, the condensation rate in the upper plenum and the differential pressure across the intact loops oscillated in phase with the water delivery. The core differential pressure also oscillated. These core differential pressure oscillations resulted in temporary increases and decreases in core cooling. However, the increases in core cooling offset the decreases.

Power Distribution

- Overall system performance was independent of the radial power profile. Specifically, two-region cooling and flow circulation in the pressure vessel were observed in tests with uniform and nonuniform radial core power profiles.

- A nonuniform radial power profile resulted in enhanced heat transfer in the high power region and degraded heat transfer in the low power region; a similar multidimensional effect was observed in cold leg injection tests (see Section 3.2.3). The magnitude of this effect on overall heat transfer was smaller in the case of combined injection.

ECC Downflow Area

- Distributing the ECC over a larger area of the core increased the water downflow region and hence the area of the core which experienced early quenching.

- However, distributing ECC over a wider region of the upper plenum, increased condensation in the upper plenum thereby increasing the temperature of the water downflow. As discussed below, increasing the temperature of the water downflow decreased core cooling.

BE vs. EM

- Overall system behavior was qualitatively the same under both EM conditions (single LPCI pump failure; decay heat 20% higher than 1971 ANS standard; high initial core temperature) and BE conditions (no LPCI pump failure; lower decay heat and initial core temperature).

- Core cooling was better under BE conditions than EM conditions, due to the higher ECC flow delivered to the core, higher circulation flow, lower core power and other factors.

ECC Temperature

- An increase in ECC temperature decreased core cooling in the two-phase upflow region because the energy removal capacity of the water downflow was lower. Also, increasing the temperature of the water downflow reduced the circulation between the upper plenum and core because the density difference between the two-phase upflow and the water downflow was less.

- In SCTF the core was adequately cooled under a wide range of ECC temperature which bounds expected PWR conditions.
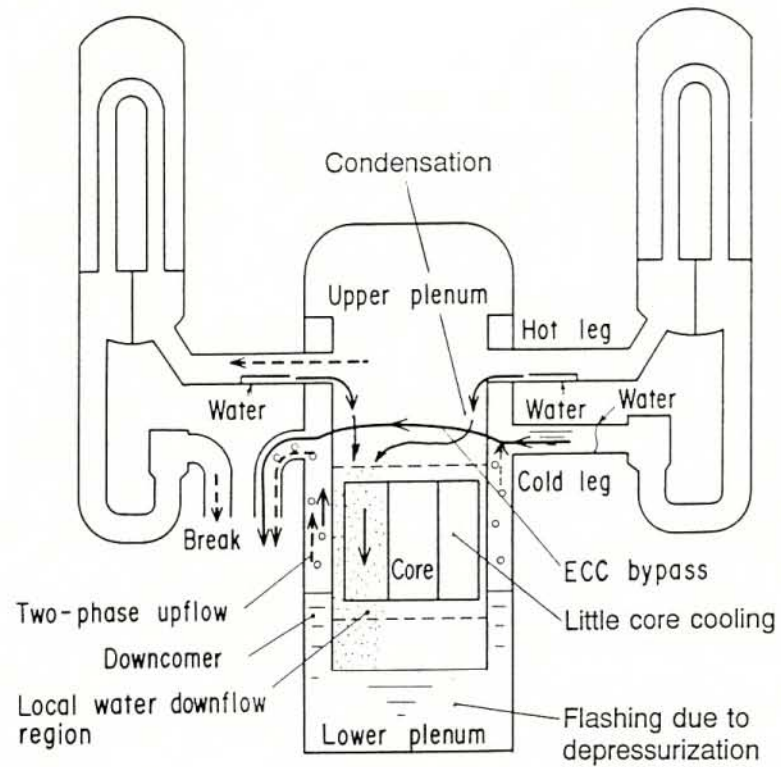
OVERALL TRANSIENT FOR COMBINED INJECTION TESTS:
END-OF-BLOWDOWN TO LOWER PLENUM REFILL

FIGURE 3.3-1
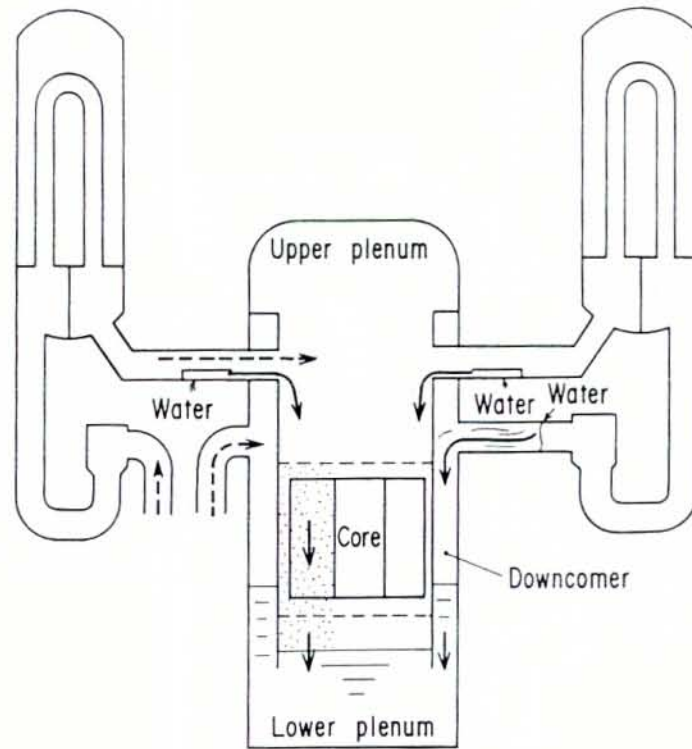
OVERALL TRANSIENT FOR COMBINED INJECTION TESTS:
LOWER PLENUM REFILL TO REFLOOD INITIATION
FIGURE 3.3-2

Weak steam binding effect
Condensation
Upper plenum
Hot leg
Water
Water   Water
Break
Water downflow region
Water upflow
Two-phase upflow region
Downcomer
Core
Flow circulation
Net negative flow
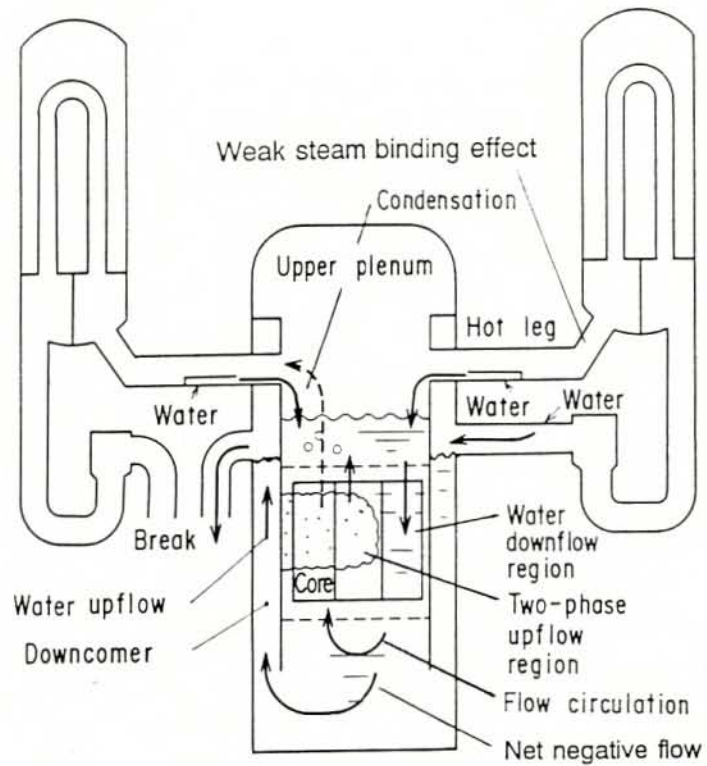
**OVERALL TRANSIENT FOR COMBINED INJECTION TESTS:
REFLOOD INITIATION TO WHOLE CORE QUENCH
FIGURE 3.3-3**

Break valves open

Pressure (MPa)

0.60
0.60
0.40
0.30
0.20

Upper plenum

Containment tank 2

○-- PT01J11
▲-- PT01B

70
60
50
40
30
20
10
0

Mass flow rate (kg/s)

To cold leg

To upper plenum

○-- FT02R5
▲-- FTUPPERPLENUM

80
60
40
20
0

Differential pressure (kPa)

Downcomer
Lower plenum
Upper plenum

Core

○-- DPDOWNCOMER
▲-- LT01R11
+-- DT03041
X-- LT01J41

80
50
40
20
0

Broken loop SG side
Intact loop
Broken loop PV side

○-- DT02H5
▲-- DT01B3
+-- DT01FS

1.00
0.75
0.50
0.25
0

Void fraction (-)

2.03m~2.57m

1.37m~1.91m

○-- VF03541
▲-- VF04541

1100
900
700
600
300

Clad temperature (K)

1.905m

2.33m

4
3
2
1
0

Quench front elevation (m)

○-- TE0641C
▲-- TE0741C
+-- QHL41C

400
300
200
100
0
-60

Heat transfer cofc · (W/m²K)

1.905m

2.33m

0   60   100   150   200

Time after flood (s)

○-- HTC-TE0641C
▲-- HTC-TE0741C

OVERALL SYSTEM RESPONSE WITH COMBINED INJECTION
TEST S3-13
FIGURE 3.3-4
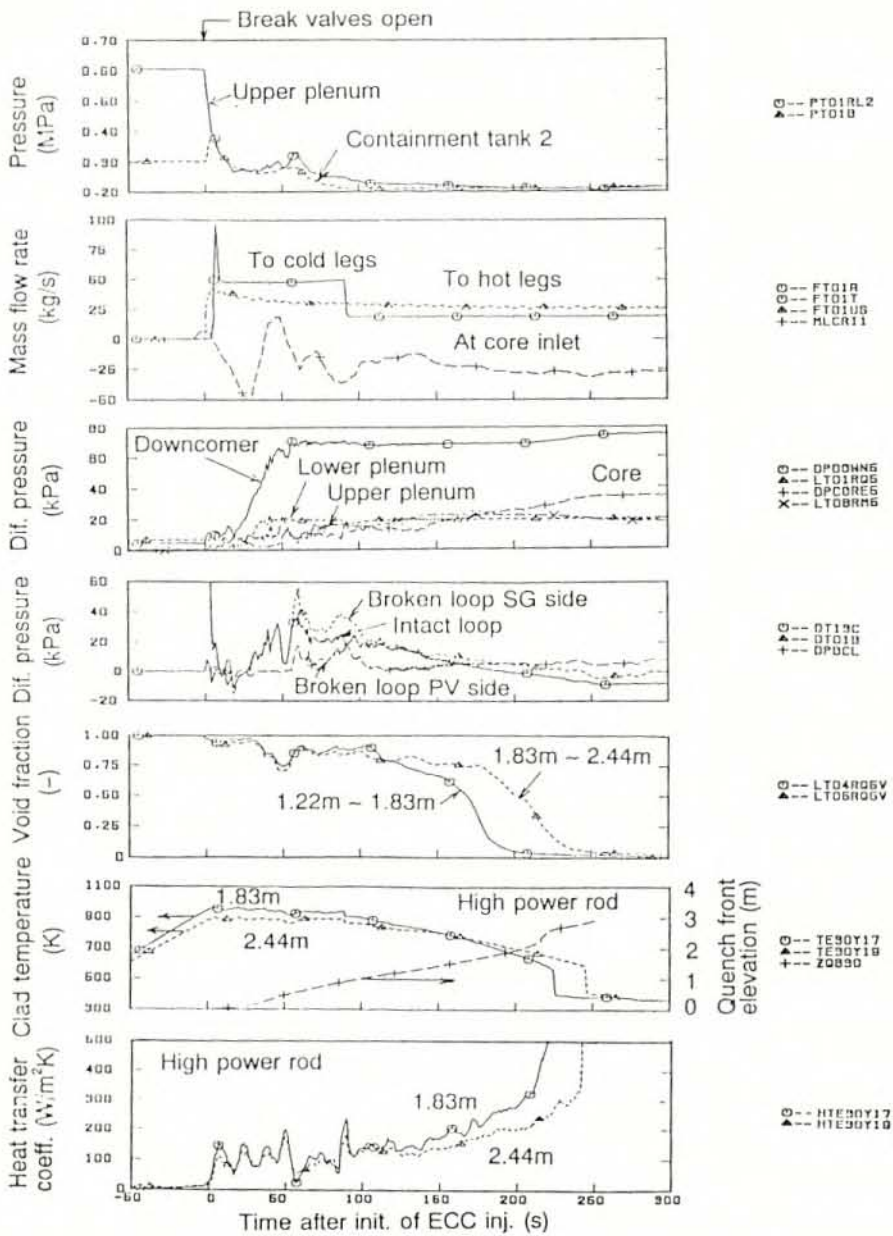
OVERALL SYSTEM RESPONSE WITH COMBINED INJECTION
TEST C2-19
FIGURE 3.3-5
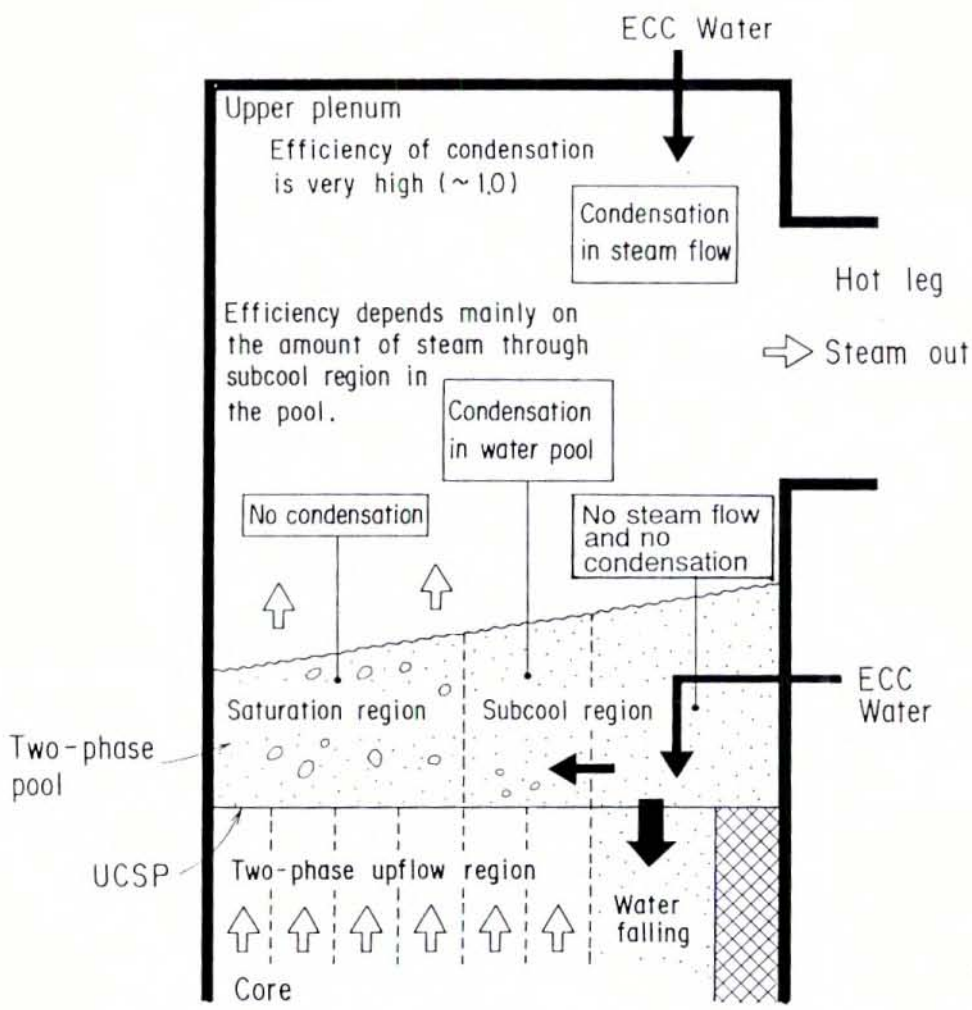
UPPER PLENUM THERMAL-HYDRAULIC BEHAVIOR
OBSERVED IN SCTF AND CCTF TESTS
FIGURE 3.3-6
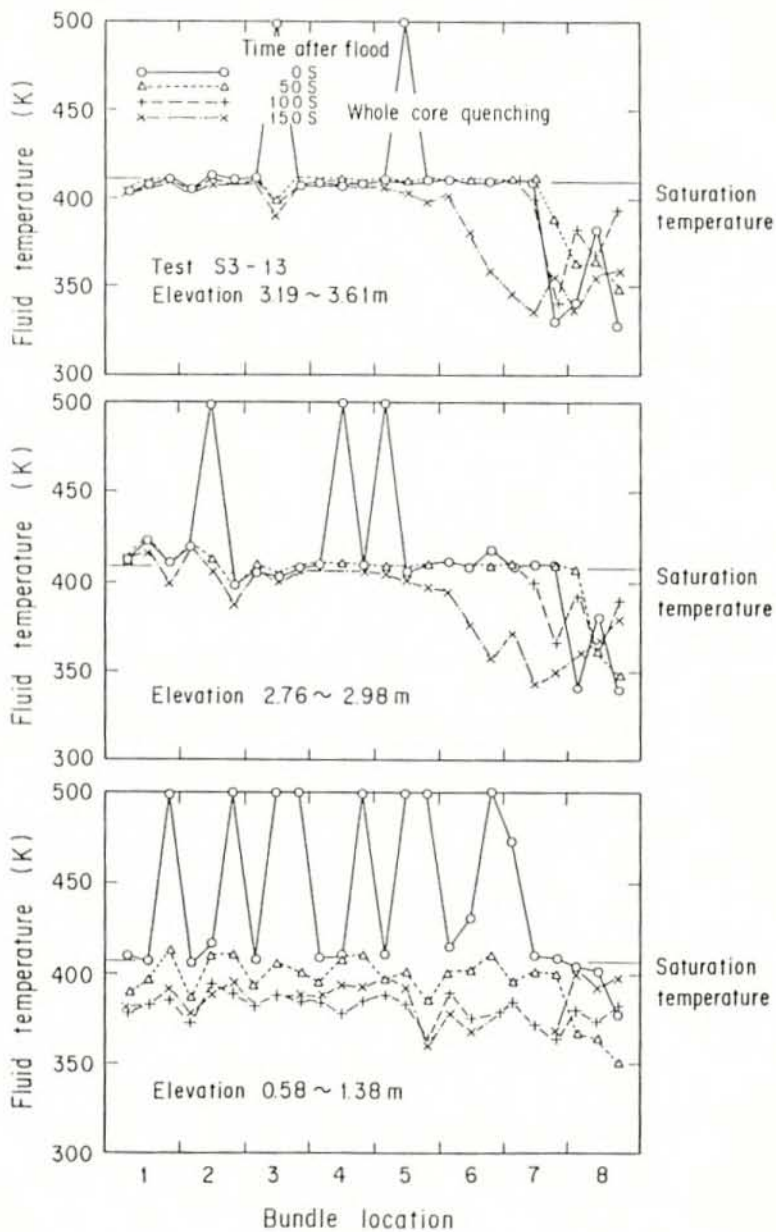
FLUID TEMPERATURE DISTRIBUTION
EFFECT OF ECC INJECTION CONFIGURATION
TEST S3-13
FIGURE 3.3-7

3.4 UPPER PLENUM INJECTION TESTS

The reflood portion of the large break LOCA (LBLOCA) transient for upper plenum injection (UPI) is described below based on the results at CCTF. Figures 3.4-1 and 3.4-2 are schematics which depict the system behavior at different times in the transient. Data plots of overall system response for Test C2-16, the UPI base case test, are provided in Figure 3.4-3.

3.4.1 Overall Transient (Figures 3.4-1, 3.4-2 and 3.4-3)

Upper plenum behavior during reflood for UPI was qualitatively similar to that for combined injection (see Section 3.3.1). Specifically, water injected in the upper plenum either accumulated in the upper plenum or penetrated through the tie plate to the core. The water delivered to the lower plenum either flowed up the downcomer to the break or back up into the core. Like combined injection, this water upflow into the core resulted in bottom flooding behavior in the core.

Steam upflow from the core entered the upper plenum where it was condensed by the ECC injection. For the base case test (i.e., single LPCI failure), only about half of the core steam generation was condensed in the upper plenum. The remainder was vented to containment via the reactor coolant loops.

Water carried over to the loops by the steam flow either accumulated in the hot legs and SG inlet plena or was entrained to the SG U-tubes. Heat transfer from the secondary side vaporized the entrained water increasing the volumetric flow, and therefore pressure drop, in the reactor coolant loops. However, because most of the steam was condensed in the upper plenum, the loop flow and pressure drop was less for UPI than for cold leg injection.

3.4.2 System Behavior

The major findings from the CCTF tests regarding system behavior with UPI are summarized below; behavior in the core is discussed in Section 3.4.3. As previously indicated, upper plenum behavior with UPI was qualitatively similar to that for combined injection.

Downcomer

- Water flow in the downcomer during reflood was upward from the lower plenum to the broken cold leg. The magnitude of the flow was determined by the difference between water downflow from the upper plenum and the core flooding rate.

- The downcomer was filled with water up to the cold leg nozzles.

Upper Plenum

- Water accumulated in the upper plenum as a two-phase mixture. The collapsed water level of this mixture was uniform across the upper plenum. For both single failure and no failure cases, the collapsed liquid level quickly increased to above the hot leg elevation.

- For the single failure case, only half the steam generated in the core was condensed in the upper plenum. The remainder was vented to containment via the reactor coolant loops.

- For the no failure case, essentially all the steam upflow from the core was condensed in the upper plenum. Hence, the steam flow in the loops was minimal.

Reactor Coolant Loops

- As indicated above, steam flow in the reactor coolant loops was minimal for the no failure case and present at a reduced rate (about half the core steam generation) for the single failure case.

- For the single failure case, water was carried over to the hot legs and steam generators by the steam flow exiting the upper plenum. Vaporization of entrained water in the steam generator U-tubes increased the volumetric flow rate, and therefore flow pressure drop, in the loops. Compared to cold leg injection, the increase in flow pressure drop was small. For the no failure case, water which spilled over into the loops accumulated in the hot legs and SG inlet plena.

3.4.3 Core Behavior

Core behavior with UPI was similar to combined injection (see Section 3.3.3). Specifically, a circulation flow path between the core and upper plenum was established. The two-phase upflow from the core to the upper plenum was returned to the core by water downflow through the tie plate. Water downflow in the core occurred over a localized region of the core.

Differences in core behavior between UPI and combined injection reflected differences in ECC injection; specifically, UPI flow was substantially less than hot leg ECC injection. The increase in water temperature in the upper plenum due to steam condensation was larger in the UPI tests because of the lower ECC flow. Consequently, the temperature of the water downflow was higher (i.e., lower subcooling). Since the circulation flow between the core and upper plenum during the middle and later stages of reflood is controlled by the density difference between the two-phase up flow and the water downflow (see Section 3.3.3), the flow circulation was not as strong for the UPI tests.

A second effect of the increased temperature of the water downflow for UPI was that thermal-hydraulic behavior was relatively uniform across the core. As discussed in Section 3.3.3 for combined injection, thermal-hydraulic behavior in the core was divided into separate regions of subcooled water downflow and saturated two-phase upflow. However, for UPI the separate regions were noted only at the top of the core; thermal-hydraulic behavior was uniform over the remainder of the core.

Thermal-hydraulic behavior in the two-phase upflow region was similar to that observed with cold leg injection (see Section 3.2.3). Other findings from the CCTF tests regarding thermal-hydraulic behavior in the core with UPI are summarized below.

Water Downflow Region

- Water downflow occurred preferentially on one side of the core for both symmetric injection and asymmetric injection.

- The enhancement of core cooling due to water downflow from the upper plenum was limited to the upper elevations of the core in the water downflow region.

Two-Phase Upflow Region

- Within a couple of seconds of reflood initiation, water entrained by the boiling process was present throughout the core. Entrained water initiated core cooling in the upper regions of the core.

- The distribution of entrained water was uniform across the core.

- Quench propagation was mainly from the bottom up and not from the top down.

3.4.4 Parameter Effects

The initial and boundary conditions were varied parametrically to determine the effect of different parameters on the transient. The major results of these tests are summarized below.

UPI Distribution

- Overall thermal-hydraulic behavior was generally the same for comparable UPI flows but different injection distributions (i.e., injection through two nozzles versus one nozzle).

- Injection through one nozzle (asymmetric UPI) enhanced core cooling in the upper part of the core compared to injection through two nozzles (symmetric UPI), due to two-dimensional thermal hydraulics.

<u>UPI Flow</u>

- Increasing the UPI flow (no failure rather than single failure) increased condensation in the upper plenum such that essentially all the steam generated in core was condensed. Hence, the steam flow, and therefore water entrainment, in the reactor coolant loops was minimal.

- Increasing the UPI flow significantly reduced cladding temperatures and quench times throughout the core. The effect was more pronounced in the water downflow region.

LEGEND

▦	Water
▨	Frothy Mixture
▨	High Quality Mixture
▦	Steam

Broken Loop

Intact Loop
(1 of 3 Shown)

LPCI

No Flow in
Broken Cold Leg

HPCI
ACC

Intact Loop Steam Flow
Completely Condensed at
ECC Port

ECC
(off)

Note: It is not clear from the
data whether UPI water
penetrated to the core during
this period. This figure shows no
penetration.
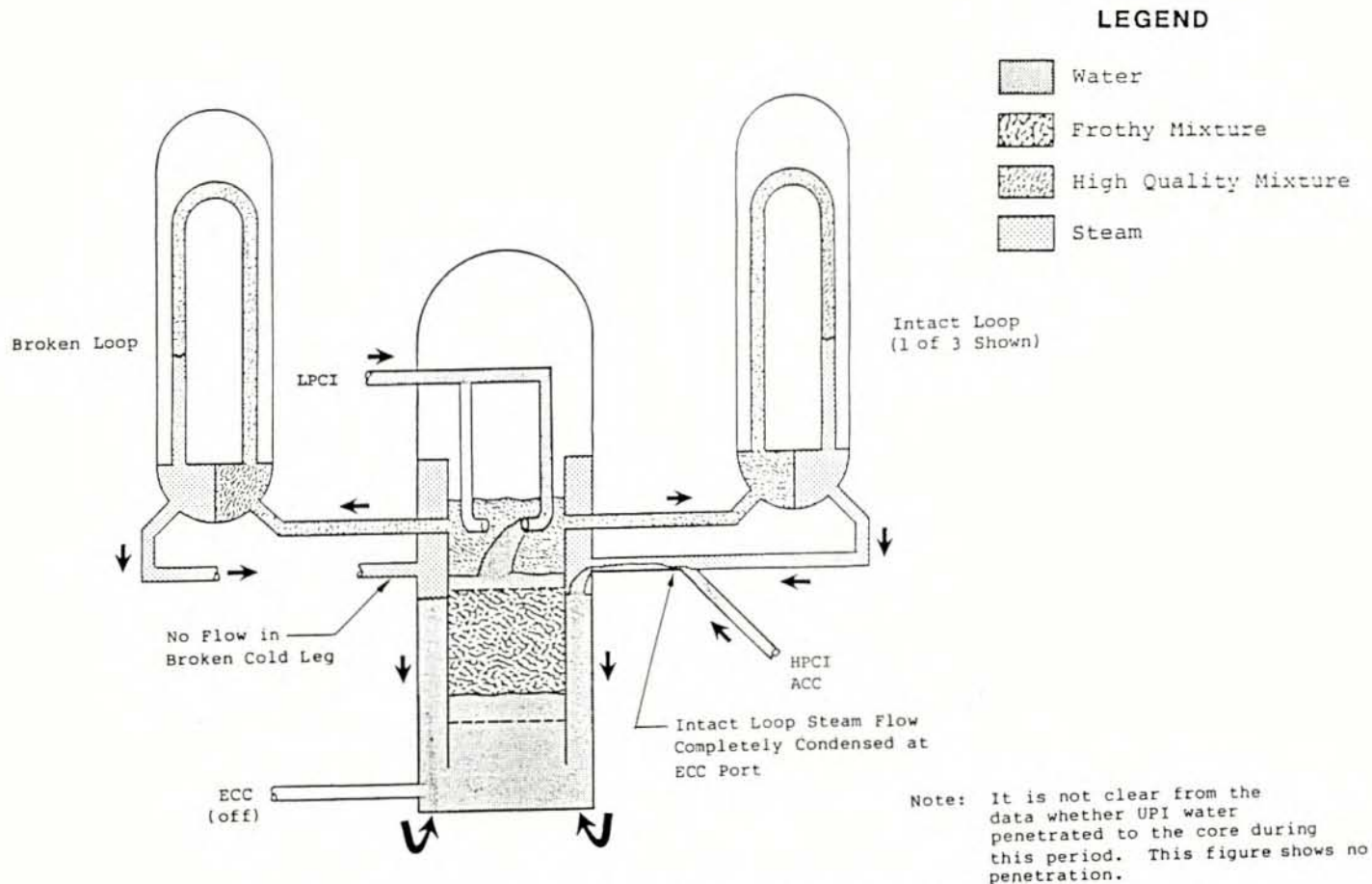
OVERALL TRANSIENT FOR UPPER PLENUM INJECTION:
REFLOOD DURING ACC INJECTION

FIGURE 3.4-1

LEGEND

Water

Frothy Mixture

High Quality Mixture

Steam

Broken Loop

Intact Loop
(1 of 3 Shown)

LPCI

HPCI

ECC
(off)
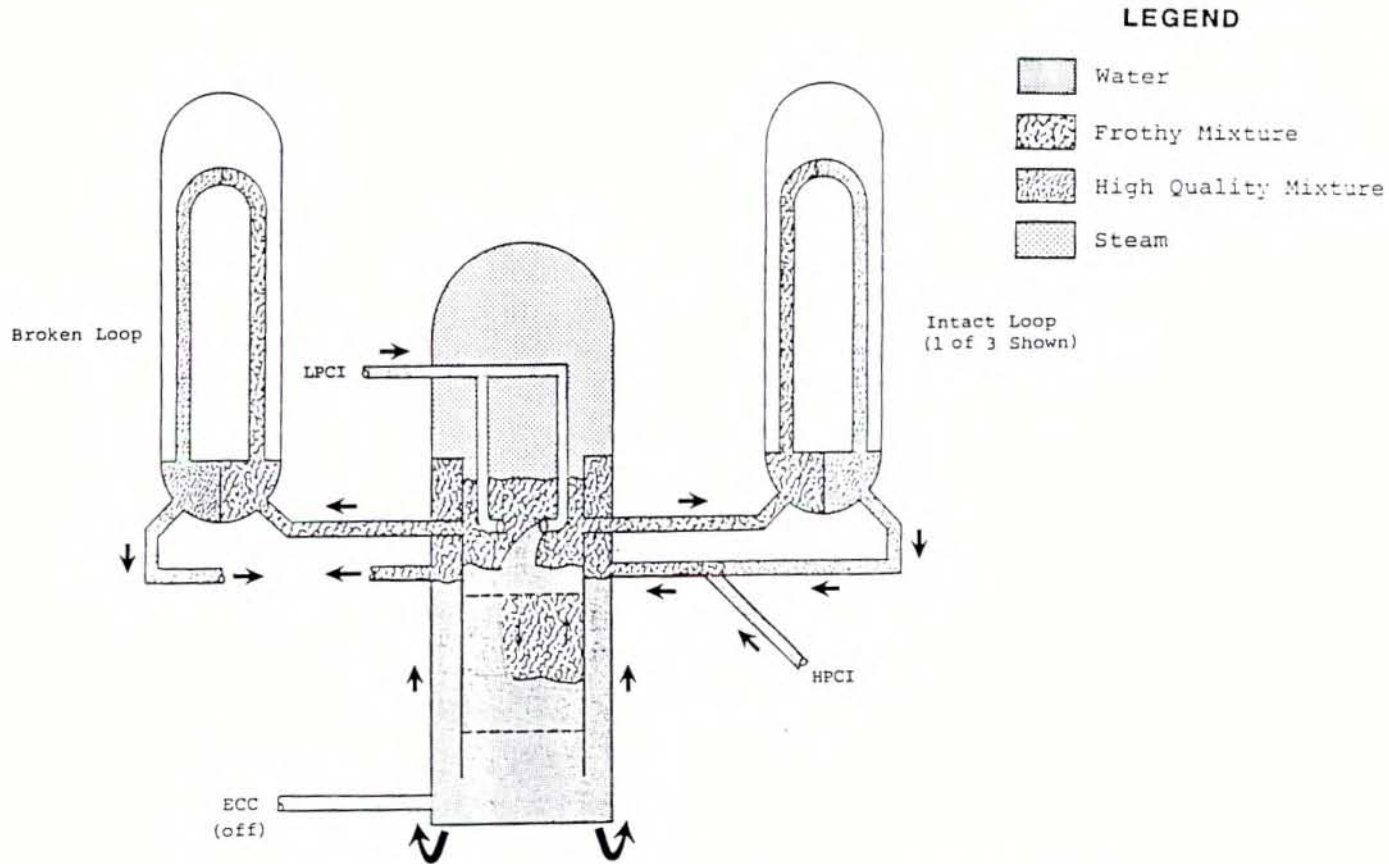
OVERALL TRANSIENT FOR UPPER PLENUM INJECTION:
REFLOOD AFTER TERMINATION OF ACC INJECTION

FIGURE 3.4-2
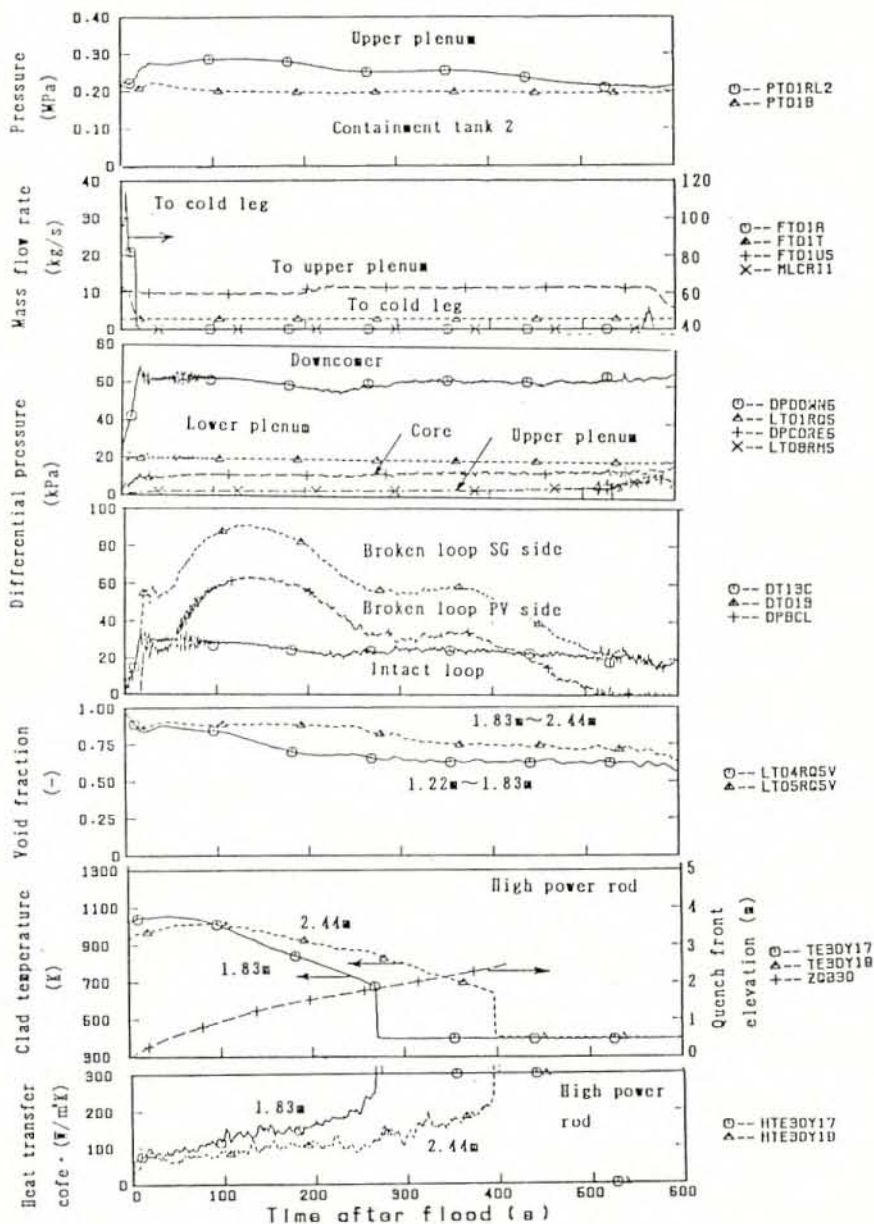
OVERALL SYSTEM RESPONSE WITH UPPER PLENUM INJECTION
TEST C2-16
FIGURE 3.4-3

3.5 DOWNCOMER INJECTION/VENT VALVE TESTS

The reflood portion of the large break LOCA (LBLOCA) transient for downcomer injection is described below based on the results of tests at CCTF. The downcomer injection tests were performed both with the vent valves locked shut (Test C2-AA2) and with the vent valves free to open (Tests C2-AS2 and C2-10); separate descriptions are provided for each type of test. Figure 3.5-1 is a schematic which depicts system behavior during reflood for downcomer injection without vent valves. Data plots of overall system response for Test C2-AA2 (vent valves closed) and Test C2-AS2 (vent valves open; loops open) are provided in Figures 3.5-2 and 3.5-3, respectively.

3.5.1 Reflood Transient for Downcomer Injection without Vent Valves
(Figure 3.5-1)

The overall thermal-hydraulic behavior during reflood for downcomer injection without vent valves was very similar to cold leg injection (see Section 3.2.1). ECC flowed down the downcomer to the lower plenum and into the core. The water upflow into the core resulted in a bottom flooding behavior in the core the same as that previously described for cold leg injection (see Section 3.2.3).

Some of the water entrained out of the core de-entrained and either fell back to the core or accumulated in the upper plenum, hot legs and steam generator inlet plena. The remainder of the water entrained out of the core was carried to the steam generator U-tubes. Heat transfer from the secondary side vaporized entrained water in the U-tubes. Hence, flow in cold legs consisted of single-phase, superheated steam.

The steam flow through the intact loops entered the downcomer where some of the steam was condensed by the ECC injection into the downcomer. However, because contact between the ECC and steam flows was limited, the condensation rate was less than for cold leg injection. Further, condensation was intermittent as U-tube oscillations of the core and downcomer water levels occurred. When the downcomer water level was below the ECC injection nozzle, steam condensation increased due to good steam access to the ECC injection stream and subcooled ECC accumulating on top of the downcomer water column. Increased condensation reduced the pressure in the downcomer relative to the core pressure which forced water out of the core and into the downcomer. The increase in steam condensation warmed the top portion of the downcomer water column to near saturation. Also, as the water level rose, steam access to the ECC injection stream was blocked by saturated water and condensation decreased. The reduction in condensation resulted in an increase of the downcomer pressure which forced water from the downcomer back into the core and started the cycle again. The oscillations followed the manometer frequency of the system (Reference J-973). The character of this oscillation in CCTF was influenced

by the vertical position of the injection nozzle slightly below the main coolant nozzles, which is typical of Japanese PWRs with downcomer injection.

Experimentally, the PCT for downcomer injection was nearly equal to that for cold leg injection, and the quench times for downcomer injection were slightly longer than for cold leg injection. This slight difference is due to the increased water temperature at the bottom of the core due to the oscillations described above.

3.5.2 Reflood Transient for Downcomer Injection with Vent Valves

For downcomer injection with vent valves, ECC flowed down the downcomer to the lower plenum and into the core. The water flow into the core resulted in steam generation in the core and two-phase upflow from the core to the upper plenum. In the upper plenum some of the water carried out of the core was de-entrained and either fell back to the core or accumulated. The remainder of the water entrained out of the core was carried by the steam flow through the vent valves to the downcomer. The loops were blocked in the test (C2-10), simulating the plant condition where loops are presumed to be blocked by plugs of water. In the unblocked loop test (C2-AS2), water plugs formed between hot legs and steam generators, and blocked steam flow through intact loops.

With the vent valves free to open, the flow exiting the upper plenum was vented to the downcomer via the vent valves rather than the reactor coolant loops. The lack of steam flow and water entrainment through the loops eliminated the increase in the core-to-downcomer differential pressure due to vaporization of entrained water in the steam generators. The core-to-downcomer differential pressures for downcomer injection with vent valves and cold leg injection without vent valves are compared in Figure 3.5-4. The differential pressures are similar for the first 15 seconds after BOCREC. However, after 15 seconds, the differential pressure for cold leg injection without vent valves was higher than that for downcomer injection with vent valves.

The low core-to-downcomer differential pressure with the vent valves free to open resulted in a higher core flooding rate than with the vent valves closed. Consequently, cladding temperatures were lower and quench times shorter.
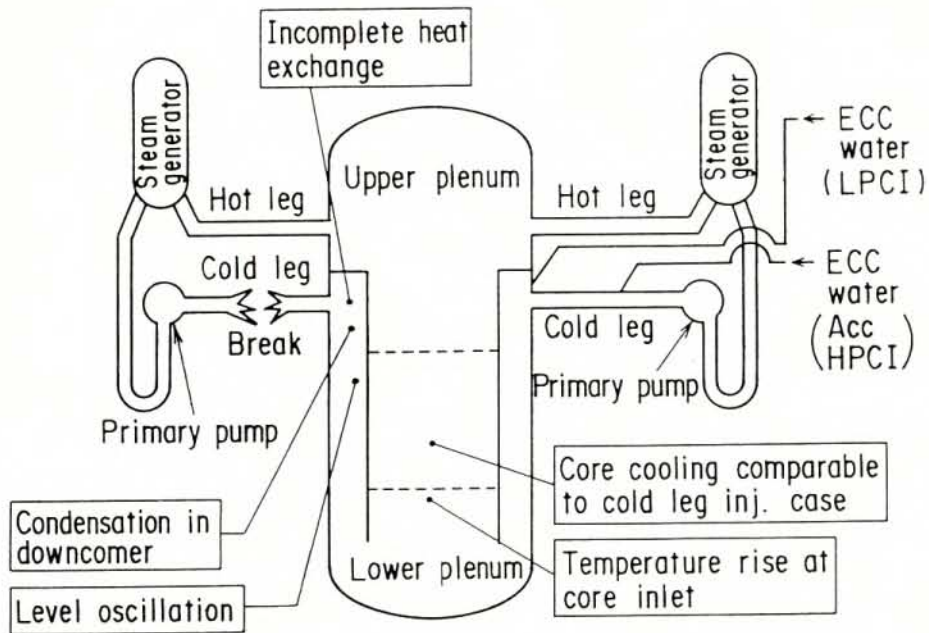
MAJOR FINDINGS ON REFLOOD BEHAVIOR
FROM CCTF TESTS WITH DOWNCOMER INJECTION
FIGURE 3.5-1
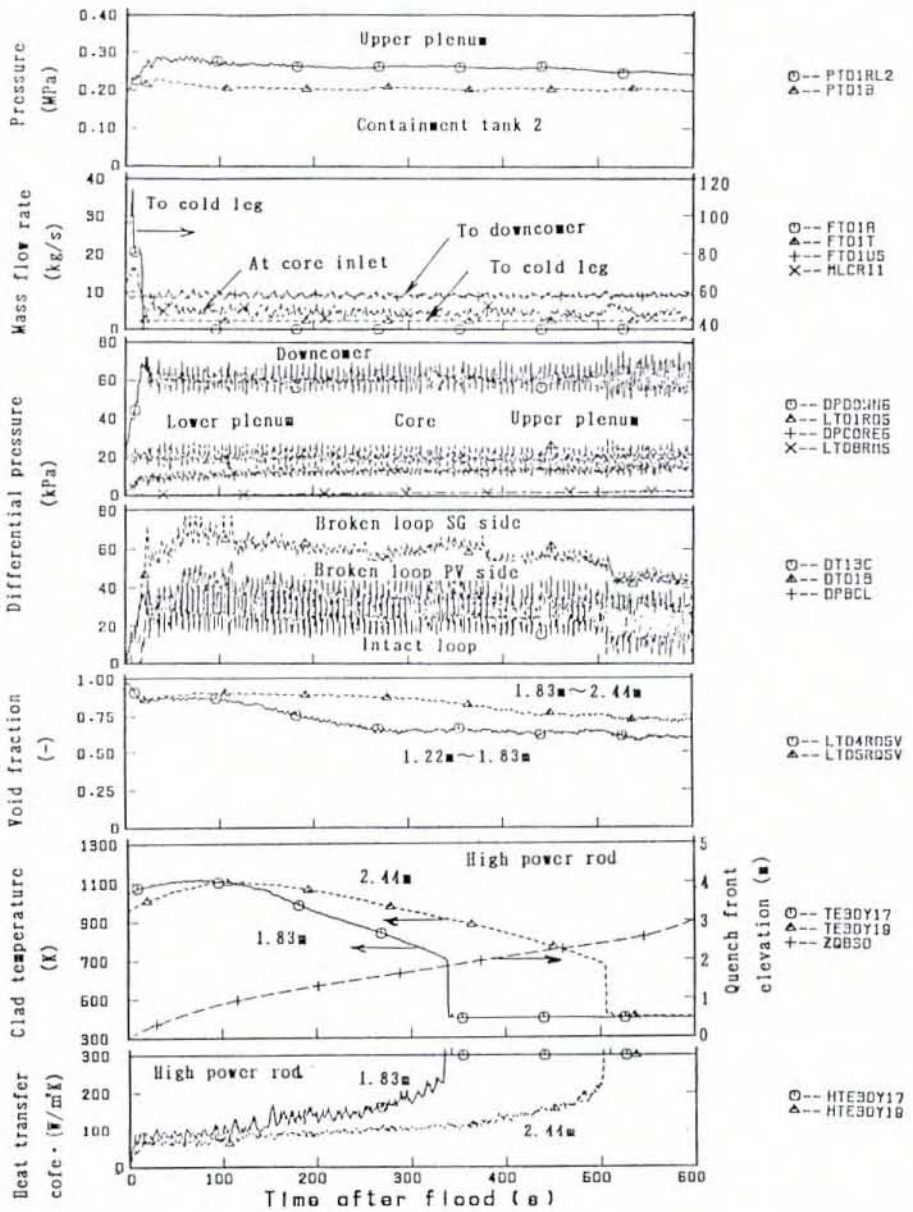
OVERALL SYSTEM RESPONSE
WITH DOWNCOMER INJECTION AND CLOSED VENT VALVES
TEST C2-AA2
FIGURE 3.5-2
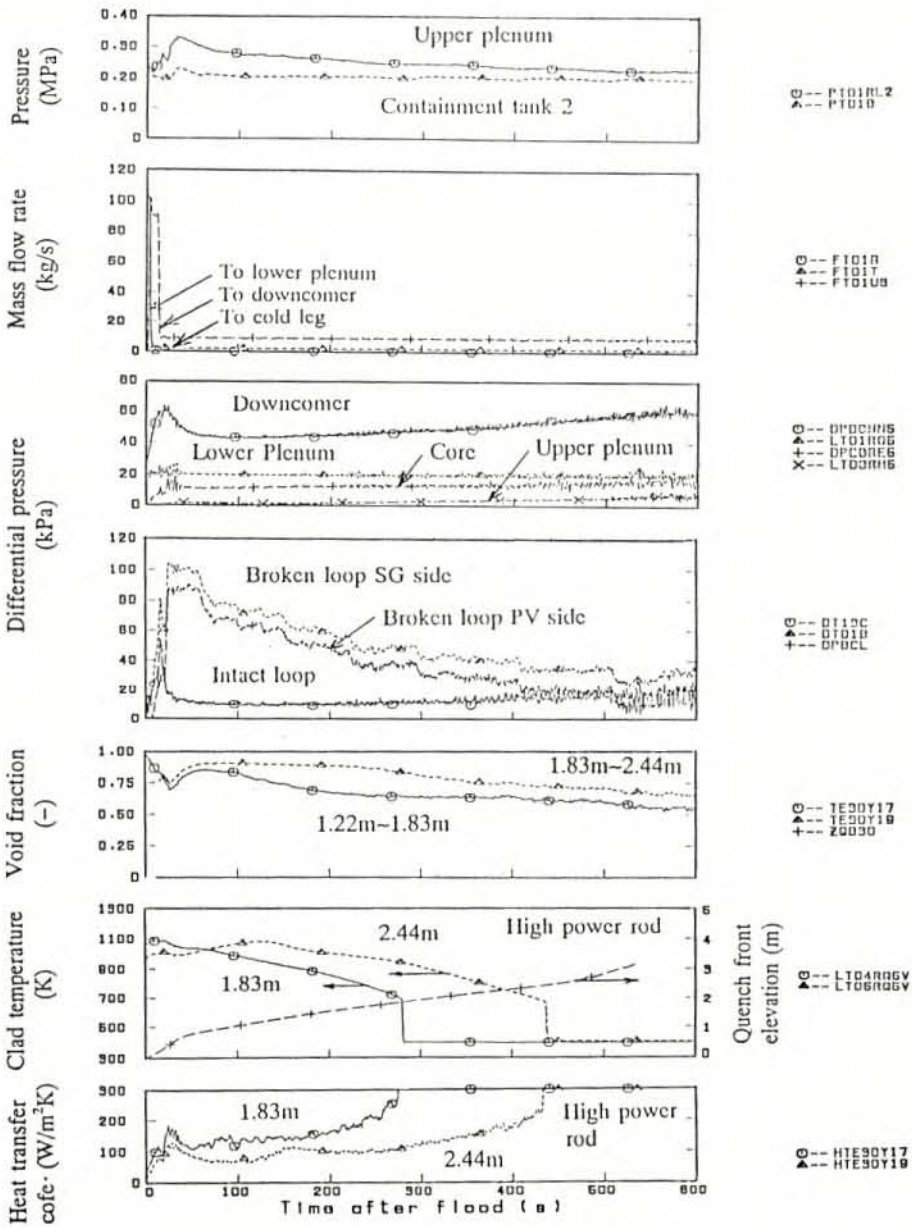
OVERALL SYSTEM RESPONSE
WITH DOWNCOMER INJECTION AND OPEN VENT VALVES
TEST C2-AS2
FIGURE 3.5-3
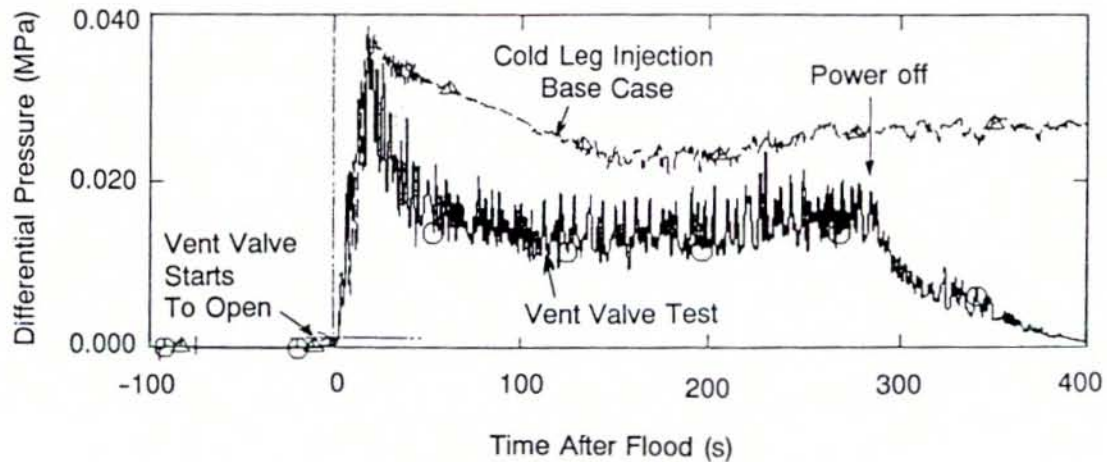
COMPARISON OF DIFFERENTIAL PRESSURES
BETWEEN UPPER PLENUM AND TOP OF DOWNCOMER
FOR COLD LEG INJECTION WITHOUT VENT VALVES
AND DOWNCOMER INJECTION WITH VENT VALVES

FIGURE 3.5-4

3.6 SUMMARY

Refill and reflood behavior with cold leg injection ECCS were tested in CCTF and SCTF across a wide range of conditions. The important findings with regard to core cooling were as follows:

- Within a few seconds of BOCREC, water entrained by the boiling process was present throughout the core and core cooling was occurring at all elevations.

- Water was distributed uniformly across the core in the horizontal direction; i.e., uniform void fraction in the lateral direction.

- Steam flow in the core was higher in the high power bundles than in the low power bundles.

These phenomena had a beneficial effect on core cooling. The CCTF and SCTF tests confirmed that the core was adequately cooled over the range of conditions investigated (including EM and BE conditions).

Refill and reflood behavior with combined injection ECCS were also investigated in CCTF and SCTF. The important findings from these tests are listed below.

- Most of the ECC injected into the hot legs entered the upper plenum and flowed down through the core.

- Two separate thermal-hydraulic regions were established in the core; i.e., water downflow region and two-phase upflow region.

- The two-phase upflow from the core to the upper plenum was returned to the core in the water downflow; i.e., a circulation flow path was established.

- Within a few seconds of BOCREC, water entrained by the boiling process was present axially throughout the two-phase upflow region of the core and core cooling was occurring at all elevations.

- Since most of the steam generated in the core was condensed by the ECC injected in the hot legs, the steam flow through the loops was minimal. Consequently, the steam binding effect was insignificant.

The tests confirmed that the core was adequately cooled over the range of conditions investigated.

The CCTF and SCTF test programs also simulated upper plenum injection and downcomer injection (both with and without vent valves) ECCS. The tests indicated that these ECC systems adequately cooled the core.

Section 4

UPTF TESTS

4.1 DESCRIPTION OF FACILITY, TEST PROGRAM, AND TEST CONDITIONS

4.1.1 Upper Plenum Test Facility (UPTF)

The UPTF was a full-scale simulation of the primary system of the four loop 1300 MWe Siemens/KWU pressurized water reactor (PWR) at Grafenrheinfeld (Figures 4.1-1 and 4.1-2). The test vessel upper plenum internals, downcomer, and primary coolant piping were replicas of the reference plant. However; important components of a PWR, such as the core, coolant pumps, steam generators, and containment were replaced by simulators which simulated the thermal-hydraulic behavior in these components during end-of-blowdown, refill, and reflood phases of a large break LOCA. UPTF simulated both hot leg and cold breaks of various sizes. The ECC injection systems at the UPTF were configured to simulate the various ECC systems of German and US/J PWRs. UPTF is described in more detail in References G-902 and G-412.

As shown in Figure 4.1.3, the UPTF primary system was divided into the investigation and simulation areas. The investigation areas, which were exact replicas of a GPWR, consisted of:

· Core/upper plenum interface, upper plenum, and hot legs (Area A on Figure 4.1-3).

· Cold legs, downcomer, lower plenum, and downcomer/lower plenum interface (Area B on Figure 4.1-3).

Knowledge of the physical phenomena occurring in these two areas during a LOCA is important for reactor safety analysis.

Realistic thermal-hydraulic behavior in the investigation areas was assured by establishing appropriate initial and boundary conditions. The boundary conditions were established using simulators. Setup and operation of the simulators were based on small-scale data and mathematical modeling.

The simulation areas included the following:

- core simulator
- steam generator simulators
- pump simulators
- containment simulator

The main components of the UPTF are described below.

Test Vessel and Internals
The dimensions of the UPTF test vessel (Figure 4.1-2) were identical to the reactor vessel of the reference PWR except for wall thickness. The entire inner surface was clad with stainless steel. Penetrations were provided for instrumentation. The vessel internals (Figure 4.1-2) consisted of lower plenum internals, core simulator, dummy fuel assemblies, and upper plenum internals. The lower plenum had the same dimensions as the reference PWR. The core region contained the core simulator and 193 quarter-length dummy fuel assemblies with end boxes.

The core simulator consisted of 17 pipes for both steam and water injection. These injection pipes subdivided into a total of 193 steam/water injection nozzles, one below each dummy fuel assembly. The core simulator was divided into 17 zones, each of which had separate injection control valves such that lateral distribution of steam and water flow rates could be obtained to simulate, for example, core radial peaking. Total flow capacities were 360 kg/s of steam and 2000 kg/s of water.

The upper plenum had actual reactor dimensions and contained 61 control rod guide tubes and 16 support columns. Eight vent valves were mounted in the core barrel above the hot leg nozzle elevation for simulation of ABB and B&W PWRs. The vent valves could be locked or unlocked depending on the type of test.

Steam Generator Simulators
Each of the three intact loops contained a steam generator simulator (Figure 4.1-4) to simulate a PWR steam generator (SG). They were designed to measure water carried into the simulators and simulate the steam generator response to carryover while preserving the flow resistance of the reference SGs. Water carryover was measured by separating the water from the steam flow using a set of 31 two-stage cyclone separators. A steam mass flow equivalent to the measured water entrainment could be injected into the simulator to simulate the thermal response of a PWR SG.

Steam/Water Separators

Steam/water separators were located in the hot and cold legs of the broken loop. Their configurations were similar to the SG simulators previously described, but the dimensions and number of cyclones were adjusted to account for the larger mass flows expected in the broken loop (Figure 4.1-4).

Emergency Core Cooling System (ECCS)

The ECC injection systems commonly used in US/J PWRs and GPWRs were simulated at UPTF using accumulators. There were a total of four accumulators; two with a capacity of 150 m^3 and two with a capacity of 125 m^3 each. Two of these could be used alternatively as nitrogen accumulators for simulation of accumulator nitrogen release in US/J PWRs.

Pump Simulators

UPTF simulated the flow resistance and key internal heights of a reactor pump with manually adjustable valves (Figure 4.1-5) installed in each intact loop between the pump seal and the cold leg injection port.

Vent Valves

Eight vent valves (Figure 4.1-6) were installed in the core barrel of the test vessel to permit simulation of ABB and B&W PWRs with vent valves.

Containment Simulator

The containment simulator was designed to simulate the containment pressure history following a LOCA in the PWR. It was divided into an upper dry well of about 500 m^3 and a wet well of about 1000 m^3. Vent pipes routed steam from the dry well into the water pool of the wet well, where it condensed.

4.1.2 Process Instrumentation and Control

The scope of the process instrumentation included a total of 414 measurements of fluid temperatures, single-phase mass flows, water levels, absolute pressures, differential pressures and valve positions. These instruments monitored test boundary conditions and supported operating the facility's auxiliary systems. The signals from 265 process instrumentation channels were also directed to the main test data acquisition system for test evaluation (see Section 4.1.3).

The process control scheme is shown in Figure 4.1-7. The boundary conditions for the investigation areas were programmed into the control computer (Siemens microcomputer SMP) as functions of time. Pre-test analyses (using thermal-hydraulic codes and subscale data) were used to define the boundary conditions.

The UPTF core simulator steam and water injection rates and steam generator simulator steam injection rates could be either preprogrammed or controlled by feedback systems. These feedback systems simulated the thermal-hydraulic responses of the PWR active core and steam generators to water penetration (Figures 4.1-8 and 4.1-9). Each feedback system is described briefly below.

Core Simulator Feedback System

To simulate the reactor core response in the case of water breakthrough from the upper plenum into the core region, a stand-alone control computer was activated by signals from the drag bodies (DBs) and breakthrough detectors (BTDs) installed at the tie plate. Steam injection into the core was increased in accordance with the measured penetration rate; separate steam flow adjustments were made to each injection zone. The algorithm simulating the core response to water breakthrough was based on analytical and experimental data from CCTF and SCTF (References G-401, J-555 and J-560).

In addition, the Core Simulator Correction System could be used to adjust steam injection based on collapsed level measured in the core to simulate the thermal-hydraulic response of the core to bottom flooding. This system could also adjust water injection to simulate changes in water entrainment due to changes in steam flow and collapsed liquid level. The algorithms for the Core Simulator Correction System were also based on analytical and experimental data from CCTF and SCTF (References G-401, J-555 and J-560).

Steam Generator Simulator Feedback System

The response of a PWR steam generator to water penetration into the tube region was simulated by the SG Feedback System. Using this system, steam was injected in response to measurements of a water plug or entrained water entering the SG simulator.

4.1.3 Instrumentation and Data Acquisition System

The instrumentation and data acquisition system provided thermal-hydraulic data from the investigation and simulation areas; and from the supply and disposal subsystems of the test facility (Figure 4.1-10). The instrumentation included conventional instrumentation supplied by FRG and advanced instrumentation supplied by the US.

Test Instrumentation

Within the test vessel, 36 flow modules and 94 BTDs were installed at the core/upper plenum interface to detect the steam and water mass flows and water breakthrough at the tie plate. The flow modules included three individual measurement systems to measure the fluid momentum flux at the tie plate as well as the local fluid velocity and the water level above the tie plate. Numerous flow temperature and pressure

measurements were located in the upper plenum and in the downcomer. Also, an array of 705 optical sensors were installed throughout the upper plenum and downcomer to sense the presence or absence of water.

Outside the test vessel, conventional thermal-hydraulic measurements were used primarily to monitor the test boundary conditions. Five pipe flowmeter systems, including drag rakes and gamma densitometers, were used to measure the mass flow rates in the hot legs and the broken cold leg. In addition, 71 conventional mass flow measurements were used.

Information on the measurement systems for both the conventional and advanced test instrumentation is provided in Reference G-413; the type and number of measuring instruments, the sensor location, the measuring ranges, the uncertainties, and the identification codes are all defined in Reference G-413. The advanced instrumentation is discussed in Section 6.

Data Acquisition System
The data acquisition systems are shown in Figure 4.1-10. Two computer systems were used to collect, store and process the test data: the stand-alone system (HP A 600) for the optical sensors in the upper plenum and downcomer, and the main system (VAX 11/750) for the other instrumentation. Both data acquisition systems were supplied by the US.

4.1.4 Test Program and Test Conditions

The UPTF Test Program consisted of 30 tests comprising a total of 80 test runs. There were two basic types of tests performed within this program:

- Separate effects tests which emphasized "transparent" boundary conditions to quantify controlling phenomena in the primary system during LOCA and to support code improvement.

- Integral tests which focused on system-wide behavior during a simulated transient to identify controlling phenomena in the primary system during a LOCA transient.

The total number of tests included 21 separate effects tests and 9 integral tests.

The 21 separate effects tests are grouped according to the region of the primary system and the thermal-hydraulic phenomena of interest.

- Countercurrent flow phenomena in the downcomer for cold leg ECC injection during end-of-blowdown and refill phases of an LBLOCA.

- Entrainment in the downcomer during reflood for cold ECC injection.

4.1-5

- Thermal-hydraulic phenomena in the upper core, tie plate and upper plenum.

- De-entrainment along the flow path from the core to the steam generators for cold leg ECC injection.

- Steam/ECC interactions in the hot and cold legs.

- Impact of vent valves on the steam/water flow in the upper plenum and the downcomer of ABB and B&W PWRs.

- Temperature distribution in the downcomer for ECC injection in the cold legs when the primary system is filled with warm water.

- Steam/water countercurrent flow in the hot legs under the boundary conditions of small and intermediate-sized breaks.

- ECC delivery to the core for HPI in the hot legs.

The integral tests are subdivided into the following groups based on ECCS type and configuration, and break location.

- Five tests simulated a cold leg break with ECC injection into the cold legs (US/J type PWR).

- Five tests simulated a hot or cold leg break with combined ECC injection into the hot and cold legs (Siemens/KWU PWR).

- One test simulated a cold leg break with ECC injection into a cold leg of an intact loop and into the downcomer, and the vent valves free-to-open (ABB PWR).

The integral tests covered the end-of-blowdown, refill and reflood phases of a large break LOCA (LBLOCA).

An overview of test objectives and basic test conditions for the UPTF tests are given in Table 4.1-1. Note, some tests consisted of several test runs which may belong to different groups of tests. Therefore, some tests are listed more than once in Table 4.1-1. The Siemens data and quick look reports for the UPTF tests are listed in the bibliography (Section 8).

Table 4.1-1

UPTF TESTS

Group	Test Objective	Test Numbers	Run Numbers	Basic Test Conditions[1]
Downcomer Behavior during End-of-Blowdown	Downcomer CCFL and ECC Bypass	4A	174	CLI; transient depressurization from 1200 kPa; loops open
		5A	063	CLI; transient depressurization from 1800 kPa; loops blocked
		5B	062	CLI; steady-state CS steam injection; loops blocked
		6	131, 132, 133, 135, 136	CLI; ECC saturated; steady-state CS steam injection; loops blocked
		7	200, 201, 202, 203	CLI; ECC saturated; steady-state CS steam injection; loops blocked
		21A	272	DCI; ECC subcooled; steady-state CS steam injection; loops blocked
		21B	274	DCI; ECC saturated; steady-state CS steam injection; loops blocked
Downcomer Behavior during Reflood	Downcomer Entrainment	25A	242	CLI; DC wall superheated; steady-state SGS steam injection; loops open
		25B	241	CLI; DC wall saturated; steady-state SGS steam injection; loops open
		21D	171	DCI; DC wall saturated; steady-state SGS steam injection; loops open
Tie Plate and Upper Plenum Behavior Tests	Simultaneous Two-Phase Upflow and Water Downflow; Breakthrough at Tie Plate; Upper Plenum Pool Formation	20	090	UPI; ECC subcooled; CS steam and water injection; no SGS steam injection
		10A	080	HLI; ECC saturated; CS steam injection; no SGS steam injection
		12	014	HLI; ECC subcooled; CS steam injection; no SGS steam injection
		13	071	HLI; ECC subcooled; CS steam and water injection (W/S=4); no SGS steam injection
		26C	232	HLI; ECC subcooled; CS steam and water injection (W/S=10); no SGS steam injection
		15A	123	HLI; ECC subcooled; CS steam and water injection (hysteresis); no SGS steam injection
		15B	127	HLI; ECC subcooled; CS steam and water injection (W/S=4); auto SGS steam injection[2]
		16A	181	HLI; ECC subcooled; CS steam and water injection (W/S=1.7); auto SGS steam injection[2]
		16B	184	HLI; ECC subcooled; CS steam and water injection (W/S=2.7); auto SGS steam injection[2]
Upper Plenum/Hot Leg De-entrainment Tests	Tie Plate CCFL; Entrainment to Upper Plenum, Hot Legs and SG	10C	082	Steady-state CS steam and water injection; loops blocked
		10B	081	Steady-state CS steam and water injection; loops open
		29	210, 211, 212	Steady-state CS steam and water injection; loops open

Table 4.1-1

UPTF TESTS

Group	Test Objective	Test Numbers	Run Numbers	Basic Test Conditions[1]
Loop Behavior Tests	Flow Pattern in Hot Legs	8A	112 (2nd portion)	HLI; ECC subcooled; CS steam injection; auto SGS steam injection[2]; low loop flow resistance
		8B	111	HLI; ECC subcooled; CS steam injection; auto SGS steam injection[2]; high loop flow resistance
		26B	231	HLI; ECC subcooled; CS steam injection; no SGS steam injection
		26A	230	HLI; ECC saturated; CS steam injection; no SGS steam injection
	Flow Pattern in Cold Legs	8A	112 (1st portion)	CLI; ECC subcooled; CS steam injection; no SG simulation; low loop flow resistance
		8B	111	CLI; ECC subcooled; CS steam injection; no SG simulation; high loop flow resistance
	Flow Pattern in Hot and Cold Legs	9A	056	CI; ECC subcooled; CS steam and water injection; auto SGS steam injection[2]; low loop flow resistance
		9B	059	CI; ECC subcooled; CS steam and water injection; auto SGS steam injection[2]; high loop flow resistance
Vent Valve Separate Effects Tests	Downcomer CCFL and ECC Bypass during End-of-Blowdown	22A	280 (1st portion)	DCI; ECC subcooled; steady-state CS steam injection; loops blocked; VV free
		22B	281, 283	DCI; ECC saturated; steady-state CS steam injection; loops blocked; VV free
		22Bs	285	DCI; ECC saturated; steady-state CS steam injection; loops blocked; VV free; TS
		22C	282	DCI; ECC saturated; steady-state CS steam injection; loops blocked; VV free
		22Cs	284	DCI; ECC saturated; steady-state CS steam injection; loops blocked; VV free; TS
	Flow Phenomena in Downcomer, Loops and Upper Plenum during Reflood	21C	273, 275	DCI; ECC subcooled; steady-state CS steam and water injection; loops open; VV blocked
		22A	280 (2nd portion)	DCI; ECC subcooled; steady-state CS steam and water injection; loops blocked; VV free
		23B	290	DCI; ECC subcooled; steady-state SGS steam injection; loops blocked; VV free; TS
		23A	291	DCI; ECC subcooled; steady-state CS steam and water injection; loops open; VV free; TS

Table 4.1-1

UPTF TESTS

Page 3 of 4

Group	Test Objective	Test Numbers	Run Numbers	Basic Test Conditions[1]
SBLOCA Separate Effects Tests	Fluid-Fluid Mixing in Cold Leg and Downcomer	1	020, 021, 023, 025, 026	CLI; ECC subcooled; primary system filled with warm water
	Hot Leg CCFL	11	030-034, 036-045	Steady-state CS steam injection; water injection into inlet plenum of broken hot leg steam/water separator; intact loops blocked
	Behavior in Hot Leg and Upper Plenum with HPI	30	141, 142	HLI; ECC subcooled; system pressure = 1500 kPa
Cold Leg ECC Injection Integral Test	System Behavior during a Simulated LOCA Transient	27A 27B 2 4B 17B 17A	256 255 101 177 151 151	CLI; BE refill/reflood simulation; nitrogen discharge from ACC CLI; BE reflood simulation; high loop flow resistance CLI; EM reflood simulation CLI; BE reflood simulation; moderate loop flow resistance CLI; BE reflood simulation; low loop flow resistance No ECC injection; BE reflood simulation; low loop flow resistance
Combined ECC Injection Integral Tests [3]	System Behavior during a Simulated LOCA Transient	3 18 28 19 14	C5 169 262 192 221	CI; cold leg break -- break size = 2A; EM refill/reflood simulation CI; cold leg break -- break size = 2A; EM refill/reflood simulation CI; cold leg break -- break size = 2A; BE refill/reflood simulation CI; cold leg break -- break size = 0.5A; EM refill/reflood simulation CI; hot leg break -- break size = 2A; EM refill/reflood simulation
Downcomer/ Cold Leg ECC Injection with Vent Valves Integral Tests	System Behavior during a Simulated LOCA Transient	24	302, 304	DCI and CLI; cold leg break; EM refill/reflood simulation; TS

Table 4.1-1

UPTF TESTS

NOTES:

1. The following abbreviations are used in the test conditions:

CI	Combined ECC injection
CLI	Cold leg ECC injection
DCI	Downcomer ECC injection
HLI	Hot leg ECC injection
UPI	Upper plenum ECC injection

ACC	Accumulators
BE	Best estimate
CS	Core simulator
EM	Evaluation model
SGS	Steam generator simulator
TS	Thermal sleeves installed in downcomer ECC injection nozzles
VV	Vent valves
W/S	Ratio of core simulator water and steam injection rates

2. "Auto SGS steam injection" indicates that the SGS feedback control system was activated to automatically inject steam based on the water flow into the SGS.

3. Break size is defined relative to the cross-sectional area of the reactor coolant piping (A).
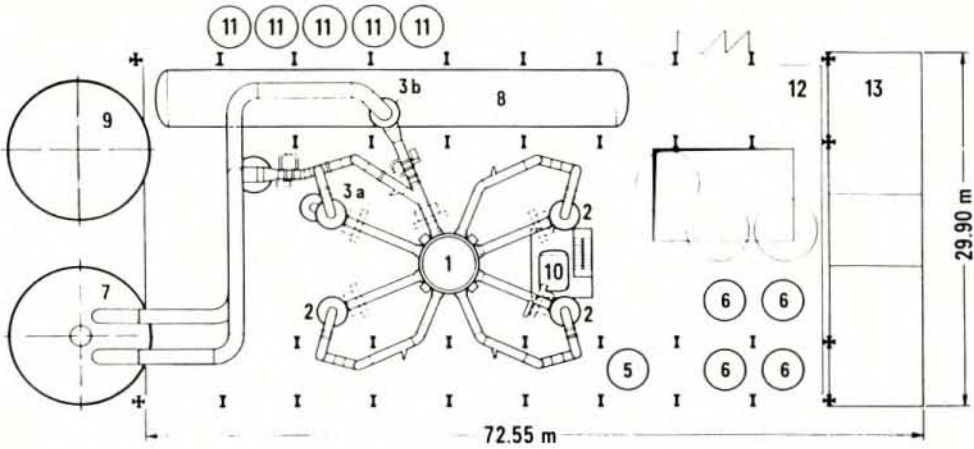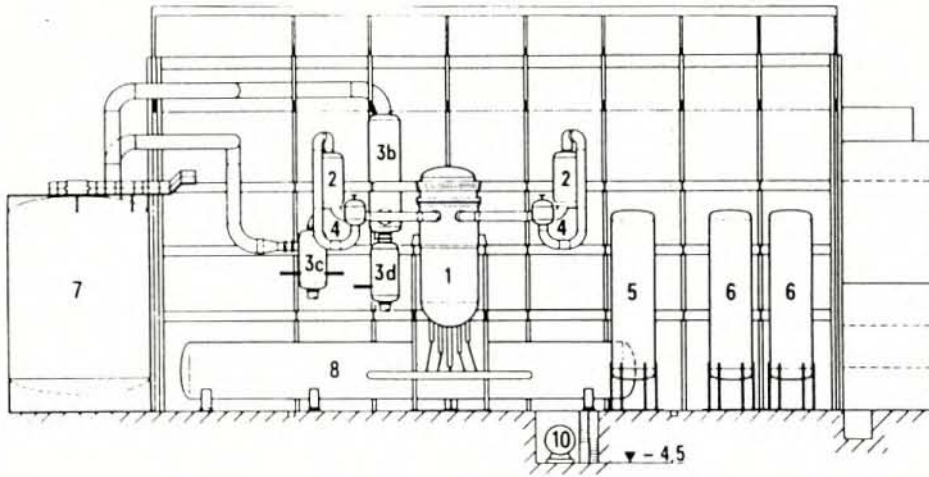
1	Test vessel	6	Accumulator
2	Steam generator simulator	7	Containment simulator
3a	Water separator (broken loop hot leg)	8	Steam storage tank
3b	Water separator (broken loop cold leg)	9	Water collecting tank
3c	Drainage vessel for broken hot leg	10	Drainage tank
3d	Drainage vessel for broken cold leg	11	Water storage tank
4	Pump simulator	12	Test building
5	Hot water storage tank	13	Switchgear building

LAYOUT OF THE UPTF
FIGURE 4.1-1

1 Test Vessel
2 Steam Generator Simulator (Intact Loop)
3a Steam Generator Simulator/ Water Separator (Broken Loop Hot Leg)
3b Water Separator (Broken Loop Cold Leg)
3c Drainage Vessel for Hot Leg
3d Drainage Vessel for Cold Leg
4 Pump Simulator
5a Break Valve (Hot Leg)
5b Break Valve (Cold Leg)
6 Containment Simulator

7 Surgeline-Nozzle
8 ECC-Injection Nozzles (Cold Leg)
9 ECC-Injection Nozzles (Hot Leg)
10 Core Simulator Injection Nozzle
11 TV-Drainage Nozzle
12 Steam Injection Nozzle
13 Drainage Nozzle

Loop II
Loop I
Loop III
Loop IV

Simulator

Test vessel cover
Test vessel flange
Vent valve
Upper plenum internals
Upper core support plate
End box
Dummy fuel assembly
Core simulator injection nozzles
Zone wall (perforated)
Core bypass structure
Resistance plate
Test vessel (lower part)
Core simulator injection pipes

Vent valve

13 489
Ø 750
210
250
Ø 4870

Note: All dimensions in mm

UPTF PRIMARY SYSTEM AND TEST VESSEL
FIGURE 4.1-2
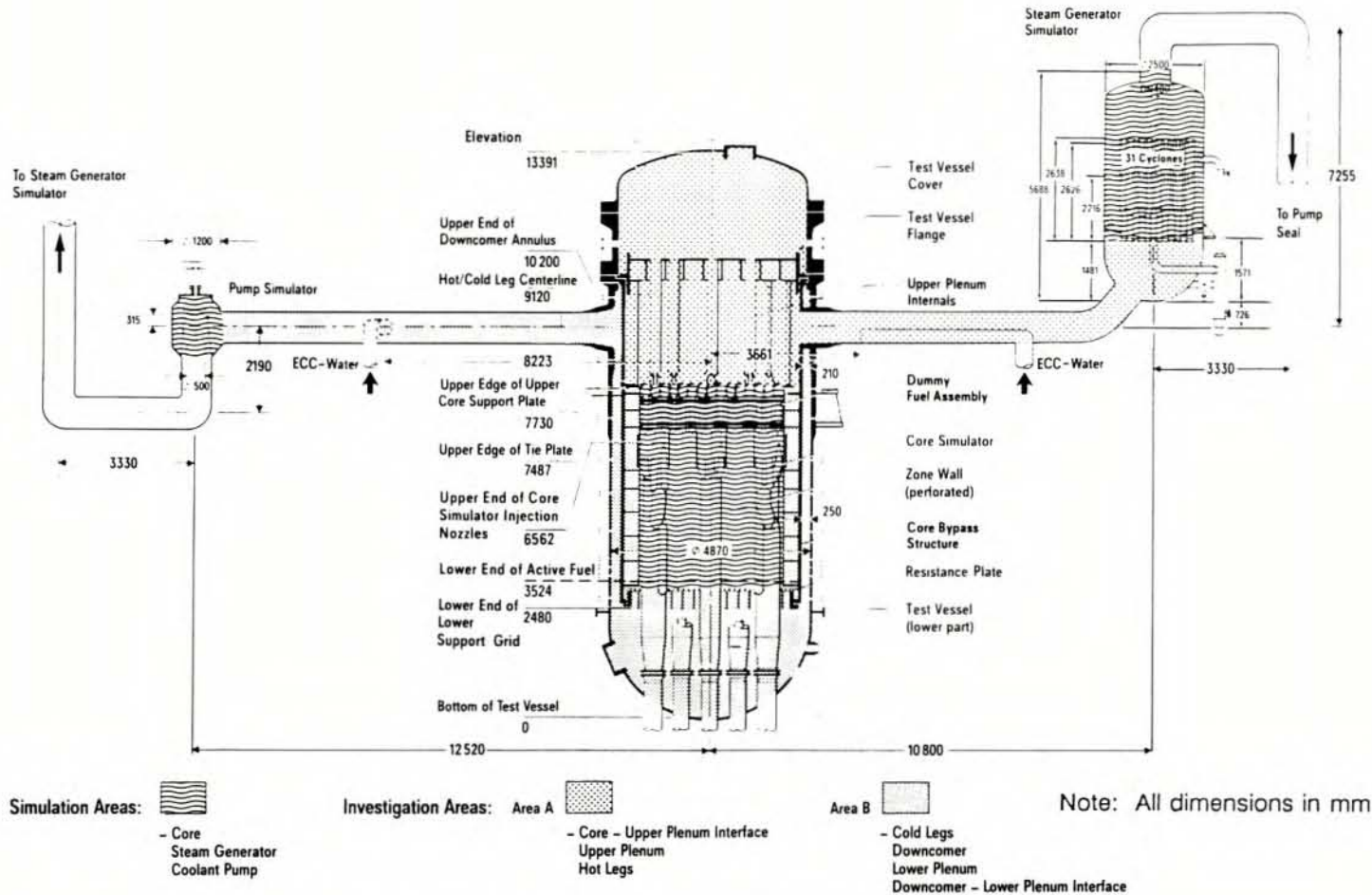
UPTF INVESTIGATION AND SIMULATION AREAS

FIGURE 4.1-3

Section A – A

Section B - B

Section C - C

Steam generator simulator
of intact loops

Steam generator simulator
(water separator)
of broken loop hot leg

Water separator of
broken loop cold leg
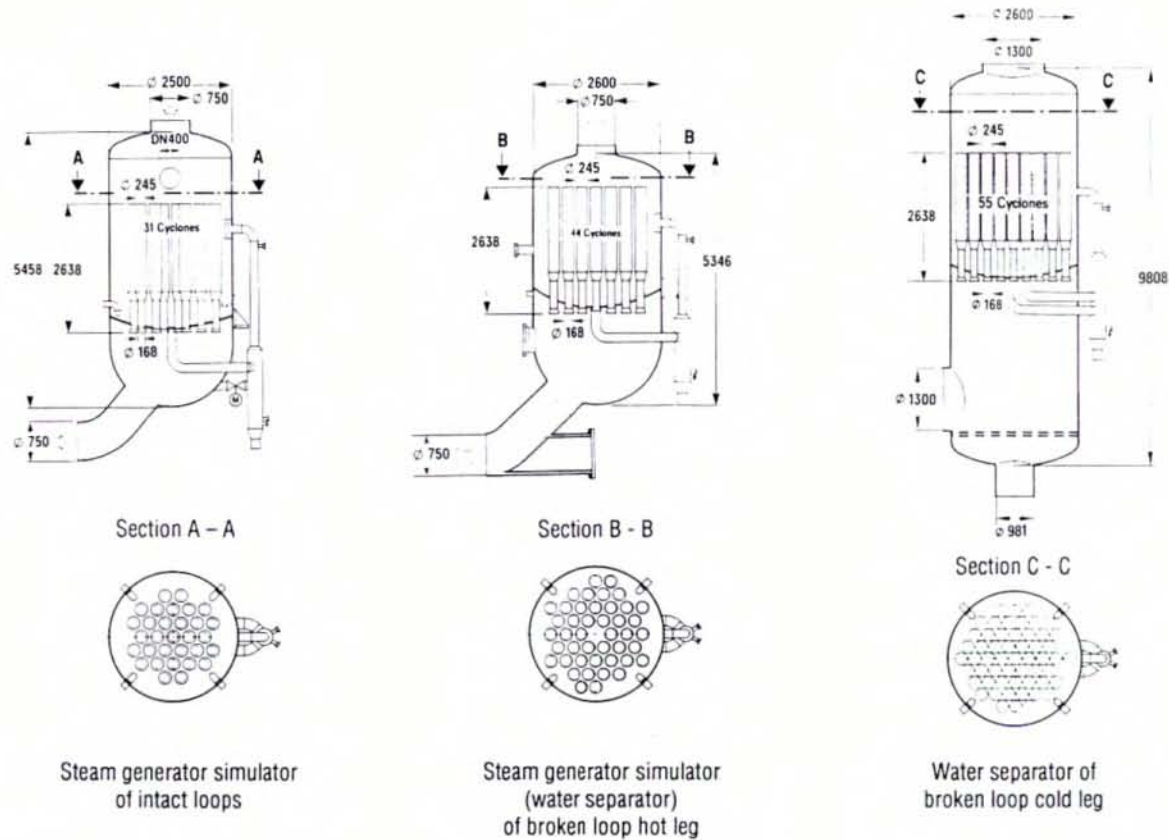
Note: All dimensions in mm

UPTF STEAM GENERATOR SIMULATORS AND WATER SEPARATORS

FIGURE 4.1-4

Section B - B

Note: All dimensions in mm
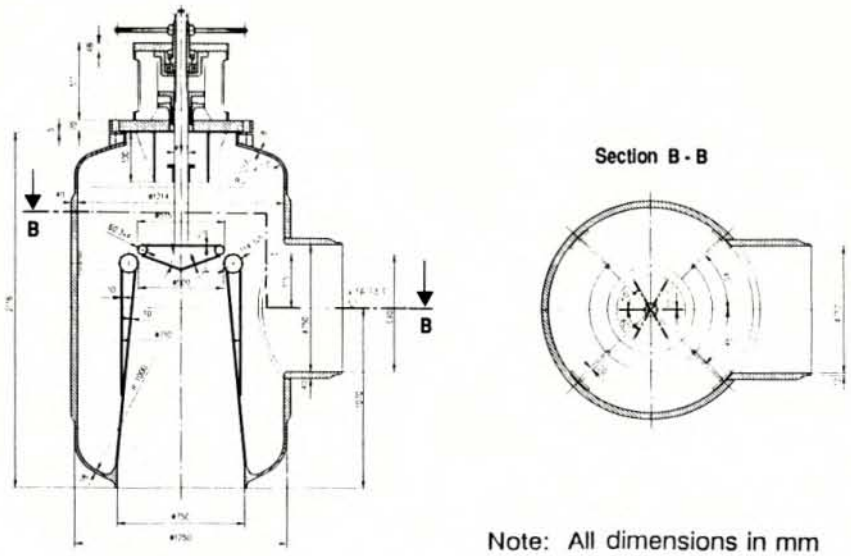
UPTF PUMP SIMULATOR
FIGURE 4.1-5

Section A - A

Core barrel

Test vessel

Hand hole
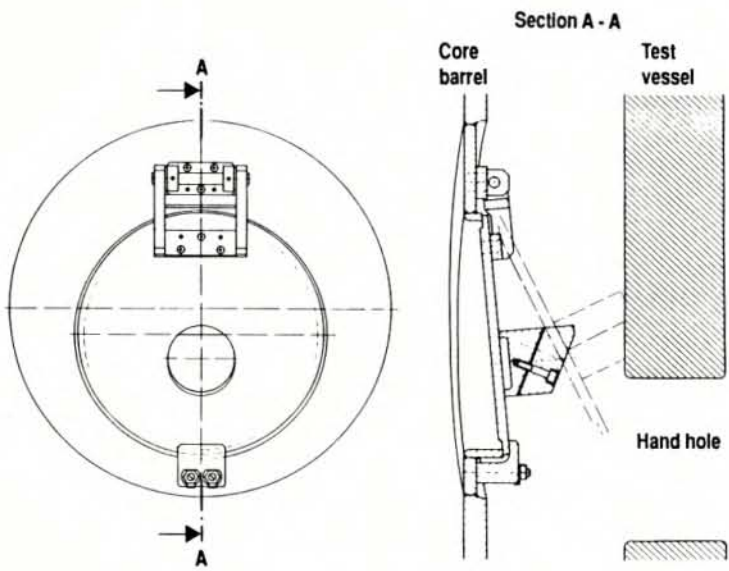
UPTF VENT VALVE
FIGURE 4.1-6
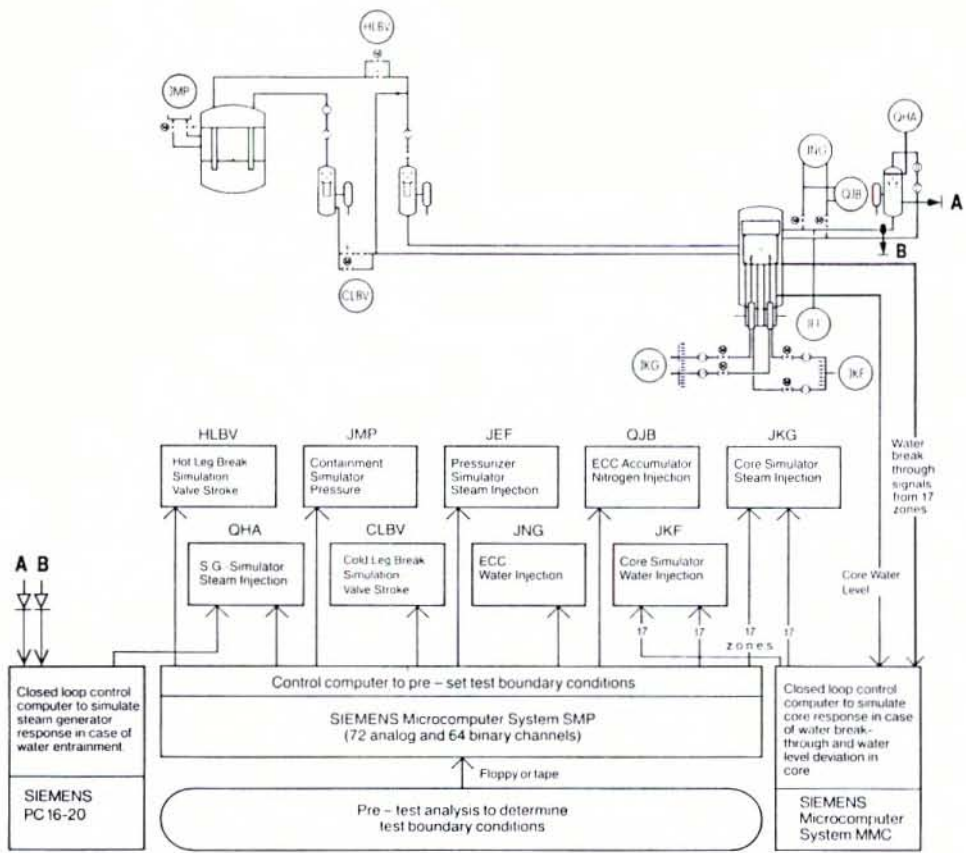
UPTF PROCESS CONTROL SCHEME
FIGURE 4.1-7
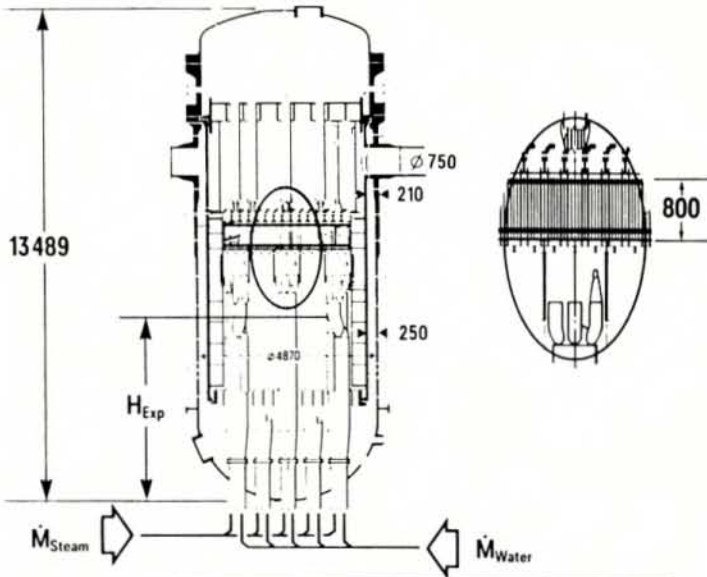
○ **Steam Injection**

$$\dot{M}_{Steam} = \dot{M}_{S,\ Base} + \dot{M}_{S,\ Break\text{-}Through} + \dot{M}_{S,\ H-Deviation}$$

$$\dot{M}_{S,\ Base} = F_1\ (t)$$

$$\dot{M}_{S,\ Break\text{-}Through} = F_2\ (\dot{M}_{W,\ Break\text{-}Through},\ E_t)$$

$$\dot{M}_{S,\ H-Deviation} = F_3\ [(H_{Exp} - H_{Calc.}),\ E_t]$$

○ **Water Injection**

$$\dot{M}_{Water} = F_4\ (\dot{M}_{Steam},\ H_{Exp})$$

○ **Energy Level of Core to be Simulated**

$$E_t = E_o + \int_o^t e\ (t)_{Decay} \cdot dt - \int_o^t \dot{M}_{Steam} \cdot r \cdot dt$$

○ **Functions**

$$F_1,\ F_2,\ F_3\ and\ F_4$$

Developed from SCTF-Test Results

Note: All dimensions in mm

UPTF CORE SIMULATOR FEEDBACK SYSTEM LOGIC
FIGURE 4.1-8
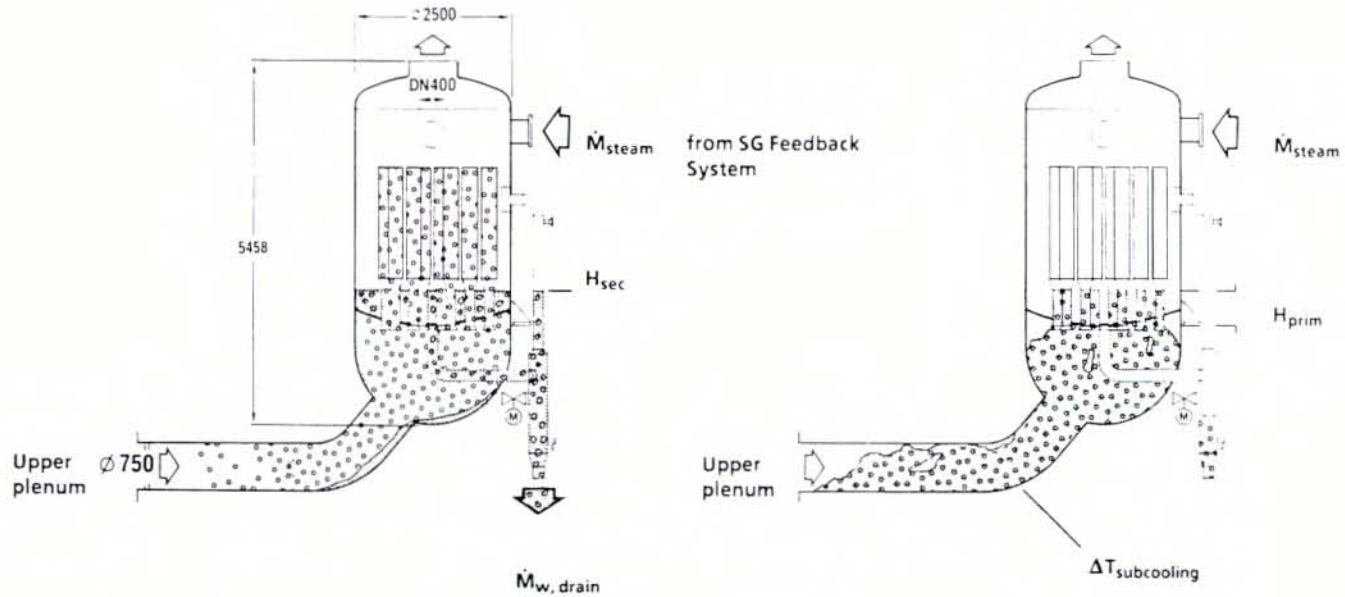
For homogeneous flow:

$$\dot{M}_{steam} = \rho \cdot A(H) \cdot \dot{H}_{sec} + \dot{M}_{w, drain}$$

For plug flow:

$$\dot{M}_{steam} = F(H_{prim} \cdot \Delta T_{subcooling})$$

UPTF STEAM GENERATOR SIMULATOR FEEDBACK SYSTEM LOGIC
FIGURE 4.1-9
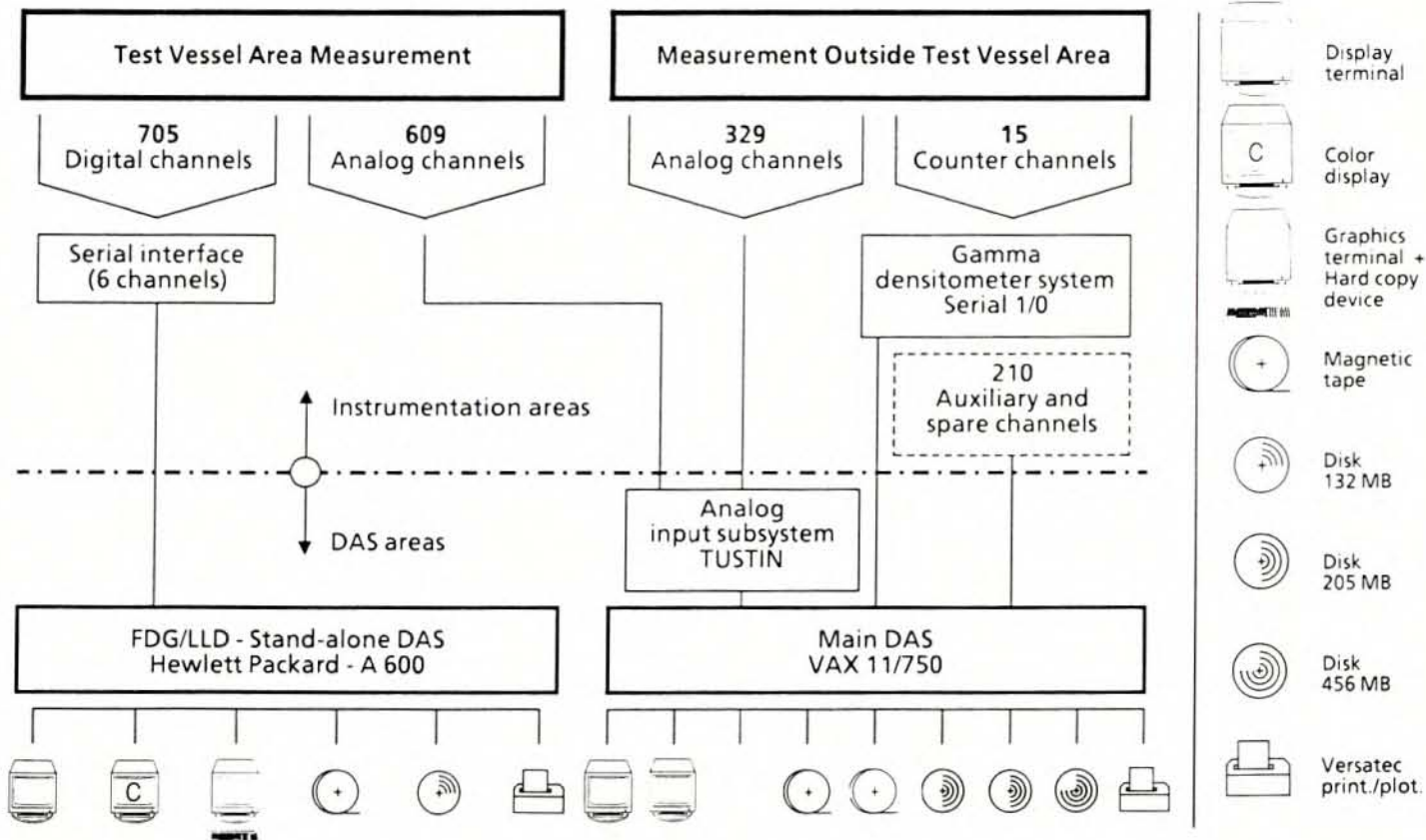
UPTF DATA ACQUISITION SYSTEM
FIGURE 4.1-10

4.2 DOWNCOMER BEHAVIOR DURING END-OF-BLOWDOWN TESTS

4.2.1 Rationale of Tests

During the end-of-blowdown, steam flows up the downcomer to escape out the broken cold leg. Due to flashing and entrainment in the lower plenum, the downcomer upflow may be two phase. This upflow initially tends to prevent the ECC from flowing down the downcomer and refilling the vessel. The upflow can carry some or all of the ECC injected into the cold legs or the downcomer directly out the broken cold leg (i.e., ECC bypass). Subscale tests have shown that, at a certain steam or two-phase upflow, ECC starts to be delivered to the lower plenum.

Downcomer CCFL and ECC bypass for cold leg ECC injection were extensively studied in the USNRC ECC Bypass Program. In this program, steam/water tests were performed at Creare and Battelle Columbus Laboratories using facilities ranging in size from 1/30 to 1/5 linear scale (References E-411, E-413, E-415, E-416, E-418, E-419, E-421 and E-901 to E-903). Outside the ECC Bypass Program, tests were performed by JAERI (Reference J-257), and Simpson and Rooney in the UK (Reference E-904). Empirical flooding correlations (for cold leg ECC injection) were developed by Creare (Reference E-001) and Battelle (Reference E-422) based on the subscale test facility data. While the subscale results have been extrapolated to full-scale, the extrapolation techniques involve some uncertainty.   The objectives of UPTF testing were to investigate downcomer flooding behavior and to determine the effect of scale on ECC bypass.

4.2.2 Scope of Testing

UPTF Separate Effects Tests 4A, 5, 6, 7, 21A and 21B were performed to investigate steam/water flow phenomena in the intact cold legs, downcomer and lower plenum of a PWR during the end-of-blowdown phase of a large break LOCA. The conditions for each test are summarized in Table 4.1-1. Each test is described briefly below.

- Tests 4A and 5A studied these phenomena during a depressurization transient for cold leg ECC injection including flashing and entrainment of water in the lower plenum. Test 5B was performed for steam upflow only under quasi-steady state conditions.

- Tests 6 and 7 were quasi-steady tests designed as counterparts to testing in subscaled facilities. Specifically, these tests injected steam and ECC at near saturation temperatures to focus on CCFL. Also, the ECC injection location was varied in these tests.

- UPTF Test 21 (Phases A and B) investigated downcomer CCFL at full-scale for downcomer ECC injection with closed vent valves. This test was a counterpart to tests with open vent valves (discussed in Section 4.7), and to tests with cold leg ECC injection (i.e., Tests 5B, 6 and 7).

The data and quick look reports for these tests are listed in the bibliography (Section 8). These tests have been evaluated by both FRG and US. The FRG evaluation is documented in References G-411, G-903 through G-907, G-910, and G-915; the US evaluation is provided in References U-455 and U-460.

4.2.3 Summary of Key Results

During the UPTF tests, flow conditions in the downcomer were heterogeneous. Figure 4.2-1 shows contour plots of fluid temperature (subcooling) in the unwrapped UPTF downcomer during a cold leg ECC injection test (Test 5B) and a downcomer ECC injection test (Test 21A). The plots show that little subcooling was measured below the ECC injection port adjacent to the break. Significant subcooling, even at the lower elevations of the downcomer, was measured below the ECC injection ports away from the break. ECC injected near the break was mainly bypassed and ECC injected away from the break penetrated to the lower plenum. This heterogeneous behavior was not observed in previous subscale tests. The detailed results of the cold leg ECC injection tests and downcomer ECC injection tests are discussed separately below.

Cold Leg ECC Injection Tests

The important phenomena observed in the UPTF cold leg injection tests are described below based on Test 5A. Immediately after the start of ECC injection, water plugs formed in the intact cold legs. After a short delay (about eight seconds), the water plugs reached the downcomer; water delivery to the downcomer was intermittent plug delivery for the duration of the transient. Initially, the ECC injected into the cold leg adjacent to the break (i.e., Cold Leg 1) was completely bypassed while some of the ECC injected in the cold legs away from the break (i.e., Cold Legs 2 and 3) penetrated to the lower plenum. Subcooled water was first detected in the lower plenum about one second after the water plugs entered the downcomer. As the downcomer upflow decreased, ECC delivery from Cold Legs 2 and 3 increased until essentially all the ECC injected in these loops was delivered to the lower plenum. However, the ECC injected into Cold Leg 1 was mostly bypassed throughout the transient.

The results of UPTF Tests 6 and 7 are presented in the three diagrams of Figure 4.2-2. These diagrams show that water delivery was mainly controlled by the cold leg arrangement with respect to the break. The water delivery curve for an ECC injection rate of about 500 kg/s into each cold leg of the three intact loops is illustrated in the upper diagram of Figure 4.2-2. This diagram shows three different flow regimes for

water penetration to the lower plenum which can be characterized by the steam injection rate:

- Complete bypass from Cold Leg 1 with partial delivery from Cold Legs 2 and 3 for high steam flow $(\dot{M}_s > 320 \text{ kg/s})$.

- Complete bypass from Cold Leg 1 and nearly complete delivery from Cold Legs 2 and 3 for intermediate steam flows $(100 \text{ kg/s} \leq \dot{M}_s \leq 320 \text{ kg/s})$.

- Partial delivery from Cold Leg 1 and complete delivery from Cold Legs 2 and 3 for low steam flows $(\dot{M}_s < 100 \text{ kg/s})$.

The relationship between cold leg location and delivery was confirmed in Test 7 by varying the injection location. These results are shown on the lower two diagrams of Figure 4.2-2. The middle diagram shows the behavior of ECC (735 kg/s) injected into only Cold Leg 1. The data shows complete bypass at steam injection rates above 102 kg/s and partial bypass for the lowest investigated steam injection rate of 30 kg/s.

The bottom diagram shows that, for ECC injection into Cold Legs 2 and 3, there was some bypass at a steam injection rate of about 100 kg/s. However, the top diagram suggests complete delivery from Cold Legs 2 and 3 for steam flows below about 270 kg/s. Apparently, there was a synergistic effect in which injection into Cold Leg 1 increased delivery from Cold Legs 2 and 3. (See References U-455 and G-411 for further discussion.)

Data from UPTF and the 1/5-scale Creare test facility for ECC injection into the three intact cold legs are compared in Figure 4.2-3 using the Wallis parameter. For UPTF, the effective steam flow was estimated by considering the condensation efficiency calculated from UPTF Test 6. Due to the strongly heterogeneous flow conditions in the downcomer of UPTF, the water delivery curves of UPTF and Creare are significantly different. For dimensionless effective steam flow, $(J^*_{s,\text{eff}})^{1/2}$, greater than 0.2 the dimensionless water downflows for UPTF are much higher than for Creare. Note, the UPTF data at low steam flows should not be directly compared to the Creare CCFL curve because these data were not CCFL data (i.e., increasing the injection in Cold Legs 2 and 3 would have increased delivery).

Downcomer ECC Injection Tests
Immediately after the start of ECC injection through the downcomer nozzles water accumulated in the upper region of the downcomer and was bypassed out the broken cold leg. A few seconds later, ECC started accumulating in Cold Legs 2 and 3, and, after a brief delay, in Cold Leg 1. Some of the ECC which accumulated in the cold legs, drained into the downcomer and contributed to penetration to the lower plenum. Flow conditions in the downcomer were heterogeneous. Specifically, Figure 4.2-1

shows that ECC injected in the nozzle adjacent to the break was completely bypassed while some of the ECC injected in the nozzle away from the break penetrated to the lower plenum. Figure 4.2-1 also shows that subcooled water was present in the upper portion of the downcomer. Apparently, the momentum of the ECC injection impinging on the core barrel dispersed the ECC around the downcomer; this phenomenon did not occur in the cold leg injection tests (Figure 4.2-1).

Dispersion and accumulation of ECC in the upper region of the downcomer affected water delivery. As shown in Figure 4.2-4, water delivery to the lower plenum was lower with downcomer injection than with cold leg injection.

Figure 4.2-4 also shows the effect of ECC subcooling on water delivery with downcomer injection. For a steam injection rate of about 300 kg/s, an increase in ECC subcooling from 56 K to 117 K increased water delivery from about 100 kg/s to 400 kg/s. This increase in water delivery was due to the decrease in steam upflow resulting from increased condensation.

4.2.4 Conclusions

The UPTF tests indicated:

- Flow conditions in the downcomer were highly heterogeneous at full-scale. This heterogeneous (or multidimensional) behavior increased water delivery rates at full-scale relative to previous tests at subscale facilities.

- Based on use of the Wallis parameter, data from subscale tests indicate lower penetration than the full-scale UPTF data.

- For similar total ECC injection rates, water delivery was lower with ECC injection through two nozzles in the downcomer rather than through nozzles in the three intact cold legs.
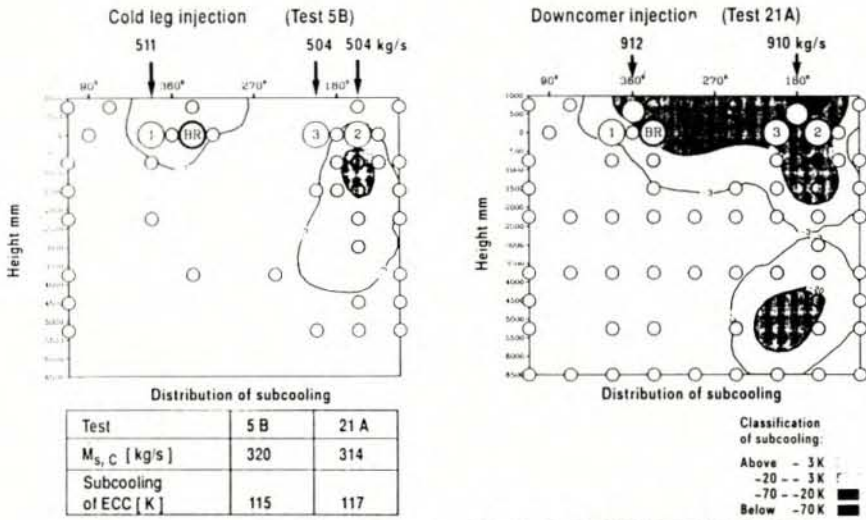
FLOW CONDITIONS IN FULL-SCALE DOWNCOMER FOR
STRONGLY SUBCOOLED ECC IN COUNTERCURRENT FLOW

FIGURE 4.2-1

Water downflow rate $\dot{M}_{w,\,df}$ (kg/s)
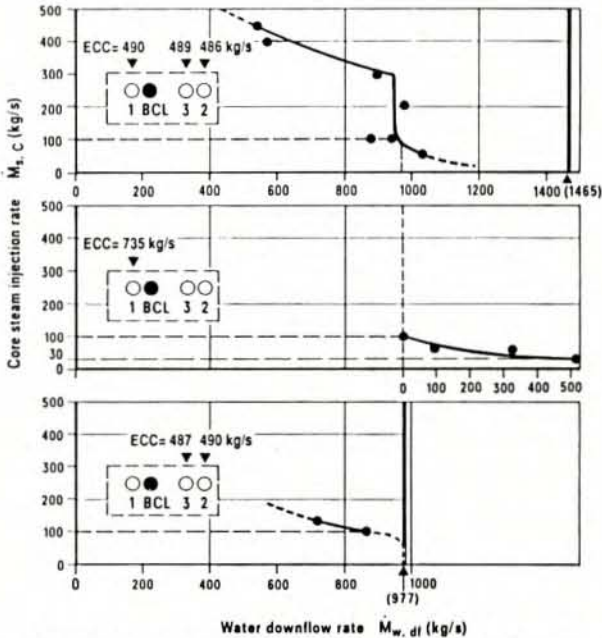
EFFECT OF LOOP ARRANGEMENT ON WATER DELIVERY TO LOWER PLENUM
FOR SLIGHTLY (< 50 K) SUBCOOLED ECC IN COUNTERCURRENT FLOW
UPTF TESTS 6 AND 7

FIGURE 4.2-2
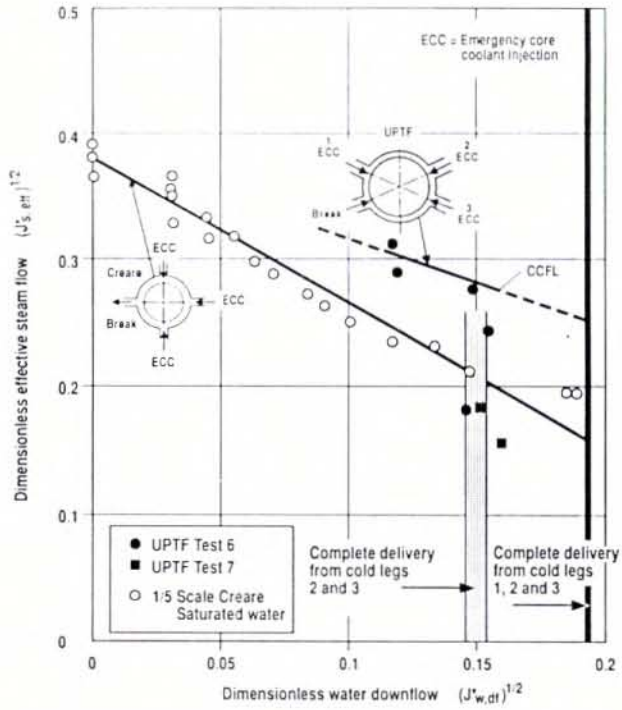
EFFECT OF SCALE ON WATER DELIVERY
TO LOWER PLENUM IN COUNTERCURRENT FLOW
FIGURE 4.2-3
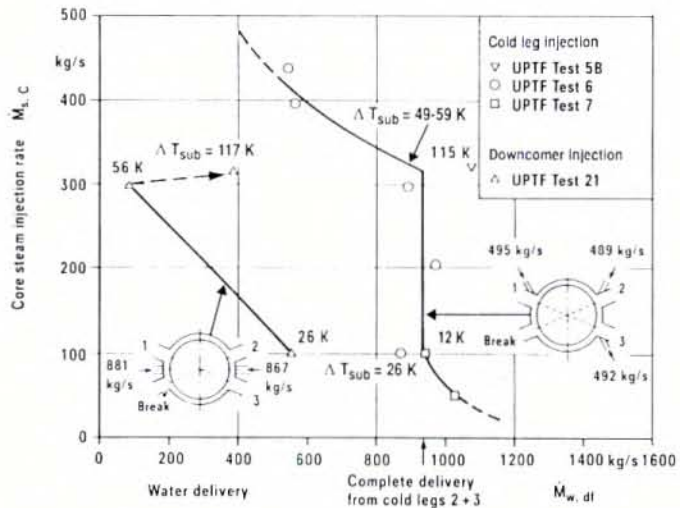
EFFECT OF ECC INJECTION CONFIGURATION
ON WATER DELIVERY TO LOWER PLENUM
IN COUNTERCURRENT FLOW
FIGURE 4.2-4

4.3 DOWNCOMER BEHAVIOR DURING REFLOOD TESTS

4.3.1 Rationale of Tests

During reflood, when ECC is injected by the LPCI system, the water level in the downcomer approaches the bottom of cold leg nozzles. Steam flowing around the downcomer and out the broken loop cold leg reduces the downcomer water level by entraining water from the downcomer out the break. The steam flow in the downcomer, and therefore entrainment out the break, is reduced by steam condensation on the ECC injected in the loops or the downcomer. This reduction in steam flow by condensation is dependent on the ECC flow rate and ECC injection configuration. Note, when the downcomer water level is at the cold leg elevation, spillover rather than entrainment is the controlling phenomenon.

The collapsed water level in the downcomer is also reduced by steam generation in the downcomer. During reflood, the reactor vessel wall is superheated because wall cooling was minimal during blowdown and refill. Heat released by the walls can, depending on the flow conditions, result in steam generation. Steam generation increases the void fraction in the downcomer thereby reducing the collapsed liquid level.

Since the downcomer water level constitutes the driving head for bottom flooding of the core, the level reduction due to entrainment and steam generation can affect core cooling during reflood.

Few experimental data are available concerning flow behavior in the downcomer of a PWR during the reflood phase of a LOCA. Subscale CCTF test results indicate that a reduction of the downcomer water level can occur due to wall steam generation and water entrainment.

In UPTF Integral Test No. 2, which simulated LOCA reflood behavior in a US/J PWR with cold leg injection, the reduction in downcomer water level was between 1.5 m and 2.0 m. This reduction was larger than that observed in the counterpart test at CCTF (Test C2-4). This difference in level reduction is attributable to downcomer scale and configuration. Specifically, the scaled CCTF had azimuthal velocities which were small relative to the reference US/J PWR and relative to UPTF (which simulates a GPWR downcomer). It appeared entrainment out the break was higher at UPTF than at CCTF. Separate effects tests were performed at UPTF to develop a more detailed understanding of entrainment/level reduction in the downcomer.

4.3.2 <u>Scope of Testing</u>

The goal of UPTF Tests 25 and 21D was to provide full-scale, separate effects data on the interaction of steam and water in the downcomer during reflood. The specific objectives are listed below. The test conditions are summarized in Table 4.1-1. The specific objectives were to:

- Determine the influence of steam flow and downcomer water level on water entrainment out the broken cold leg with cold leg ECC injection (Test 25) and downcomer injection Test 21D).

- Evaluate the effect of reactor vessel wall temperature on the downcomer water level reduction and entrainment (Test 25A).

The data and quick look reports for these tests are listed in the bibliography to this report (Section 8). These tests have been evaluated by both FRG and US. The FRG evaluation is documented in Reference G-411; the US evaluation is provided in References U-455 and U-460.

4.3.3 <u>Summary of Key Results</u>

During Test 25, manometer oscillations between the downcomer and core were observed. Entrainment out the broken cold leg oscillated at the same frequency. Apparently, as the downcomer level increased, water entrainment out the break increased. The increase in entrainment increased the pressure in the downcomer which forced the downcomer level down and the core level up. However, as the downcomer level decreased, entrainment out the break and the pressure in the downcomer decreased.

The water level measurements in the downcomer revealed that the water level was higher in front of the broken cold leg nozzle than at other azimuthal positions. The magnitude of the local increase in water level depended on the steam/water flow out the broken cold leg and average downcomer water level; the maximum increase was 0.7 m.

At steam flows less than the condensation potential of the ECC injection, the steam flow was completely condensed resulting in plug flow in the cold legs. However, at loop steam flow rates greater than the steam condensation potential of the ECC injection, stratified steam/water flow occurred in the cold legs. In this case, the water was continuously delivered to the downcomer with a subcooling of less than 5 K. Behavior in the loops is covered in Section 4.6.

Figure 4.3-1 is a plot of the downcomer level vs. water entrainment rate for different steam flows based on Test 25 (cold leg injection). As shown in the figure, water entrainment through the broken cold leg increased with steam flow and downcomer level. Also, the collapsed water level in the downcomer for given steam and ECC injection rates was about the same in the test run with superheated vessel walls as in the test run with saturated walls. The maximum superheat of the downcomer walls was limited to about 60K in the UPTF tests.

Water entrainment through the broken loop cold leg for downcomer ECC injection is shown in Figure 4.3-2. Even at a low water levels, the broken cold leg entrainment flow exceeded the ECC injection rate into one injection nozzle. This suggests all ECC injected through the nozzle near the broken cold leg was entrained directly out the break.

Separate correlations for the level/entrainment/steam flow data from Test 25 were developed by FRG and the US. While the assumptions and approaches of the two correlations are different, both correlations are consistent with the test data and predict about the same level reduction for given flow conditions. Each correlation is described briefly below.

- The correlation developed by FRG (Siemens) assumes that the steam flow entering the downcomer carries water droplets which were entrained in the cold legs. The correlation also assumes that additional entrainment only occurs in front of the broken cold leg nozzle because the steam velocity and water level are highest at that location. This correlation is based on fundamental hydraulic equations, while the shear stress coefficient and constants in the correlation were determined from UPTF tests. Since the steam flow in the correlation is the total steam flow out the break, steam generation in the downcomer is taken into account. Figure 4.3-3 is a plot of the correlation with the test data. The development of this correlation is discussed in detail in References G-411 and G-912.

- The correlation developed by the US (MPR) assumes entrainment can occur throughout the downcomer due to the azimuthal steam flow. Wall steam generation is taken into account by correcting the measured void height (difference between the collapsed water level and the bottom of the cold leg) for the estimated voiding due to the steam generation. Inherent in this approach is the assumption that the level reductions due to entrainment and steam generation are separate and additive. Figure 4.3-4 is a plot of this correlation with the Test 25 data. A detailed description of the development of this correlation is provided in Reference U-455.

Both correlations indicate water entrainment in the downcomer and the level reduction depend on the downcomer configuration; specifically, the downcomer height and downcomer gap.

4.3.4 Conclusions

UPTF test results indicated:

- Water entrainment out the break and the reduction of the downcomer water level were significant at high steam flows.

- Water entrainment increased with increasing broken cold leg steam flow and with increasing downcomer water level.

- Subscale CCTF tests showed less entrainment and level reduction than comparable tests at the full-scale UPTF. Analytical evaluations of the tests indicate, that for full-height facilities where the vertical flow area in the downcomer is scaled by the scale factor, water entrainment in the steam flow increases with scale.

- In Test 21 with downcomer ECC injection, all ECC injected through the nozzle near the broken cold leg was entrained directly out the break, even at low levels in the downcomer.

- At ECC injection rates with a condensational potential greater than the loop steam flow, the steam flow is completely condensed in the cold legs. Hence, there is no steam flow into the downcomer and no level reduction due to entrainment.

Figure 4.3-1

Broken loop cold leg

Collapsed water level in DC

m

9.0

8.745

8.0

7.0

6.0

0   100   200   300   400

Water entrainment through BCL, $\dot{M}_w$ in kg/s

$\dot{M}_{steam}$

$\dot{M}_{water}$

Downcomer

BCL steam flow kg/s	ECC injection, kg/s 246 (3 × 82)	426 (3 × 142)
47-52	O	
36	□	
25	×	
16-19	△	▲
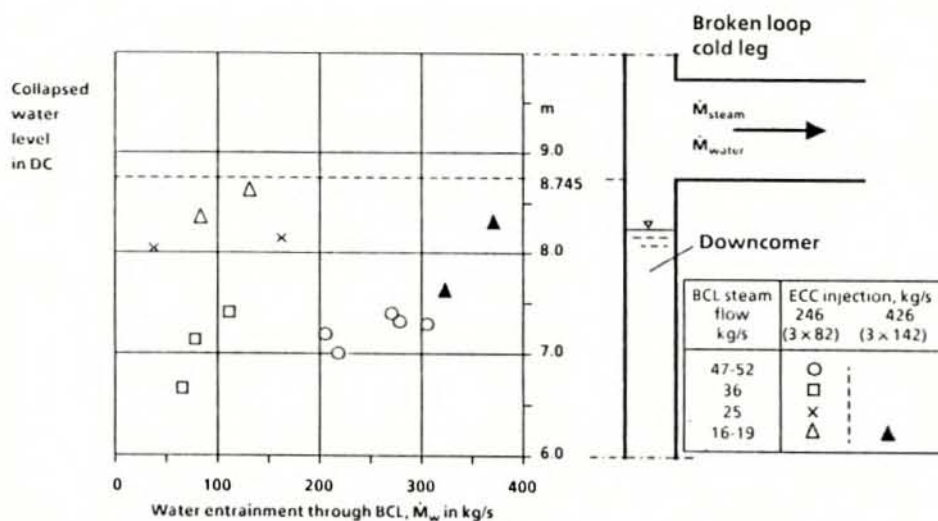
WATER ENTRAINMENT THROUGH BROKEN COLD LEG
FOR ECC INJECTION INTO COLD LEGS UPTF TEST 25
FIGURE 4.3-1

Figure 4.3-2

Broken loop cold leg

Collapsed water level in DC

m

9.0

8.745

8.0

7.0

6.0

0   100   200   300   400

Water entrainment through BCL, $\dot{M}_w$ in kg/s

$\dot{M}_{steam}$

$\dot{M}_{water}$

Downcomer

BCL steam flow kg/s	ECC injection, kg/s 2 × 125
51-55	Φ
43-46	Φ
30-37	✳
15-19	Δ
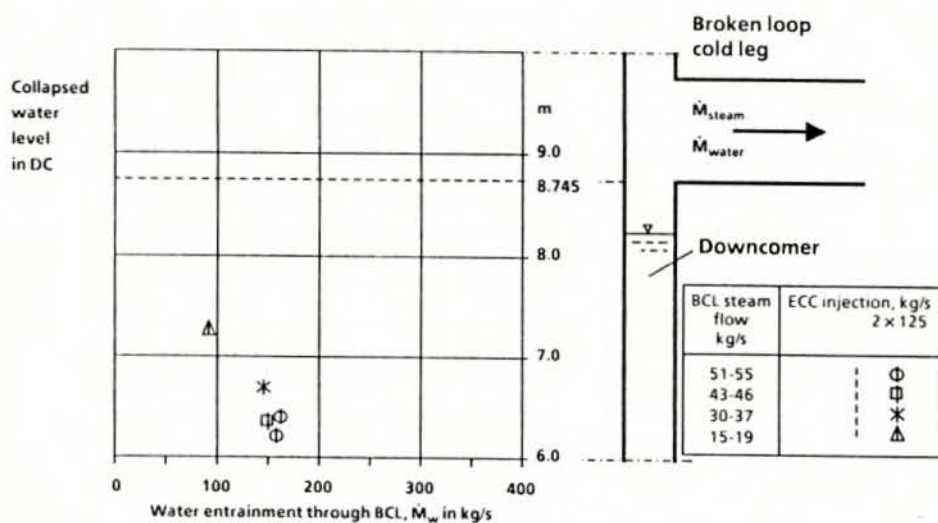
WATER ENTRAINMENT THROUGH BROKEN COLD LEG
FOR ECC INJECTION INTO DOWNCOMER
UPTF TEST 21D
FIGURE 4.3-2

$$\sqrt[3]{M_w} \cdot (H + H_T)^2 \cdot \rho_s = M_s^2 \left(C_1 \cdot \frac{M_{ECC}^{0.5}}{M_s} + C_2 \right)$$
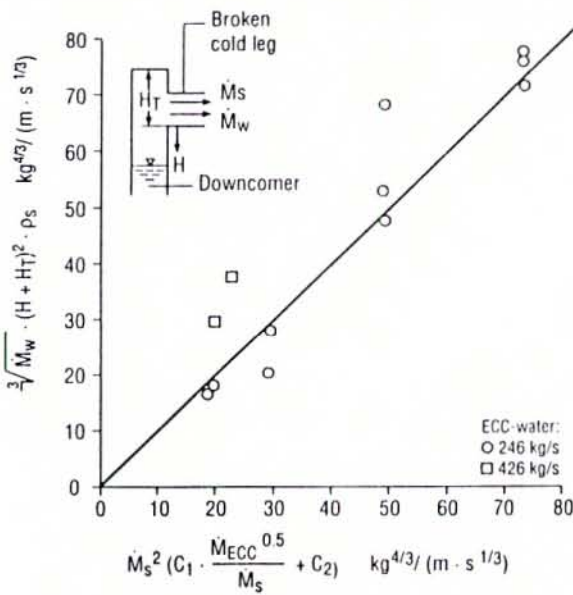
M_s = Steam flow rate

M_w = Water flow rate

M_{ECC} = Total ECC injection rate into cold legs

$$C_1 = 0.044 \; \frac{s^{7/6}}{kg^{1/6} \cdot m}$$

$$C_2 = 0.0187 \; \frac{s^{5/3}}{kg^{2/3} \cdot m}$$

C_1, C_2 dependent on pressure and geometry /G411/

ECC-water:
O 246 kg/s
□ 426 kg/s

Vertical axis: $\sqrt[3]{M_w} \cdot (H + H_T)^2 \cdot \rho_s$ kg$^{4/3}$/ (m · s $^{1/3}$)

Horizontal axis: $M_s^2 \left(C_1 \cdot \frac{M_{ECC}^{0.5}}{M_s} + C_2 \right)$ kg$^{4/3}$/ (m · s $^{1/3}$)

WATER ENTRAINMENT CORRELATION AS
A FUNCTION OF DC WATER LEVEL, BCL-STEAM FLOW
AND ECC INJECTION RATE
UPTF TESTS 25A AND 25B

FIGURE 4.3-3

Legend:

    o   Phase A (Hot Walls)

    *   Phase B (No Hot Walls)

$$J_{g,eff}^{*} = J_{g}^{*} - 0.8 \cdot J_{g,cond}^{*}$$

$$H_{v,top} = 0.35 \, (J_{g,eff}^{*} / J_{f,ent}^{* \, \frac{1}{4}})^{2}$$

Typical Void Height Fluctuation

Top Downcomer Void Height, $H_{v,top}$ (m)

$J_{g,eff}^{*} / J_{f,ent}^{* \, \frac{1}{4}}$
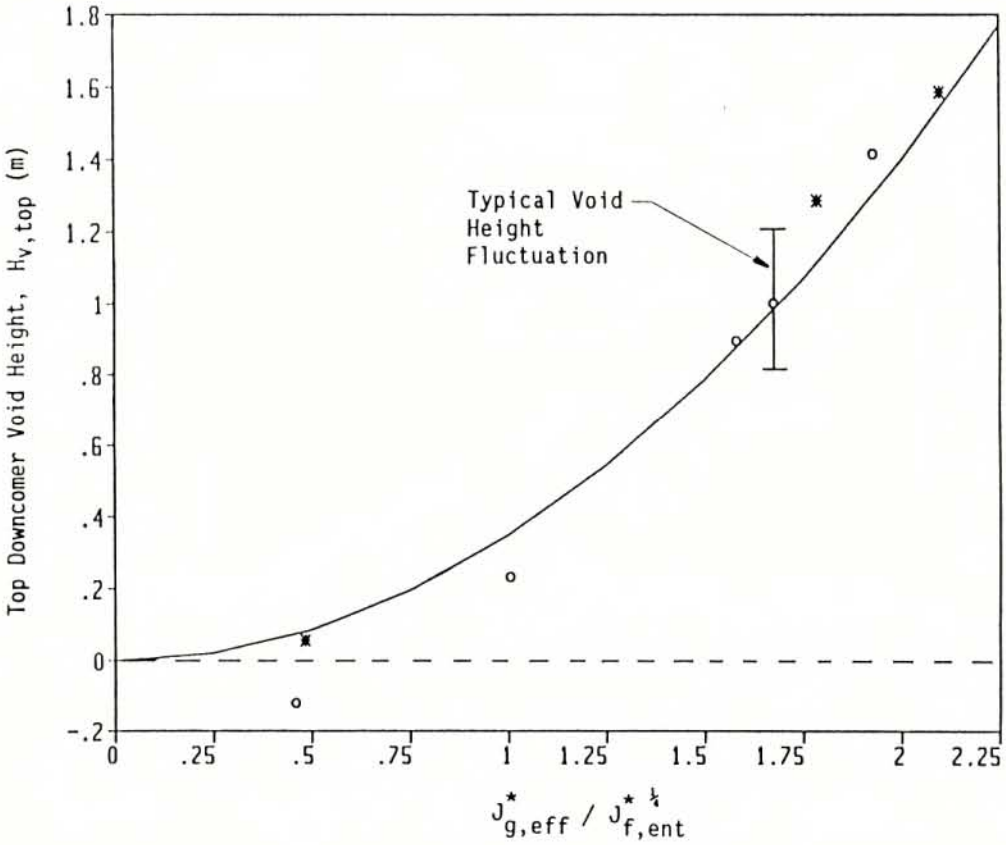
CORRELATION OF TOP DOWNCOMER VOID HEIGHT
ENTRAINMENT AND STEAM FLOW
UPTF TEST 25
FIGURE 4.3-4

4.4 TIE PLATE AND UPPER PLENUM BEHAVIOR TESTS

4.4.1 Rationale of Tests

Countercurrent flow phenomena at the tie plate are different with different types of ECC Systems. For PWRs with cold leg or downcomer injection, countercurrent flow at the tie plate occurs during the reflood phase of an LBLOCA as water entrained by the core steam flow de-entrains in the upper plenum and falls back through the tie plate into the core. (De-entrainment phenomena in the upper plenum and loops are discussed in Section 4.5.) The water is not subcooled.

For PWRs which inject ECC into the hot legs (i.e., combined injection) or upper plenum, countercurrent flow phenomena at the tie plate involve simultaneous two-phase upflow from the core and local downflow of subcooled water to the core. In PWRs with UPI, only low pressure pumped ECC is injected into the upper plenum; consequently, tie plate countercurrent flow occurs only during the reflood portion of an LBLOCA. In combined injection PWRs, accumulator and pumped ECC is injected through the hot leg injection nozzles and tie plate countercurrent flow occurs during all phases of an LBLOCA and some SBLOCA scenarios. Small break phenomena are discussed in Section 4.8.3.

Countercurrent flow phenomena at the tie plate were previously investigated at small-scale test facilities (References E-471, E-931 to E-933, and G-901). These facilities simulated the tie plate using small perforated plates. The maximum size of the facilities was equivalent to one fuel assembly. Using the subscale data, Naitoh, Chino and Kawabe proposed an analytical model based on the pressure balance at the tie plate and the principle of maximum water downflow (Reference E-934).

UPTF integral tests with combined ECC injection indicated that countercurrent flow behavior at the tie plate at full-scale was quite different from that observed at small-scale. Separate effects tests were performed at UPTF to investigate tie plate countercurrent flow.

4.4.2 Scope of Testing

At UPTF, several separate effects tests were performed to investigate countercurrent flow phenomena at the tie plate. Test 10C focused on the countercurrent flow limitation for two-phase upflow from the core. The objective of this test was to determine the core simulator water injection rate necessary to produce a given net flow into the upper plenum (Reference U-903). The other tests (Nos. 10A, 12, 13, 15, 16, 20, 26C) investigated countercurrent flow phenomena associated with ECC injection into the upper plenum or hot legs. The specific objectives of these tests are listed below. The test conditions are summarized in Table 4.1-1.

- Determine the portion of injected ECC which penetrates through the tie plate to the lower plenum.

- Determine the location and magnitude of the water penetration area.

- Determine the collapsed water level and the water distribution in the upper plenum.

- Evaluate the effect of water subcooling at the tie plate on water penetration (Test 10A).

- Determine the delay between initiation of ECC injection and initiation of local water breakthrough.

- Quantify the tie plate countercurrent flow hysteresis effect (Test 15A).

- Evaluate the influence of the momentum of hot leg water plugs on water penetration (Tests 15B, 16).

- Investigate water entrainment into the hot leg and SG simulator for UPI PWRs (Test 20).

The data and quick look reports for these tests are listed in the bibliography for this report (Section 8). Evaluation of these tests by FRG is provided in References G-411, G-906, G-915, and G-925. Separate evaluations of Tests 10C and 20 by the US are documented in References U-453 and U-903, and Reference U-454, respectively.

4.4.3 Summary of Key Results

UPTF Test 10C was a basic test for quantifying the combined CCFL behavior of the core simulator (i.e., steam/water injection nozzles and dummy fuel rods), end box and tie plate. In this test, the steam/water upflow from the core and water fallback through the tie plate were uniform across the vessel. The steam upflow and water fallback rates for Test 10C are plotted in Figure 4.4.-1. For comparison, the corresponding data from the Karlstein Calibration Test Facility (one fuel assembly) are also presented in Figure 4.4-1. The figure shows that the flooding curves for the full-scale and small-scale facilities are nearly the same. Hence, the CCFL at the tie plate for uniform steam/water upflow is independent of scale. The upper plenum collapsed water level did not exceed 0.3 m during Test 10C. The results of Test 10C were used in both the specification of test conditions and evaluation of data from other UPTF tests.

For tests with ECC injection into the hot legs, flow phenomena at the tie plate and in the upper plenum were heterogeneous (i.e., multidimensional). Specifically, as shown in Figures 4.4-2 and 4.4-3, water downflow occurred in discrete regions. The water downflow regions were located in front of intact loop hot legs where injection was occurring. Collapsed water levels in the upper plenum were also multidimensional with increased water levels over the downflow regions.

Figure 4.4-2 includes a plot of saturated water downflow vs. steam upflow based on the results of Test 10A. The figure shows that water downflow increased with decreasing steam flow, as expected. Due to the heterogeneity of tie plate countercurrent flow described above, water downflow with hot leg ECC injection was significantly greater than that predicted by the CCFL correlation determined from Test 10C (Figure 4.4-2).

In Test 12, complete breakthrough of subcooled ECC occurred at core simulator steam injection rates as high as 284 kg/s, the highest steam flow tested. For comparison, the average steam production in a 1300 MWe GPWR during reflood is 150 kg/s. The maximum subcooling measured in the water downflow just below the tie plate was 70 K.

Tests 13, 16 and 26C investigated the effect of core simulator water injection on countercurrent flow phenomena by variations in the ratio of core simulator water and steam injection rates. A Kutateladze plot of the steam upflow vs. water downflow for these tests is provided in Figure 4.4-4 (left graph). The graph shows that, for a given steam flow, water downflow decreases with increasing core simulator water injection rate. Hence, tie plate CCFL and water downflow depend on the total upflow through the tie plate and not simply the steam flow.

Test 26C demonstrated that existence of a two-phase pool of saturated water in the upper plenum at initiation of hot leg ECC injection had only a minor effect on the water breakthrough at the tie plate. Water penetration to the core region followed the ECC delivery to the upper plenum without significant delay. Formation of a local subcooled water pool in the upper plenum combined with a local increase in collapsed liquid level provided the necessary conditions for water breakthrough at the tie plate.

Increasing or decreasing core simulator injection rates had a significant effect on the water breakthrough at the tie plate. In Test 15A the core simulator injection rates were decreased and then increased to investigate this hysteresis effect. During the period of decreasing core simulator injection rates, the water downflow rates in Test 15A (2 ECC injection ports) were the same as Test 13 (3 ECC injection ports), which also had decreasing core simulator upflow rates (Figure 4.4-4, right graph). However, during the period of increasing core simulator upflow rates in Test 15A, water downflow at a given steam upflow rate was much higher than in Test 13. This

hysteresis effect resulted from differences in steam condensation below the tie plate for increasing and decreasing core simulator injection rates. Specifically, condensation was higher during the period with increasing core simulator injection rates because the "initial" downflow of subcooled water for a given injection rate was higher. The higher condensation rate reduced the steam upflow and increased water downflow.

In Test 15B ECC delivery to the upper plenum was intermittent due to plug flow in the hot leg. The time-averaged water breakthrough at the tie plate was not significantly affected by intermittent delivery.

To simulate flow conditions representative of different times in an EM transient (i.e., single LPCI failure) for UPI PWRs, the core simulator and ECC injection rates were lower for Test 20 than for the other tests with hot leg ECC injection. In this test, about 40% of the core simulator steam injection was condensed by the ECC-water; the condensed steam was returned to the core region with the water downflow. Due to steam condensation in the upper plenum, the maximum water subcooling at the tie plate was only 25 K. The collapsed water level in the upper plenum was small (upflow region: 0.05 m, downflow region: 0.2 m).

A Kutateladze-type CCFL correlation was developed to predict water breakthrough with hot leg ECC injection (Reference G-906). In addition, an analytical model for tie plate countercurrent flow was developed based on the pressure balance in the water downflow and two-phase upflow regions; this model shows good agreement with UPTF tests results (Reference G-925).

4.4.4 Conclusions

The UPTF test results revealed tie plate countercurrent flow behavior with hot leg ECC injection is quite different from that without hot leg ECC injection, even with saturated ECC injection. Without hot leg ECC injection, flow phenomena at the tie plate were uniform; for this case, tie plate CCFL was independent of scale. With hot leg ECC injection, flow phenomena at the tie plate and in the upper plenum were multidimensional. Specifically, water downflow through the tie plate and upflow from the core occurred in separated regions; the water downflow regions were located in front of the hot legs. Also, water accumulation in the upper plenum was greater over the downflow regions than over the upflow region. Due to these multidimensional phenomena, water downflow through the tie plate was significantly higher than predicted by the tie plate CCFL correlation based on uniform steam/water flow at the tie plate (i.e., Test 10C).

UPTF: 193 Fuel assemblies (FA)

Karlstein
Calibration Test: 1FA

$\dot{M}_{s, C}$ $\dot{M}_{w, C}$

$\dot{M}_{w,down}$

$\sqrt{K^*_s}$

Karlstein Tests
■ 1.0 kg /s /FA ($\dot{M}_{w,C}$)
● 2.0 kg /s /FA ($\dot{M}_{w,C}$)

UPTF Test 10 C
◇ 0.3 kg /s /FA ($\dot{M}_{w,C}$)
□ 0.8 kg /s /FA ($\dot{M}_{w,C}$)
○ 1.3 kg /s /FA ($\dot{M}_{w,C}$)
△ 2.5 kg /s /FA ($\dot{M}_{w,C}$)

$\sqrt{K^*_{w, down}}$
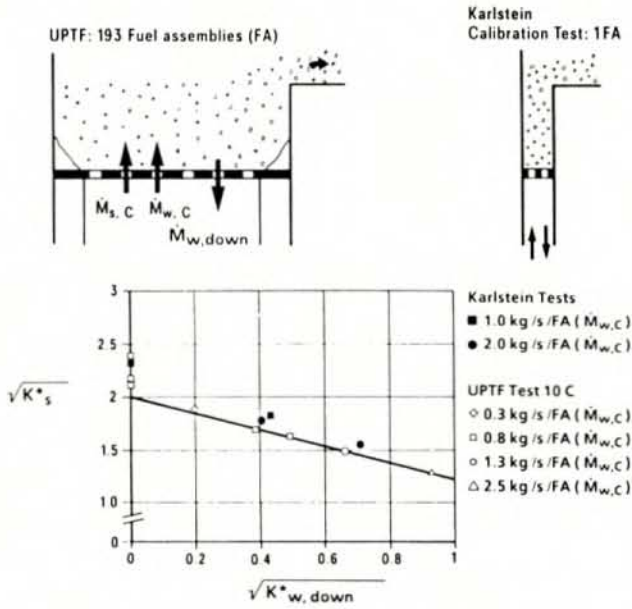
COUNTERCURRENT FLOW OF SATURATED STEAM
AND WATER AT THE TIE PLATE
FIGURE 4.4-1

$\dot{M}_W$ = 2x100 kg/s

HL1   HL2

HL4
Break   HL3

$\dot{M}_W$, $T_W = T_{sat}$

$\dot{M}_{s, C}$ $\dot{M}_{w, down}$

$\dot{M}_W$ = 400kg/s

HL1   HL2

HL4
Break   HL3

Core steam flow $\dot{M}_{s,C}$ kg/s

ECC Injection
O $\dot{M}_W$= 2x100 kg/s
+ $\dot{M}_W$= 1x400 kg/s

CCFL
Correlation

Water downflow , $\dot{M}_{w, down}$
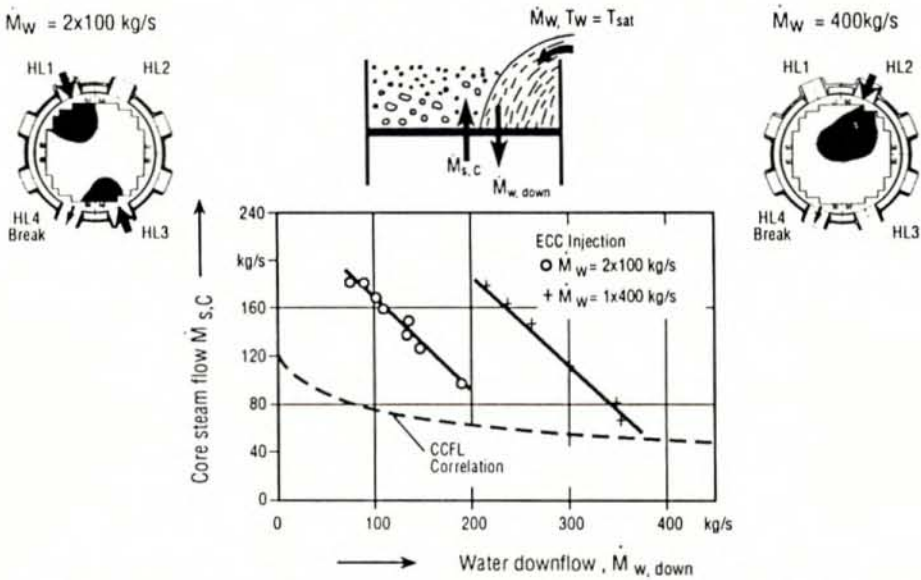
COUNTERCURRENT FLOW OF STEAM AND SATURATED WATER
INJECTED INTO HOT LEG UPTF TEST 10A
FIGURE 4.4-2

ECC injection:
$\dot{M}_W = 3 \times 400$ kg/s

Core simulator steam injection:
$\dot{M}_{S,C} = 284 \Rightarrow 156$ kg/s

Force /N/

0 15 – 1 00 Upward
–0 15 – 0 15 Intermittent
–2 00 – –0 15 Downward
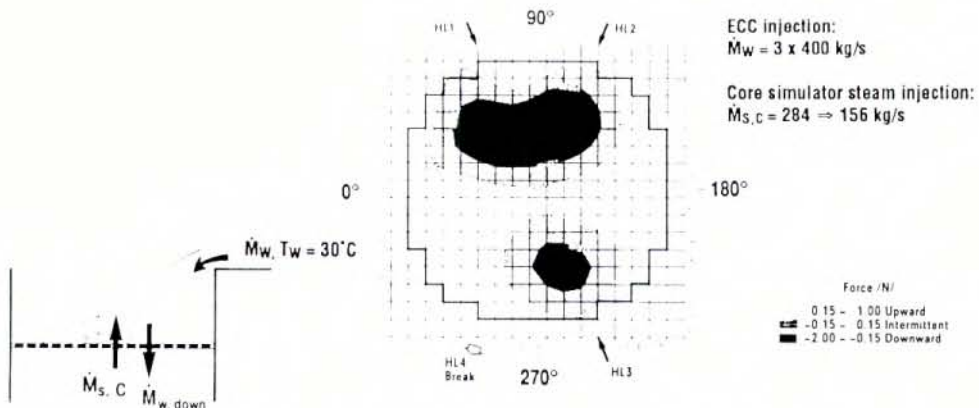
COUNTERCURRENT FLOW OF STEAM AND SUBCOOLED
WATER DURING HOT LEG ECC INJECTION
UPTF TEST 12
FIGURE 4.4-3

$$K^*_i = \frac{\dot{M}_i}{A \quad \sqrt{\rho_i} \quad \sqrt[4]{g \, \sigma \Delta \rho}}$$

$A = 193 \cdot (0.23)^2 \cdot 0.37 \ m^2$

Test	w/s
□ 26C	9
+ 13	4
○ 16A	1 7
◇ 16B	2 7

+ Test 13
(descending only)
○ Test 15A
(descending + ascending)
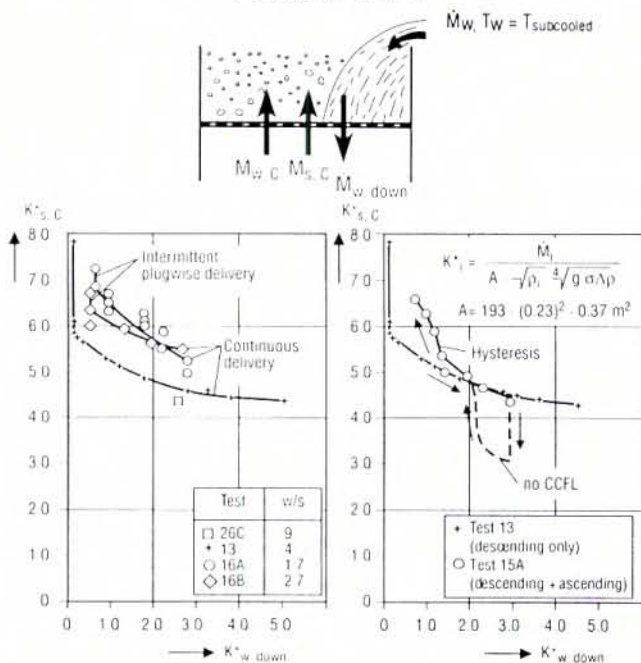
COUNTERCURRENT FLOW OF TWO-PHASE UPFLOW AND
SUBCOOLED WATER DOWNFLOW DURING HOT LEG ECC INJECTION
FIGURE 4.4-4

4.5 UPPER PLENUM/HOT LEG DE-ENTRAINMENT TESTS

4.5.1 Rationale of Tests

In an US/J-type PWR, ECC is injected into the cold legs during the reflood phase of a large cold leg break LOCA. Part of the water injected into the cold legs flows through the downcomer and lower plenum to the core. In the core, the water is either accumulated, vaporized by heat transferred from the fuel rods, or entrained by the steam flow exiting the core. The water entrained by the steam flow is either de-entrained at the tie plate, de-entrained in the upper plenum, or carried over to the hot legs and steam generators with the steam flow. The water which de-entrains in the upper plenum can either fall back to the core or form a pool in the upper plenum.

At this time in the transient, the temperature in the secondary side of the steam generators (SG) is higher than saturation temperature at the primary side pressure. Consequently, entrained water which reaches the U-tubes is evaporated. Vaporization of water in the SG's contributes to steam binding which reduces the core flooding rate and degrades core cooling.

Water accumulation in upper plenum, hot legs and SG inlet plena is beneficial in that it delays carryover to the SG U-tubes. However, it also creates an additional pressure difference which needs to be overcome to vent steam from the core during reflood. In addition, the hot metal surfaces in these regions evaporate water and thereby contribute to steam binding; this contribution to steam binding is small compared to the SG U-tubes.

Data regarding upper plenum accumulation were obtained at the Karlstein One-bundle Test Facility as part of the final calibration tests for the UPTF tie plate flow modules (Reference G-802). Tests related to these phenomena were also performed at SCTF. Preliminary comparisons between SCTF and UPTF test results have shown the collapsed liquid level in the upper plenum was typically much lower at UPTF than at SCTF, even for coupled test conditions.

Testing at UPTF was intended to provide data on de-entrainment and accumulation in the upper plenum and loops for a realistic PWR configuration at full-scale.

4.5.2 Scope of Testing

At UPTF, Tests 10B and 29 (Phases A and B) were performed to investigate de-entrainment in the upper plenum and loops for US/J-type PWRs. The specific objectives for Tests 10B and 29 were as follows.

- Provide separate effects data on mass distribution in the upper plenum, hot legs, SG simulator (SGS) inlet plena, and SGS tube regions for several sets of constant core simulator steam and water injection rates.

- Provide a steam/water flow transient in UPTF which has the same upper plenum level transient as observed in SCTF Test S3-10 (Test 29 only). (Note, tests at SCTF typically had collapsed levels in the upper plenum which were much higher than initial UPTF tests.)

The data and quick look reports for those tests are listed in the bibliography (Section 8). Evaluation of Tests 10B and 29 is documented in References G-411 and U-456.

4.5.3 Summary of Key Results

Upon initiation of core simulator water injection, water de-entrainment and accumulation started first in the upper plenum, then the SGS inlet plena and finally, the hot legs. As the inventories in these regions approached a state of equilibrium, water carryover to the SGS tube regions started. Once the equilibrium states (or inventories) were attained, all the water exiting the core reached the SGS tube regions. The equilibrium states reached in the upper plenum, hot legs and SGS inlet plena were dependent on the core simulator injection rates.

The distribution of water between the upper plenum, hot legs, SGS inlet plena, and SGS tube regions for Tests 10B and 29A is shown in Figures 4.5-1 and 4.5-2, respectively. For Test 10B, which had a maximum core simulator water injection rate of 60 kg/s, the collapsed water level in the upper plenum was small (0.02 to 0.05 m). The upper plenum water level, however, was higher in Test 29A which had higher water injection rates. As shown in Figure 4.5-3, the transient portion of Test 29A was able to achieve water levels similar to the reference SCTF test. However, the core simulator water injection rates necessary to achieve these levels were much higher than typically used in US/J PWR tests at UPTF (i.e., Test 17).

The upper plenum water levels for UPTF Test 29 are compared to data from the Karlstein One-bundle Test Facility (steady-state data only) in Figure 4.5-4. The figure shows good agreement between the full-scale and subscale data. Comparison of UPTF data to ORNL air/water (3 fuel assemblies) and steam/water (1 fuel assembly) showed similar agreement (Reference U-456). Figure 4.5-4 shows that the water level in the upper plenum increased with increasing water injection. The Karlstein data indicate that upper plenum water level increased with decreasing steam injection; this trend was also noted at UPTF. The fact that Karlstein data indicate lower water level for the same water flow but higher steam flow implies the differential pressure in the upper plenum is dominated by accumulated water and not by friction losses.

Based on the UPTF data, semi-empirical correlations were developed to define the relationship between the water accumulation in the upper plenum, hot leg and SGS inlet plena and the core simulator steam and water injection rates (Reference G-411). Also, a methodology was developed for determining water distribution as a function of time. The correlations and methodology are described in Reference U-456.

4.5.4 Conclusions

The UPTF tests showed that accumulation in the upper plenum, hot legs and SGS inlet plena delayed carryover to the SGS tube regions by approximately 30 seconds.

UPTF Test No. 10B
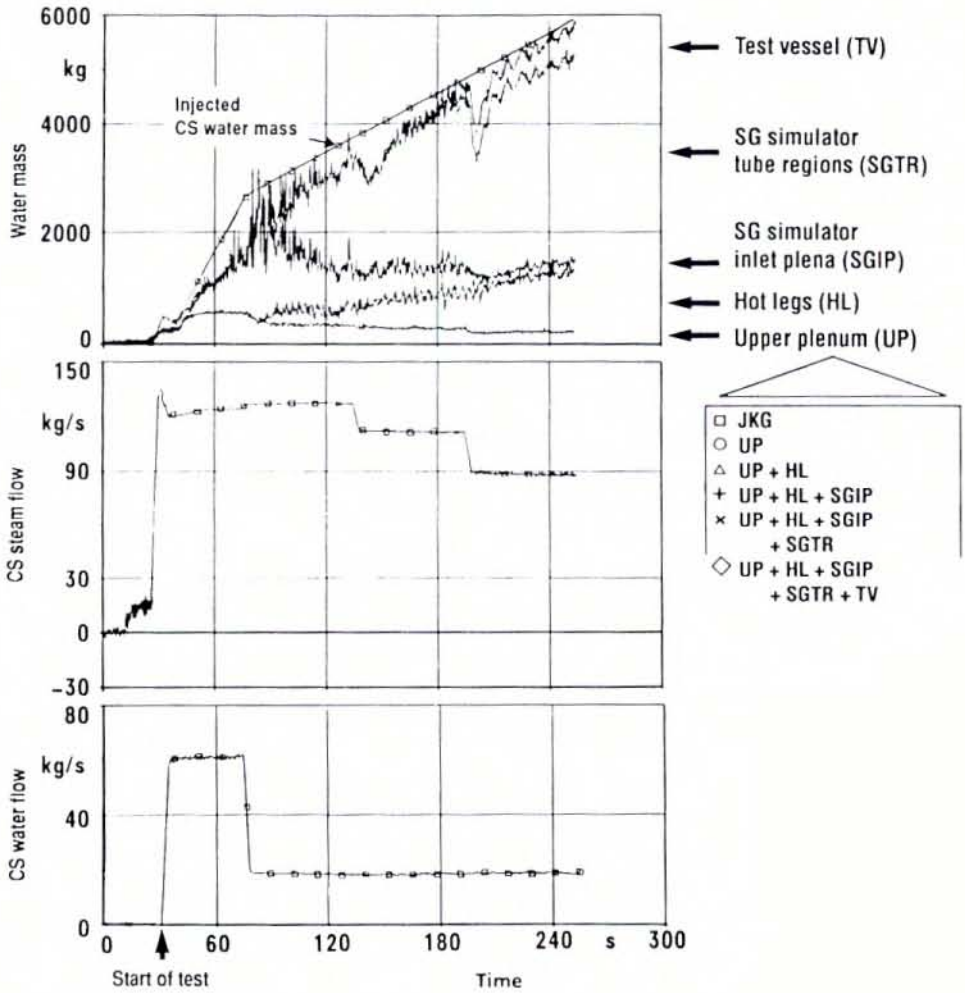
WATER ACCUMULATION IN UPPER PLENUM,
HOT LEG, STEAM GENERATOR SIMULATOR
INLET PLENA AND TUBE REGIONS
UPTF TEST 10B
FIGURE 4.5-1
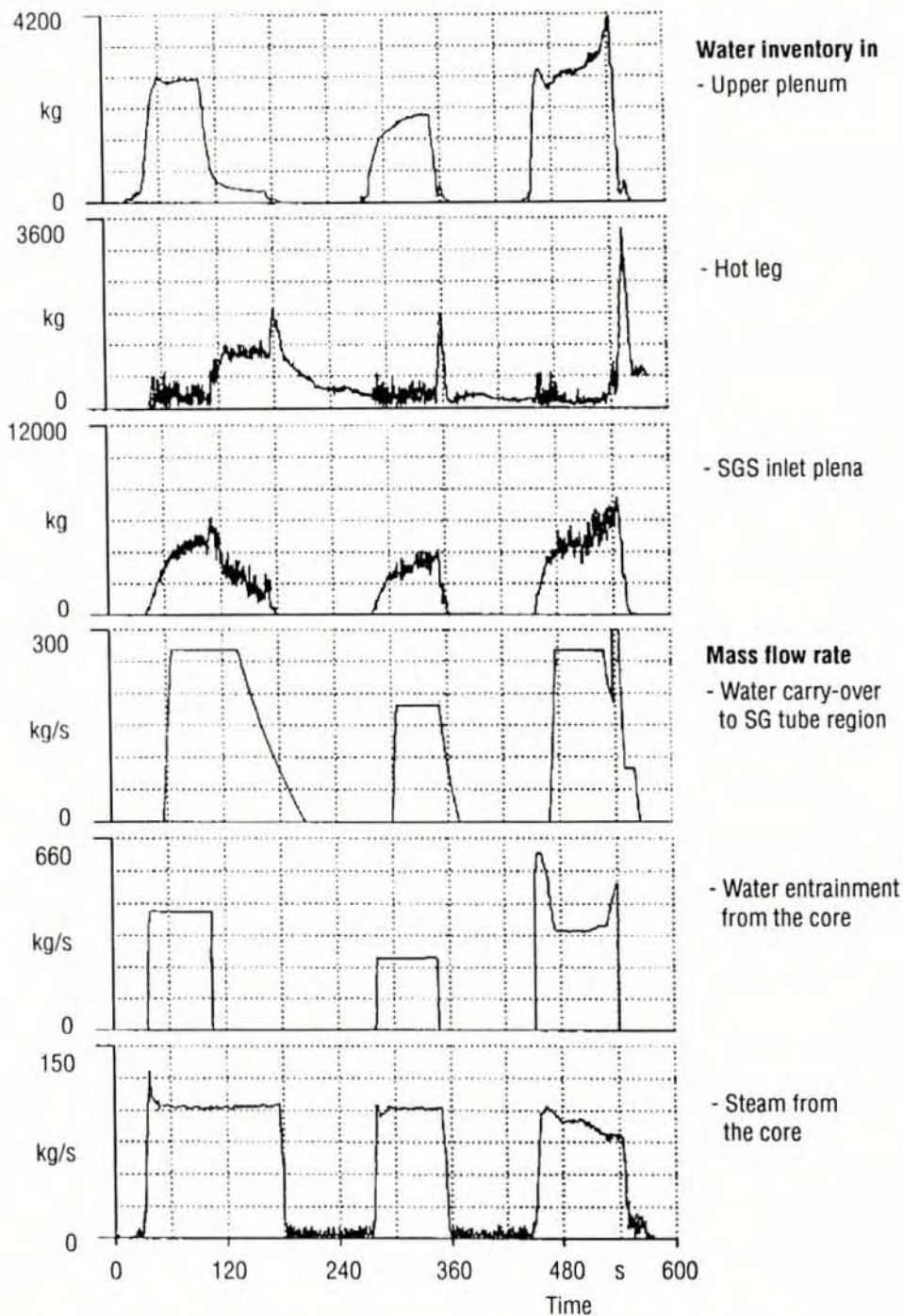
ACCUMULATION OF WATER MASS IN INDIVIDUAL COMPONENTS
UPTF TEST 29A
FIGURE 4.5-2

COMPARISON OF UPPER PLENUM WATER LEVELS
FOR UPTF AND SCTF TESTS
FIGURE 4.5-3
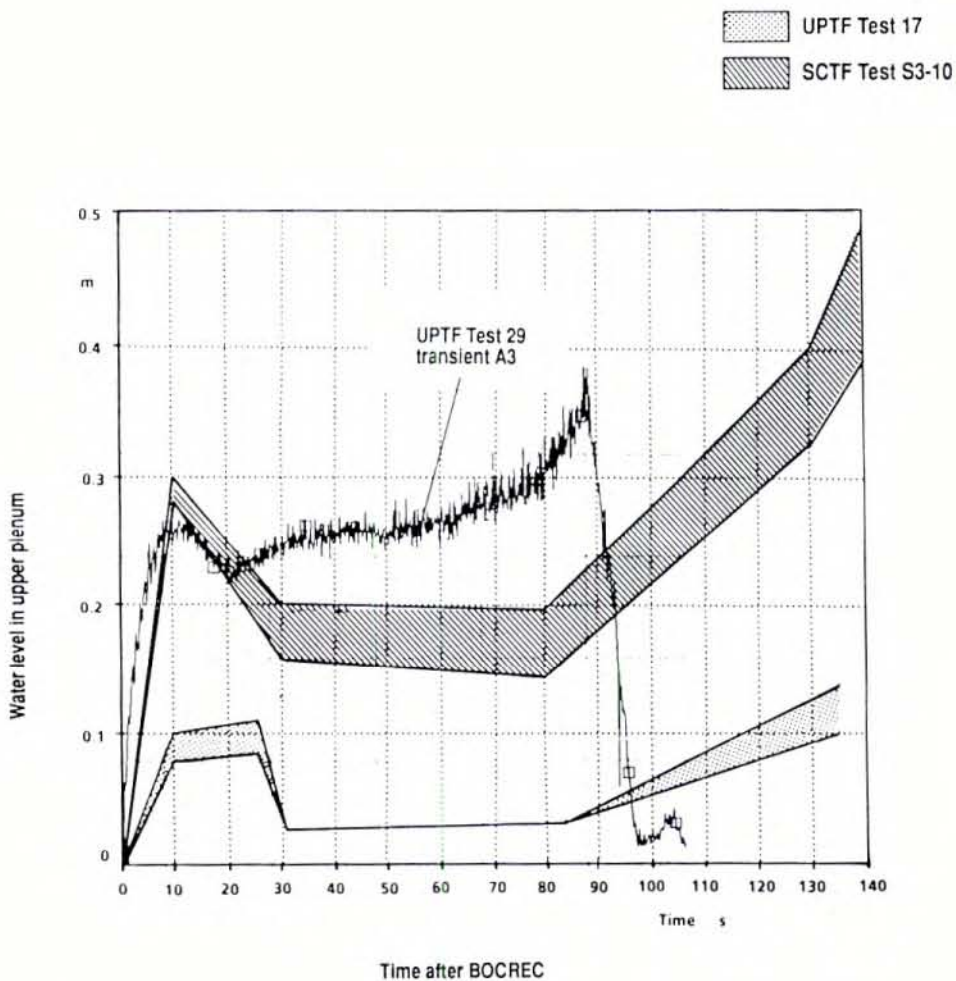
Note: The core simulator steam and water injection rates for UPTF Test 17 were coupled to the measured flow conditions for SCTF Test S3-10. Transient A3 of UPTF Test 29 was essentially a repeat of Test 17 but with much higher core simulator water injection rates.

Water level in upper plenum m

0.5
0.4
0.3
0.2
0.1
0

$\dot{M}_{w,UPTF} = 193 \times \dot{M}_{w,FA}$

0   1   2   3   4   5   6   kg/s   7

Tie plate water flow rate per FA $\dot{M}_{w,FA}$

UPTF Test No. 29, Phases A and B (RUN 212):

p = 3 bar

■ 100 kg/s core simulator steam flow

Karlstein Calibration Tests (CAL 1 - CAL 177):

p = 2.5 bar

▲ 0.4 to 0.49 kg/s/FA steam flow
   (corresponding to 85 kg/s in UPTF core simulator)

● 0.6 to 0.65 kg/s/FA steam flow
   (corresponding to 120 kg/s in UPTF core simulator)

COMPARISON OF UPPER PLENUM WATER LEVELS
IN KARLSTEIN CALIBRATION TESTS AND UPTF TEST 29
FIGURE 4.5-4

4.6 LOOP BEHAVIOR TESTS

4.6.1 Rationale of Tests

During a LOCA, subcooled ECC interacts with steam in the primary loops near the injection nozzles. The steam is partially or completely condensed by the ECC. The extent of condensation strongly affects the flow regime and the delivery of ECC to the vessel. Depending on the flow conditions, water plugs which completely fill the pipe cross-section can form.

Plug formation in the cold legs was previously investigated at several subscale facilities ranging in size from 1/20-scale to 1/3-scale (References E-435, E-436, E-912, E-916 and J-904). These tests indicated that plug flow can be either steady or oscillating.

Hot leg plug formation was investigated in subscale tests (1/10- and 1/5-scale) performed by Creare (Reference E-434). The tests revealed complete ECC reversal and plug formation can occur at higher steam flows and water injection rates. These test results supported the analytical model of Daly and Harlow (Reference E-914) which predicted the flow conditions at which reversal of ECC would occur in the hot leg of a GPWR.

Finally, TRAC calculations for both cold leg injection PWRs and combined injection PWRs have predicted plug formation in reactor coolant piping during LBLOCA conditions (References U-701, U-702, U-703, U-707, U-747, and U-748).

UPTF testing was intended to investigate loop flow patterns at full-scale and determine the thermal-hydraulic boundary conditions for the transition between the different flow regimes.

4.6.2 Scope of Testing

UPTF Tests 8, 9, 25B, and 26 investigated the flow pattern in the reactor coolant loops for typical LOCA flow conditions. These tests included ECC injection into only the cold legs, only the hot legs, and both the hot legs and cold legs. The test conditions are summarized in Table 4.1-1.

The data and quick look reports for these tests are listed in the bibliography of this report (Section 8). These tests have been evaluated by both FRG and US. The FRG evaluation, which covers all of the tests, is documented in References G-411 and G-911; the US evaluation, which covers only the tests related to cold leg injection PWRs is provided in Reference U-458.

4.6.3 <u>Summary of Key Results</u>

In the UPTF tests, three different flow regimes were observed in the reactor coolant piping; specifically, stable plug flow, stratified flow and unstable plug flow. Each of these flow regimes is described below.

- In stable plug flow, a quasi-steady water plug formed adjacent to the ECC injection nozzle. In the cold legs, the plugs either remained stationary or oscillated upstream and downstream from the injection nozzle. ECC delivery to the downcomer was continuous with stationary plugs and fluctuated with oscillating plugs.

  For high steam flows in the hot legs, the ECC flow was completely reversed and the plug grew toward the steam generator simulator. The plug was discharged into the upper plenum when either the hydrostatic head of the plug or the pressure increase due to steam injection in the SGS exceeded the loop differential pressure. In this case, ECC delivery to the upper plenum fluctuated over time.

- In stratified flow, steam flowed in the top part of the pipe and water flowed along the bottom of the pipe. In the cold legs, the steam and water flows were cocurrent and ECC delivery to the downcomer was continuous.

  In the hot legs, the steam and water flows were countercurrent. Stratified flow with continuous delivery occurred at low steam flows. At high steam flows, the water flow was reversed by the steam flow and delivery of ECC to the upper plenum fluctuated.

- Unstable (or intermittent) plug flow was characterized by cyclic formation and decay of water plugs in the piping; i.e., the flow regime alternated between plug flow and stratified flow. The cyclic formation and decay of water plugs resulted in large oscillations in pressure and flow conditions.

Figures 4.6-1 and 4.6-2 are plots of steam flow vs. condensation potential of the ECC which indicate the flow regime established under different conditions. A discussion of the basis for these figures is provided in Reference G-411. Included on each figure is a line which shows the condition when the condensation potential and steam flow are equal (i.e., a thermodynamic ratio, R_T, of one). These figures show that plug flow (either stable or unstable) occurred only when the condensation potential of the ECC exceeded the steam flow (i.e., $R_T > 1$). The data points with high condensation potentials correspond to high ECC injection rates typical of accumulator injection.

When the condensation potential was less than the steam flow (i.e., $R_T < 1$), flow in the piping was stratified to provide a vent path for the uncondensed steam flow. As shown in Figure 4.6-1, stratified flow occurred in the cold legs for some cases where

R_T slightly exceeded 1.0. In these cases, thermal stratification of the water layer in the bottom of the cold leg limited condensation and prevented plug formation. The low condensation potentials associated with stratified flow correspond to low ECC injection rates typical of LPCI injection in US/J PWRs.

Figures 4.6-1 and 4.6-2 also indicate plug flow was stable at high steam flows and unstable at low steam flows. According to calculations performed by Siemens, at low steam flows, the plug decayed shortly after it formed because the momentum of the mean steam flow was not sufficient to maintain a stable water plug. Alternate formation and decay of water plugs resulted in steam flow oscillations.

Siemens calculated the minimum steam flow for stable plug flow assuming that a plug is stable when the flow force acting on the end of the plug balances or exceeds the hydrostatic pressure on the plug end (References G-411 and 911). The calculations predict that, for a given system pressure, the minimum steam mass flux for stable plug flow in the cold legs is dependent on the pipe diameter but is independent of the condensation potential of the ECC. However, the minimum steam mass flux for stable plug flow in the hot legs does depend on the condensation potential. The calculations also predict that there is a minimum steam condensation potential at which the momentum flux of the steam flow is sufficient to form a plug. For steam condensation potentials less than this minimum value, the calculations indicate that stratified flow will occur, even if R_T is greater than 1.0. The results of these calculations are compared to the UPTF data in Figures 4.6-1 and 4.6-2. As shown in these figures, the calculated minimum steam flow for stable plug flow is consistent with the data.

4.6.4 Conclusions

The UPTF tests demonstrated:

·   Plug flow occurred with high ECC injection rates typical of accumulator injection.

·   Stratified flow occurred with low (i.e., LPCI) ECC injection rates typical of LPCI in US/J PWRs.

·   The flow regime established in the loops was determined by the instantaneous thermal-hydraulic boundary conditions in the loops.

·   ECC delivery to the vessel fluctuated for plug flow.

·   For stratified flow in the cold legs, ECC delivery to the downcomer was continuous. However, for stratified flow in the hot legs, ECC delivery to the upper plenum was continuous at lower steam flows and fluctuated at high steam flows.
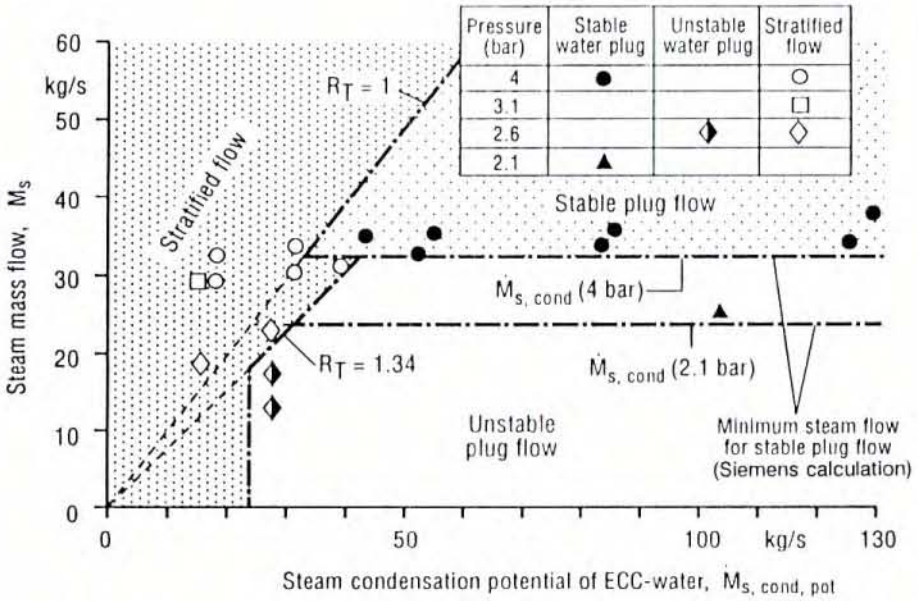
FLOW PATTERNS FOR COCURRENT FLOW IN THE COLD LEG
FIGURE 4.6-1
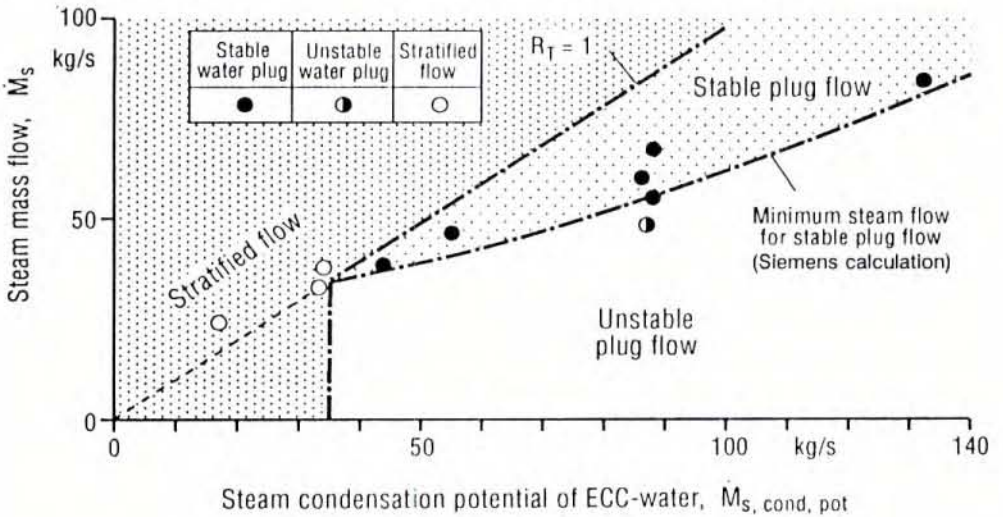
FLOW PATTERNS FOR COUNTERCURRENT FLOW IN THE HOT LEG
FIGURE 4.6-2

4.7 SEPARATE EFFECTS TESTS WITH VENT VALVES

4.7.1 Rationale of Tests

Babcock & Wilcox (B&W) and Brown Boveri Reaktor (BBR -- now ASEA Brown Boveri or ABB) PWRs are different from other US/J-type PWRs and GPWRs in that ECC is injected through nozzles in the downcomer and there are vent valves in the core barrel. The purpose of these vent valves is to provide an alternate steam flow path for LOCA conditions. Flow through the vent valves can have a significant impact on LOCA behavior.

During the end-of-blowdown (EOB), steam flows up the downcomer to escape out the broken cold leg. This upflow limits ECC penetration to the lower plenum. With vent valves, the steam upflow in the downcomer is reduced because a portion of the steam in the reactor vessel flows through the vent valves rather than around the bottom of the core barrel. The reduction in steam upflow tends to result in increased ECC delivery to the lower plenum.

During reflood, steam generated in the core vents to containment via the downcomer and broken cold leg. In PWRs without vent valves, steam enters the downcomer from the intact loop cold legs. In the PWRs with vent valves, steam enters the downcomer from the vent valves and possibly also the intact cold legs. Flow through the vent valves bypasses the intact loops and tends to reduce the core-to-downcomer differential pressure. Also, vent valves influence the steam flow distribution in the downcomer which can affect water entrainment from the downcomer out the broken cold leg.

ECC penetration during EOB and downcomer entrainment during reflood were evaluated in other UPTF tests with cold leg and downcomer ECC injection and no vent valves (see Sections 4.2 and 4.3). Tests with vent valves were performed at the BBR Pie Wedge Vent Valve Test facility, a 1/8-scale facility. The BBR tests focused on steam/water flow phenomena in the upper plenum. The UPTF vent valve separate effects tests were intended to be counterparts to the UPTF tests without vent valves and to the subscale BBR tests.

4.7.2 Scope of Testing

The UPTF vent valve separate effects tests consisted of Tests 22 and 23. These tests investigated EOB and reflood phenomena for downcomer ECC injection with vent valves. The ID of the downcomer injection nozzles was reduced part way through the tests by the installation of thermal sleeves. The conditions for each test are summarized in Table 4.1-1. Each test is described briefly below.

- Test 22 studied ECC penetration to the lower plenum for downcomer ECC injection with vent valves. In most phases, steam and ECC were injected at near saturation temperature to focus on CCFL; however, one phase involved subcooled ECC. ECC injection location was also varied in this test. Phases B and C were repeated after installation of the thermal sleeves.

- Test 23, which consisted of three phases, investigated reflood phenomena for downcomer ECC injection with vent valves. Phase A (or Test 23A) simulated typical reflood conditions for an ABB/BBR raised loop PWR. (Test 21 Phase C also provided information on the effect of vent valves by using conditions similar to Test 23A but with vent valves locked shut.) Phases B and C (or Tests 23B and 23C [1]) studied the relationship between steam flow in the downcomer, downcomer water level, and entrainment out the broken cold leg using flow conditions typical of B&W PWRs. Flow through the vent valves was single-phase steam flow in Phase B and two-phase (steam with entrained water) in Phase C. Phase C also provided data on water de-entrainment in the upper plenum.

UPTF Test 21 investigated ECC penetration to the lower plenum during EOB and downcomer entrainment during reflood for downcomer ECC injection without vent valves (see Sections 4.2 and 4.3, respectively). The effect of vent valves on these phenomena can be evaluated by comparing the results of Test 21 to the results of Tests 22 and 23.

The data and quick look reports for these tests are listed in the bibliography (Section 8). Evaluations of these tests are documented in References G-411 and U-460.

4.7.3 Summary of Key Results

The results of the vent valve separate effects tests are summarized below by the phenomena investigated; specifically, ECC penetration during EOB, downcomer entrainment during reflood, and system behavior in an ABB/BBR raised loop PWR during reflood.

ECC Penetration during End-of-Blowdown

Countercurrent flow phenomena in the downcomer were heterogeneous with downcomer injection and vent valves. Specifically, ECC injected through the nozzle near the break was largely bypassed out the break while ECC injected through the nozzle away from the break penetrated to the lower plenum. The results of Test 22 are plotted in Figure 4.7-1. The figure shows essentially complete bypass of ECC

---

[1] Phase C of Test 23 and Phase A of Test 22 were combined into a single test run. In Table 4.1, Test 23C is denoted as the second portion of Test 22A.

injected near the break for steam injection rates as low as 100 kg/s. Conversely, nearly all ECC injected in the nozzle away from the break penetrated to the lower plenum for steam injection rates as high as 300 kg/s. As discussed in Section 4.2, similar heterogeneous behavior was noted in tests with cold leg injection (Tests 4, 5, 6 and 7) and in tests downcomer injection and no vent valves (Tests 21A and 21B).

The results of Test 22 also show that the installation of thermal sleeves in the injection nozzles had a negligible effect on ECC penetration.

The results of Tests 21A and 21B are included on Figure 4.7-1. For similar steam injection rates and ECC subcooling, ECC penetration to the lower plenum was higher with the vent valves free to open (Test 22) than with the vent valves closed (Test 21). This difference in ECC penetration is due to differences in the amount of steam upflow in the downcomer and the steam flow pattern in the top of the downcomer. Specifically, with the vent valves free to open, the steam upflow was lower because a significant portion of the steam injection (about 34%) flowed through the vent valves. The vent valve flow created a significant circumferential flow in the downcomer which appeared to reduce/redirect downcomer upflow and facilitate ECC penetration.

Figure 4.7-2 compares downcomer injection with vent valves to cold leg injection. The figure shows that ECC penetration to the lower plenum with the two systems is similar due to complete delivery of ECC injected away from the break.

Entrainment from Downcomer during Reflood
Water entrainment out the broken cold leg was high in Tests 23B and 23C. Specifically, even at relatively low water levels in the downcomer, entrainment out the break exceeded the ECC injection rate through one nozzle. Since thermocouples directly below the downcomer injection nozzle near the break measured no subcooling, it can be concluded that all ECC injected through this nozzle was entrained directly out the break. This substantial entrainment prevented the downcomer level from increasing to a steady-state value during some test phases. As discussed in Section 4.3, similar behavior was observed in Test 21D with closed vent valves.

Figure 4.7-3 is a plot of downcomer void height (i.e., the difference between the collapsed water level and the bottom of the cold leg) versus steam flow in the downcomer. Included in the plot are data from Tests 21D, 23B, 23C and 25A (cold leg injection) with similar steam and ECC flow conditions. This figure shows that downcomer void height increased as the steam flow increased. Note that the downcomer void height was higher for downcomer injection without vent valves (Test 21D) than downcomer injection with vent valves (Test 23B). However, the void height for downcomer injection with vent valves was similar to or only slightly exceeded that for cold leg injection (Test 25A). The data for Test 23C (downcomer ECC injection with two-phase flow through the vent valves) do not follow the same

trend as the other tests; instead, the void height was essentially constant near the maximum values observed in the tests. This suggests the water flow through the vent valves has an effect similar to that of increased steam flow.

Reflood Behavior in an ABB/BBR Raised Loop PWR
For the discussion below, it should be noted that the geometry of the ABB/BBR raised loop design, especially the loop arrangement and the once-through steam generators, are not precisely simulated in UPTF.

Steam/water flow phenomena in the upper plenum and loops for Test 21C were similar to that described in Section 4.5. Specifically, water entrained out of the core accumulated in the upper plenum, hot legs, and SGS inlet plena, and was carried over to the SGS tube regions. Within a few seconds of initiation of core simulator injection, accumulation in the upper plenum reached an equilibrium value. This equilibrium value increased with increased water injection. At low steam flows (<30 kg/s) water accumulated in the hot legs; however, at higher steam flows the momentum of the flow through the hot leg was sufficient to prevent accumulation. Water was carried over to the SGS tube regions at all steam flows tested.

The steam flow through the intact loops flowed around the downcomer and out the broken cold leg. Water in the downcomer was entrained out the break by this steam flow. At high steam injection rates, most of the ECC injected through the nozzle near the break was entrained directly out the break. The downcomer water level was higher in front of the ECC injection nozzles due to the local decrease in pressure from steam condensation at the injection nozzles.

Overall steam/water flow phenomena in Test 23A, in which the vent valves were free to open, were similar to that described above for Test 21C; however, in Test 23A a substantial portion of the two-phase flow from the core flowed through the vent valves rather than the loops. Due to the decrease in loop steam flow the core-to-downcomer differential pressure was lower; consequently, the core water level was higher in Test 23A than Test 21C. The lower loop steam flows also resulted in more accumulation in the upper plenum and hot legs, and less carryover to the SGSs. At low core simulator steam injection rates, there was no water carryover to the SGSs.

Injection of a small amount of nitrogen with the ECC to simulate dissolved nitrogen in ACC water significantly affected thermal-hydraulics in the downcomer and broken cold leg. Specifically, steam flowed from the containment simulator through the broken cold leg to the downcomer when nitrogen was not injected (i.e., Test 21C) but not when nitrogen was injected (i.e., Test 23A). Steam backflow from the containment simulator occurred when nitrogen was not injected because the high condensation rates reduced the pressure in the downcomer. Nitrogen injection suppressed condensation which increased the pressure in the downcomer and prevented backflow from the containment simulator.

4.7.4 Conclusions

The conclusions based on the UPTF vent valve separate effects tests are listed below by phenomena investigated.

ECC Penetration during End-of-Blowdown

- ECC penetration to the lower plenum during EOB was heterogeneous with complete bypass of the ECC injected through the nozzle near the break and penetration of ECC injected through the nozzle away from the break.

- The reduction of injection nozzle diameter by installation of thermal sleeves did not significantly affect ECC penetration.

- For similar steam injection rates and ECC subcooling, ECC penetration was higher with the vent valves free-to-open than with the vent valves closed because a significant portion of the steam flowed through the vent valves.

- For the range of steam flows tested, water delivery to the lower plenum for ECC injection through two nozzles in the downcomer with vent valves free-to-open was comparable to that for ECC injection through nozzles in the three intact cold legs with the vent valves locked shut.

Downcomer Entrainment during Reflood

- Under reflood conditions all ECC injected through the nozzle near the broken cold leg was entrained directly out the break.

- For similar steam and ECC flow conditions, the downcomer void height with the vent valves free-to-open was significantly less than with the vent valves closed.

- For similar steam and ECC flow conditions, the downcomer void height for downcomer injection with the vent valves free-to-open was similar to that for cold leg injection with the vent valves shut.

Reflood Behavior in an ABB/BBR Raised Loop PWR

- Flow through the vent valves reduced steam flow through the loops and therefore water carryover to the SGS tube regions.

- The reduction in loop steam flow resulted in a decrease in the core-to-downcomer differential pressure which is favorable for core cooling.

- Injection of a small amount of nitrogen with the ECC to simulate dissolved nitrogen in the ACC water affected thermal-hydraulic behavior in the downcomer by decreasing steam condensation.

600 kg/s

Steam injection rate $\dot{M}_s$

500

400

300

200

100

0

DC injection into 2 nozzles
+ UPTF Test 22 with VV no TS
× UPTF Test 22 with VV and TS
△ UPTF Test 21 no VV no TS

DC injection into nozzle at 0°
▽ UPTF Test 22 with VV no TS
□ UPTF Test 21 no VV no TS

DC injection into nozzle at 180°
▲ UPTF Test 22 with VV no TS

56K $\Delta T = 117K$ 112K   53K   +
112K 52K × +

37K ×+
$\Delta T = 37 K$

845–912 kg/s 1   2 835–910 kg/s
0° 180°
Break 3

30K   26K   ▲
26K

Complete delivery from one DC injection nozzle

0   200   400   600   800   1000   1200   1400 kg/s 1600

Water delivery

$\dot{M}_{w, df}$

VV = Vent valve
TS = Thermal sleeve
DC = Downcomer

EFFECT OF VENT VALVES ON WATER DELIVERY
TO LOWER PLENUM IN COUNTERCURRENT FLOW
FOR DOWNCOMER INJECTION

FIGURE 4.7-1

Legend (as labeled in figure):

- Dimensionless steam injection rate $(J_s^*)^{1/2}$ (y-axis)
- Dimensionless water downflow rate $(J_{w,df}^*)^{1/2}$ (x-axis)

Loop injection

ECC CL 1   ECC CL 2
Break
CL 3 ECC

Downcomer injection

1   2
ECC ← → ECC
Break   3

Loop injection into 3 cold legs

- ● UPTF Test 6, $\Delta T = 59–26$ K
- ■ UPTF Test 7, $\Delta T = 12/2$ K
- ▼ UPTF Test 5B, $\Delta T = 115$ K

Downcomer injection into 2 nozzles with VV

- △ UPTF Test 22, $\Delta T = 112$ K
- ◇ UPTF Test 22, $\Delta T = 53–26$ K
- ◁ UPTF Test 22, $\Delta T = 52/37$ K (with thermal sleeves)

112 K
115 K

Complete delivery from one DC injection nozzle

Complete delivery from cold legs (CL) 2 and 3

VV = Vent valve
ECC = Emergency core coolant
DC = Downcomer

COMPARISON OF DIMENSIONLESS WATER DELIVERY
FOR ECC INJECTION INTO COLD LEGS AND
DOWNCOMER WITH VENT VALVES

FIGURE 4.7-2
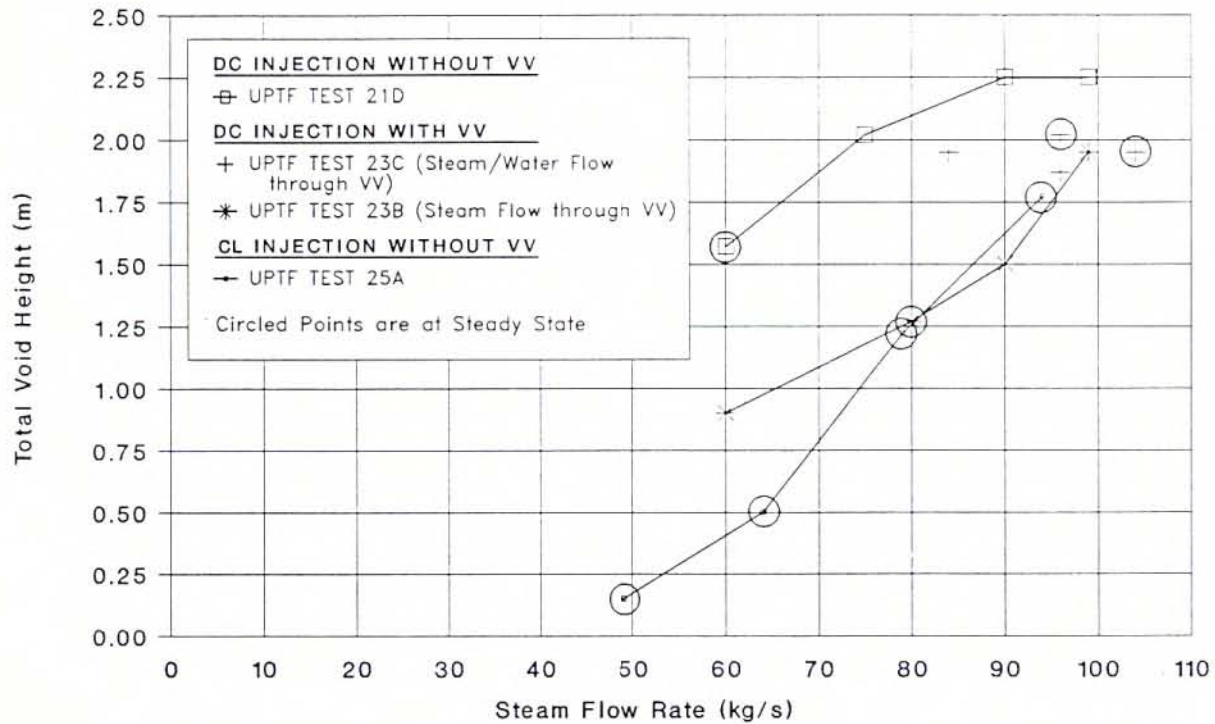
COMPARISON OF DOWNCOMER VOID HEIGHT
FOR DOWNCOMER AND COLD LEG ECC INJECTION
FIGURE 4.7-3

4.8 SMALL BREAK LOCA TESTS

In UPTF three tests were performed to investigate selected phenomena which can occur in a small break LOCA (SBLOCA). These phenomena included:

- Fluid-fluid mixing in the cold leg and downcomer (Test 1).

- Countercurrent flow in the hot leg (Test 11).

- Steam/water countercurrent flow phenomena at the tie plate during high pressure ECC injection (Test 30).

4.8.1 Fluid-fluid Mixing

4.8.1.1 Rationale of Test

This test investigated water mixing phenomena which occur in the downcomer of a PWR as a result of high pressure coolant injection (HPCI) into the cold leg at a time when the reactor coolant system is at an elevated temperature. This mixing relates to the overall reactor safety issue of pressurized thermal shock (PTS). In PTS, the concern is over simultaneous occurrence of:

- High pressure

- Sudden, localized reduction of reactor vessel wall temperature

- Reduced reactor vessel metal ductility due to prolonged irradiation

- Existing flaw in weld metal of reactor vessel

Hypothesized scenarios by which these conditions could occur simultaneously include inadvertent HPCI actuation and an SBLOCA with HPCI. A key concern is how the injected water mixes with primary coolant. In general, if the mixing is good, a slow and drawn-out cooldown occurs, which provides sufficient time to prevent the development of significant temperature gradients in the vessel wall. Good mixing occurs when there is flow (even natural circulation) in the loops.

In certain SBLOCA scenarios, however, it is possible to create a stalled flow condition in one or more loops, which creates the potential for "ECC-streaming" through the cold leg and into the downcomer (Figure 4.8-1). This stream of ECC could possibly cool local regions of the vessel wall, leading to wall temperature gradients and to a reduction of wall temperatures. The extent of this cooldown depends on the natural mixing which occurs between the ECC and the hot, stagnant primary coolant. This mixing was investigated analytically and experimentally in several scaled test facilities

and found to be significant; i.e., the cold stream of water reaching the reactor vessel is substantially heated in the cold leg pipe, and the plume entering the vessel is quickly dissipated in the downcomer (Reference E-925).

A single UPTF test was performed to obtain full-scale data on the mixing of a cold stream of ECC water injected in the cold leg with stagnant hot primary fluid. Of particular interest were the temperature distributions and associated mixing obtained in the downcomer region. The UPTF full-size geometry is suitable to realistically simulate this complete three-dimensional mixing region.

4.8.1.2 Scope of Testing

UPTF Test 1 consisted of five phases, or test runs. For each phase, the primary system was initially filled with hot water and cold ECC was injected into a single cold leg. Since there was no heating during the test, each phase was a gradual cooldown of the entire system. The range of ECC injection rates tested covered the range of HPCI flows for US/J PWRs and GPWRs. The test conditions are summarized in Table 4.1-1.

Pre-test evaluation of the side-mounted ECC injection pipe in UPTF and GPWRs showed that mixing was poor and not typical of US/J PWRs which inject ECC into the top of the cold leg. To simulate mixing phenomena more typical of US/J PWRs, a modified ECC injection nozzle was used in UPTF (Figure 4.8-2). The design of the modified nozzle was developed by the USNRC (Reference U-931).

The data and quick look reports for UPTF Test 1 are provided in References G-001 and G-201, respectively. Evaluation of the test results is documented in Reference U-457.

4.8.1.3 Summary of Key Results

Figure 4.8-3 shows the fluid and wall temperatures measured in the cold leg for two phases of Test 1. These measurements show that flow in the cold leg was thermally stratified. Specifically, a cold stream flowed along the bottom of the cold leg from the injection nozzle to the downcomer and a hot stream flowed along the top of the cold leg countercurrent to the cold stream. While the temperature difference between the hot and cold streams increased with increasing ECC injection, the cold stream entering the downcomer was significantly warmer than the ECC injection for all ECC flows tested (Figure 4.8-3).

Figure 4.8-3 also indicates that the cooldown of fluid in the cold leg between the injection nozzle and the pump simulator followed a "well mixed" transient; i.e., the fluid temperatures were relatively uniform for ECC flow rates greater than 20 kg/s.

The cold stream from the cold leg penetrated down the downcomer as a plume. Temperature measurements in the downcomer indicate that, due to mixing in the cold legs and at the cold leg/downcomer interface, the temperature of the plume was significantly higher than the temperature of the ECC injection. Also, the plume decayed within approximately four cold leg diameters (Figure 4.8-4).

4.8.1.4 Conclusions

The UPTF tests showed that due to mixing in the cold leg, the cold stream entering the downcomer from the cold leg was significantly warmer than the ECC injection. Also, the plume of cold water in the downcomer decayed quickly.

4.8.2 Hot Leg Countercurrent Flow

4.8.2.1 Rationale of Test

Reflux condensation refers to the cooling mode of an SBLOCA in which steam is the continuous phase above the reactor core and in the primary loops. Heat is transferred from the core to the secondary side of the steam generators by evaporation of the water in the core and subsequent condensation of that steam in the steam generator U-tubes. Part of the condensate returns to the reactor vessel by flowing countercurrent to the steam flow in the hot legs (Figure 4.8-5). Depending on the countercurrent flow limitation (CCFL) the steam flow may inhibit the water flow to the reactor.

Countercurrent flow in horizontal pipes was studied at subscale facilities and in small diameter pipes. Testing at UPTF was intended to provide CCFL data for full-size reactor cooling piping.

4.8.2.2 Scope of Testing

The objectives of Test 11 were to investigate hot leg CCFL at full-scale and to verify the margin between the PWR reflux condensation conditions and the flooding limit. Test 11 consisted of 15 separate test runs. Fourteen test runs mapped out the CCFL curve over a range of steam flows at two system pressures and one test run simulated representative PWR SBLOCA flow conditions. Countercurrent flow in the UPTF hot leg was established by injecting water in the inlet plenum of a steam generator simulator and steam in the core simulator (Figure 4.8-6). The test conditions are summarized in Table 4.1-1.

The data and quick look reports for Test 11 are provided in References G-011 and G-211, respectively. Evaluation of the results of this test are documented in References G-411, U-452 and U-904.

4.8.2.3 Summary of Key Results

Figure 4.8-6 is a steam flow versus countercurrent water flow plot of the results of
Test 11. The steam and water flows are plotted using the Wallis parameter (J*).
Included on the figure is a best-fit correlation of the UPTF data. The data show that
water runback to the test vessel decreased as the steam flow increased. At high
steam flows, there was complete turnaround of the water flow. Based on the
correlation, the minimum steam flow for complete turnaround corresponded to a Wallis
parameter of 0.47 (i.e., $J^*_g{}^{1/2} = 0.69$).

Note that Figure 4.8-6 includes data at 300 kPa and 1500 kPa. The close agreement
of the data at the two pressures indicates that the Wallis parameter is suitable for
pressure scaling.

The UPTF results are compared to CCFL correlations developed from tests at
subscale facilities in Figure 4.8-7. The Krolewski correlation (Reference E-491)
underpredicts water runback at UPTF and the Ohnuki correlation (Reference J-947)
overpredicts runback. The Richter correlation (Reference E-493), which is based on
data from a 1/3.7-scale (cold leg diameter) facility with a geometrical configuration
similar to UPTF, passes through the UPTF data.

The flow conditions for the UPTF test run which simulated typical PWR SBLOCA
conditions are included in Figure 4.8-6. As shown in the figure, the SBLOCA condition
is well below the CCFL correlation. This suggests that water runback to the reactor
vessel during reflux condensation is not inhibited by the steam flow through the loop.

A full-range drift-flux model has been developed and verified against the UPTF data.
This model is based on the drift-flux and the envelope theories and is applicable to
both horizontal pipes and inclined pipes. Development of this model and comparison
to the UPTF data are documented in References G-643 and G-924.

4.8.2.4 Conclusions

The UPTF test demonstrated that a substantial margin exists between the flooding limit
(CCFL conditions) and the typical conditions expected in a PWR during the reflux
condensation cooling mode of an SBLOCA.

4.8.3 Countercurrent Flow at the Tie Plate during High Pressure Injection

4.8.3.1 Rationale of Test

During an SBLOCA in which the core uncovers and heats up at elevated pressure
(about 8,000 kPa), the only source of ECC for cooling the core and replenishing the

reactor coolant system inventory is the high pressure injection system (HPIS). In GPWRs with combined injection, the HPIS injects ECC through nozzles in the hot legs. The ECC flow into the upper plenum from the hot legs can either accumulate in the upper plenum or flow down through the tie plate to the core. The rate of water downflow to the core is determined by the countercurrent flow limitation with the upflow of steam generated in the core.

Countercurrent flow at the tie plate with hot leg ECC injection was investigated in other UPTF tests for LBLOCA. Test 30 was performed to investigate these phenomena using flow conditions more representative of expected SBLOCA conditions.

4.8.3.2 Scope of Testing

UPTF Test 30 consisted of two test runs which covered a range of steam and ECC flows. The system pressure for the test was limited to 1500 kPa (the maximum operating pressure of UPTF), whereas system pressure during an SBLOCA is typically about 8000 kPa. The steam and ECC flows for the test were selected to provide the "best simulation" of GPWR conditions given the lower pressure. The test conditions are summarized in Table 4.1-1.

The data and quick look reports for UPTF Test 30 are provided in References G-030 and G-230, respectively. The test results are also discussed in Reference G-411.

4.8.3.3 Summary of Key Results

Water downflow to the core began within two seconds of the start of ECC injection. Downflow increased with increasing ECC injection. Due to steam condensation in the upper plenum, water downflow to the core was greater than ECC injection. Temperature measurements below the tie plate indicate the maximum subcooling of the water downflow was as high as 50 K.

Steam/water countercurrent flow phenomena at the tie plate were heterogeneous (i.e., multidimensional). Specifically, water downflow occurred only in localized regions in front of the hot legs with ECC injection (Figure 4.8-8). Steam upflow from the core occurred over the remainder of the vessel. As discussed in Section 4.4, similar heterogeneity occurred in the tests which simulated LBLOCA conditions.

The steam which was not condensed in the upper plenum flowed out through the loops. In the hot legs with ECC injection, the steam flow toward the steam generator simulator passed over the subcooled ECC flow toward the vessel (i.e., countercurrent, stratified flow). ECC entrained by the steam flow accumulated in the hot leg between the Hutze and the hot leg bend. The maximum collapsed water level measured near the hot leg bend was 0.18 m.

4.8.3.4 Conclusions

The test demonstrated that, for representative SBLOCA conditions, water downflow through the tie plate was not inhibited by the steam upflow from the core. Consequently, essentially all ECC injected into the hot legs penetrated to the core. The actual water downflow to the core was greater than the ECC injection rate due to steam condensation in the upper plenum.

Test Vessel

Downcomer

Cold Leg Closed at Pump Simulator

Cold Leg

Stratification

High Pressure
Injection
ECC – Water

A

A

Section A – A

Cold Water Plume
in the Downcomer
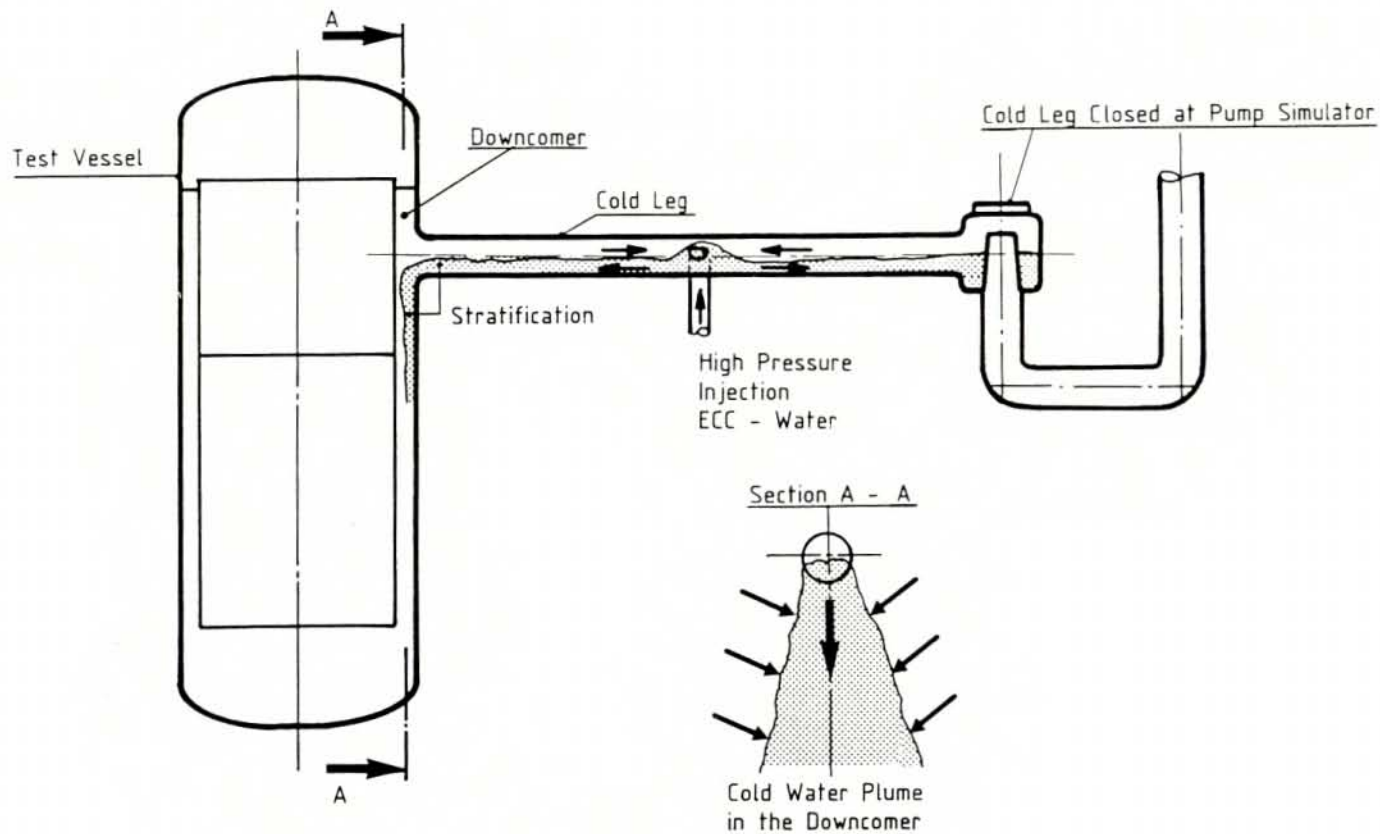
**COLD AND HOT WATER STREAMS IN
UPTF FLUID-FLUID MIXING TEST
UPTF TEST 1
FIGURE 4.8-1**
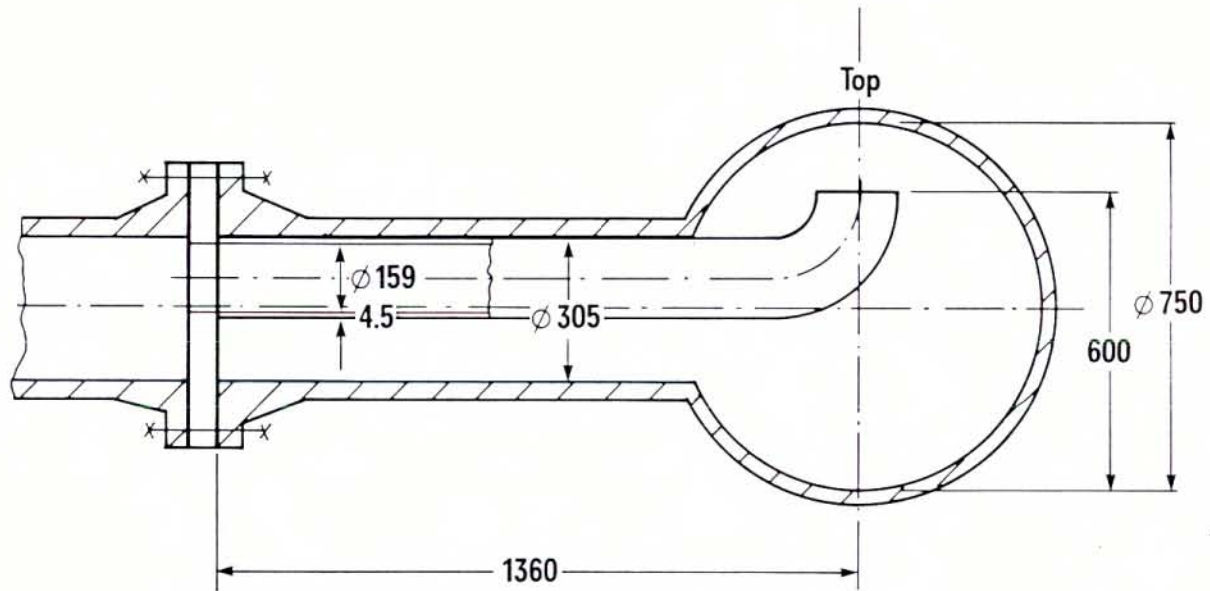
CONFIGURATION OF UPTF HIGH PRESSURE
ECC INJECTION NOZZLE
UPTF TEST 1
FIGURE 4.8-2
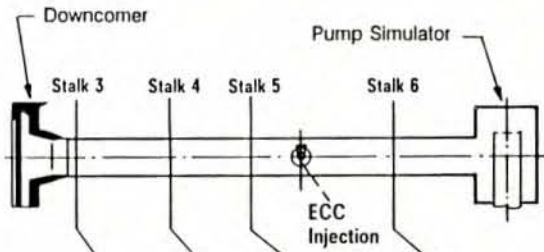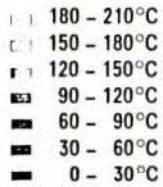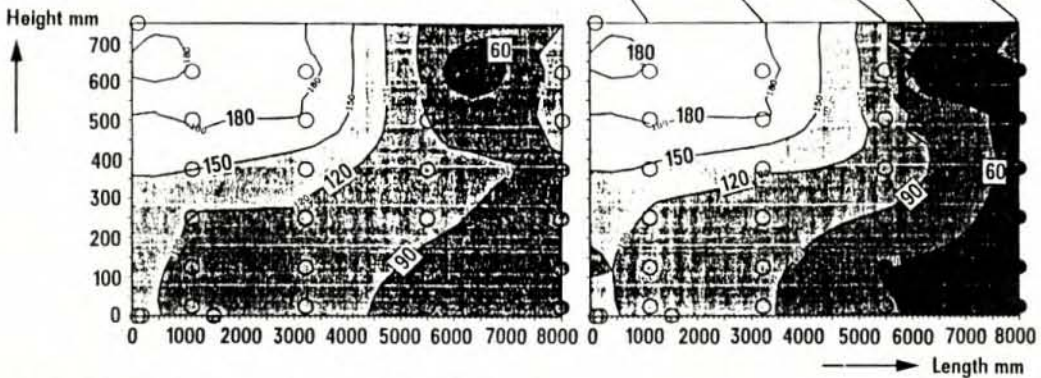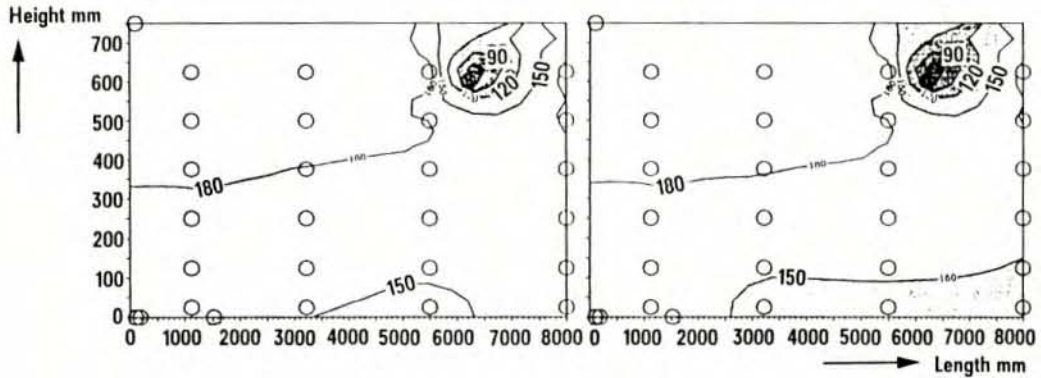
VERTICAL FLUID TEMPERATURE DISTRIBUTION IN LOOP 2
UPTF TEST 1
FIGURE 4.8-3

T   – Fluid temperature in DC
T_O – Temperature of stagnant fluid in DC at start of test
T_{ECC} – ECC Fluid temperature $(25-35°C)$

Dimensionless temperature $\dfrac{T - T_{ECC}}{T_O - T_{ECC}}$

Time = 500 s after start of ECC

Elevation
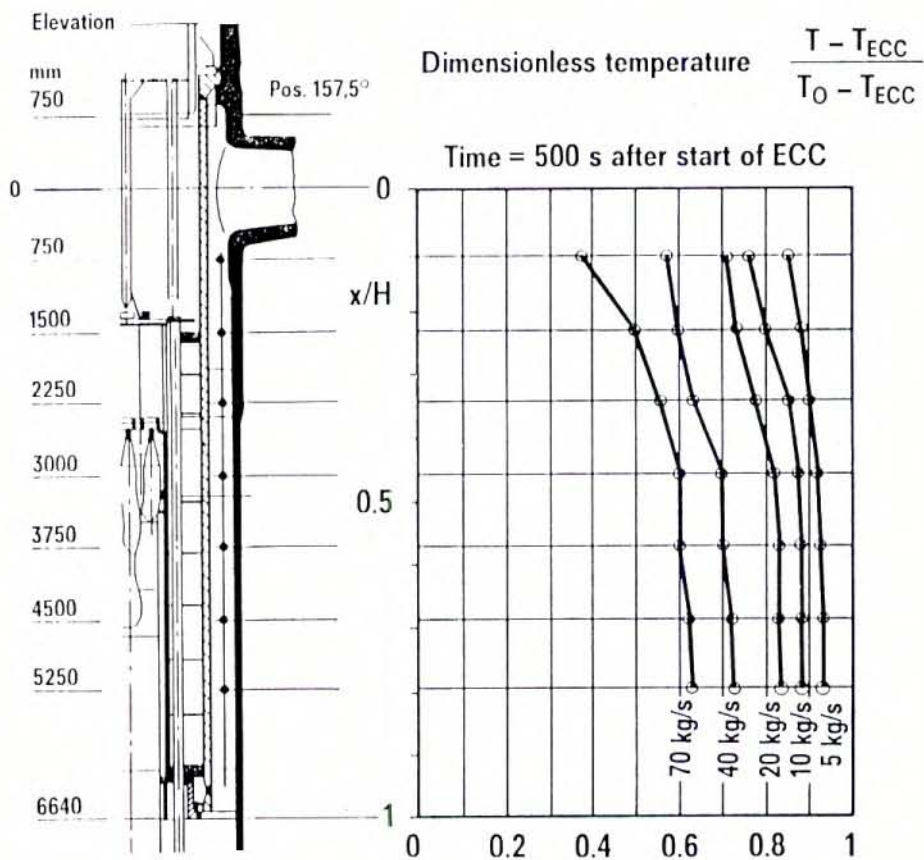
DIMENSIONLESS FLUID TEMPERATURE ALONG DOWNCOMER
CENTERLINE 500 SECONDS AFTER START OF ECC INJECTION
UPTF TEST 1
FIGURE 4.8-4
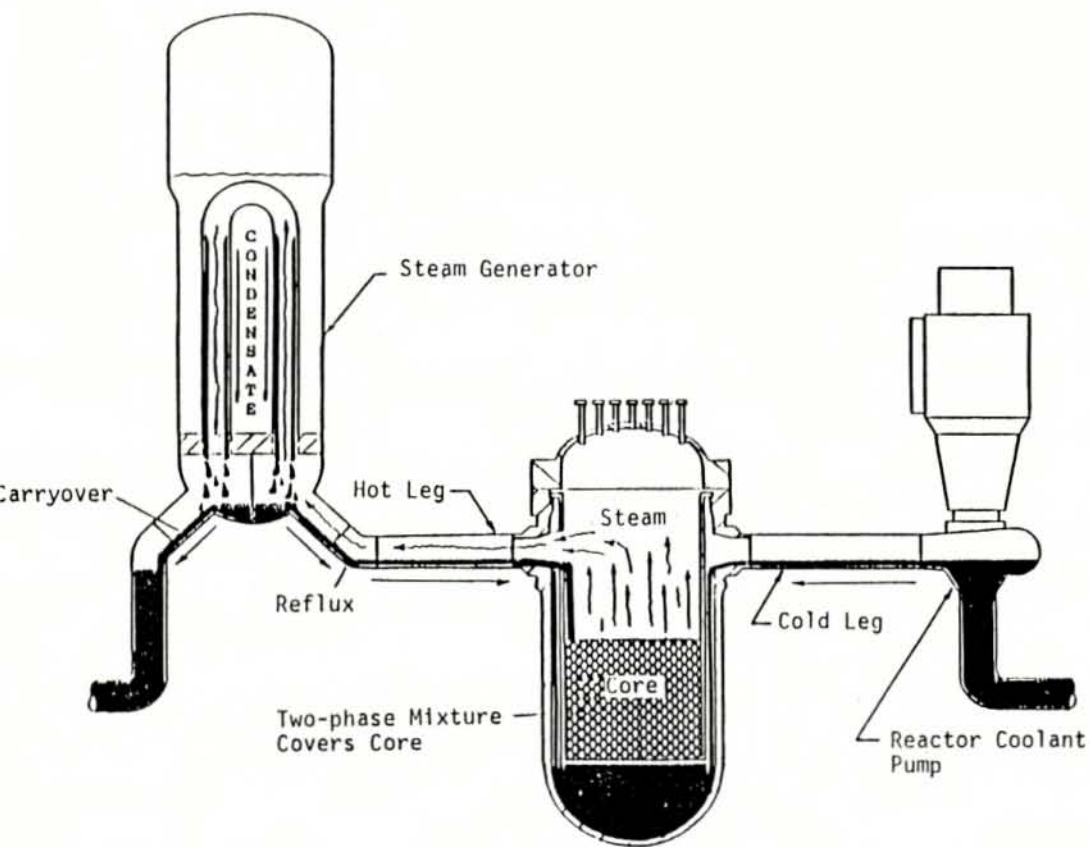
REFLUX CONDENSATION FLOW PATHS
FIGURE 4.8-5

0.8

× = 15 Bar Data
● = 3 Bar Data

Complete Turnaround Points

0.7

This point, assumed
not to be a CCFL
point, falls directly
on derived CCFL
correlation.

(Dimensionless Superficial Steam Velocity)$^{1/2}$, $\sqrt{j_g{}^*}$

0.6

$\sqrt{j_f{}^*} = 0.7955 - 1.1564 \sqrt{j_g{}^*}$

0.5

Least Squares Fit to CCFL Data

0.4

0.3

Data Point
for Typical
PWR SBLOCA
Conditions

These points had
complete water
penetration and
are not necessarily
CCFL points

0.2

0.1

0.0

0.00   0.05   0.10   0.15   0.20   0.25

(Dimensionless Superficial Countercurrent Water Velocity)$^{1/2}$, $\sqrt{j_f{}^*}$

Notes: 1:   The dimensionless superficial velocity, or Wallis parameter,
is defined as:

$$j^* = \frac{\dot{M}}{\rho A} \sqrt{\frac{\rho}{\Delta \rho g \bar{D}}}$$

2.   The flow area and hydraulic diameter used to calculate the
dimensionless superficial velocities are based on the "hutze"
region of the hot leg. [A = 0.397m^2 (616 in^2); D = 639mm (25.2 in)]

UPTF HOT LEG COUNTERCURRENT FLOW RELATIONSHIP
UPTF TEST 11
FIGURE 4.8-6
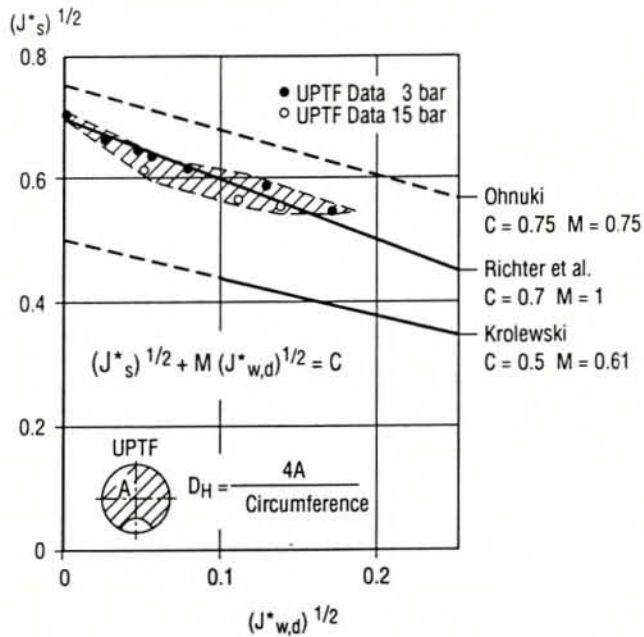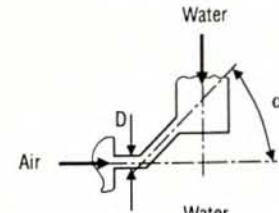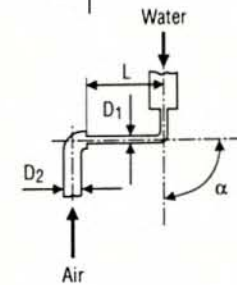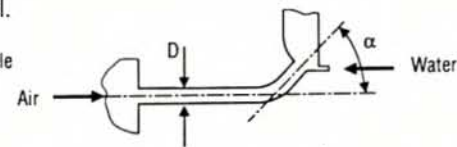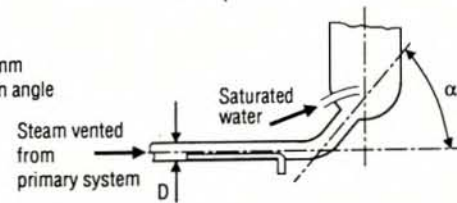
COMPARISON OF UPTF DATA WITH CORRELATIONS OF RICHTER ET AL.
OHNUKI AND KROLEWSKI

FIGURE 4.8-7
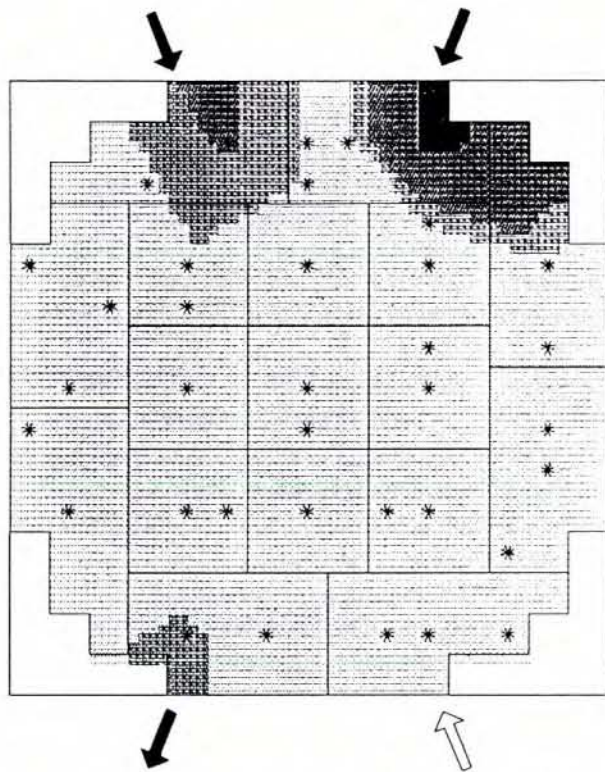
UPTF TEST 30
(RUN 142)

Fluid temperatures

10 mm below tie plate

DT = Tsat - Tfluid (K)

Time (s)=200.00

DT (K)   -10   -5   0   5   15   50

FLUID TEMPERATURES 10mm BELOW TIE PLATE
UPTF TEST 30
FIGURE 4.8-8

4.9 INTEGRAL TESTS WITH COLD LEG ECC INJECTION

4.9.1 Rationale of Tests

During the end-of-blowdown, steam flows up the downcomer and out the broken cold leg. Due to flashing and entrainment in the lower plenum, the downcomer upflow may be two-phase. This upflow initially tends to prevent ECC from flowing down the downcomer and refilling the vessel. The downcomer upflow can carry some or all of the ECC injected into the cold legs directly out the broken cold leg (i.e., ECC bypass). However, as the system pressure decreases, the two-phase upflow decreases and ECC penetration to the lower plenum increases.

Reflood begins as water enters the core from the lower plenum. During the reflood phase in a PWR, part of the water injected into the cold legs flows through the downcomer and lower plenum to the core. In the core, the water is accumulated, vaporized to steam, or entrained by the steam flow exiting the core. The water entrained by the steam flow is either de-entrained at or above the tie plate (i.e., in the end box or upper plenum), or carried over to the hot legs and steam generators. Heat transfer from the secondary side of the SG vaporizes water carried over to the SG U-tubes (i.e., steam binding).

The steam exiting the intact loop SGs flows out the break via the cold legs and downcomer. In the cold legs, some of the steam is condensed by the subcooled ECC injection. Depending on the flow conditions, this interaction between the steam and ECC can result in either plug flow or stratified flow. The resultant flow regime affects ECC delivery to the downcomer. The uncondensed steam vents to containment by flowing around the downcomer and out the broken cold leg. This steam flow in the downcomer can reduce the downcomer water level by entraining water out the break.

Shortly after initiation of core reflood, ECC injection changes from accumulator (ACC) injection to LPCI. When the ACCs are depleted, the nitrogen used to pressurize the ACCs is rapidly discharged into the reactor coolant system through the ECC piping. ACC nitrogen discharge affects core cooling by temporarily pressurizing the intact cold legs and downcomer which forces a surge of water into the core.

Integral tests with cold leg ECC injection have been performed in several scaled test facilities to investigate system behavior under a wide range of conditions. Of special importance are the tests performed in the Semi-scale Test Facility at INEL (1:1600), in the PKL Test Facility at Siemens/KWU (1:145-scale relative to 1300 MWe Siemens/KWU PWR) and tests performed in CCTF and SCTF (1:21-scale relative to Trojan USPWR and Ohi JPWR) at JAERI. Integral tests were performed at UPTF to investigate system behavior at full-scale.

4.9.2 Scope of Testing

Five integral tests with cold leg ECC injection were performed at UPTF to simulate, at full-scale, steam/water flow conditions during the refill and reflood phases of an LBLOCA. The tests covered both evaluation model (EM) and best-estimate (BE) conditions. The test conditions are summarized in Table 4.1-1. Each test is described briefly below.

- Test 2 simulated, at full-scale, the reflood transient of an EM test at CCTF (Test C2-4). The metal surfaces were initially superheated to simulate structure heat release.

- Test 17 simulated a BE reflood transient based on SCTF Test S3-10; conditions for Test S3-10 were based on a TRAC analysis of a Westinghouse PWR. Test 17 consisted of two phases with identical core simulator injection rates. Phase A had no ECC injection whereas Phase B had ECC injection.

- Test 4B was a BE reflood transient similar to UPTF Test 17.

- Test 27A simulated the EOB and refill phases of an LBLOCA based on a TRAC analysis for a Westinghouse PWR. Test 27A included simulation of ACC nitrogen discharge.

- Test 27B was a BE reflood simulation. The test conditions were based on CCTF Test C2-SH2 and a TRAC analysis of a Westinghouse PWR.

The data and quick look reports for these tests are listed in the bibliography (Section 8).   FRG evaluation of these tests is provided in Reference G-411. Evaluations of these tests by the US are covered by phenomena in References U-455 (downcomer entrainment during reflood), U-456 (water carryover/steam binding), U-458 (loop flow regime) and U-459 (ACC nitrogen discharge).

4.9.3 Summary of Key Results

The integral tests were used to study the controlling phenomena and the system interactions in a PWR LOCA. Individual phenomena were studied in more detail in separate effects tests at UPTF. The integral tests were also used to assess the predictive capability of computer codes such as TRAC (see Section 5). The key results of the cold leg injection integral tests are summarized below.

End-of-Blowdown, Refill, and Accumulator Nitrogen Discharge (Test 27A)
The high ECC flow corresponding to ACC injection completely condensed the steam flow through the intact loops. Consequently, water plugs formed in each of the intact loop cold legs (Figure 4.9-1, top diagram). These plugs oscillated in the cold legs resulting in fluctuations in the delivery of ECC to the downcomer.

Temperature measurements in the downcomer indicate ECC penetration to the lower plenum was heterogeneous (i.e., multidimensional). Specifically, as shown in Figure 4.9.2 (top diagram), subcooling was measured below the cold legs away from the break (Cold Legs 2 and 3) while no subcooling was detected below the cold leg next to the break (Cold Leg 1). This suggests all the ECC injected into Cold Leg 1 was bypassed out the break while some of the ECC injected into Cold Legs 2 and 3 penetrated to the lower plenum.

As the system pressure approached containment pressure, the steam upflow in the downcomer decreased and ECC penetration increased. By the end of depressurization, the lower plenum was filled to about the bottom of the core barrel. The water level reached the bottom of the core shortly after depressurization was complete.

To simulate steam generation and water entrainment in the core during reflood, the core simulator steam and water injection rates were increased rapidly as water entered the core. The differential pressure for flow out of the core and through the loops increased the absolute pressure in the core relative to that in the downcomer. Consequently, the downcomer water level increased relative to the core water level (Figures 4.9-3 and 4.9-4).

About ten seconds after the beginning of reflood, nitrogen was injected directly into the primary system to simulate nitrogen discharge from the ACCs. Nitrogen injection resulted in a sudden increase in downcomer pressure which forced water from the downcomer into the core. The surge in core water level (about 1.5 m) activated the FASS which terminated the test.

Reflood (Tests 2, 4B, 17B, and 27B)
System behavior during reflood is described below based on Test 27B. The results from the other integral tests with cold leg ECC injection were qualitatively similar. Plots of the boundary conditions and system response for Test 27B are provided in Figures 4.9-5 and 4.9-6.

During the initial portion of reflood, the high ECC injection rate simulating ACC injection completely condensed the steam flow through the intact loops. Consequently, subcooled water plugs formed in the intact cold legs between the injection nozzle and the downcomer. The high ECC flow rapidly filled the downcomer

with subcooled water. The downcomer water level stabilized at the cold leg elevation as water spilled out the broken cold leg.

When the ECC injection rate was reduced to simulate LPCI, only part of the loop steam flow was condensed. The resultant flow regime in the cold leg was cocurrent, stratified flow of steam and saturated water to the downcomer (Figure 4.9-1, bottom diagram). The steam flow from the intact cold legs entrained water from the downcomer out the break and reduced the water level in the downcomer. The downcomer water level was 0.75 to 1.25 m below the bottom of the cold legs (Figure 4.9-6). Flow out the broken cold leg was oscillatory throughout the LPCI period (Figure 4.9-7).

Water entrained out of the core was either de-entrained in the upper plenum or carried over to the loops. Water which de-entrained in the upper plenum either accumulated in the upper plenum or fell back to the core. Figure 4.9-6 includes a plot of the collapsed water level in the upper plenum for Test 27B. The plot shows that the collapsed water level history in the upper plenum reflected changes in the core simulator water injection rate. The maximum collapsed water level measured in Test 27B was 0.12 m.

Water carried over to the loops was either de-entrained and accumulated in the hot legs and SGS inlet plena, or carried over to the SGS tube regions. As shown in Figure 4.9-8, carryover to the SGS tube regions constituted about 40% of the water injected in the core simulator. The data also show that de-entrainment and accumulation upstream of the tube regions delayed carryover to the tube regions by approximately 20 seconds. Carryover to the tube regions was higher in the broken loop hot leg than in the intact loops because the steam flow was higher. Carryover to the tube regions was similar in the three intact loops.

4.9.4 Conclusions

The controlling phenomena during an LBLOCA which were identified from the integral tests at UPTF are listed below.

- ECC bypass during end-of-blowdown.

- Downcomer entrainment during reflood.

- Water carryover/steam binding during reflood.

- Steam/ECC interaction in the loops.

- Nitrogen discharge from the ACCs.

Except for nitrogen discharge effects, each of these phenomena has been studied in detail in separate effects tests at UPTF (see Sections 4.2, 4.3, 4.5 and 4.6).

The key findings from the cold leg injection integral tests are summarized below.

- The lower plenum was filled to the bottom of the core barrel when blowdown was complete.

- The flow regime in the intact cold legs was plug flow during ACC injection (i.e., EOB, refill, and early reflood) and stratified flow during LPCI (i.e., late reflood).

- During the LPCI portion of reflood, the steam flow through the downcomer entrained water from the downcomer out the break and thereby reduced the downcomer water level below the cold leg elevation.

- Due to de-entrainment and accumulation in the upper plenum, hot legs and SGS inlet plena, water carryover to the SGS tube regions did not start until about 20 seconds after initiation of reflood (i.e., BOCREC).

- Discharge of nitrogen from the ACCs resulted in sudden pressurization of the downcomer which forced water from the downcomer into the core.
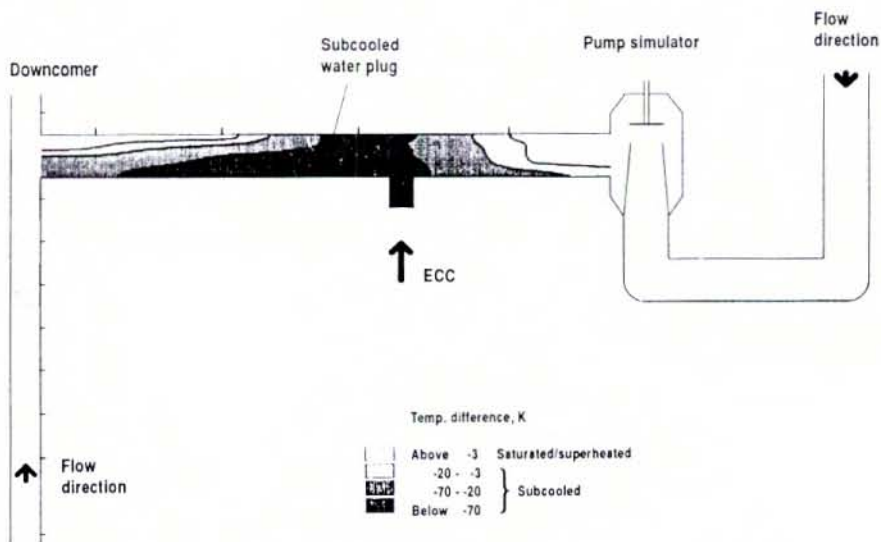
**PLUG FORMATION IN COLD LEG 2 DURING
END OF BLOWDOWN PHASE AT 38 S, PHASE A**
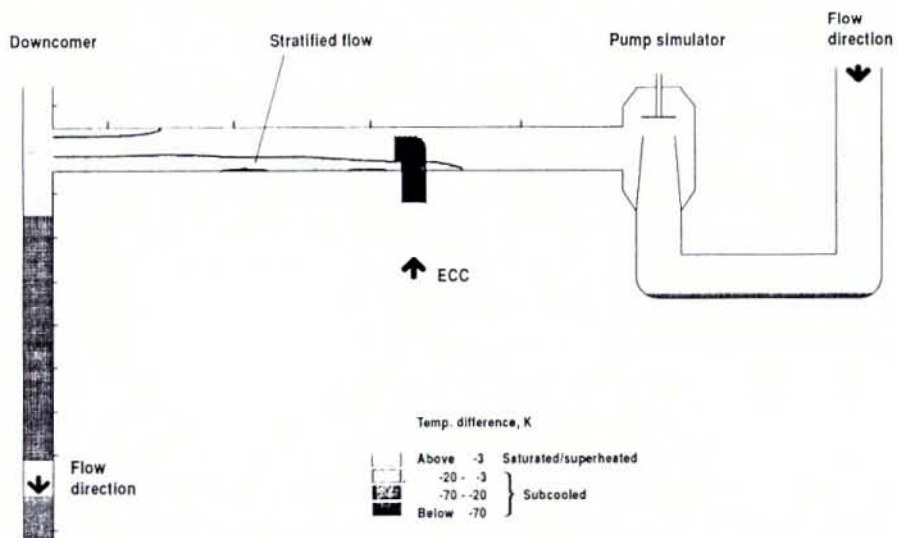
STRATIFIED FLOW IN COLD LEG 2 DURING REFLOOD PHASE AT 65 S

COLD LEG FLOW REGIME
UPTF TEST 27

FIGURE 4.9-1
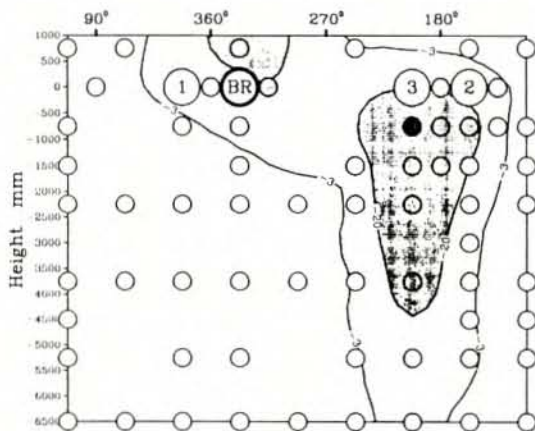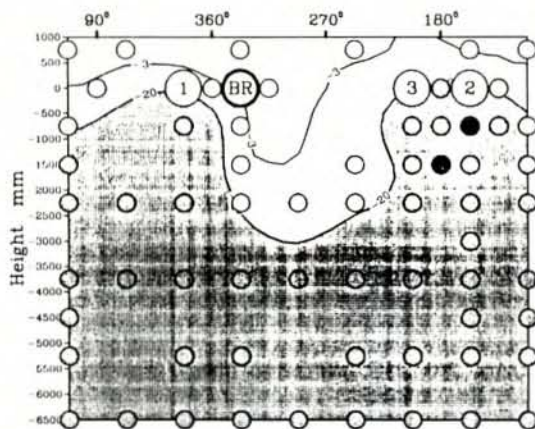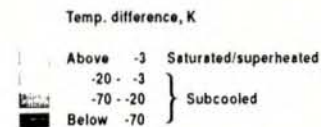
CONTOUR PLOTS
OF FLUID SUBCOOLING IN DOWNCOMER
UPTF TEST 27A
FIGURE 4.9-2

BOUNDARY CONDITIONS FOR UPTF TEST 27A
FIGURE 4.9-3

Figure content (labels):

ABSOLUTE PRESSURE

1500 KPA
1000
500
0

□ JAA01CP001H
  Upper plenum
○ JAA01CP002H
  Downcomer
△ JMP01CP001
  Containment
  simulator

WATER LEVEL

12 M
8
4
0

Bottom of core

Lower plenum + core
□ C2A08:58PCU9 •
○ CJAA01CL003 •

Downcomer

0   20   40   60   80   100
TIME   S

⚓ START OF TEST   ⚓ 74.1S FASS
⚓ 6.0 BAR

* Referred to inside
bottom of test vessel
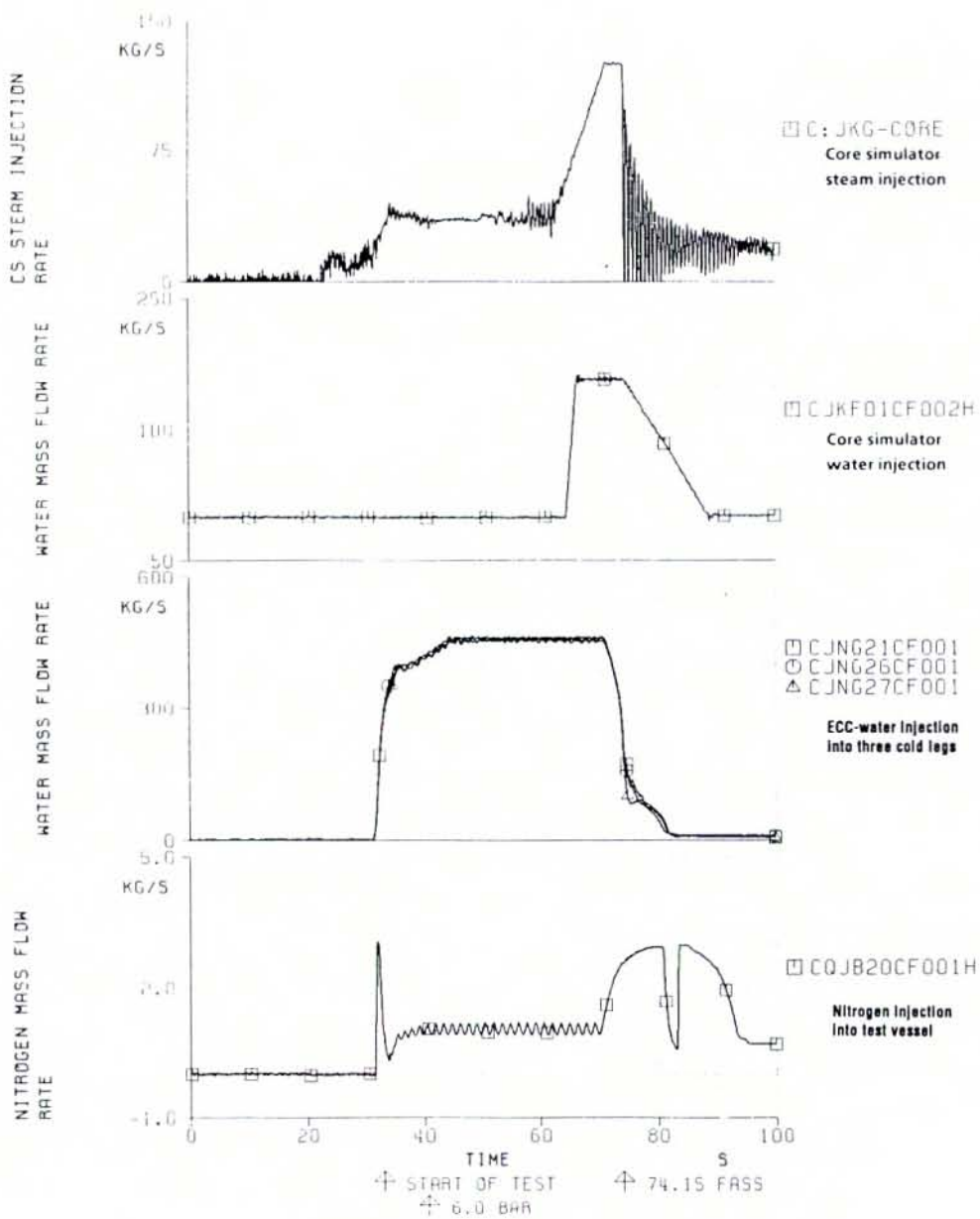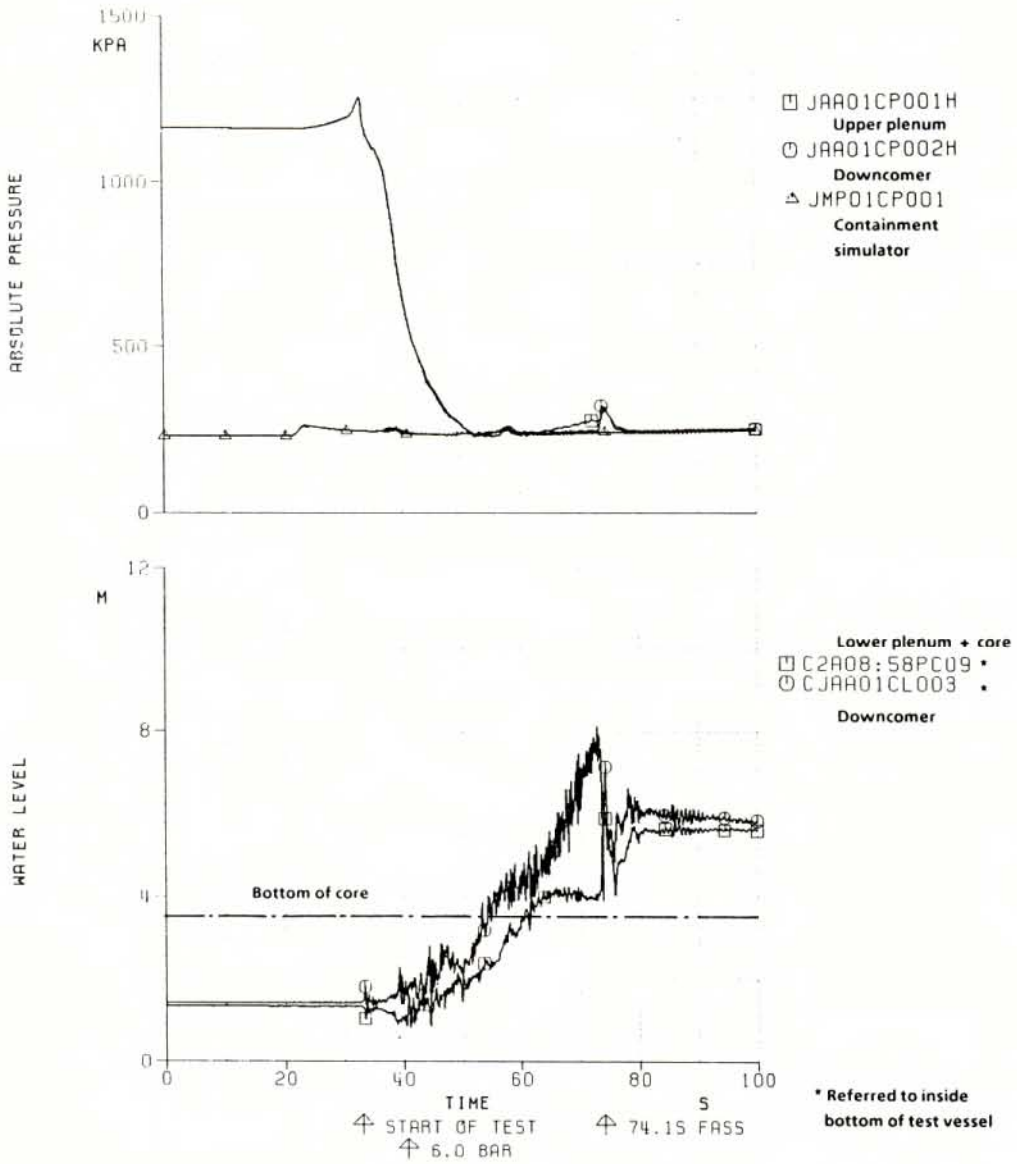
OVERALL SYSTEM RESPONSE IN UPTF TEST 27A
FIGURE 4.9-4
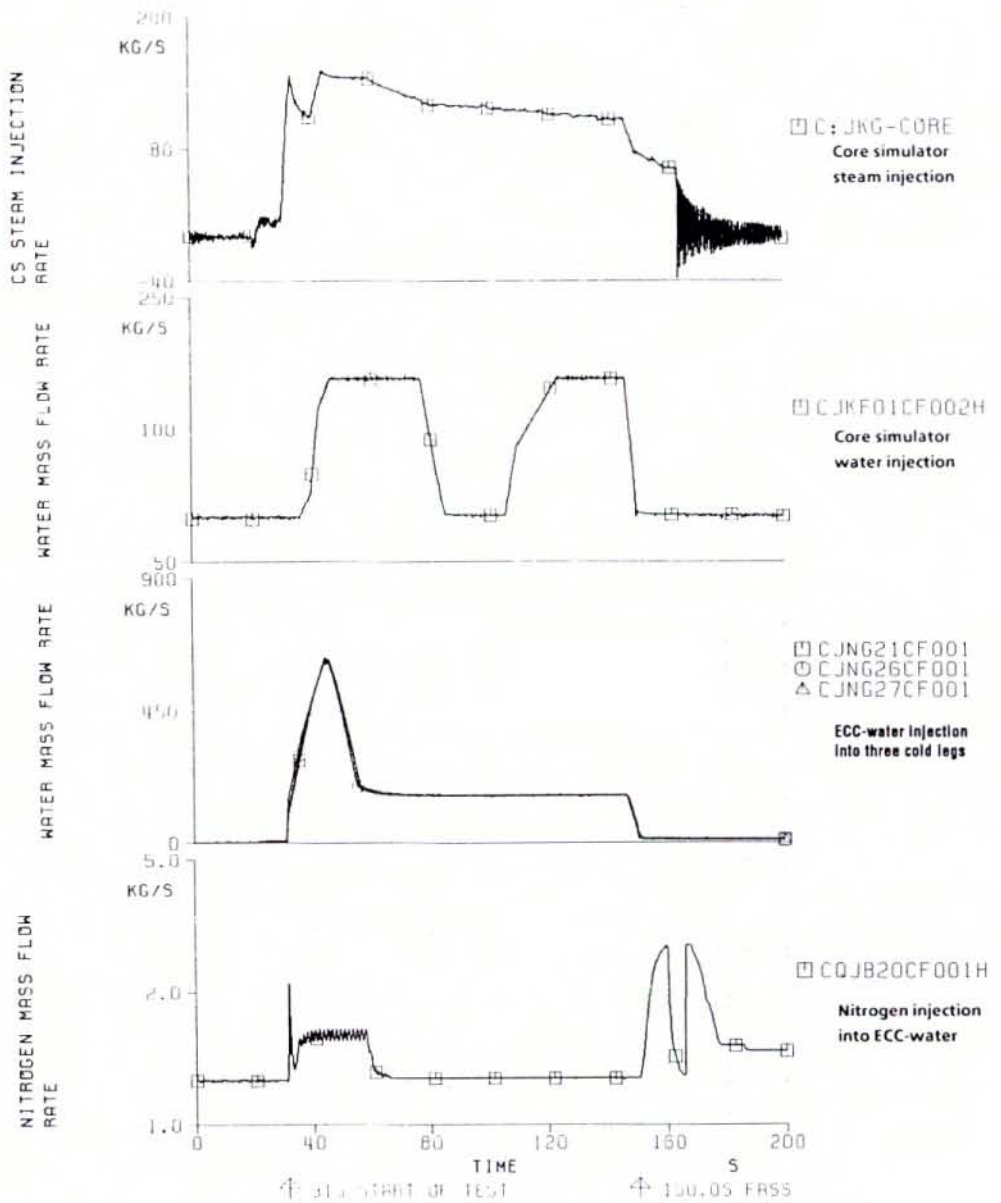
BOUNDARY CONDITIONS FOR UPTF TEST 27B
FIGURE 4.9-5
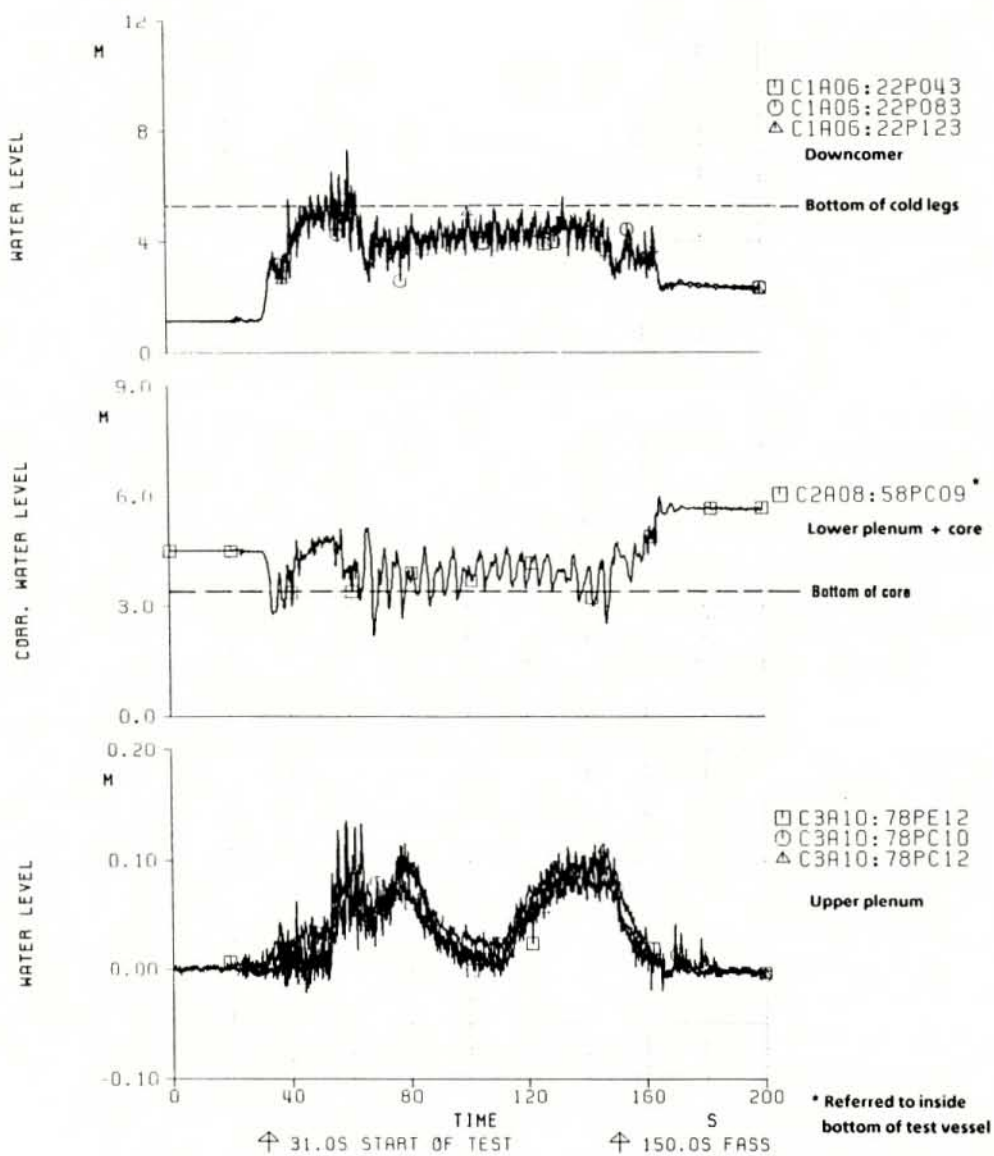
OVERALL SYSTEM RESPONSE IN UPTF TEST 27B
FIGURE 4.9-6
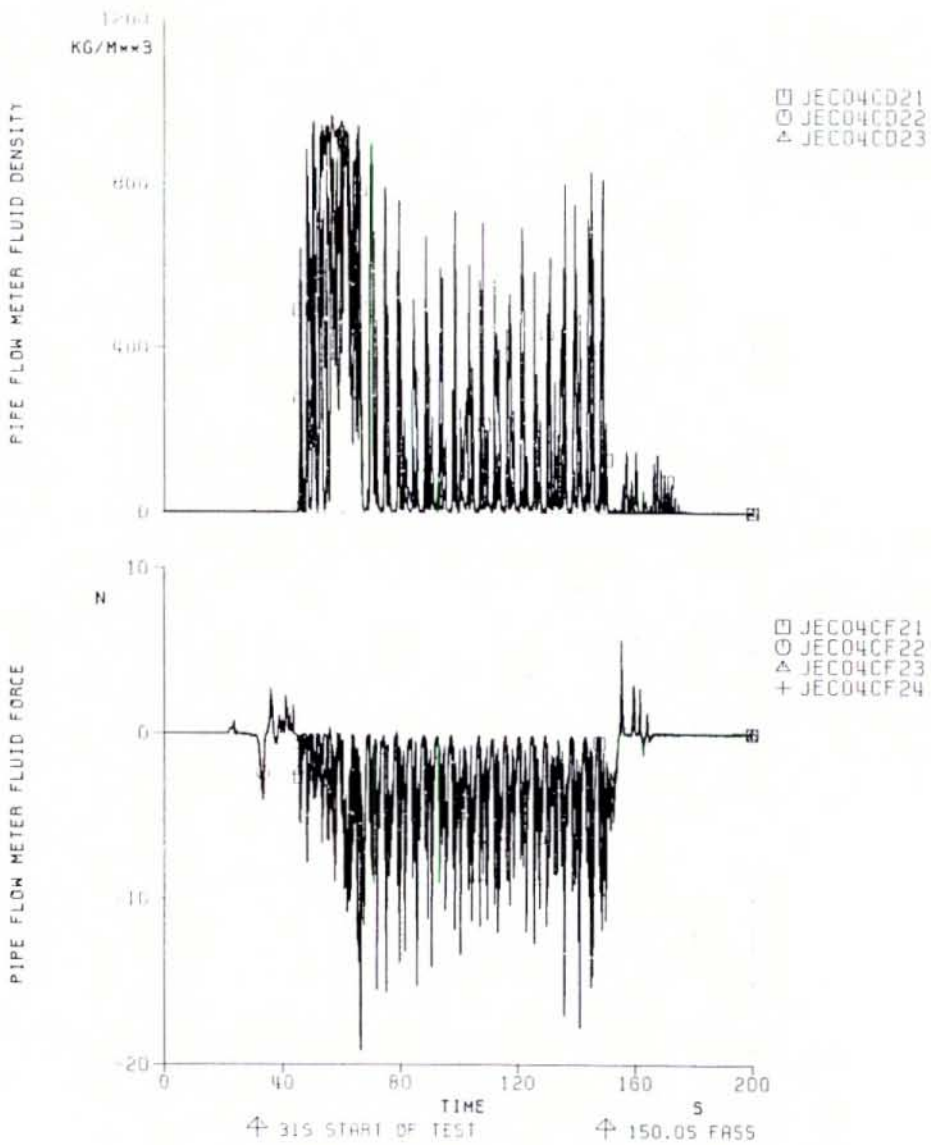
FLUID OSCILLATION IN BROKEN COLD LEG
UPTF TEST 27B
FIGURE 4.9-7
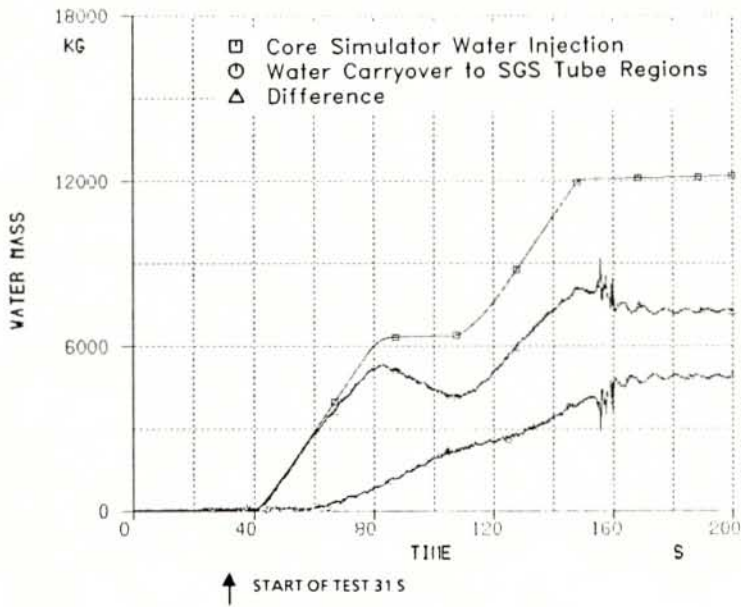
WATER CARRYOVER TO SGS TUBE REGIONS
UPTF TEST 27, PHASE B
FIGURE 4.9-8

4.10 INTEGRAL TESTS WITH COMBINED ECC INJECTION

4.10.1 Rationale of Tests

Combined injection refers to ECC injection into the cold legs and hot legs. During a LOCA in a PWR with combined injection, ECC injected into the hot legs needs to pass through the upper plenum to reach the core, and ECC injected into the cold legs needs to pass through the downcomer and lower plenum to reach the core. Interaction of ECC with steam and two-phase flow in the hot legs, upper plenum, cold legs, downcomer, and lower plenum can affect core cooling.

During the end-of-blowdown phase of a cold leg break LOCA, flow is predominantly downward in the upper plenum and core, and upward in the downcomer. This flow condition promotes delivery of hot leg ECC injection through the upper plenum and core to refill the lower plenum. Significant local core cooling can occur due to the ECC delivery through the core. Although the flow conditions inhibit delivery of cold leg ECC to the lower plenum, countercurrent flow in the downcomer can permit some of the cold leg ECC injection to contribute to refill.

During reflood, steam generated in the core and entrained water vent upward to the upper plenum. Although this flow tends to inhibit delivery of hot leg ECC injection to the core, countercurrent flow in the upper plenum can permit hot leg ECC to be delivered to the core. Further, steam condensation by ECC can reduce the steam flow, which improves ECC delivery and reduces steam binding in the loops. During reflood, cold leg ECC injection flows into the downcomer and helps to maintain the driving head for reflood.

During the end-of-blowdown, refill and reflood phases, formation of ECC liquid plugs in the loops can influence overall system behavior. A particularly important phenomenon is the movement of hot leg plugs into the steam generator tube regions, which can lead to a significant surge in steam generation affecting the system.

Several of the phenomena discussed above are scale-dependent, particularly:

- ECC countercurrent flow in downcomer.

- ECC countercurrent flow in upper plenum.

- Behavior of ECC plugs in the hot legs and cold legs.

Full-scale UPTF separate effects tests were carried out to study each of these areas, see Sections 4.2, 4.4 and 4.6, respectively. Overall system behavior with combined ECC injection was investigated in tests at subscale facilities including the PKL facility at Siemens/KWU (1:145-scale relative to a 1300 MWe German PWR), and CCTF and

SCTF (both 1:21-scale relative to an 1100 MWe US/J PWR). To complement the sub-scale integral tests and to investigate full-scale behavior under transient conditions, UPTF integral tests with combined injection were also performed, as described in this section.

4.10.2 Scope of Testing

Five integral tests with combined ECC injection were performed at UPTF. These tests covered both cold leg and hot leg breaks and simulated both evaluation model (EM) and best-estimate (BE) conditions. The principal objective of the tests was to investigate overall system behavior and transient thermal-hydraulic phenomena in the upper plenum (including tie plate region), downcomer and loops. The test conditions for the five tests are summarized in Table 4.1-1. Each test is described briefly below.

- Test 18 simulated the end-of-blowdown, refill and reflood phases of an EM transient for a double-ended cold leg break LOCA. ECC was injected into two hot legs and three cold legs. Core simulator flow conditions were based on prior SCTF tests, and included feedback responses to ECC breakthrough.

- Test 3 had conditions similar to Test 18. It was conducted earlier in the UPTF program and did not utilize the automatic SG feedback system.

- Test 19 had conditions similar to Test 18 except the simulated cold leg break was only one-half of the pipe area.

- Test 14 had conditions similar to Test 18 except a hot leg break was simulated.

- Test 28 simulated a BE transient for double-ended cold leg break LOCA. ECC was injected into four hot legs and three cold legs.

The data and quick look reports for these tests are listed in the bibliography (Section 8). The results of the tests are also discussed in Reference G-411.

4.10.3 Summary of Key Results

Key results of the cold leg break tests are explained using observations and data from Test 18, which covered the end-of-blowdown, refill and reflood phases.

The test started with a "conditioning" phase during which the primary system depressurized from 1800 kPa to 1050 kPa. The purpose of this phase was to establish the desired transient flow conditions. The "test" phase consisted of the portion of the test after a pressure of 1050 kPa was reached. The test phase included

further depressurization (end-of-blowdown), followed by refill and reflood. Key test boundary conditions and system response data are shown in Figures 4.10-1 and 4.10-2.

An important observation was that hot leg ECC injection was delivered to the core during all three LOCA phases. Delivery of cold leg ECC injection was slightly delayed during the end-of-blowdown due to downcomer CCFL. The combination of hot and cold leg ECC injection led to a quick refill of the lower plenum and reflood of the core. The facility was automatically shut down by high core water level 23 seconds after the start of reflood.

Figure 4.10-3 shows overall facility behavior diagrams at four times during Test 18. Each diagram shows the liquid accumulation in the cold leg, downcomer, lower plenum, core, upper plenum, hot leg, and steam generator simulator. Steam flow in the loops and in the core simulator and SG simulator are also shown. Finally, the rate of water breakthrough from the upper plenum to the core is shown. The top diagram of Figure 4.10-3 shows the conditions at the start of the "test" phase. As seen, there is a small amount of water in the lower plenum and the steam and ECC flows are active.

During the end-of-blowdown, water plugs formed in the cold legs. Figure 4.10-4 shows an enlarged diagram of the water plugs in this region. ECC flowed from the cold legs into the downcomer, where a mixture of ECC delivery and bypass (out the broken cold leg) were observed. This behavior was attributable to the strongly heterogeneous conditions which were observed in the downcomer (Figure 4.10-5). As discussed more extensively in Section 4.2, ECC delivery was favored on the side of the vessel away from the break, and bypass was favored on the side near the break.

The lower plenum level increased due to delivery of hot leg and cold leg ECC injection during end-of-blowdown. Following blowdown, continued delivery occurred leading to start of reflood. ECC delivery to the downcomer and upper plenum was unsteady due to the movement of water plugs in the cold legs and hot legs. The plug movements were caused by condensation effects and system pressure balance effects. Figure 4.10-6 shows an enlarged diagram of phenomena in the hot legs and upper plenum/tie plate at two different times during reflood. In the upper diagram a plug has formed and is moving away from the pressure vessel, resulting in very little delivery to the upper plenum and very little breakthrough to the core. In the lower diagram the plug has been reversed and forced into the vessel by increased steam generation (simulated) at the SG; there is substantial breakthrough into the core.

Water breakthrough across the tie plate into the core occurred in discrete regions which were adjacent to hot legs in which injection was occurring (Figure 4.10-7). Two-phase upflow through the tie plate existed in regions where breakthrough was not

occurring. Water subcooling up to 70 K was measured in breakthrough regions just below the tie plate. Water breakthrough at the tie plate was not affected by the increased core simulator steam flow (feedback response) which simulated PWR core response. The collapsed level in the upper plenum was multidimensional, with the maximum level (up to 1 m) occurring above breakthrough zones.

Overall, essentially all of the core steam generation was condensed by ECC, and over 88% of the ECC was retained in the primary system to contribute to refill and reflood. An energy balance of the simulated PWR core was performed to determine the "virtual" core energy response and quench time. Total input energy was the initial calculated stored energy relative to the saturation temperature (based on GPWR EM calculation) plus decay heat. Energy removal was determined from the amount of steam generation (steam injection in UPTF). Figure 4.10-8 shows the results of this analysis for two core zones in Test 18. The upper curve is input energy and the lower curve is energy removal. Quench is complete at the time when the curves intersect. Quench occurs about 20 seconds sooner in the zone with water breakthrough than in the other zone. The band just above the lower curve shows the effect of assuming a quench temperature 100 K above saturation; i.e., quench is advanced by about five seconds. Figure 4.10-9 shows core stored energy diagrams at four times for the conditions of Test 18. Based on the results of these energy balance calculations for Test 18, the PWR reflood duration (BOCREC to quench) was estimated to be 35 seconds.

Test 19 simulated a 50% (0.5A) cold leg break with 5/8 ECC injection. The core simulator steam and water injection rates during reflood were based on SCTF Test S3 - 13. The main test phase, which was initiated at 1050 kPa, was preceded by a conditioning phase (1800 to 1050 kPa) which established the basic flow pattern in the UPTF primary system.

The phenomena and the overall system behavior in Test 19 were similar to that described above for Test 18 (200% cold leg break) except the system depressurization rate was lower. During the end-of-blowdown most of the ECC injected into the cold legs was either bypassed out the broken cold leg or accumulated in the upper downcomer. Water breakthrough from the upper plenum to the core occurred immediately after initiation of hot leg ECC injection. Due to condensation near the injection nozzles, ECC delivery to the upper plenum and to the downcomer was intermittent. Massive water penetration through the tie plate to the core region and the high steam condensation rates in the upper plenum, hot legs and cold legs resulted in a rapid increase in the core water level during reflood.

Test 14 simulated a 200% hot leg break. The boundary conditions were the same as for Test 18. The effect of the different break location on the overall system behavior was found to very limited. With a hot leg break, steam vented to containment during the end-of-blowdown by flowing through the upper plenum to the break rather than

up the downcomer to the break. Consequently, the cold leg ECC injection flowed down the downcomer to the lower plenum and was not bypassed. Lower plenum refill initiated immediately after the start of the test phase at a system pressure of 1050 kPa. After BOCREC, the core water level increased rapidly due to massive water breakthrough from the upper plenum. Entrainment of hot leg ECC injection out the broken hot leg was negligible even at high core simulator steam injection rates. The difference of collapsed water levels in downcomer and core region was lower than in the cold leg break test because the hot leg break provided slightly better depressurization of the upper plenum.

4.10.4 Conclusions

The key findings from integral tests with combined ECC injection are summarized below.

- ECC delivery to the lower plenum occurs during the end-of-blowdown from both hot leg and cold leg ECC injection.

- Reflood initiates very shortly after blowdown terminates.

- ECC delivery from hot leg and cold leg injection leads to rapid core cooling and core quench.

- Hot leg ECC injection penetrates through the tie plate to the core in local regions adjacent to hot legs.

- Water plugs form in the loops; movement of these plugs results in intermittent ECC delivery.

Top panel legend:
□ JKG - core
Core simulator
Total injected steam

Base steam mass flow

Correction system

Mass Flow (kg/s): 200, 80, -40

Middle panel legend:
□ CJKF01CF001
○ C: JKF - core
Core simulator
Total injected water

Mass Flow (kg/s): 1200, 800, 400, 0

Bottom panel legend:
□ CJNG21CF001
○ CJNG22CF001
△ CJNG25CF001
+ CJNG26CF001
X CJNG27CF001

ECC injection into two hot legs and three cold legs

Mass Flow Rate (kg/s): 600, 300, 0

Time (s): 30, 40, 50, 60, 70, 80

10.5 bar   52.9 s BOCREC   76.0 s FASS

BOUNDARY CONDITIONS FOR UPTF TEST 18
FIGURE 4.10-1
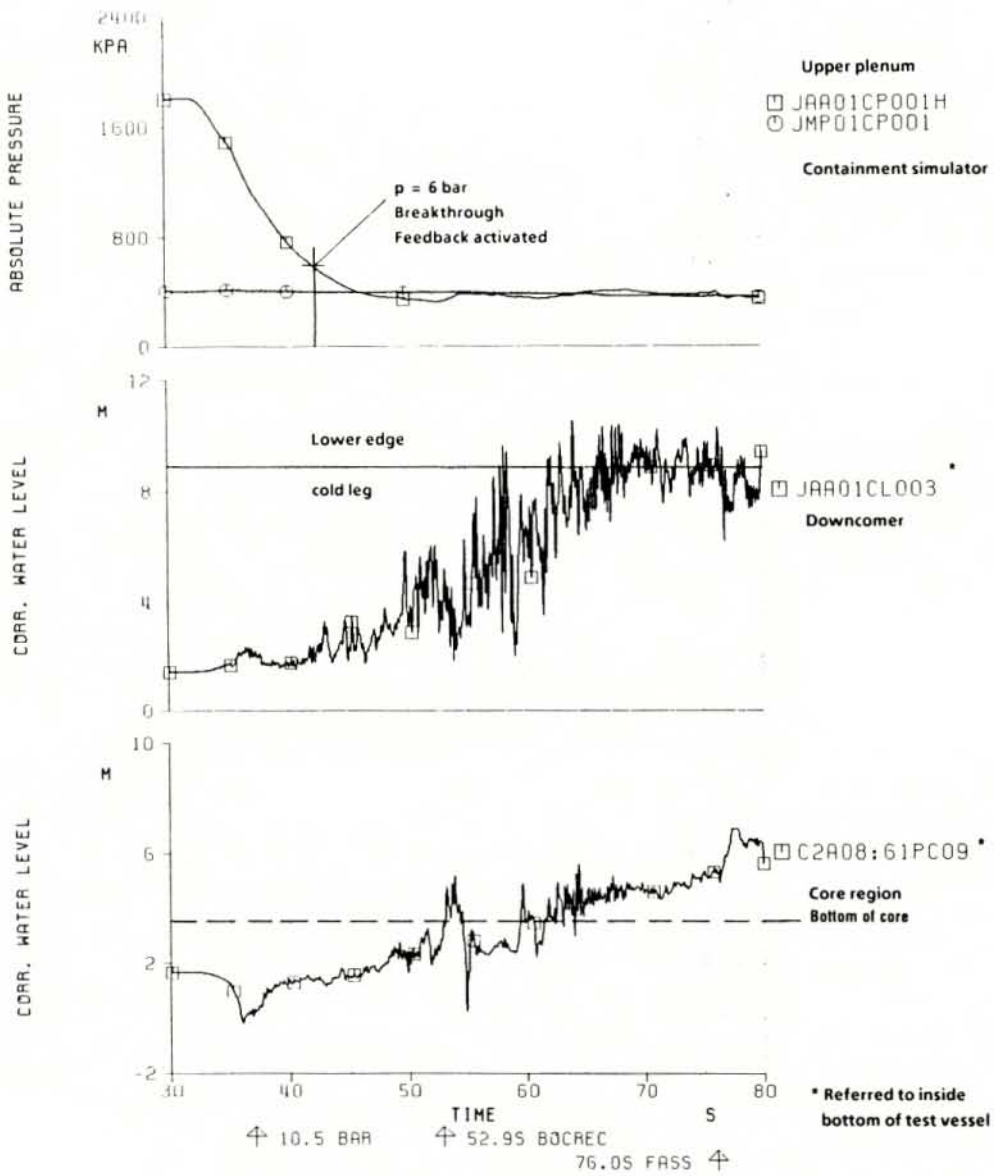
OVERALL SYSTEM RESPONSE IN UPTF TEST 18
FIGURE 4.10-2

Start of main test phase
37.5 s

System pressure
P = 1080 kPa

← Steam

Steam mass flow

↑ ECC   ↓ ECC

ECC Bypass

P = 390 kPa

End-of-blowdown
46.5 s

P = 320 kPa

Bottom of core recovery
52.9 s

P = 380 kPa

End of test phase
76.0 s
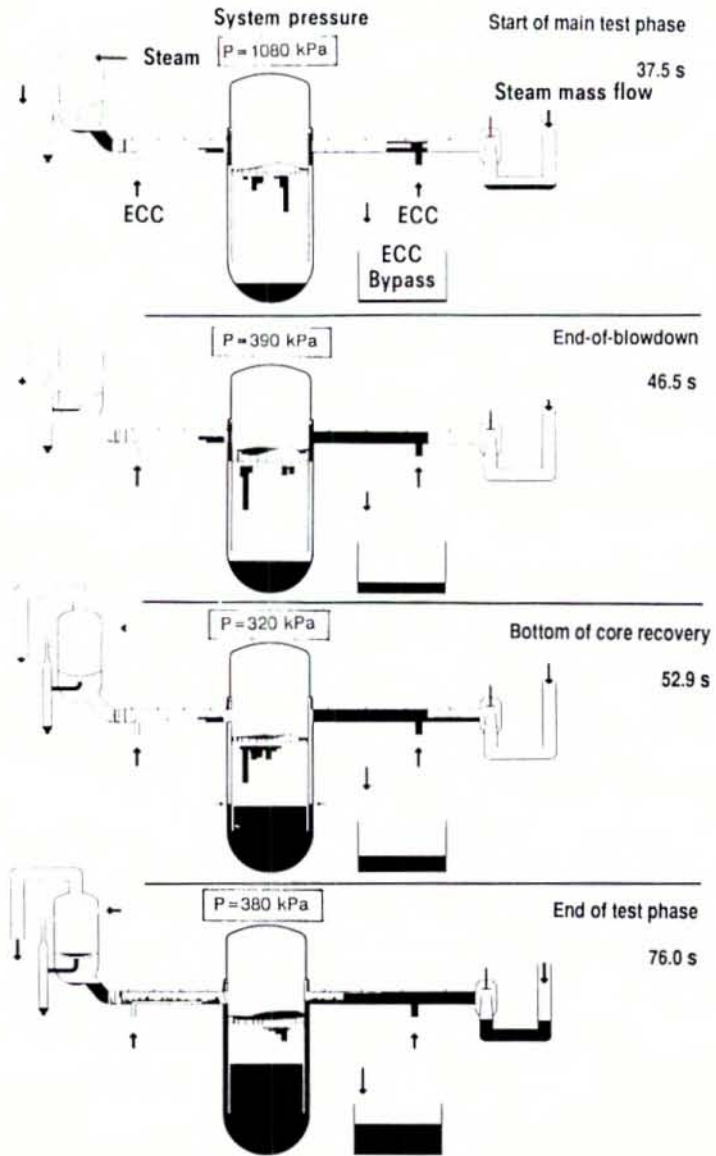
OVERALL SYSTEM BEHAVIOR IN UPTF TEST 18
FIGURE 4.10-3

Downcomer Water plug Pump simulator Flow direction

ECC

Flow direction

Temp. difference, K

	Above -3	Saturated/superheated
	-20 - -3	
	-70 - -20	Subcooled
	Below -70	
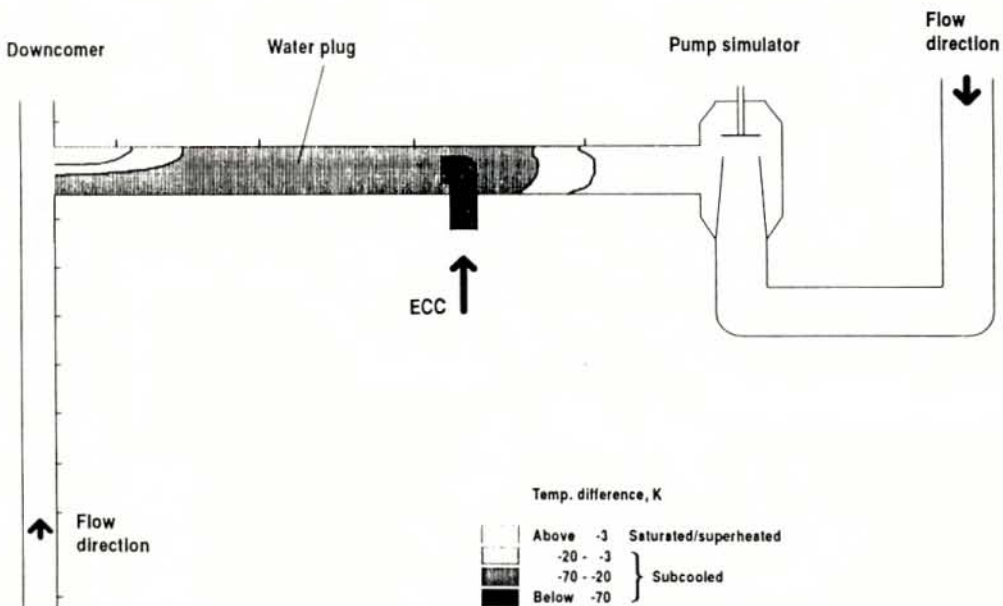
PLUG FORMATION AND FIRST WATER DELIVERY FROM
COLD LEG 2 TO DOWNCOMER AT 40 S
UPTF TEST 18
FIGURE 4.10-4
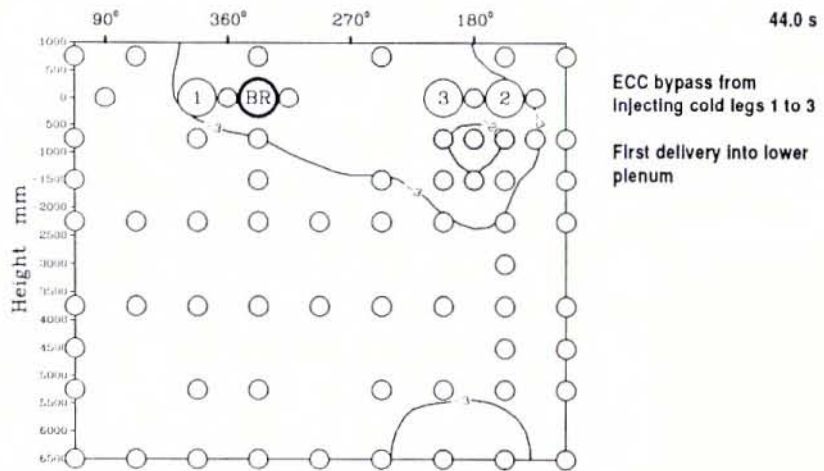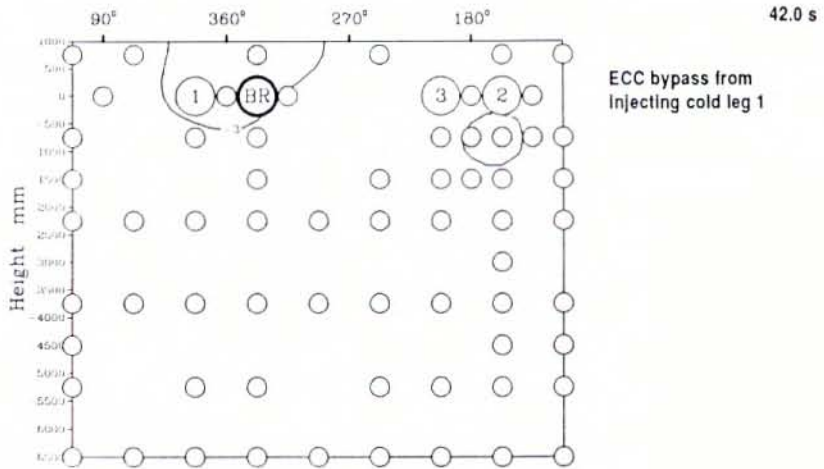
CONTOUR PLOTS OF FLUID SUBCOOLING IN DOWNCOMER
UPTF TEST 18
FIGURE 4.10-5

BTD force, N

	0.15 – 1.00	Upflow
	–0.15 – 0.15	Intermediate
	–2.00 – –0.15	Downflow

Temp. difference, K

	Above –3	Saturated/superheated
	–20 – –3	
	–70 – –20	} Subcooled
	Below –70	

Mass flow

Steam

Density

Water plug

56 s

Fluid force

Tie plate

ECC

Mass flow

Steam

Density

Stratified flow

64 s

Fluid force

Tie plate

ECC
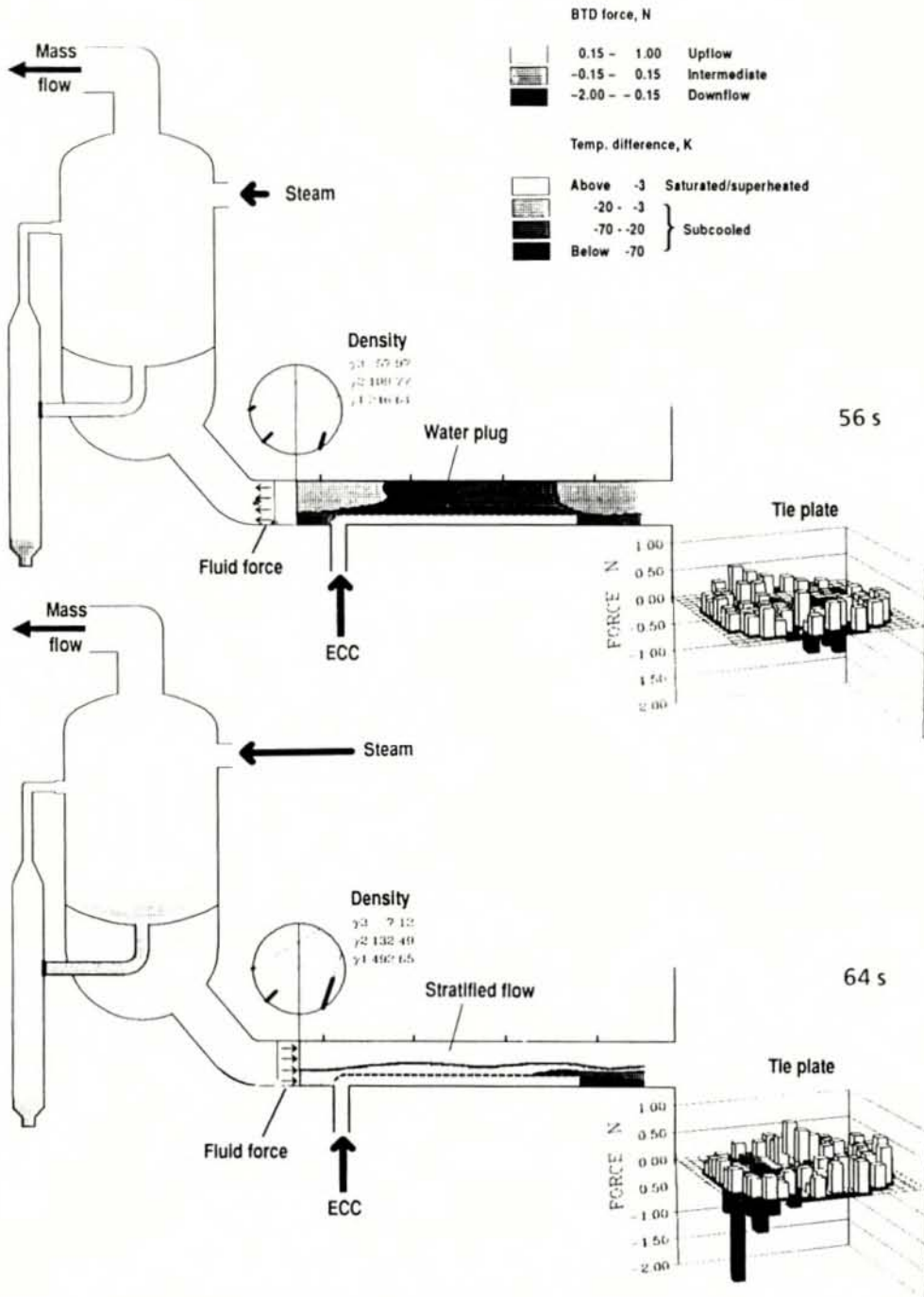
FLOW PHENOMENA IN HOT LEG AND TIE PLATE AREA
UPTF TEST 18
FIGURE 4.10-6

68 s

74 s

kg/s

```
☐      -5.00  –   25.00   Intermediate / Upflow
▨    -10.00  –   -5.00  }
■    -45.00  –  -10.00  } Downflow
```
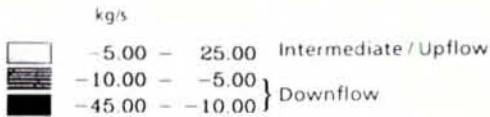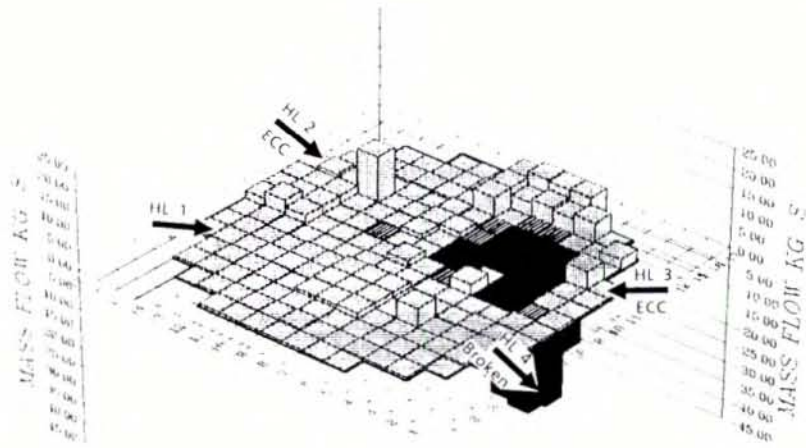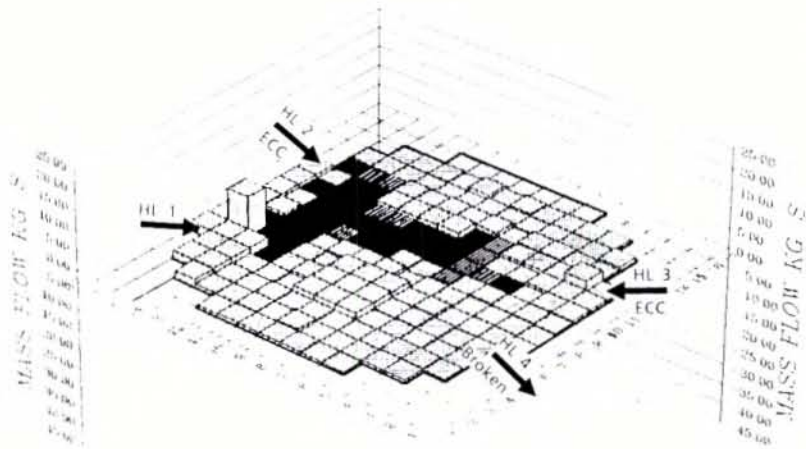
WATER MASS FLOW RATES ACROSS TIE PLATE
UPTF TEST 18
FIGURE 4.10-7
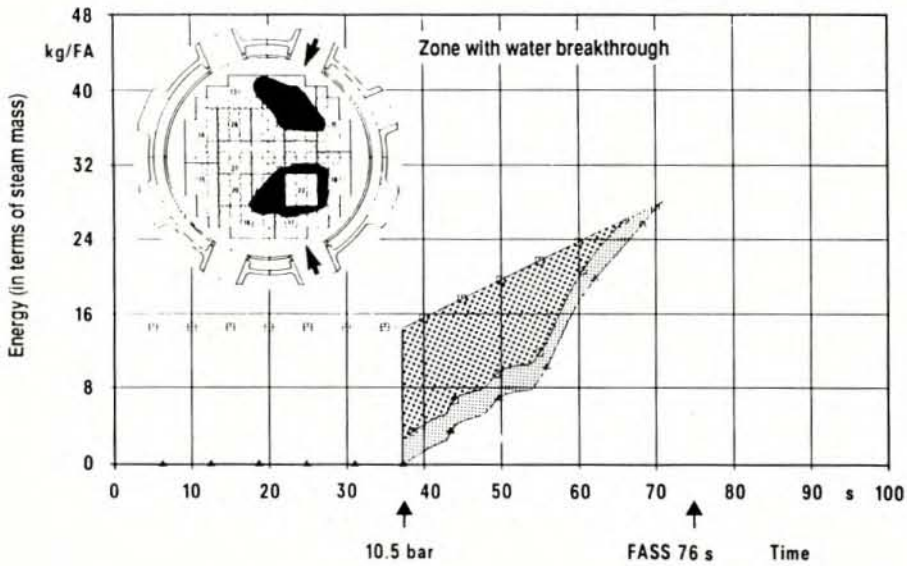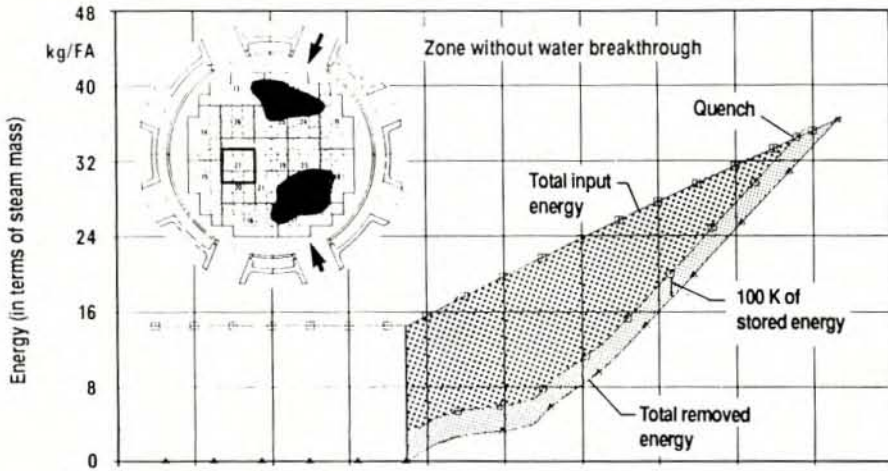
ENERGY BALANCE FOR TWO SIMULATED PWR CORE ZONES
UPTF TEST 18
FIGURE 4.10-8

Energy balance   Test 18
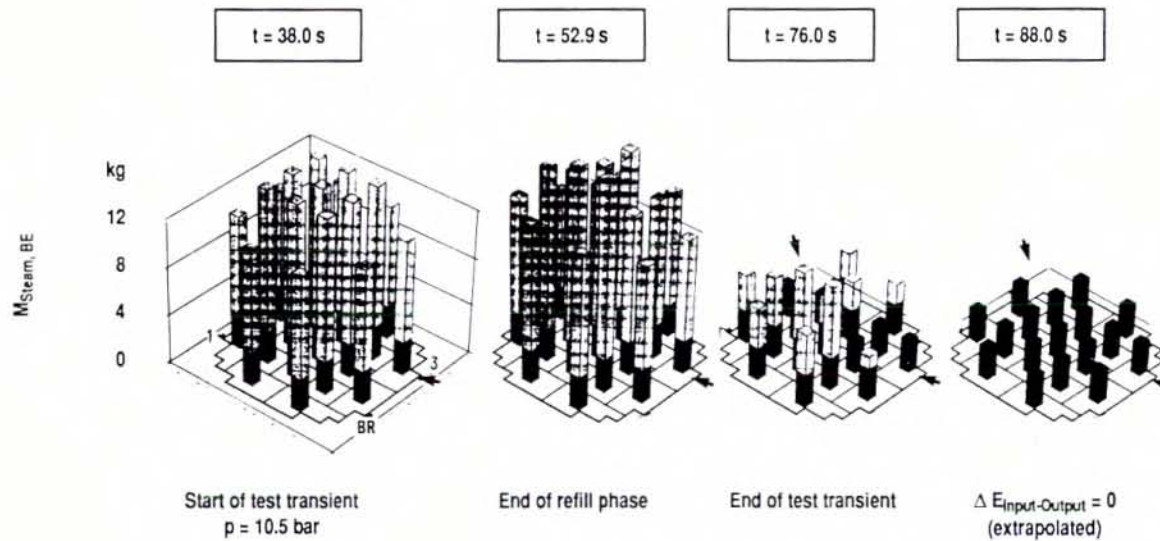
CALCULATED STORED ENERGIES OF SIMULATED PWR CORE
AT DIFFERENT TIMES IN TRANSIENT
UPTF TEST 18
FIGURE 4.10-9

4.11 INTEGRAL TEST WITH COLD LEG/DOWNCOMER ECC INJECTION AND VENT VALVES

4.11.1 Rationale of Test

One UPTF integral test simulated the end-of-blowdown, refill, and reflood phases of an LBLOCA in an ABB/BBR PWR like the Muelheim-Kaerlich (MK) PWR. The MK PWR is a 2 x 4 loop PWR with vent valves in the core barrel. The ECC system consists of four separate systems. Two of the systems inject ECC directly into the downcomer and two systems inject ECC into the loops. For each loop, ECC is injected into only one of the two cold legs. Each system consists of three types of injection; namely, high pressure coolant injection (HPCI), accumulator (ACC) injection, and low pressure coolant injection (LPCI).

During end-of-blowdown, steam in the reactor vents out the broken cold leg by flowing around the bottom of the core barrel and up the downcomer to the break, and by flowing through the vent valves and around the downcomer to the break. The upflow in the downcomer entrains some of the ECC injected in the downcomer and intact loop cold leg out the break thereby limiting ECC delivery to the lower plenum. However, the vent valves provide an alternative steam flow path which reduces the upflow and promotes ECC delivery.

During reflood, steam generated in the core is vented to containment via the upper plenum and either the vent valves or the reactor coolant loops. Flow through the vent valves bypasses the loops and tends to reduce the core-to-downcomer differential pressure which improves core cooling. The vent valves also influence the steam flow distribution in the downcomer which can affect water entrainment from the downcomer out the broken cold leg.

Section 4.7 described key phenomena and results from separate effects tests performed to determine the effect of reactor vessel vent valves on LOCA behavior. An integral test was performed to investigate overall system behavior for a simulated transient.

4.11.2 Scope of Testing

One integral test (Test No. 24) was performed at UPTF to simulate the end-of-blowdown, refill and reflood phases of a large cold leg break LOCA in the MK PWR. ECC was injected through two downcomer injection nozzles and one intact cold leg nozzle. Six vent valves were free to open during the test; the two vent valves directly in front of the downcomer ECC injection nozzles were locked shut. Two test runs were performed, as described below.

- Run 302 used core simulator steam flow conditions based on the results of SCTF Test S3-17 (Run 721), which was the BBR coupling test (Reference J-568). Other conditions were based on a TRAC analysis of the MK plant and pretest ("conditioning") TRAC calculations (References G-414, G-631 and G-662).

- Run 304 was similar to Run 302 except considerably higher steam flow was used.

TRAC pretest calculations were performed to determine an appropriate method to "condition" the facility at the start of the test (Reference G-631). A method which injected steam in the core simulator, SG simulators, and pressurizer simulator during depressurization from 1800 kPa to 1000 kPa was found to yield suitable conditions at 1000 kPa. During the reflood portion of the tests, the core simulator steam and water flows were adjusted by the core simulator feedback system according to measured core water level. In addition, SGS steam injection was activated based on the separated water measured in the SG simulators. The data and quick look reports for Test 24 are provided in References G-024 and G-224, respectively.

4.11.3 Summary of Key Results

The results are described based on the behavior observed in Run 302. During the conditioning phase, the pressure decreased from 1800 kPa to 1000 kPa. At a pressure of 1000 kPa, the depressurization rate was about 200 kPa/sec, which was the desired value. Depressurization from 1000 kPa was rapid and the primary system pressure went below the containment pressure by about 60 kPa due to the condensation on subcooled ECC.

ECC penetrated to the lower plenum during end-of-blowdown, primarily on the side of the vessel away from the break. After blowdown terminated, completion of refill and reflood occurred rapidly. During the entire test, the pressure in the upper plenum exceeded the pressure in the downcomer by up to 12 kPa (Figure 4.11-1). This value was less than that observed in tests without vent valves, reflecting the effect of the vent valve flow path. As a result, the level in the core was only about 1 m below the level in the downcomer (Figure 4.11-1).

During the entire test (including end-of-blowdown) a steam/water upflow from the core to the upper plenum was observed. This was different from integral tests without vent valves which had a reversal from end-of-blowdown (downflow) to reflood (upflow). The vent valve flow path directly from the upper plenum to the downcomer caused this effect.

Because of the high ECC injection rates, complete steam condensation and plugging were observed in the cold leg into which ECC was injected. Further, the downcomer contained subcooled fluid throughout, which suppressed wall boiling. Subcooling was detected in the break outflow during end-of-blowdown.

During reflood, some of the water carried out of the core de-entrained and accumulated in the upper plenum. The measured level was up to 0.07 m. Due to the short duration of the reflood phase (nine seconds), very little water was carried into the intact loops and essentially no water was measured in the SG simulators.

In Run 304, the higher core simulator steam injection caused the upper plenum to downcomer pressure difference to be about 20 kPa (Figure 4.11-2). The corresponding water level difference between the core and downcomer was 2.5 m. Upper plenum water accumulation to a level of 0.2 m occurred. Also, after about 30 seconds, water collection in the tube regions of the SG simulators was observed.

4.11.4 Conclusions

The transient LOCA simulation of the MK PWR showed that:

- There is substantial ECC penetration to the lower plenum during the end-of-blowdown, leading to rapid refill and reflood.

- The upper plenum-to-downcomer pressure difference is maintained at a low value due to the presence of the vent valves, allowing the core level to rise quickly during reflood.
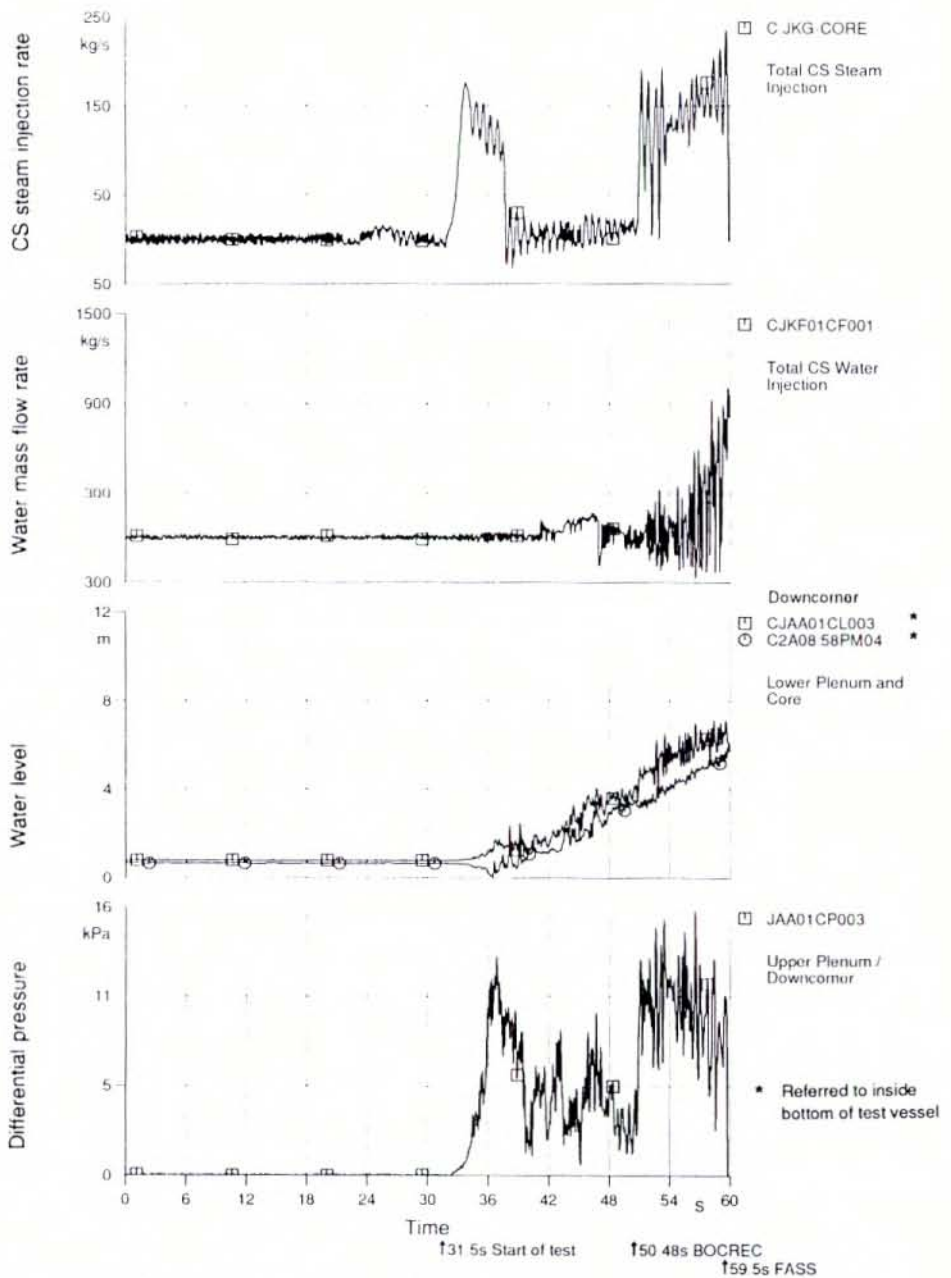
WATER LEVEL IN DOWNCOMER AND CORE SIMULATOR,
DIFFERENTIAL PRESSURE FROM UP TO DC,
AND CORE SIMULATOR INJECTION RATES
UPTF TEST 24 (RUN 302)
FIGURE 4.11-1
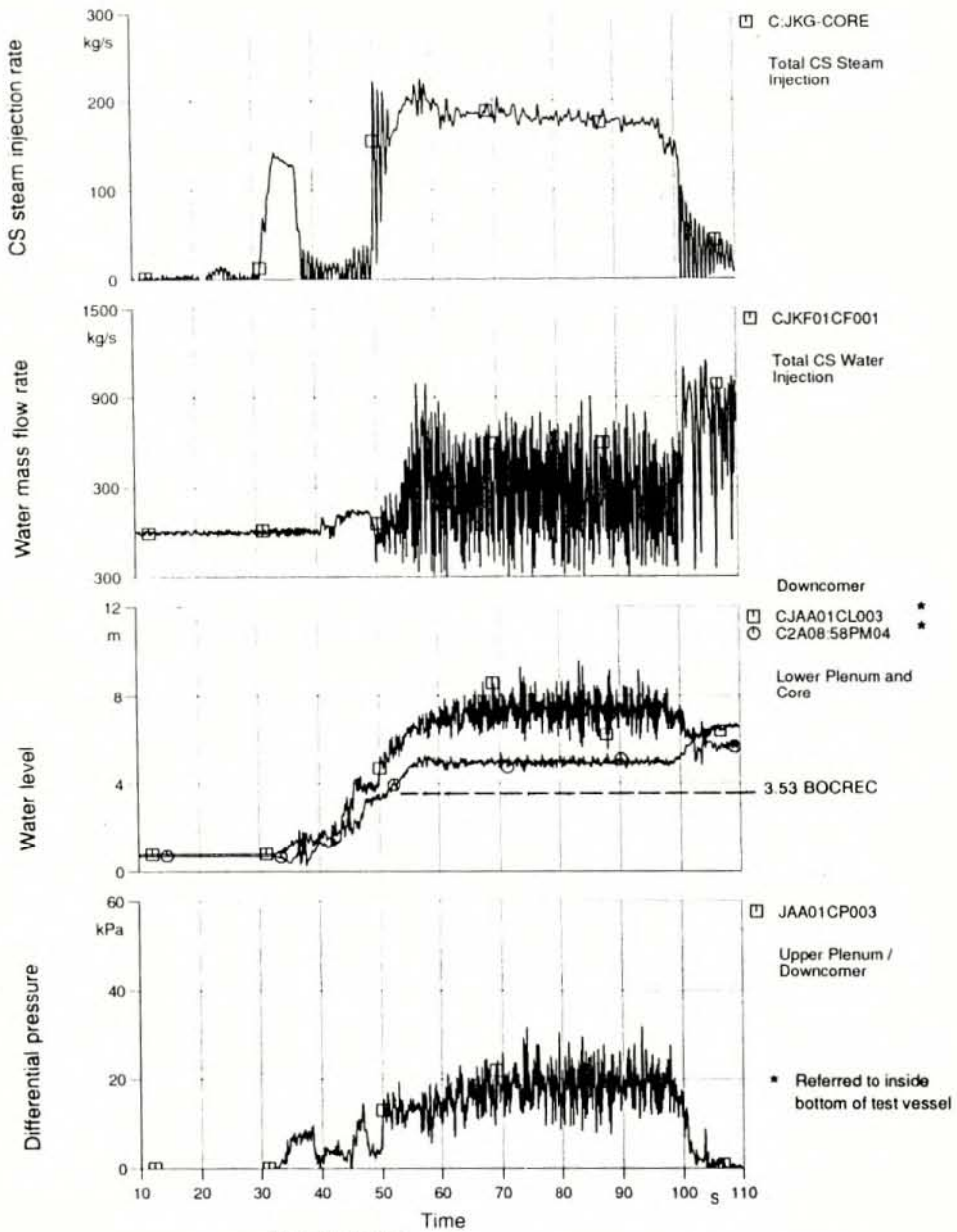
WATER LEVEL IN CORE SIMULATOR AND DOWNCOMER,
DIFFERENTIAL PRESSURE FROM UP TO DC,
AND CORE SIMULATOR INJECTION RATES
UPTF TEST 24 (RUN 304)
FIGURE 4.11-2

Section 5

TRAC ANALYSES

5.1 INTRODUCTION

As part of the USNRC contribution to the 2D/3D Program, the Transient Reactor Analysis Code (TRAC), developed by Los Alamos National Laboratory (LANL), was provided to the other participants in the program. In addition, LANL carried out an analytical support program using TRAC under the direction of the USNRC. Selected TRAC calculations were also carried out by the other program participants.

The objectives of the USNRC analytical support program were to utilize TRAC to:

- Provide analysis support during the design phase of UPTF and SCTF.

- Evaluate the location, type, and desired accuracy of instrumentation in UPTF, SCTF and CCTF.

- Help specify test boundary and initial conditions.

- Perform pretest predictions and post-test analyses.

- Provide analytical coupling between UPTF and SCTF.

- Checkout and validate TRAC to form a basis for credible prediction of the behavior of a full-size PWR during the end-of-blowdown, refill, and reflood phases of an LBLOCA.

The remainder of this section provides an overview of TRAC and discusses assessment results obtained as part of the 2D/3D Program. This section is intended to provide an overview of TRAC and its capabilities with respect to LBLOCA phenomena occurring from the end-of-blowdown through refill and reflood. Calculations were generally performed using the latest version of TRAC available at the time. In discussing results, the emphasis is placed on results obtained with TRAC-PF1/MOD1 and MOD2. These code versions are still in use so assessment information on them is of current interest. Results obtained using earlier versions were important in their contribution to an understanding of test results and in their impact on code development. At the time of this writing, the only TRAC versions recommended for use are TRAC-PF1/MOD1 and MOD2.

5.2 OVERVIEW OF TRAC

5.2.1 History

At the beginning of the 2D/3D Program, TRAC was an experimental code for reactor safety analysis. Concurrent with the 2D/3D Program, TRAC was developed into a sophisticated and mature computer code for the analysis of thermal-hydraulic transients in reactor systems. The use of TRAC as a part of the 2D/3D Program contributed significantly to its development as code experience and data from the 2D/3D Program were continually fed back to the code developers. The 2D/3D Program provided the best and most complete set of experimental data for assessing TRAC against large-break LOCA (LBLOCA) phenomena. TRAC has gone through several major releases with a number of versions of each release. The last code version used as part of the 2D/3D Program was TRAC-PF1/MOD2, version 5.3, which was released in June 1990.

A preliminary TRAC version consisting of only one-dimensional components was completed in December 1976. Although this version was not released publicly nor documented formally, it was used in TRAC-P1 development and formed the basis for the one-dimensional loop component modules. The first publicly released version, TRAC-P1, was completed in December 1977.

TRAC-P1 was designed primarily for analysis of LBLOCAs in PWRs. It could be applied to many analyses ranging from blowdowns in simple pipes to integral LOCA tests in multiloop facilities. A refined version, TRAC-P1A, was released to the National Energy Software Center in May 1979. Although it treated the same class of problems, TRAC-P1A was more efficient than TRAC-P1 and incorporated improved hydrodynamic and heat transfer models.   TRAC-PD2 (released in April, 1981) contained improvements in reflood heat transfer models and numerical solution methods. Although TRAC-PD2 was an LBLOCA code, it was applied successfully to small-break problems and to the Three Mile Island transient.

TRAC-PF1 was designed to improve the ability of TRAC-PD2 to handle small-break LOCAs and other transients. TRAC-PF1 used a full two-fluid model with two-step numerics in the one-dimensional components. The two-fluid model, in conjunction with a stratified-flow regime, handled countercurrent flow better than the drift-flux model used previously. The two-step numerics allowed large time steps for slow transients.   A one-dimensional core component permitted simpler calculations, although the three-dimensional vessel option was retained. A noncondensible gas field was added to the one- and the three-dimensional hydrodynamics. Significant improvements were also made to the trip logic and the input. TRAC-PFl was released publicly in July 1981.

TRAC-PF1/MOD1 (Reference E-603) provided full balance-of-plant modeling through the addition of a general capability to model plant control systems. The steam generator model was improved and a special turbine component was added. The physical models were also modified, with the condensation model containing the most significant changes. Wall heat transfer in the condensation and film-boiling regimes was improved. Finally, the motion equations were modified to include momentum transport by phase change, and to preserve momentum conservation in the three-dimensional vessel. TRAC-PF1/MOD1 was released in April, 1986.

TRAC-PF1/MOD2 was released in June 1990. It contained several improvements including a generalized heat structure capability with fully implicit axial conduction, improved constitutive models, better heat-transfer and drag correlations, an improved reflood model, and several additional refinements for a variety of components. These upgrades are discussed in more detail in Section 5.2.3.

5.2.2 TRAC-PF1/MOD1 and TRAC-PF1/MOD2 Characteristics

TRAC-PF1/MOD1 is described in References E-602, E-603 and E-604, and TRAC-PF1/MOD2 is described in References E-605, E-606, E-607 and E-608. Key characteristics of the TRAC-PF1/MOD1 and TRAC-PF1/MOD2 are summarized below.

- Variable-Dimensional Fluid Dynamics. A one-dimensional or three-dimensional (r, θ, z) flow calculation can be used within the reactor vessel. Flow within the loop components is treated one-dimensionally. Three-dimensional modeling provides explicit calculations of multidimensional flow patterns inside the reactor vessel that are important in determining ECC penetration during blowdown. Multidimensional core flow effects, upper plenum pool formation, and core penetration during reflood can be treated directly.

- Nonhomogeneous, Nonequilibrium Modeling. A full two-fluid (six-equation) hydrodynamic model describes the steam-water flow, thereby allowing important phenomena such as countercurrent flow to be treated explicitly. A stratified flow regime is included in the one-dimensional hydrodynamics. A seventh field equation (mass balance) describes a noncondensible gas field, and an eighth field equation tracks solutes in the liquid.

- Flow-Regime-Dependent Constitutive Equation Package. The thermal-hydraulic equations describe the transfer of mass, energy, and momentum between the steam-water phases and the interaction of these phases with the heat flow from the system structures. Because these interactions are dependent on the flow topology, a flow-regime-dependent constitutive equation package has been incorporated into the code.

- Consistent Analysis of Entire Accident Sequences. An important TRAC feature is its ability to address entire accident sequences, including computation of initial conditions, with a consistent and continuous calculation. For example, the code models the blowdown, refill, and reflood phases of a LOCA. This modeling eliminates the need to perform calculations using different codes to analyze a single accident. In addition, a steady-state solution capability provides self-consistent initial conditions for subsequent transient calculations.

- Component and Functional Modularity. TRAC is completely modular by component. The components in a calculation are specified through input data. Available components allow the user to model a wide range of PWR designs or experimental configurations. This feature also allows component modules to be improved, modified, or added without disturbing the remainder of the code. TRAC component modules currently include accumulators, breaks and fills, heat structures, pipes, plenums, pressurizers, pumps, steam generators, tees, turbines, valves, and vessels with associated internals (downcomer, core, upper plenum, etc.).

  TRAC is also modular by function; that is, major aspects of the calculations are performed in separate modules. For example, the basic one-dimensional hydrodynamics solution algorithm, the wall-temperature field solution algorithm and other functions are performed in separate routines that can be accessed by all component modules. This modularity allows the code to be upgraded readily as improved correlations and test information become available.

- Comprehensive Heat-Transfer Capability. TRAC-PF1/MOD2 incorporates detailed heat-transfer analyses of the vessel and the loop components. Included is a two-dimensional (r,z) treatment of fuel-rod heat conduction with dynamic fine-mesh rezoning to resolve both bottom-flood and falling-film quench fronts. The heat transfer from the fuel rods and other system structures is calculated using flow regime-dependent heat-transfer coefficients obtained from a generalized boiling curve based on a combination of local conditions and history effects.

- Machine Independent Programing. The code was originally designed for the Control Data Corporation CDC 7600 computer. TRAC may also be run on Cray computers (1-s, X-MP, Y-MP) using the Cray operating system, UNICOS, or the Cray Timesharing System (CTSS) used at LANL, the IBM using VM or MVS operating systems, and Cyber 205, Amdahl, and FACOM computers. Efforts have been made to make the programming as machine independent as possible.

5.2.3 Changes from TRAC-PF1/MOD1 to TRAC-PF1/MOD2

Several improvements were made between the MOD1 and MOD2 versions of TRAC-PF1. The improvements are listed below.

- The MOD2 models and correlations (Reference E-606) are more defensible.

- MOD2 runs faster than MOD1. Depending on the type of transient and the noding, it will run between 1.2 and 10.0 times faster than MOD1.

- The improved post-CHF heat transfer and interfacial models in MOD2 accurately simulate separate-effects tests.

- MOD2 has an improved reflood model based on mechanistic and defensible models.

- There are improved constitutive models in MOD2 for downcomer penetration, upper plenum de-entrainment, hot/cold leg ECC injection, vertical stratification in the vessel component, and condensation and evaporation in the presence of noncondensibles.

- Generalized heat structure capability in MOD2 allows the user to accurately model complicated configurations.

- An improved valve model based on experimental data for partially closed valves was implemented in MOD2.

- Improved vessel numerics that eliminate mass errors even at large time step sizes that can occur in small breaks or operational transients were included in MOD2.

- An offtake model is available in MOD2 to accurately represent small breaks in the bottom, top, or side of a pipe.

- The American Nuclear Society (ANS) 1979 Decay Heat Standard was implemented as a default model in MOD2.

- A countercurrent flow limitation (CCFL) model was implemented in both the one-dimensional and three-dimensional components in MOD2.

- An improved subcooled boiling model based on published correlations was implemented in MOD2.

- The momentum solution was forced to be conserving in MOD2.

- The external thermocouple model developed by the United Kingdom Atomic Energy Authority (UKAEA) was implemented in MOD2.

- The fully implicit axial conduction solution developed by the Japan Atomic Energy Research Institute (JAERI) was implemented in MOD2.

5.2.4 TRAC Assessment Descriptors

In the course of TRAC assessment using 2D/3D data, it was recognized that a standardized, consistent terminology needed to be developed to describe the code performance in post-test calculations. LANL developed this terminology in the form of four code assessment "descriptors", as defined below:

- Excellent agreement applies when the code exhibits no deficiencies in modeling a given behavior. Major and minor phenomena and trends are correctly predicted. The calculated results are judged to agree closely with the data. The calculation will, with few exceptions, lie within the uncertainty bands of the data. The code may be used with confidence in similar applications. (The term major phenomena refers to the phenomena that influence key parameters such as rod cladding temperature, pressure, differential pressure, mass flow rate, and mass distribution.   Predicting major trends means that the prediction shows the significant features of the data. Significant features include the magnitude of a given parameter through the transient, slopes, and inflection points that mark significant changes in the parameter.)

- Reasonable agreement applies when the code exhibits minor deficiencies. Overall, the code provides an acceptable prediction. All major trends and phenomena are correctly predicted. Differences between calculation and data are greater than deemed necessary for excellent agreement. The calculation will frequently lie outside but near the uncertainty bands of the data. However, the correct conclusions about trends and phenomena would be reached if the code were used in similar applications. The code models and/or facility noding model should be reviewed to see if improvements can be made.

- Minimal agreement applies when the code exhibits significant deficiencies. Overall, the code provides a prediction that is only conditionally acceptable. Some major trends or phenomena are not predicted correctly, and some calculated values lie considerably outside the uncertainty bands of the data. Incorrect conclusions about trends and phenomena may be reached if the code were used in similar applications, and an appropriate warning needs to be issued to users. Selected code models and/or facility noding need to be reviewed, modified and assessed before the code can be used with confidence in similar applications.

- Insufficient agreement applies when the code exhibits major deficiencies. The code provides an unacceptable prediction of the test. Major trends are not predicted correctly. Most calculated values lie outside the uncertainty bands of the data. Incorrect conclusions about trends and phenomena are probable if the code is used in similar applications, and an appropriate warning needs to be issued to users. Selected code models and/or facility noding need to be reviewed, modified and assessed before the code can be used with confidence in similar applications.

These descriptors are used in this report.

5.3 PRESSURIZED WATER REACTOR (PWR) CALCULATIONS WITH TRAC

During the course of the 2D/3D Program, a number of PWR calculations were performed with TRAC. Plant calculations were particularly important in the 2D/3D Program because the tests did not simulate the entire LBLOCA transient. Hence, specification of initial and boundary conditions for 2D/3D Program tests entailed trying to simulate mid-transient conditions of a LOCA. In this regard, the TRAC PWR analyses provided useful guidance for selecting test conditions. The code calculations also provided a link from subscale experiments to full-scale plants. The PWR calculations are listed in Table 5.3-1 and are discussed briefly below.

5.3.1 US/J PWR Calculations

Six US/J PWR calculations were performed using the latest version of TRAC available at the time of the calculation. Code versions are documented in Table 5.3-1. In the calculations, a 200% cold leg break LOCA in a generic four-loop PWR was assumed. Fuel assemblies of either 15x15 or 17x17 were simulated depending upon the calculation. Three types of boundary conditions were used in the calculations, including conservative conditions, minimum safeguards conditions and most-probable conditions.

These TRAC calculations were used to determine test conditions for 2D/3D tests. Specifically, tests with low initial cladding temperatures at reflood initiation were added to the CCTF, SCTF, and UPTF test matrices to obtain experimental data under the best-estimate conditions covered in the TRAC calculations. Also, a test to investigate the nitrogen surge at the end of accumulator injection was added to the UPTF test matrix.

As an example, key results from a US/J PWR calculation are given below. This calculation was for a 200% cold leg break LOCA in a generic four-loop PWR. The analysis noding is shown in Figure 5.3-1. Three-dimensional vessel noding with four radial rings and eight tangential sectors was used. The initial and boundary conditions represented the minimum safeguards conditions at 102% power. Minimum safeguards conditions include: maximum fuel power peaking and stored energy, single active failure in the ECCS, and loss-of-offsite power. Important results of this analysis were:

- The PCT of 933 K for the hot-channel best-estimate (BE) rod (34.74 kW/m peak linear power) and 897 K for the highest powered average rod (29.95 kW/m) occurred during early blowdown at 3.5 seconds (Figure 5.3-2).

- The end of bypass and end of late blowdown occurred at 25 seconds.

- ECC liquid entered the core at 39 seconds (beginning of core recovery).

- Accumulator nitrogen began to flow into the cold legs at 45 seconds, producing an increase in cold-leg pressure and a surge of liquid into the core. Accumulators in the intact loops emptied of water at 49 seconds.

- The PCT of the BE rod during the refill and reflood phases of the transient was 854 K, at a time of 40 seconds.

- The end of accumulator flow was followed by a slow filling of the core. All of the average rods were quenched at 160 seconds, the hot-channel BE rods at 177 seconds.

5.3.2 GPWR Calculations

Six GPWR calculations were performed as part of the 2D/3D Program. These are listed as part of Table 5.3-1. These calculations were used to specify the initial and boundary conditions for SCTF-III tests and UPTF tests which simulated a GPWR with combined ECC injection. They were also used in specifying the steam generator simulator operational characteristics in UPTF.

As an example, key results from a GPWR calculation for a 200% cold leg break in a Siemens/KWU 4-loop PWR follow. The vessel noding is shown in Figure 5.3-3. Three-dimensional vessel noding with four radial rings and eight azimuthal sectors was used. The initial conditions were steady-state operation at 100% power. The key boundary condition was five of eight ECC systems available (two in hot legs, three in cold legs), which is the minimum licensing condition. Important results of this analysis were:

- The PCT of 833 K (average power rod) and 973 K (high power rod) occurred during blowdown at about five seconds (Figure 5.3-4).

- During blowdown, local enhanced heat transfer and quenching occurred in a region of the core under the Loop 2 hot leg, due to water from the pressurizer flowing through this region.

- There was about 2500 kg of water in the lower plenum (about 10% full) at the conclusion of blowdown.

- ECC water plugs formed in the hot and cold legs and oscillated with significant amplitude. ECC was delivered to the vessel in an intermittent manner.

- During reflood, ECC from the hot leg injectors penetrated from the upper plenum to the core in local regions adjacent to the hot legs. Upflow was calculated in the remaining regions of the core.

- The PCT during reflood was about 800 K (average power rod) and 970 K (high power rod). See Figure 5.3-4.

- In breakthrough areas, quench occurred by 55 seconds. In other regions, quench occurred by 88 seconds (average power rod) and 133 seconds (high power rod).

5.3.3 ABB/BBR and B&W Type PWR Calculations

Within the 2D/3D Program, two ABB/BBR and B&W type PWR calculations were performed; one for the ABB/BBR PWR and one for the B&W PWR (Table 5.3-1). Both of these plant types use a two hot leg, four cold leg (i.e., 2 x 4) loop arrangement with once-through steam generators. The ABB/BBR plant has a raised loop configuration with no part of a loop below the cold leg nozzle elevation. The B&W calculation was for a lowered loop plant which has part of the loops below the cold leg nozzle elevation. The ABB/BBR plant is also about 1/3 larger than the B&W plant that was the subject of the plant calculation. Both of these plant types have vent valves between the upper plenum and the downcomer to provide a flow path alternative to the loops.

The B&W plant calculation was a 200% cold leg break with technical specification conditions. The assumed operating conditions included 2% initial core overpower, full availability of the two core flooding tanks, one low-pressure-injection pump, and one high-pressure injection pump. Important results of this analysis were:

- The PCT of 1284 K for the hot channel rod (57.7 kW/m peak linear power) and 995 K for the highest average powered rod (28.7 kW/m) occurred during blowdown at 8 seconds.

- Flow from the core flooding tanks began at 11.5 seconds as the system depressurized to the check valve set point.

- Blowdown ended at 23 seconds.

- Reflood of the core started at 26.5 seconds after the lower plenum was refilled.

- The core region quenched completely by 160 seconds.

- The percent bypass was 41% where the bypass is defined as the percentage of the total core flooding tank water flowing out the cold leg break (vessel side).

- During reflood, 46% of the net steam flow exiting the core passed through the vent valves.

The ABB/BBR calculation was also for a double-ended cold leg break LOCA. The initial and boundary conditions were based on EM conditions which included 5% initial core overpower, 120% decay heat, and reduced number of operational ECC systems. Important results are summarized below.

- The PCT of 1193 K for a high powered rod occurred at the end of refill.

- Blowdown ended at 20 seconds and reflood started at 26 seconds.

- The region with the highest power was quenched at 150 seconds and the entire core was quenched at 250 seconds.

- During reflood, about 60% of the steam generated in the core flowed through the vent valves. The remaining 40% flowed out the hot legs.

5.3.4 Conclusions

The TRAC calculations for PWRs gave useful information to aid in specifying the initial and boundary conditions for CCTF, SCTF, and UPTF tests.

Table 5.3-1

TRAC PWR AND RELATED CALCULATIONS

(Note: The most recent calculations are listed first for each PWR type.)

PWR Type	Report Title	Source	Reference	TRAC Version
US/J	TRAC-PF1/MOD1 US/Japanese PWR Conservative LOCA Prediction	INEL	U-727	PF1/MOD1 v. 14.3
US/J	TRAC-PF1/MOD1 Analysis of a Minimum-Safeguards Large-Break LOCA in a US/Japanese PWR with Four Loops and 15x15 Fuel	LANL	U-726	PF1/MOD1 v. 12.2
US/J	TRAC-PF1/MOD1 Analysis of a 200% Cold Leg Break in a US/Japanese PWR with Four Loops and 15x15 Fuel	LANL	U-723	PF1/MOD1 [1]
US/J	TRAC-PF1/MOD1 Analysis of a Minimum-safeguards Large-break Loss-of-Coolant Accident in a 4-loop PWR with 17x17 Fuel	LANL	U-724	PF1/MOD1 [1]
US/J	TRAC-PF1 Analysis of a Best-estimate Large-break LOCA in a Westinghouse PWR with Four Loops and 17x17 Fuel	LANL	U-722	TRAC-PF1

Table 5.3-1

TRAC PWR AND RELATED CALCULATIONS

(Note: The most recent calculations are listed first for each PWR type.)

PWR Type	Report Title	Source	Reference	TRAC Version
US/J	A TRAC-PD2 Analysis of a Large-Break Loss-of-Coolant Accident in a Reference US PWR	LANL	U-721	PD2
GPWR	Calculation of a Double Ended Break in the Cold Leg of the Primary Coolant Loop of a German Pressurized Water Reactor with a 5/8 Emergency Cooling Injection	GRS	G-661	PF1/MOD1 v. 12.5
GPWR	Calculation of a Double Ended Break in the Hot Leg of the Primary Coolant Loop of a German Pressurized Water Reactor with a 5/8 Emergency Coolant Injection	GRS	G-663	PF1/MOD1 v. 12.5
GPWR	TRAC-PF1 Analysis of a 200% Hot-leg Break in a German PWR	LANL	U-748	PF1/MOD1 v. 8.2

Table 5.3-1

TRAC PWR AND RELATED CALCULATIONS

(Note: The most recent calculations are listed first for each PWR type.)

PWR Type	Report Title	Source	Reference	TRAC Version
GPWR	Comparison Between a TRAC GPWR Calculation and a CCTF Test with Combined Injection and EM Boundary Conditions for the Reflood Phase of a German PWR-LOCA	JAERI	J-608	PF1/MOD1 [1]
GPWR	GPWR-1982 TRAC-PF1 Base Case Results	LANL	U-747	PF1, PF1/MOD1
GPWR	A TRAC-PF1 Calculation of a Reference German PWR at the Initiation of ECC Injection	LANL	U-744	PF1
GPWR	GPWR-1982 TRAC-PF1 Input Deck Description	LANL	U-746	PF1
GPWR	TRAC-PD2 Calculation of a Double-Ended Cold-Leg Break in a Reference German PWR	LANL	U-743	PD2
BBR	GPWR Analysis with TRAC-PF1/MOD1 Version 12.5 BBR Type Reactor, 200% Cold Leg Pump Discharge Break EM-Condition	GRS	G-662	PF1/MOD1 v. 12.5

Table 5.3-1

TRAC PWR AND RELATED CALCULATIONS

(Note: The most recent calculations are listed first for each PWR type.)

PWR Type	Report Title	Source	Reference	TRAC Version
B&W	TRAC-PF1/MOD1 Analysis of a 200% Cold Leg Break in a Babcock & Wilcox Lowered-loop Plant	LANL	U-725	PF1/MOD1 v. 11.1

NOTES: 1. Code version not documented in report.

Downcomer

Core Boundary

Barrel-Baffle Region

Core Barrel

R1 = 1.090 m
R2 = 1.690 m
R3 = 1.940 m
R4 = 2.200 m
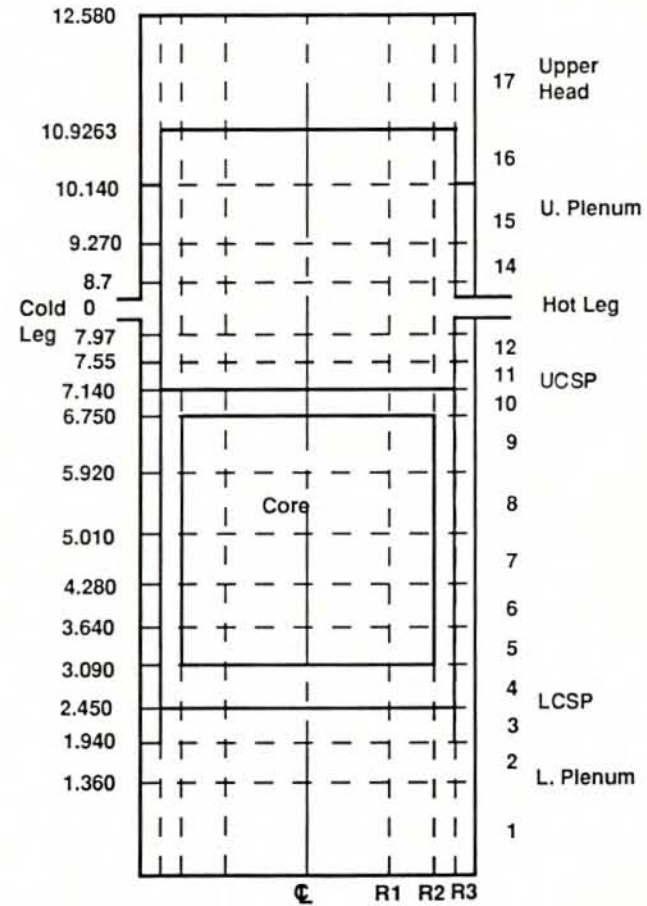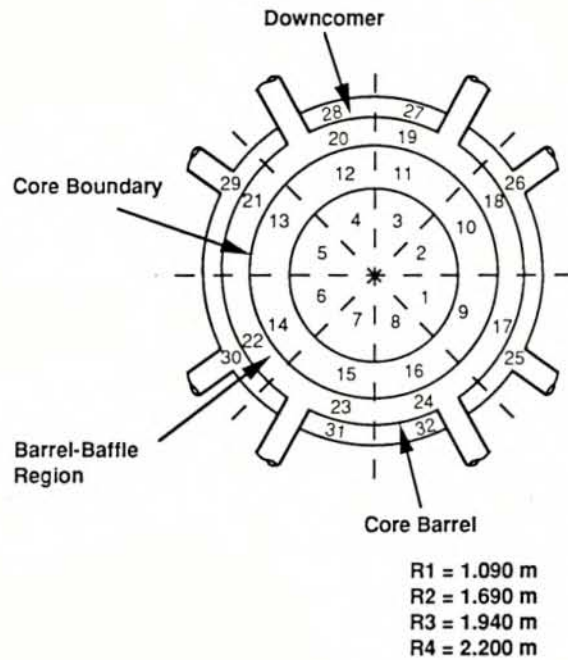
VESSEL NODING FOR US/J PWR TRAC ANALYSES
FIGURE 5.3-1
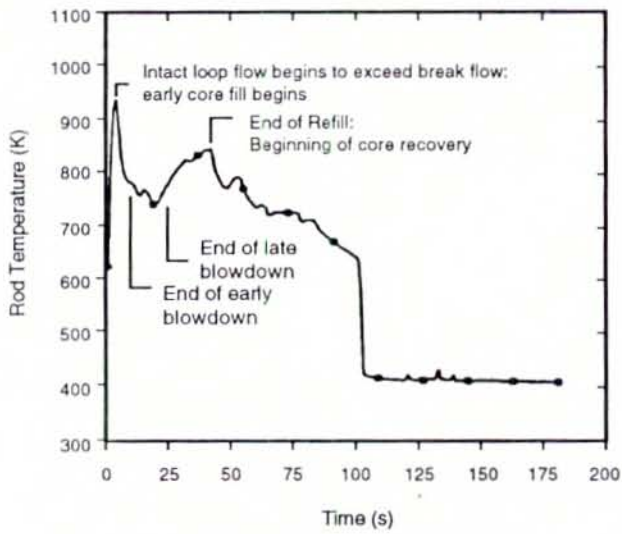
Maximum BE rod temperature
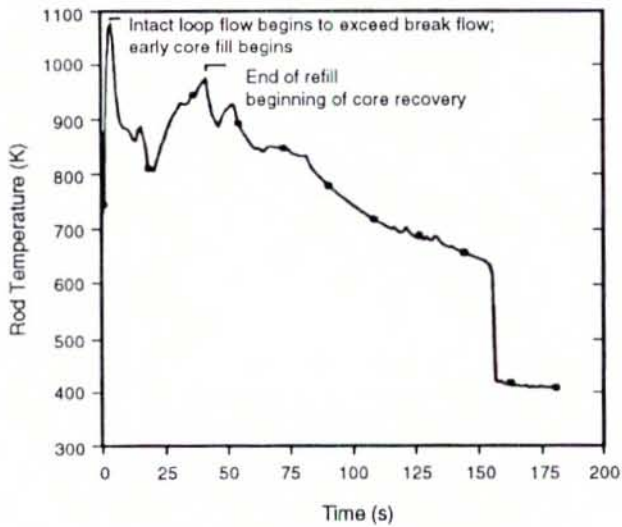
Maximum EM rod temperature

CALCULATED ROD TEMPERATURES FOR US/J PWRS
FIGURE 5.3-2
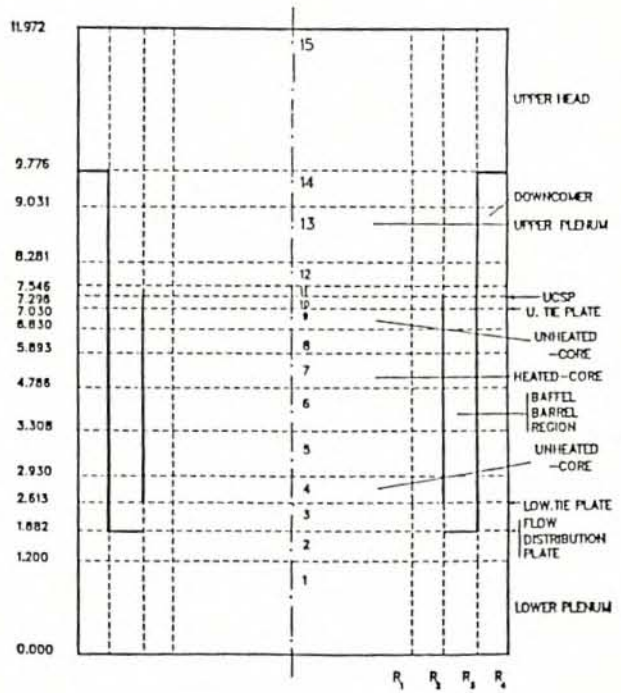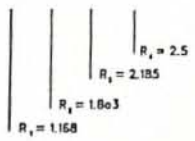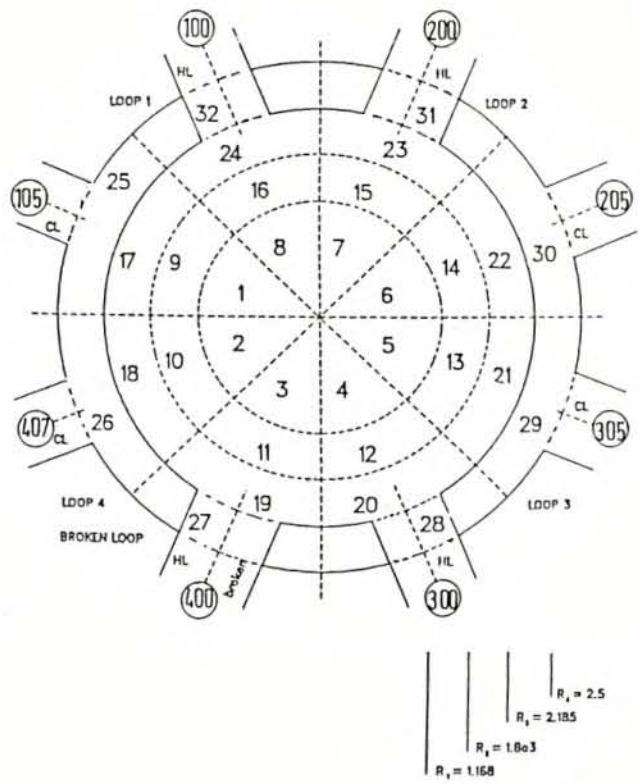
VESSEL NODING DIAGRAM FOR GPWR TRAC ANALYSES

FIGURE 5.3-3

GPWR 200% CLB, 5/8 ECC

MAXIMUM AVERAGE ROD TEMPERATURE

MAXIMUM HOT ROD TEMPERATURE
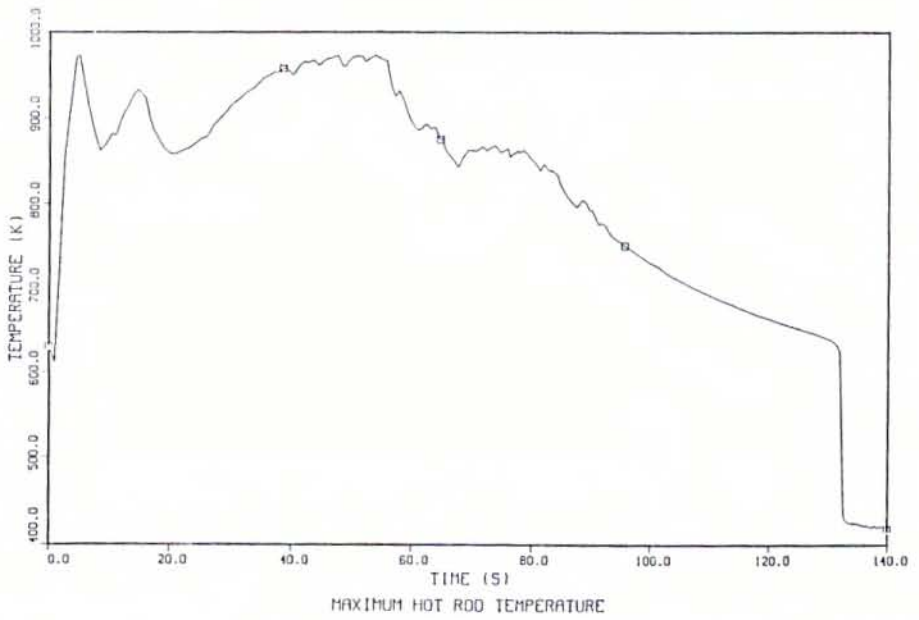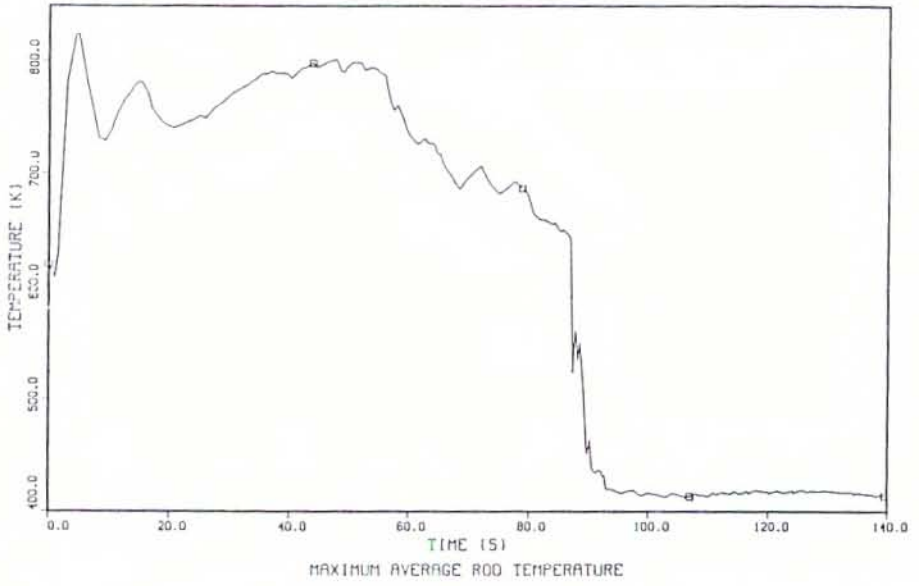
CALCULATED ROD TEMPERATURES FOR GPWRS
FIGURE 5.3-4

5.4 CCTF CALCULATIONS WITH TRAC

Because CCTF was already fully designed at the outset of the 2D/3D Program, design support calculations were not performed using TRAC. However, TRAC calculation results were used to evaluate the location, type, and desired accuracy of US-supplied instrumentation in CCTF-II, and to specify the initial and boundary conditions of the CCTF BE test (Run 71). A BE US/J PWR calculation had shown initial rod temperatures at the beginning of reflood that were much lower than rod temperatures obtained under conservative conditions. Consequently, the BE test was added to the CCTF test matrix.

CCTF calculations with TRAC were mainly post-test calculations for code assessment which have been documented in individual reports (listed in Tables 5.4-1 and 5.4-2) and in summary reports. The CCTF Core-1 summary report is Reference U-601; the CCTF Core-II summary report (except Upper Plenum Injection) is Reference U-621; and the Upper-Plenum Injection summary report is Reference U-622.

5.4.1 CCTF Core-I TRAC Calculation Results

Nine tests from the CCTF Core-I test series were analyzed using the TRAC-PD2 and TRAC-PF1 codes. Table 5.4-1 lists the CCTF-I tests analyzed with the code version and report citation. Most of the calculations were performed using a three-dimensional vessel component with either fine noding (four radial rings, four azimuthal sectors and 16 axial levels) or coarse noding (two radial rings, two aximuthal sectors and 16 axial levels). The assessment calculations for the CCTF Core- I tests covered reflood tests with parametric variations including loop K-factor, ECC flow rate, system pressure, and initial radial rod temperature profile.

The TRAC-PD2 code predicted the transient cladding temperature well, especially the PCT. Various deficiencies were found in the assessment calculations. The most significant of these was the TRAC-PD2 code did not correctly predict liquid entrainment and liquid distribution in the core. Results from these calculations were fed back to the TRAC code developers and affected later code development.

5.4.2 CCTF Core-II TRAC Calculation Results

Twenty tests from the CCTF Core-II test series were analyzed by LANL and JAERI using the TRAC-PF1/MOD1 and TRAC-PF1/MOD2 codes. Table 5.4-2 lists the calculations, the bibliography citations, and key results.

In the CCTF-II tests, various types of ECC injection were investigated including cold leg injection, downcomer injection with and without vent valves, upper plenum injection, and combined injection.

For cold leg injection, 11 tests were analyzed. Two base case tests (Runs 53 and 62) simulated reflood under conservative conditions for the US/J-type PWR. Eight reflood tests (Runs 51, 54, 55, 63, 64, 67, 70 and 75) were parametric variations on the base case tests covering changes in core power level, initial cladding temperature, system pressure, core radial power profile (steep or flat) and the end-of-blowdown and refill. The BE test (Run 71) simulated BE conditions based on a US/J PWR TRAC calculation.

For upper plenum injection (UPI), five tests were analyzed. These tests included tests under high power (Run 57), single failure (Run 59), symmetric (Run 72) and asymmetric (Run 76) injection, and BE (Run 78) conditions. The parameters varied were core power, core-stored energy, core radial power profile, UPI flow, UPI symmetry, system pressure, and the addition of the refill phase.

For downcomer injection, two tests were analyzed: downcomer injection without vent valves (Run 58) and downcomer injection with open vent valves (Run 69). For combined injection, two tests were analyzed: combined injection under EM conditions (Run 79) and combined injection under BE conditions (Run 80).

Most CCTF-II calculations were performed using a noding scheme with an intermediate level of detail. The vessel model used four radial rings, two azimuthal sectors and 16 axial levels. In this intermediate noding scheme the intact loops were combined into a single loop. A fine noding scheme was used for UPI tests, combined injection tests, and several reflood tests. It used a vessel with the same axial and radial noding but with four azimuthal sectors. In this fine noding scheme, each intact loop was modeled individually using cells with the same length as the cells in the combined intact loop of the intermediate noding scheme. Figure 5.4-1 shows a typical intact loop noding diagram.

5.4.2.1 Cold Leg Injection Tests

Core Thermal-hydraulic Behavior
TRAC calculations yielded reasonable to excellent agreement with measured peak rod temperatures, which ranged from 1000 to 1150 K. TRAC was generally able to predict PCT within 50 K as shown in Figure 5.4-2. Transient rod temperatures were predicted with reasonable to excellent agreement in the lower and middle elevations of the core, and reasonable agreement in the upper core elevations. TRAC-PF1/MOD1 tended to slightly underpredict cladding temperatures at upper core elevations and to predict early quench times at the core midplane. These discrepancies were caused by TRAC

deficiencies in predicting liquid distribution within the core. Figure 5.4-3 shows a comparison of calculated and measured differential pressure for the upper and lower halves of the core for Test C2-16 (Run 76), a UPI test. (The "spikes" in differential pressure indicate intermittent penetration from the upper plenum to the core.) As seen, the TRAC calculation tends to stratify the liquid more strongly than observed in the test.

A post-test calculation for CCTF Test C2-4 (Run 62) was performed as part of the 2D/3D Program using MOD2. MOD2 results were similar to MOD1 results. Rod temperature predictions were in reasonable agreement with the data and the major trends and phenomena were predicted. The MOD2 core reflood model did an improved job of predicting entrainment above the quench front and into the upper plenum. However, the core liquid inventory above the quench front was under predicted (Figure 5.4-4) while the upper plenum liquid level and liquid carryover from upper plenum to hotlegs were overpredicted.

Overall, TRAC-PF1/MOD1 predictions of thermal-hydraulic behavior in the vessel were in reasonable agreement with data. However, TRAC underpredicted the core inlet flow by about 25% because boiloff of liquid in the downcomer (i.e., downcomer voiding) caused underprediction of the downcomer head. In addition, calculated fluid temperatures at the core inlet exceeded measured values because of the excessive condensation in the cold leg and lack of thermal stratification in the TRAC plenum model. The reduced subcooling did not have a significant effect on core heat transfer or reflood rates.

For every test, TRAC correctly predicted an initial surge of liquid into the core during accumulator injection. The core liquid inventory at the end of this surge was a weak function of core power or power distribution in the experiments. TRAC predictions of the liquid inventory, while in reasonable to excellent agreement with the experimental data, showed a stronger dependence on core power, yielding overpredicted inventories at high power and underpredicted inventories at lower power. The amount of liquid in the upper half of the core and the upper plenum was predicted with minimal to excellent accuracy depending upon the test parameters; this matter deserved further study (see below).

Neither TRAC-PF1/MOD1 nor TRAC-PF1/MOD2 does a satisfactory job of predicting liquid distribution in the core during reflood. Models pertaining to core reflood were completely replaced in the conversion from MOD1 to MOD2. The models selected for MOD2 were chosen as a package that reflected the state-of-the-art for modeling the quenching process and associated phenomena. Results for core liquid distribution were only marginally better than results obtained with MOD1. Further study led LANL to conclude that this failure to predict core liquid distribution results from the inability of either version to model a simultaneous liquid upflow of droplets and downflow of films and/or rivulets on unheated structures. TRAC uses two-fluid modeling with

5.4-3

closure relations based on instantaneous, averaged local conditions with no history effects. It appears that further improvement in the modeling of these conditions would require modifying these fundamental assumptions and increasing the level of complexity.

Downcomer Thermal-hydraulic Behavior
TRAC-PF1/MOD1 predicted axisymmetrical water accumulation in the downcomer as observed in the CCTF tests. The downcomer water level showed a slight decrease after the initial fill to the bottom level of the cold leg nozzle. The decrease is attributed to the boiling due to the heat release from the superheated downcomer wall to the liquid carryover to the broken cold leg. The TRAC-PF1/MOD1 code predicted the decrease of the downcomer water level qualitatively although the decrease was sometimes overpredicted and sometimes underpredicted.

Upper Plenum Thermal-hydraulic Behavior
The pressure in the upper plenum was generally underestimated because the pressure drop through the broken cold leg of the pressure vessel side was underestimated. The predictions of the liquid level in the upper plenum vary in a complex manner from minimal to reasonable between tests. The TRAC-PF1/MOD1 code predicted almost complete water entrainment to the hot legs at high steam flow rates and no water entrainment to the hot legs at low steam flow rates. The entrainment rate was sensitive to the steam flow rate in the TRAC-PF1/MOD1 calculations. The liquid level in the upper plenum was sometimes underestimated because little water was entrained from the core due to the deficiency in the modeling of the core liquid distribution. This is one of the MOD1 code deficiencies identified during the program. The MOD2 calculation for Test C2-4 (Run 62) overpredicted the upper plenum liquid level. The reflood model in MOD2 gives significantly more entrainment above the quench front than the reflood model in MOD1.

Loop Behavior
The agreement of predicted loop differential pressures and mass flow rates with data was strongly correlated with agreement of the downcomer differential pressures. When the differential pressure in the downcomer was predicted well, these other parameters were also predicted well. When the differential pressure was overpredicted or underpredicted, so were these parameters. Overall, the agreement was judged to be reasonable even though the broken cold leg differential pressure was generally underpredicted. In one test (Run 71), excessively large oscillations were calculated by TRAC as a result of an overprediction of the condensation occurring in the loops.

The overprediction of condensation in CCTF cold leg ECC injection tests was identified as a code deficiency. Potential model changes that improved condensation modeling in CCTF were not incorporated into TRAC because they degraded condensation modeling for tests from a variety of other facilities.

TRAC calculations of liquid entrainment into the hot legs were reasonable at very high and very low steam flow rates, but TRAC tended to underpredict the liquid entrainment at intermediate flow rates. The modeling of steam generator heat transfer was reasonable.

5.4.2.2 Upper Plenum Injection (UPI) Tests

Five UPI tests were performed in the CCTF Core-II test program. Each test was analyzed with TRAC-PF1/MOD1 to assess the ability of the code to predict the phenomena of these tests and to determine code deficiencies associated with the phenomena. The TRAC-PF1/MOD1 calculations for four of the five UPI tests (Runs 59, 72, 76 and 78) are in overall reasonable agreement with the data. The prediction for the fifth test (Run 57) showed insufficient agreement with the data.

TRAC-PF1/MOD1 was able to qualitatively predict the channeling effect, asymmetric core reflood, the negative net core-inlet flow, and breakthrough location (Figure 5.4-5) with sufficient noding detail in the input models. The predicted rod temperatures in most cases were in reasonable agreement with the data.

As a consequence of these UPI assessment calculations, several deficiencies were identified. These are: (1) condensation modeling, (2) prediction of the CCFL at the tie plate, (3) prediction of entrainment/de-entrainment in the upper plenum, and (4) prediction of the core void fraction distribution.

As part of one study, the relationship between noding practice and the prediction of breakthrough location was examined. For very low UPI flows, a much finer noding (eight azimuthal sectors instead of four) was required to produce reasonable agreement in breakthrough location. User guidelines and noding recommendations were made for use in UPI input modeling.

5.4.2.3 Alternative ECCS Tests

The tests in the alternative ECCS series differed from the cold leg injection tests in the manner and location of emergency coolant injection. Run 58 investigated the effect of injecting ECC water directly into the downcomer. Except for the location of ECC injection, test conditions were identical to those of the base case test for cold leg injection (Run 62). Run 69 examined the effects of downcomer injection with vent-valves of the type used in Babcock & Wilcox reactor systems in the US and ABB/BBR reactors in the FRG. Initial conditions and the ECC-injection schedule were almost identical to the base case test for cold leg injection (Run 62).

Run 79 was performed to study the effects of ECC injection in both the hot and cold legs. This arrangement was characteristic of German PWRs. Run 79 simulated the "5/8 injection mode," in which only two hot leg and three cold leg injectors functioned. This is the worst case assumed for licensing in the FRG.

TRAC calculations and the experimental data agree that none of the alternative ECC system methods provides either significantly better or worse cooling of the core; all results are fairly similar to the baseline (cold-leg injection) in terms of peak rod temperatures. Overall, TRAC-PF1/MOD1 was able to consistently predict the major thermal-hydraulic phenomena in the vessel and the loops as well as the thermal behavior of the heated rods in the core. In particular, TRAC showed reasonable to excellent agreement with measured peak rod temperatures in the core under a wide variety of test boundary conditions.

The deficiencies identified were largely similar to those identified for cold leg injection and UPI tests (see Sections 5.4.2.1 and 5.4.2.2). These deficiencies are: (1) prediction of condensation in the hot legs, upper plenum and downcomer; (2) prediction of CCFL at the tie plate; (3) prediction of entrainment/de-entrainment in the upper plenum; (4) prediction of the core void fraction distribution; and (5) modeling of the vent valves.

5.4.3 Conclusions

The TRAC series of computer codes were extensively assessed against data from the CCTF Core-I and Core-II tests to check the predictive capability of the codes and to identify model deficiencies. In addition, a TRAC PWR calculation was used to specify the initial and boundary conditions of the BE CCTF reflood test. The assessment results provided an excellent technical basis for development and validation of the codes for prediction of the full-size PWRs during the end-of-blowdown, refill, and reflood phases of an LBLOCA.

The assessment results showed that the TRAC codes can be used to predict the cladding temperature transient during reflood in a PWR utilizing the ECC systems investigated in the CCTF tests. However, several deficiencies of TRAC (PD2, PF1, and PF1/MOD1) closure models were identified and recommendations were made to improve these models. The deficiencies identified included: (1) the prediction of the core void distribution, (2) entrainment/de-entrainment in the upper plenum, (3) condensation in the cold legs and downcomer with cold leg or downcomer injection, (4) condensation in hot leg and upper plenum with upper plenum or hot leg injection, (5) CCFL at the tie plate, and (6) vent valve model. TRAC-PF1/MOD2 code development was undertaken, in large part to address these deficiencies to the extent possible using recent models from the published literature.

Table 5.4-1

TRAC ANALYSES OF CCTF CORE-I TESTS

Test/Run Number	Description	Reference	TRAC Version
C1-01/10	Loop K-factor	U-603	PD2
C1-05/14	Base case	U-602 U-604 U-605 U-606 U-617	PD2
C1-05/14	Base case	J-985	PF1/M0D1 v. 8.2
C1-06/15	ECC flow	U-602 U-607 U-617	PD2
C1-10/19	System pressure	U-602 U-609 U-617	PD2
C1-11/20	Reproducibility	U-610 U-611	PD2
C1-12/21	System effect	U-602 U-612 U-617	PD2
C1-16/25	FLECHT coupling	U-613	PD2
C1-16/25	FLECHT coupling	J-601	PD2
C1-19/38	EM	U-614 U-615 U-618	PD2
C-1-19/38	EM	J-603 J-604	PD2
C1-20/39	Multidimensional effect	U-616	PD2
Summary	--	U-601	--

Table 5.4-2

TRAC ANALYSES OF CCTF CORE-II TESTS

Test/Run Number	Description	Reference	TRAC Version	Overall Agreement	Parameters Predicted	Deficiencies	
						Overpredicted	Underpredicted
C2-AC1/51	Low temperature	U-623	PF1/MOD1 v. 9.9	Reasonable	Maximum DC and LP differential pressures, core upper half and UP liquid level, hottest rod temperature, rod temperature history below core midplane	Core inlet liquid temperature, SG outlet temperature	DC differential pressure, system pressure, loop differential pressures and mass flow rates., peak rod temperature above core midplane
C2-SH1/53	Base case	U-624	PF1/MOD1 v. 8.1	Reasonable to excellent	DC, core, LP differential pressures; system pressure; loop mass flow rates; hottest rod temperature	Core inlet liquid temperature, SG outlet temperature	Liquid in core upper half and UP, peak rod temperature above core midplane
C2-SH2/54	Low power	U-625	PF1/MOD1 v. 11.8	Reasonable	Peak cladding temperatures, quench times	Condensation on cold leg ECC	Carryover from upper plenum to loops
C2-1/55	High pressure	J-609	PF1/MOD1 v. 12.5	Minimal to reasonable	Turnaround time and temperature	Void fraction in core, quench time in lower core	Liquid mass in core
C2-AA1/57	UPI, High Power	U-626 U-627	PF1/MOD1 v. 12.5	Insufficient	Multidimensional reflood	Liquid entrainment into hot legs and steam binding, amount of liquid downflow	Core water accumulation
C2-AA2/58	Downcomer injection	U-628	PF1/MOD1 v. 12.7	Reasonable	LP differential pressure; peak rod temperatures; rod temperature history below quench front; loop differential pressure and mass flow rate; system pressure	Liquid inventory in core and DC, oscillations in vessel differential, SG outlet temperature	Quench time above core midplane
C2-AS1/59	UPI, Single Failure	U-629	PF1/MOD1 v. 11	Reasonable	Multidimensional reflood, negative core inlet flow, rod temperatures (average values), amount of downflow	Condensation in cold legs	—
C2-4/62	Base case	J-607 J-609	PF1/MOD1 v. 12.5	Reasonable	Rod temperatures, turnaround time, quench time	Condensation in cold legs, liquid in core lower half	Liquid in core upper half
C2-4/62	Base case	U-714	PF1/MOD2 v. 5.3	Reasonable	Rod temperatures in lower half of core, carryover from core to upper plenum	Carryover to hot legs	Liquid in core upper half

Table 5.4-2

TRAC ANALYSES OF CCTF CORE-II TESTS

Page 2 of 3

Test/Run Number	Description	Reference	TRAC Version	Overall Agreement	Parameters Predicted	Deficiencies	
						Overpredicted	Underpredicted
C2-5/63	Low power	J-609	PF1/MOD1 v. 12.5	Minimal to reasonable	Turnaround time and temperature; quench time	Void fraction in core	Liquid mass in core
C2-5/63	Low power, steep profile	U-630	PF1/MOD1 v. 11.0	Reasonable to excellent	Maximum DC differential pressure; LP, core and UP liquid inventories; rod temperature histories at all locations; liquid flow in loops	SG outlet temperature	DC differential pressure, system pressure, loop differential pressures and mass flow rates
C2-6/64	Low power, flat profile	U-630	PF1/MOD1 v. 10.3	Reasonable to excellent	Maximum DC differential pressure; LP, core and UP liquid inventories; rod temperature histories at all locations; liquid flow in loops	SG outlet temperature	DC differential pressure, system pressure, loop differential pressures and mass flow rates
C2-8/67	Low pressure	J-609	PF1/MOD1 v. 12.5	Minimal to reasonable	Turnaround temperature, quench time	Void fraction in core	Liquid mass incore
C2-10/69	Vent valves	U-631	PF1/MOD1 v. 12.7	Minimal to reasonable	LP differential pressure; core inlet liquid temperature; upper core and UP liquid inventories; system pressure; rod temperature histories	DC differential pressure; core liquid inventory (lower half); system pressure	ECC bypass during BOCREC
C2-11/70	Refill	U-632	PF1/MOD1 v. 11.0	Minimal to reasonable	Overall trends	Sweepout of liquid from the LP, depressurization during the blowdown phase, downcomer inventory during the refill period	---
C2-12/71	Best estimate	J-609	PF1/MOD1 v. 12.5	Insufficient	---	---	Turnaround temperature, quench time, liquid mass in core
C2-12/71	Best estimate	U-633	PF1/MOD1 v. 12.3	Minimal to reasonable	DC and LP differential pressures, average system pressure, rod temperature histories at or below midplane, average loop differential pressures	Liquid temperature at core inlet; quench time above midplane; condensation oscillations and pressure oscillations in cold leg; SG outlet temperature	Core and UP liquid inventories

Table 5.4-2

TRAC ANALYSES OF CCTF CORE-II TESTS

Test/Run Number	Description	Reference	TRAC Version	Overall Agreement	Parameters Predicted	Deficiencies	
						Overpredicted	Underpredicted
C2-13/72	UPI, Symmetric	U-634	PF1/MOD1 v. 12.1	Reasonable	Multidimensional reflood, negative core inlet flow, location of liquid downflow, rod temperatures	Condensation in cold legs, amount of downflow	—
C2-15/75	FLECHT coupling	U-635	PF1/MOD1 v. 11.2	Reasonable	DC and LP differential pressures, core inlet temperature, core liquid distribution, system pressure, rod temperature history below midplane, loop pressure drop and mass flow rates	Cooling at core midplane (especially in periphery), manometer oscillations at BOCREC, SG outlet temperature	UP liquid inventory
C2-16/76	UPI, Asymmetric	U-636	PF1/MOD1 v. 12.3	Reasonable	Multidimensional reflood, negative core inlet flow, rod temperatures	Condensation in cold legs, amount of downflow	—
C2-18/78	UPI Best Estimate	U-637	PF1/MOD1 v. 12.3	Reasonable	Multidimensional reflood, negative core inlet flow, location of liquid downflow, rod temperatures	Condensation in cold legs, amount of downflow	—
C2-19/79	Combined injection	U-638	PF1/MOD1 v. 11.5	Minimal to reasonable	Average DC, LP, and core liquid inventories; LP temperature, average system pressure; top down quenching; rod temperature histories in all regions	Condensation oscillations	UP liquid inventory
C2-20/80	Combined injection	J-997	PF1/MOD1 v. 12.5	—	—	Condensation in hot legs and upper plenum	—
Summary	Non-UPI Tests	U-621	—	—	—	—	—
Summary (UPI)	All UPI Tests	U-622	—	—	—	—	—
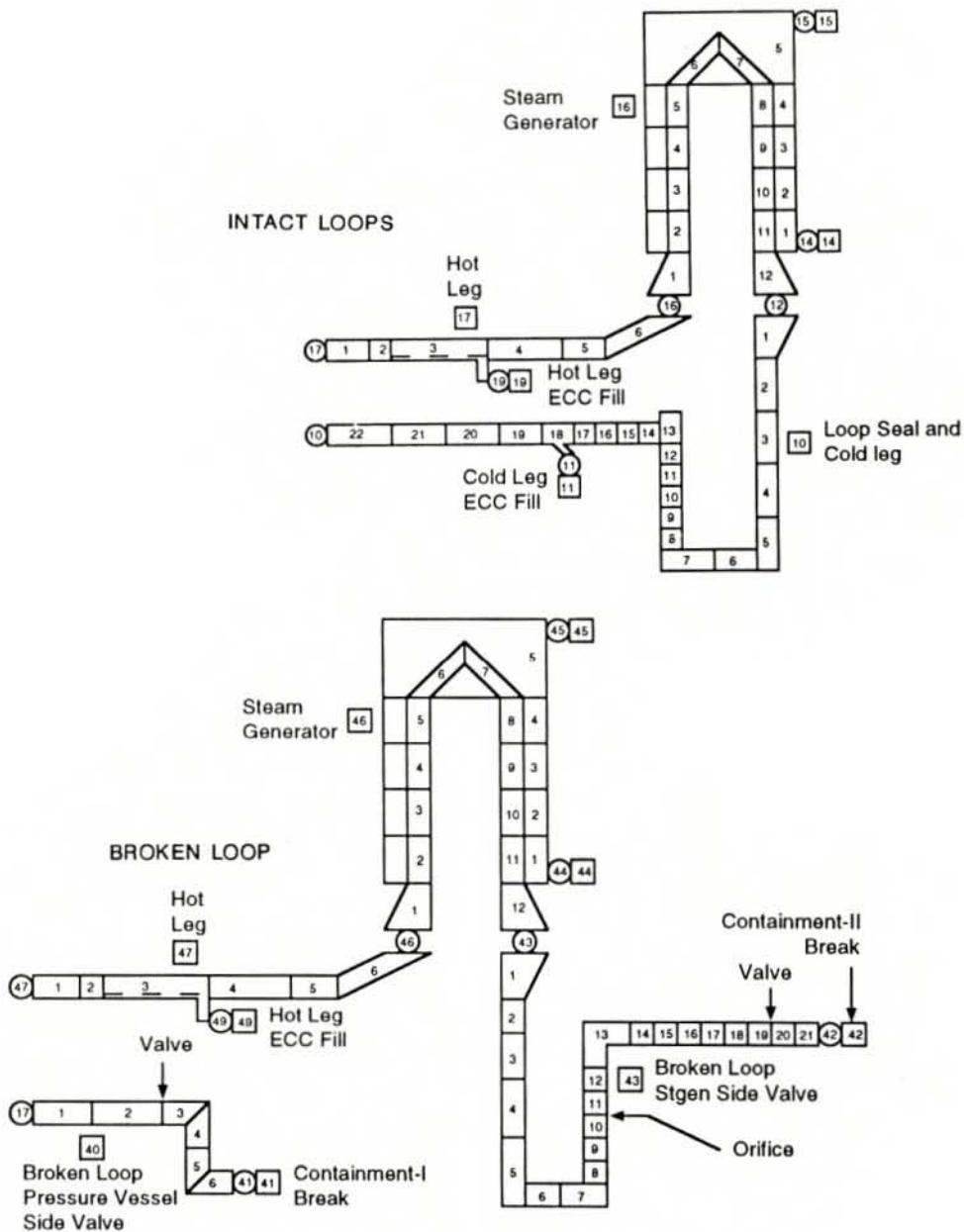
LOOP NODING FOR CCTF TRAC ANALYSES
FIGURE 5.4-1
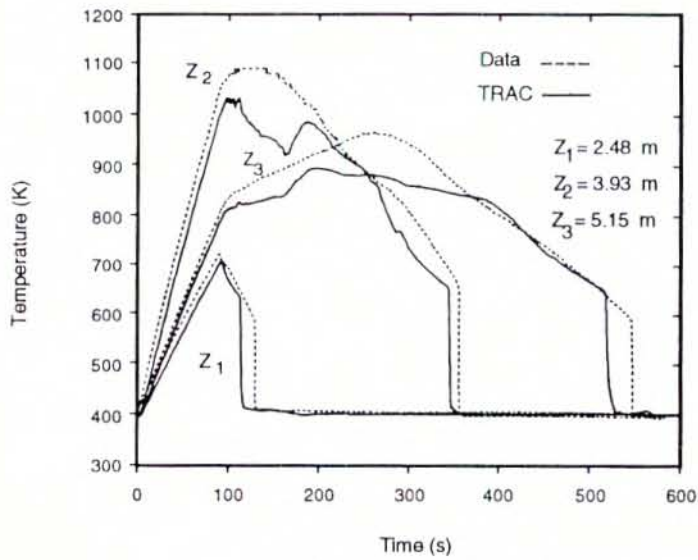
TEST C2-SH2 (RUN 54)
(TRAC-PF1/MOD1 V. 11.8)
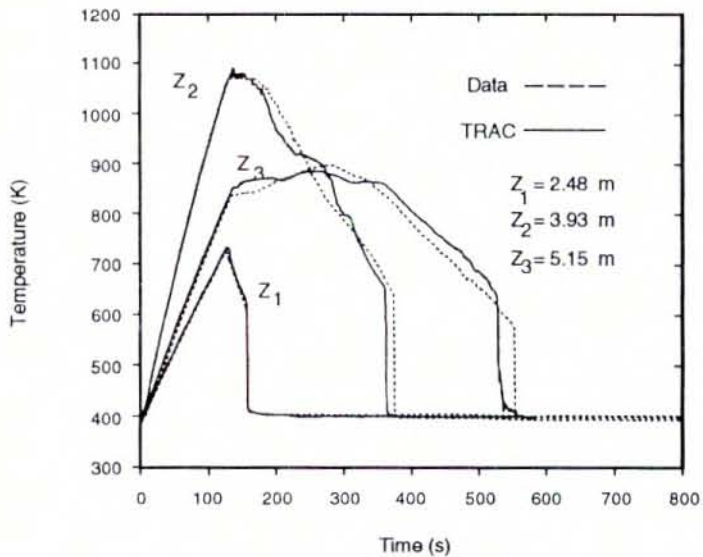
TEST C2-5 (RUN 63)
(TRAC-PF1/MOD1 V. 11.0)

TRAC/DATA COMPARISON OF HIGH POWERED ROD TEMPERATURES
CCTF TESTS C2-SH2 (RUN 54) AND C2-5 (RUN 63)

FIGURE 5.4-2
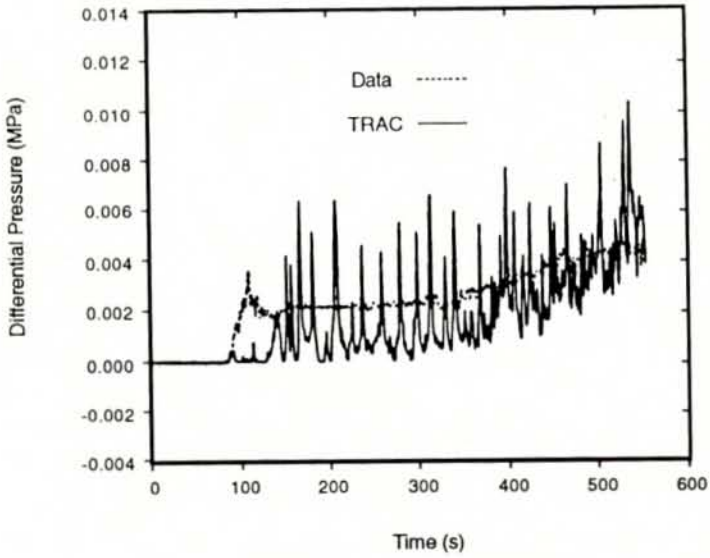
Core upper-half ΔP comparison
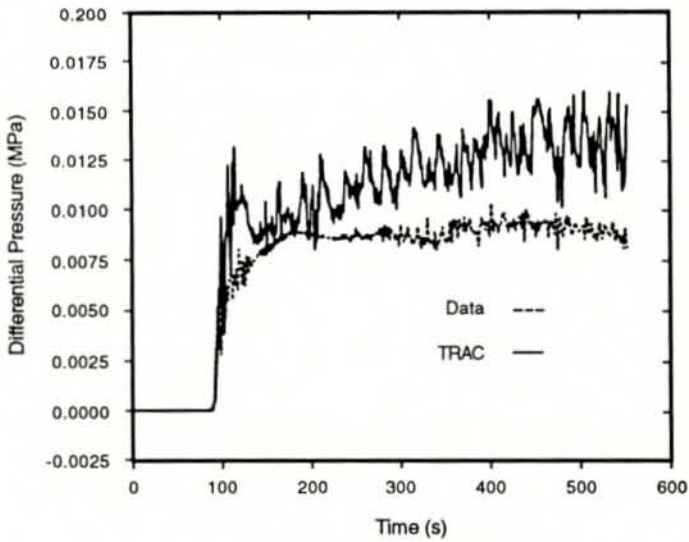
Core lower-half ΔP comparison

TRAC/DATA COMPARISON OF CORE DIFFERENTIAL PRESSURES
CCTF TEST C2-16 (RUN 76)
FIGURE 5.4-3
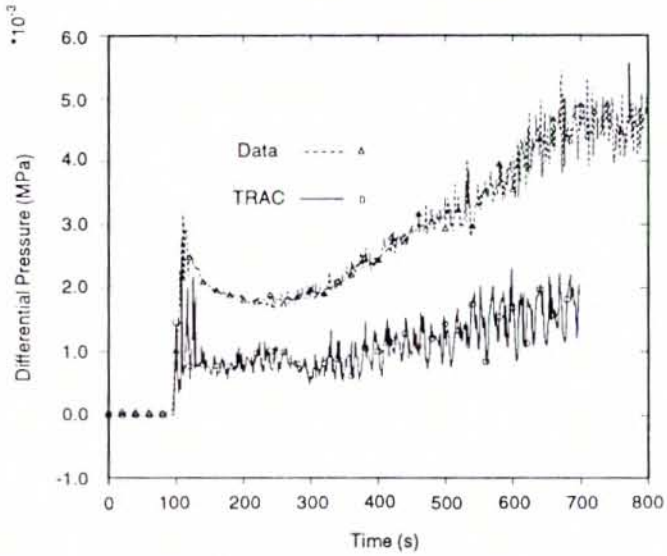
Core upper–half ΔP comparison
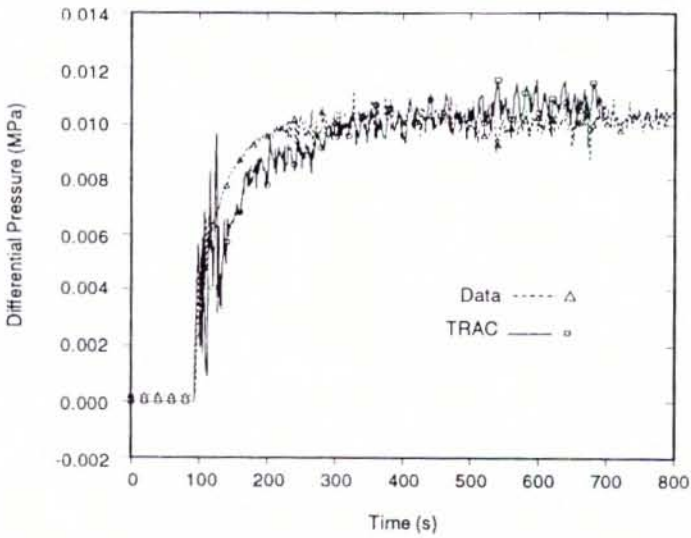
Core lower–half ΔP comparison

TRAC/DATA COMPARISON OF CORE DIFFERENTIAL PRESSURES
CCTF TEST C2-4 (RUN 62)
FIGURE 5.4-4

TRAC-PF1/MOD1 V. 12.3

Plant North

CCTF Results

☐ CCFL

▨ Small Tie Plate Downflow

▩ Large Tie Plate Downflow

TRAC Results
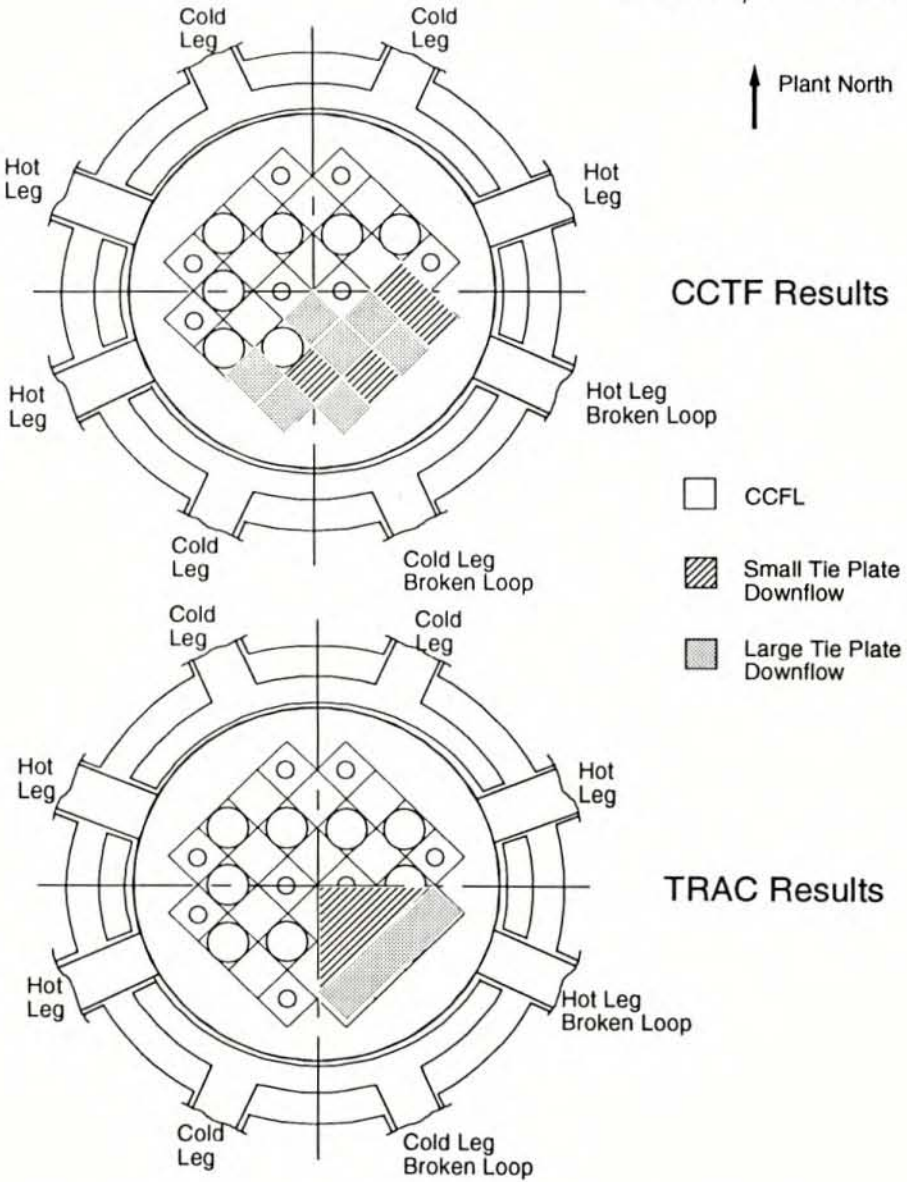
TRAC/DATA COMPARISON OF CORE DOWN FLOW REGIONS
CCTF TEST C2-16 (RUN 76)
FIGURE 5.4-5

5.5 SCTF CALCULATIONS WITH TRAC

TRAC calculations were used to a limited extent in supporting the design of SCTF. Specifically, TRAC calculations were performed to evaluate the SCTF steam supply and to evaluate operational approaches for combined injection (References U-642 and U-682). TRAC calculation results were used to evaluate the location, type, and desired accuracy of US-supplied instrumentation in SCTF, and to specify the initial and boundary conditions of the SCTF BE tests (Runs 614 and 714).

Most SCTF calculations with the TRAC codes were performed as post-test analyses to check the predictive capability of the TRAC codes. The results of these assessment calculations have been documented in individual reports (listed in Tables 5.5-1, 5.5-2 and 5.5-3) and in summary reports. The SCTF Core-I summary report is Reference U-641, the SCTF Core-II summary report is Reference U-661, and the SCTF Core-III summary report is Reference U-681.

5.5.1 Analytical Support for Design and Operation of SCTF

TRAC calculations were performed to evaluate the SCTF steam supply and evaluate operational approaches for combined injection. A series of parametric calculations were performed with TRAC-PD2 for the steam supply system of SCTF to resolve the issue of whether or not an external source of steam would be necessary to achieve refill and reflood behavior typical of a full-scale PWR. The conclusion from this study was that the external steam source was not necessary, but its inclusion would add flexibility to future SCTF tests.

An operational study was performed using TRAC-PF1/MOD1 to examine whether the GPWR transient (combined injection) could be simulated with the SCTF. Initial and boundary conditions were selected from a TRAC analysis of a GPWR and used for a TRAC SCTF calculation. Because the results from the SCTF calculation were in reasonable agreement with the TRAC-calculated GPWR results, it was concluded that appropriate initial and boundary conditions for the SCTF simulation of GPWR could be determined.

TRAC results for US/J PWR calculations were used to specify the initial and boundary conditions for the SCTF BE tests for US/J PWRs. In the specification of the test conditions, the initial cladding temperature at reflood initiation was determined based on the TRAC results. The specified temperature was much lower than conditions based on conservative rather than BE conditions.

5.5.2 SCTF Core-I TRAC Calculation Results

Thirteen tests in the SCTF Core-I test series were analyzed using the TRAC-PD2 and TRAC-PF1 codes. Table 5.5-1 lists the tests with the citations for the reports describing the analysis results. Most of the calculations of SCTF Core-I tests were performed using TRAC-PD2 with a finely noded two-dimensional vessel component (11 radial rings, 1 azimuthal sector and 13 axial levels).

The assessment calculations for the SCTF-I tests included various parametric effects such as system pressure, core radial power profile, core power level and core inlet flow rate and temperature. The assessment calculations were important in their contribution to an understanding of the phenomena in the tests and their impact on further code development. Information from 2D/3D assessment calculations, including SCTF-I, was continually fed back to the code developers. TRAC-PD2, which was used for most of the SCTF-I calculations has been superseded by three major code releases.

TRAC-PD2 predicted rod cladding temperature transients well, especially the peak cladding temperature which occurred right after the initiation of reflood. The total core differential pressure was predicted reasonably, including that the core's full-height axial differential pressure was nearly identical in all eight bundles. The primary deficiency identified in the SCTF-I calculations was that TRAC-PD2 did not correctly predict liquid entrainment and axial liquid distribution in the core.

5.5.3 SCTF Core-II TRAC Calculation Results

TRAC-PF1/MOD1 was used to perform post-test calculations for 12 SCTF Core-II tests. These are listed in Table 5.5-2 with reference citations and a summary of key results. A summary of the tests which were analyzed is as follows:

- Acceptance tests investigating high ECC flow rates (Runs 601 and 602).

- Power effects tests, including Runs 604, 605, 611, 617, 619 and 621, which had different power profiles.

- Tie plate CCFL tests, including Run 608 with zero power and Run 610 with constant power.

- A FLECHT-SET coupling test with low temperature ECC injection (Run 613).

- BE test with low initial cladding temperature (Run 614).

For SCTF calculations, a two-dimensional vessel model was used. Figure 5.5-1 shows a typical noding diagram.

5.5.3.1 Cold Leg Injection Tests

<u>Core Thermal-hydraulic Behavior</u>
Predictions for SCTF-II tests using TRAC-PF1/MOD1 were generally reasonable for the rod cladding temperature transient under conservative test conditions (such as Runs 604, 605, 611, 617, 619 and 621). Figure 5.5-2 shows an example comparison of predicted and measured rod surface temperatures. In general, the effects of core power profile, initial cladding temperature, and forced-feed injection on rod temperatures were predicted. In the tests, turnaround temperatures with a steep power profile (Run 611) were 40-100 K lower in high-powered rods than would have been expected for the same power applied in a flat power distribution due to multidimensional flow in the core (i.e., the "chimney effect"). This beneficial effect of multidimensional flow was predicted by TRAC. Another beneficial effect of the two-dimensional core flow was that rod quench times were not significantly later for steep power as compared to flat power. The TRAC-predicted quench times occurred somewhat later than observed in the test but were in overall reasonable agreement with the data.

The objective of the initial cladding temperature series (Runs 604 and 614) was to investigate vessel thermal-hydraulic behavior for two core stored energy levels: EM (Run 604, with an initial cladding temperature of 1073 K) and BE (Run 614 with an initial cladding temperature of 573 K). TRAC-predicted peak rod temperatures, turnaround times, and quench times were in reasonable agreement with data for the high initial cladding temperature case (Run 604). In the BE case (Run 614), TRAC predicted turnaround times and quench times in reasonable agreement with data, but the predicted turnaround temperatures were somewhat low; there was minimal agreement with data.

The objective of the forced-feed power effects tests (Runs 617, 619, and 621) was to observe thermal-hydraulic behavior of the system with the downcomer blocked off at the lower plenum entrance and ECC injection into the lower plenum. For these tests, turnaround temperatures and turnaround times in the high-power rods were predicted reasonably well by TRAC. TRAC-predicted rod quench times were in reasonable agreement with data in the core lower half but were somewhat early in the core upper half. Overall, TRAC results were about the same as for gravity feed tests; there was reasonable agreement with the test data.

The objective of Run 613 was coupling with FLECHT-SET experiment 2714B. Run 613 used the same system pressure and injection water subcooling as for the FLECHT experiment. TRAC predictions agreed reasonably well with the data for system pressure, liquid levels in the first half of the transient, and rod temperatures for the core lower half.

Generally, TRAC predictions of the cladding temperature transient were in reasonable agreement with data. The analysis for Run 605 (flat power) showed that heat transfer is nearly uniform which is consistent with data. In the power effects test series, a power profile existed in the radial direction for Runs 604 and 611. Heat transfer was enhanced in high-power bundles because of multidimensional flow (chimney effect). TRAC predicted the radial temperature distribution caused by the radial power profile with reasonable agreement to the test data.

In comparison to SCTF data, the axial and radial distributions of core void fractions were not predicted well with the TRAC-PF1/MOD1 code. TRAC underestimated the liquid above the quench front, and overestimated the liquid below the quench front, but calculated the total core liquid content in reasonable agreement with the data. The liquid carryover rate from the core to upper plenum was underestimated with TRAC-PF1/MOD1 in the early period of the reflood and overestimated in the later period of reflood.

Upper Plenum Thermal-hydraulic Behavior
In general, TRAC-PF1/MOD1 predicted a flatter distribution of liquid in the upper plenum than the data showed. An upper-plenum noding study was performed using the TRAC model of SCTF Run 605 as a basis; the objective was to learn more about phenomena affecting the upper-plenum liquid inventory and radial liquid distribution. Initial and boundary conditions were obtained from Run 605 data. It was found that by increasing the number of radial and axial calculational cells in the upper plenum, the amount of de-entrainment increased and the upper plenum liquid level also increased. These results also showed a marked improvement in de-entrainment and liquid level when the correct core exit flow was imposed on the model rather than that calculated by TRAC. Figure 5.5-3 shows the upper plenum liquid level comparison as originally calculated and Figure 5.5-4 shows the comparison with the imposed core exit flow conditions and fine nodalization.

5.5.3.2 Combined Injection Tests

Tie-plate Countercurrent Flow
The objective of the CCFL evaluation tests (Runs 608 and 610) was to investigate water penetration through the tie plate with water injection into the upper plenum against injected steam flow. In Run 608, saturated water was injected into the upper plenum with no core power (steam injected into the cold leg flowed down the downcomer and up through the core). In Run 610, subcooled water was injected into the upper plenum with core power on.

Liquid penetration from the upper plenum into the core was underestimated by TRAC-PF1/MOD1. In the TRAC calculations, an almost uniform distribution of steam upflow in the radial direction was predicted while nonuniform steam flow was observed

in the SCTF tests. The steam flow in the peripheral bundle, where water downflow occurred, was lower than that in the central bundle where no water downflow occurred in the SCTF tests. The assessment results suggested the need for model improvements to better predict countercurrent flow at the tie plate.

5.5.4 SCTF Core-III TRAC Calculation Results

TRAC-PF1/MOD1 was used to perform post-test calculations for nine SCTF-III tests. Table 5.5-3 lists the calculations with reference citations and a summary of key results. The predictions for all nine of the tests analyzed with TRAC are in overall reasonable agreement with the data. A summary of the SCTF-III tests which were analyzed is as follows:

- Two GPWR core cooling tests (Runs 703 and 711).

- Two GPWR integral tests (Runs 704 and 717).

- One tie-plate CCFL test (Run 709).

- Two US/J power profile effect tests (Runs 719 and 720).

- Two US/J integral tests (Runs 713 and 714).

5.5.4.1 Cold Leg Injection Tests

Core Thermal-hydraulic Behavior
The effects of a radial power profile on core thermal-hydraulic behavior were discussed with the CCTF and SCTF test results in Section 3 and also in the TRAC analyses of SCTF-II tests (see Section 5.5.2). In the SCTF-III assessment calculations, two tests (Runs 719 and 720) were analyzed with additional radial power parameterizations. Run 719 had an inclined radial power distribution with Bundles 1 and 8 receiving the highest and lowest relative powers, respectively. Run 720 had a steep radial power distribution in which the peak power occurred near the center of the core in Bundle 4 and power was lower at the edge of the core in Bundles 1 and 8.

TRAC-PF1/MOD1 predicted an upward flow in the highest powered bundle (i.e., Bundle 1 for Run 719 and Bundle 4 for Run 720) and a downward flow in the lowest powered bundle (i.e., Bundle 8 for Run 719, and Bundles 1 and 8 for Run 720) at the core inlet. The nonuniform power profile induced a flow circulation in the TRAC calculations. In the tests, measurements at the top of the core indicated a flow circulation within the core for a nonuniform power profile. Hence, the TRAC prediction of flow circulation in the core was consistent with the test results. The comparisons for void fraction data showed similar results to those for the SCTF-II tests, mentioned above.

A statistical analysis of turnaround temperature was performed for this set of tests. Predicted and measured temperatures were compared at three elevations (quarter height, mid height, and three-quarter height) in four bundles yielding 12 comparisons per test. The results are shown in Figure 5.5-5. The mean difference or bias was -19.4 K and the standard deviation (one-sigma value) was 59.8 K. The negative bias indicates TRAC had an overall tendency to underpredict cladding temperatures in these tests. By separately plotting and examining the data at each core elevation, it was found that the majority of the TRAC predictions at the quarter height and three-quarter height were lower than measured. At the mid-core height TRAC had a bias toward the overprediction of cladding temperature. Since the mid-core temperatures were the highest in the facility, the TRAC prediction of the highest turnaround temperature in each bundle was biased toward values higher than measured. Overall, TRAC-PF1/MOD1 predictions of SCTF Core-III turnaround temperatures are in reasonable agreement with measurements.

5.5.4.2 Combined Injection Tests

Core Thermal-hydraulic Behavior
In the combined injection EM base case test (Run 717), a large fraction of the ECC injected into the upper plenum before BOCREC fell downward through the core into the lower plenum and flowed up into the downcomer. Little water accumulation was observed in the upper plenum and the core. The same result was calculated by TRAC. In the test, the core thermal-hydraulic behavior could be divided into two regions. The first region, encompassing Bundles 7 and 8, was characterized as a water downflow region where good core cooling was observed (for injection above Bundles 7 and 8). The second region, encompassing Bundles 1 through 6, was characterized as having essentially no core cooling before BOCREC and, by implication, little liquid downflow. The same result was calculated by TRAC.

After BOCREC, most ECC injected into the upper plenum flowed down through the core, up the downcomer, and out the broken cold leg. TRAC calculated the same behavior. In the SCTF test (Run 717), approximately 40% of the steam generated in the core was condensed in the core; condensation of core-generated steam in the upper plenum was small. For the TRAC calculation about 35% of the steam generated in the core was condensed in the core. TRAC also indicates about 50% of the steam entering the upper plenum was condensed. Hence, the calculated rate of upper plenum condensation was higher than the test.

During reflood, the core thermal-hydraulic behavior could be separated into two regions: (1) a region of water downflow and enhanced heat transfer, and (2) a two-phase upflow region. In Run 717, the region with enhanced heat transfer encompassed Bundles 7 and 8. TRAC calculated the same behavior. Specifically, TRAC calculated that water injected into the upper plenum above Bundles 7 and 8 flowed downward through Bundle 8; minor and short-lived breakthroughs were

calculated above Bundles 6 and 7. There were no breakthroughs calculated above Bundles 1 through 5. These bundles were cooled by the upward flow of two-phase fluid. Similar cooling occurred in Bundles 6 and 7, although TRAC calculated that these bundles also experienced brief breakthroughs and the associated enhanced cooling.

Overall, the TRAC-PF1/MOD1 calculation of core reflood phenomena under combined injection conditions was in reasonable agreement with data. In particular, calculated rod cladding temperatures were in reasonable agreement with the data. Phenomena that effect PCT (e.g., core flooding rate, vessel inventory, and loop differential pressures) were also calculated with reasonable agreement. It appears the code can be used for PWR operational evaluations under similar conditions.

Tie-Plate Countercurrent Flow
The downward flow of liquid through the tie plate and into the core region is a phenomenon of great interest in plants with either upper plenum or combined injection. TRAC successfully calculated the major tie plate countercurrent flow trends for each of the four SCTF Core-III runs examined. TRAC correctly calculated the existence of two thermal-hydraulic flow regimes, namely, a region of liquid downflow and a two-phase upflow region. Also, TRAC correctly calculated the location of the liquid downflow and two-phase upflow regions. TRAC generally overpredicted the flow rate in the liquid downflow region, typically by about 30%. It was found tie plate behavior was more accurately calculated if the TRAC-CCFL model was used. (The TRAC-CCFL model is an option for axial flow in a three-dimensional vessel component. This model uses a Bankoff correlation and coefficients input by the user--see Reference E-604.)

SCTF Run 709 was specifically designed to investigate tie plate countercurrent flow for uniform, or homogeneous, flow conditions at the tie plate. Steam injected into the cold leg flowed upward through the core to the tie plate and water injected in the upper plenum flowed downward to the tie plate. Water injection was constant and evenly distributed across the upper plenum, while steam injection decreased over the course of the test. The TRAC-PF1/MOD1 calculation of Run 709 failed to predict the correct water penetration rate at the highest steam flow but correctly predicted the average tie plate penetration rate for the test.

5.5.5 Conclusions

The TRAC series of computer codes were extensively assessed against data from the SCTF Core-I, Core-II and Core-III tests to check the predictive capability of the codes and to identify model deficiencies. The assessment results provided an excellent technical basis for development and validation of the codes for prediction of full-size PWRs during the end-of-blowdown, refill and reflood phases of an LBLOCA.

The assessment results showed that TRAC can predict the cladding temperature transient with reasonable agreement. Also, TRAC-PF1/MOD1 predicted flow circulation within the core with a radial power profile. Finally, for UPI or combined injection, TRAC predicted the water downflow location and averaged downflow rate even though water downflow rates were underpredicted for high steam upflows.

Several model deficiencies of the code were identified in the assessment study with SCTF test data. The deficiencies identified included: (1) core void distribution, (2) condensation in the upper plenum, (3) liquid downflow through the tie plate, and (4) entrainment/de-entrainment in the upper plenum.

Table 5.5-1

TRAC ANALYSES OF SCTF CORE-I TESTS

Test/Run Number	Description	Reference	TRAC Version
S1-SH2/506	High pressure	U-645 U-651 J-612	PD2
S1-01/507	Base-case	U-646 U-651 U-649 U-652 J-612	PD2
S1-02/508	Low pressure	U-647 U-651 J-612	PD2
S1-04/510	High subcooling	U-648 J-612	PD2
S1-05/511	Low LPCI	U-652	PD2
S1-06/512	High power	---	PD2
S1-07/513	Flat power	U-649	PD2
S1-08/514	Steep power	U-649 U-655	PD2
S1-09/515	High ECC	U-652	PD2
S1-10/516	Base case	U-648	PD2
S1-11/517	Flat power	---	PD2
S1-13/519	SCTF/CCTF/FLECHT-SEASET coupling	U-653	PD2, PF1
S1-SH4/529	Combined injection	U-656	PF1
Summary	---	U-641	---

Table 5.5-2

TRAC ANALYSES OF SCTF CORE-II TESTS

Test/Run Number	Description	Reference	TRAC Version	Overall Agreement	Parameters Predicted	Deficiencies	
						Overpredicted	Underpredicted
S2-AC1/601	Acceptance test	U-661	PF1/MOD1 v. 14.3	Reasonable	Lower core rod temperatures, system pressure	Upper core rod temperatures	Core entrainment, UP liquid level
S2-AC2/602	Acceptance test	U-661	PF1/MOD1 v. 14.3	Reasonable	Lower core rod temperatures, system pressure	Upper core rod temperatures	Core entrainment, UP liquid level
S2-SH1/604	Base case	U-662	PF1/MOD1 v.12.0	Reasonable	Lower core rod temperatures, system pressure	Upper core rod temperatures	Core entrainment, UP liquid level
S2-SH2/605	Flat power profile	U-663 U-664	PF1/MOD1 v. 12.7	Reasonable	Lower core rod temperatures, system pressure	Upper core rod temperatures	Core entrainment, UP liquid level
S2-03/608	Tie plate CCFL	U-665	PF1/MOD1 v. 12.0	Reasonable	Upper plenum liquid level	Tie plate break-through, lower plenum liquid level	System pressure
S2-05/610	Tie plate CCFL	U-666	PF1/MOD1 v. 12.0	Minimal	Hot leg mass flow	Tie plate break-through, lower plenum liquid level	System pressure, rod turnaround temperature
S2-06/611	Steep power and temp profiles	U-667	PF1/MOD1 v. 12.0	Reasonable	Lower-half rod temperatures, 3D reflood, enhanced rod heat transfer, system pressure	Upper-half rod temperatures	Core entrainment, UP liquid level
S2-08/613	FLECHT coupling	U-668	PF1/MOD1 v. 12.0	Reasonable	System pressure, rod temperatures	—	Core upper half collapsed liquid level

Table 5.5-2

TRAC ANALYSES OF SCTF CORE-II TESTS

Test/Run Number	Description	Reference	TRAC Version	Overall Agreement	Parameters Predicted	Deficiencies	
						Overpredicted	Underpredicted
S2-09/614	Low stored energy	U-669	PF1/MOD1 v. 12.0	Reasonable	System pressure, lower core quench time	Upper core rod temperatures	Core upper half collapsed liquid level, upper plenum liquid level
S2-12/617	Steep power profile	U-670	PF1/MOD1 v. 12.0	Reasonable	System pressure, lower core rod temperatures, lower core quench time	—	Core upper half collapsed liquid level
S2-14/619	Flat power	J-609 J-615	PF1/MOD1 v. 12.5	Reasonable	Rod temperatures, system pressure	Liquid mass in lower core	Liquid mass in upper core
S2-16/621	Steep power	J-615	PF1/MOD1 v. 12.5	Reasonable	Rod temperatures, enhanced heat transfer in high powered bundle, system pressure	Liquid mass in lower core, mass flow to hot leg in later period	Liquid mass in upper core, liquid carryover to hot leg in early period
Summary	—	U-661	—	—	—	—	—

Table 5.5-3

TRAC ANALYSES OF SCTF CORE-III TESTS

Test/Run Number	Description	Reference	TRAC Version	Overall Agreement	Parameters Predicted	Deficiencies	
						Overpredicted	Underpredicted
S3-SH1/703	GPWR core cooling	U-683	PF1/MOD1 v.14.3	Reasonable	Peak cladding temperatures, rod quench times, mass distributions, mass flows, system pressure	Liquid hold-up in upper plenum early in test	Core upper half collapsed liquid level
S3-SH2/704	GPWR EM integral	U-684	PF1/MOD1 v. 14.3	Reasonable	Peak cladding temperatures, rod quench times, mass distributions mass flows, system pressure	Liquid hold-up in upper plenum, carryover to hot legs	---
S3-05/709	CCFL, nonuniform	U-685	PF1/MOD1 v. 14.3	Reasonable	Tie plate breakthrough	System pressure, rod temperatures	Penetration to lower plenum early in transient
S3-07/711	GPWR core cooling	U-681	PF1/MOD1 v. 14.3	Reasonable	Peak cladding temperatures, rod quench times, mass flows, mass distributions, system pressure	Liquid hold-up in upper plenum early in test	ECC flow to Bundle 3
S3-09/713	US/J EM integral	U-686	PF1/MOD1 v. 13.1	Reasonable	Peak cladding temperatures and rod quench times for high and low power bundles, mass flows, mass distributions, system pressure	Liquid below quench front	Rod temperatures at upper elevations, liquid above quench front
S3-10/714	US/J BE integral	U-687	PF1/MOD1 v. 13.0	Reasonable	Peak cladding temperatures, rod quench times, mass flows, mass distributions, system pressure	Core liquid stratification	Quench time at upper elevations, upper plenum liquid
S3-13/717	GPWR EM integral	U-681	PF1/MOD1 v. 14.3	Reasonable	Peak cladding temperatures, rod quench times, mass distributions, mass flows, system pressure	Carryover to hot legs	Collapsed liquid level in core
S3-15/719	Inclined power profile	U-688	PF1/MOD1 v. 14.3	Reasonable	Peak cladding temperatures, rod quench times, mass distributions, mass flows, system pressure	Rod temperatures at core midplane, upper plenum liquid level	System pressure rod temperatures at elevations, core upper half collapsed liquid level
S3-16/720	Steep power profile	U-689	PF1/MOD1 v. 14.3	Reasonable	Peak cladding temperatures, rod quench times, mass distributions, mass flows, system pressure	Upper plenum liquid level	System pressure, rod temperatures at upper eleva-tions.
Summary	---	U-681	---	---	---	---	---
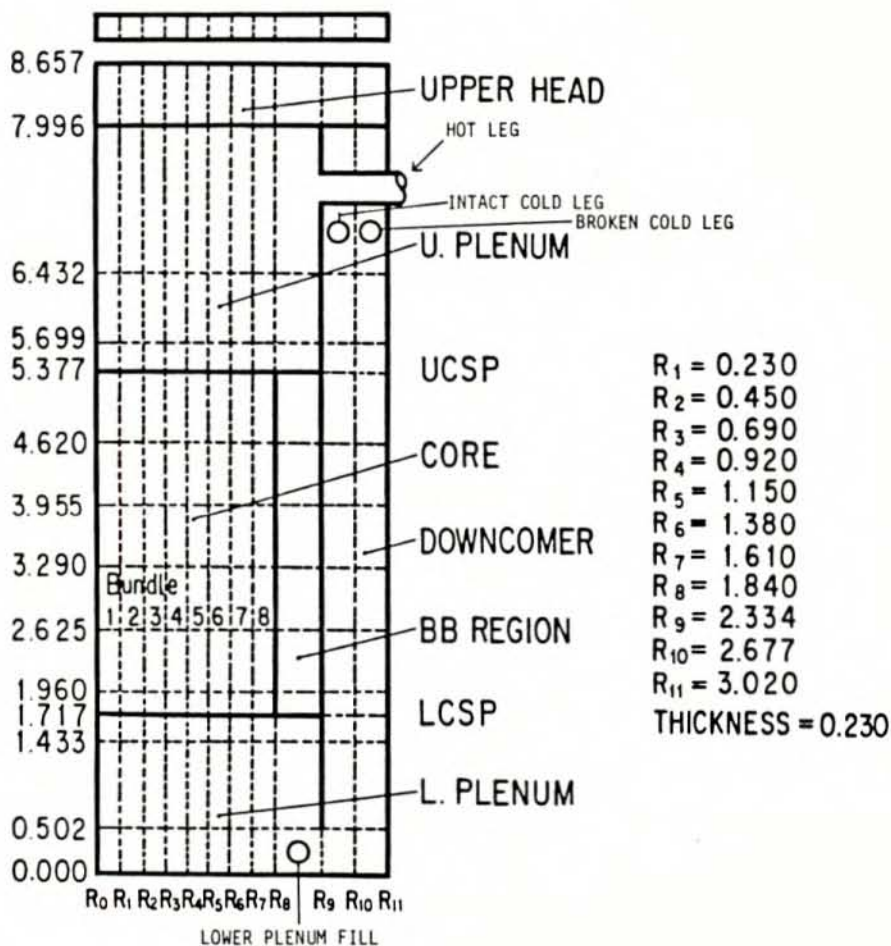
TYPICAL VESSEL NODING FOR SCTF ANALYSES
FIGURE 5.5-1

TRAC-PF1/MOD1 V. 14.3
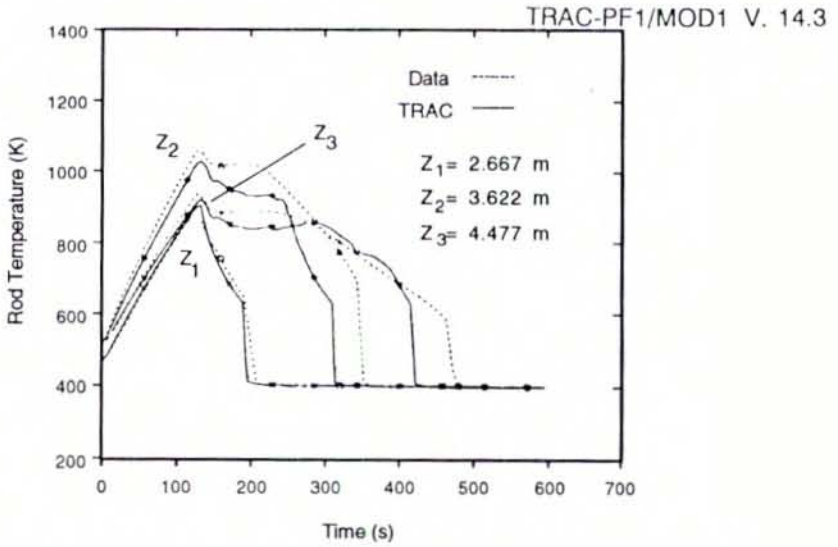
TRAC/DATA COMPARISON OF ROD TEMPERATURES
SCTF TEST S2-AC1 (RUN 601)
FIGURE 5.5-2

TRAC-PF1/MOD1 V. 12.0
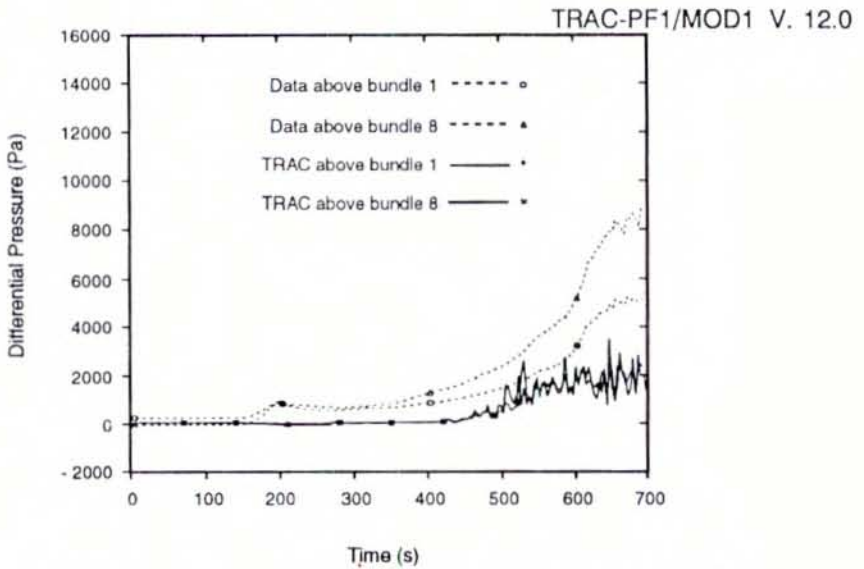
TRAC/DATA COMPARISON OF UPPER PLENUM
DIFFERENTIAL PRESSURE
SCTF TEST S2-SH1 (RUN 604)
FIGURE 5.5-3
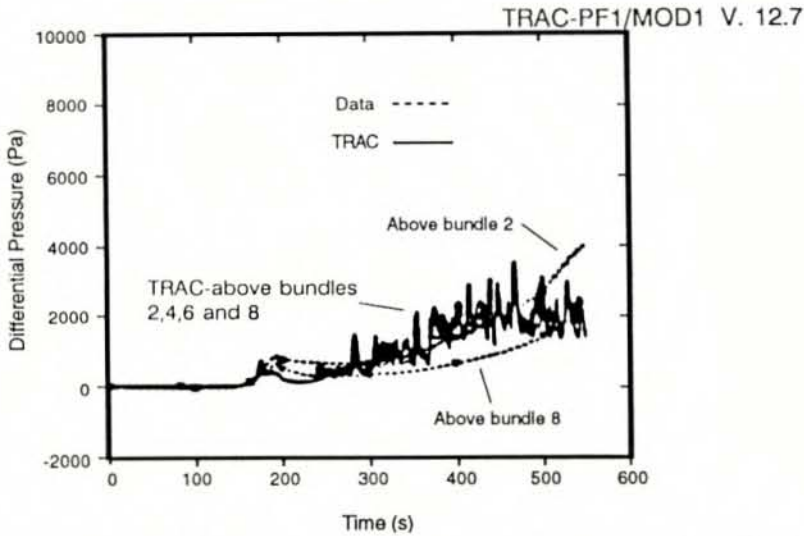
TRAC/DATA COMPARISON OF UPPER PLENUM DIFFERENTIAL
PRESSURE BASED ON STANDALONE PROGRAM
SCTF TEST S2-SH2 (RUN 605)

FIGURE 5.5-4
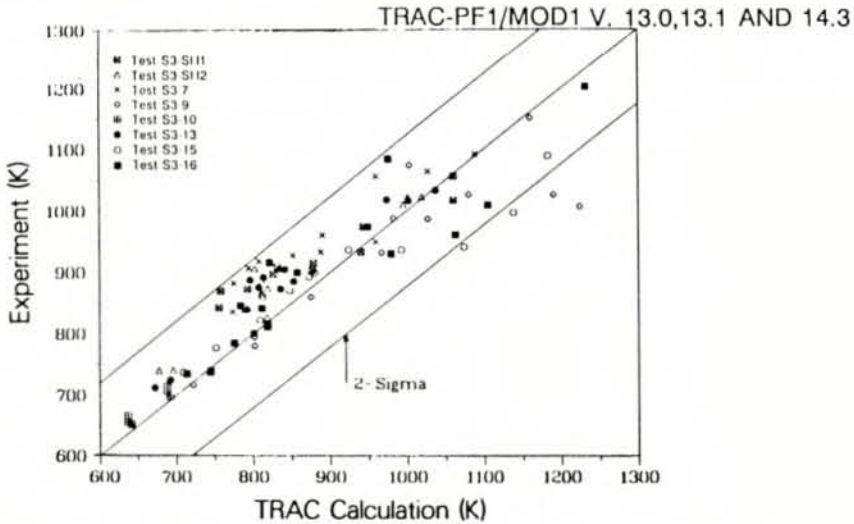
Notes: 1. The tests shown in this figure include cold leg injection
tests and combined injection tests.

2. Turnaround temperature comparisons for each test are made at three heights in
each of four bundles.

STATISTICAL ANALYSIS OF TRAC TURNAROUND TEMPERATURE
PREDICTIONS FOR SCTF TESTS

FIGURE 5.5-5

5.6 UPTF CALCULATIONS WITH TRAC

TRAC calculations were used to a limited extent in supporting the design and operation of UPTF. Also, pretest analyses were performed to evaluate operating approaches. Most of the UPTF calculations, however, were post-test analyses performed to assess the predictive capability of TRAC. The results of the assessment calculations are documented in individual reports which cover either the calculation of a given test, or the calculations of several tests related to a single phenomena (Table 5.6-1).

5.6.1 Analytical Support for Design and Operation of UPTF

TRAC calculations were used to support the design and operation of UPTF. Specifically, calculations were performed to evaluate water plugging in the loops and the effect of loop configuration (References U-701, U-702, and U-741). TRAC calculations of the core/upper plenum flow conditions in a GPWR were performed to evaluate the UPTF core simulator and to evaluate the location, type, and desired accuracy of instrumentation at the core/upper plenum interface (U-742).

Pretest analyses were performed for each of the major types of tests (References U-703, U-705, U-706, U-707, and G-631). These pretest analyses included parametric studies to evaluate selected test operating approaches. Finally, TRAC PWR calculations described in Section 5.3 were used to help develop initial and boundary conditions for UPTF tests.

5.6.2 UPTF TRAC Calculation Results

UPTF data initially became available when the last version of TRAC-PF1/MOD1 was completed. UPTF testing was completed shortly before the release of TRAC-PF1/MOD2. TRAC post-test calculations for UPTF were performed with TRAC-PF1/MOD1, preliminary versions of TRAC-PF1/MOD2 and the released versions of TRAC-PF1/MOD2. MOD2 was changed enough through the course of development that some of the earlier MOD2 versions produced substantially different results than the released version. Accordingly, results obtained with preliminary versions may not reflect the predictive capability of the released version. Table 5.6-1 lists the UPTF post-test calculations done with TRAC including reference citations and a summary of key results. As shown, 21 post-test analyses were performed. The results of these calculations are summarized below by phenomena and region.

5.6.2.1 Thermal Hydraulic Phenomena in Core and Upper Plenum

TRAC-PF1/MOD2 was used to perform post-test calculations for US/J-type PWR integral reflood tests (Tests 2 and 17). Agreement between predictions and data was insufficient. TRAC failed to predict many significant phenomena particularly liquid

distributions. The cause was the inability of the computer model of the UPTF core simulator to adequately model flow conditions below the tie plate. Specifically, water was not entrained into the core and upper plenum in the TRAC calculation as it was in the tests. This deficiency in prediction of the test boundary conditions propagated to other deficiencies throughout the primary system. Since flow conditions below the tie plate in PWR calculations are determined by the core reflood model, the results of these UPTF analyses regarding water carryover from the core are not considered indicative of the ability of TRAC to predict PWR phenomena. As seen in the CCTF and SCTF calculations, the heated core model works adequately.

A calculation with MOD2 for Test 29, Phase B, showed insufficient agreement between predictions and data. This was a test designed to investigate the entrainment/de-entrainment phenomena above the core related to the steam binding issue. An investigation into problems with the calculation showed that the inability to adequately predict phenomena above the core simulator was the key problem. In addition, it appears that phenomena in the upper plenum involve simultaneous upflow of liquid droplets carried by steam and downflow of liquid films on structural members. TRAC models two-phase flows with one liquid field and one vapor field and cannot simulate simultaneous liquid upflows and downflows. Further, TRAC node sizes cannot be realistically reduced to the level needed to separate the flows. This means that TRAC attempts to represent a two-phase flow phenomena as an average when an average may not be appropriate. However, it has been shown that this deficiency produces only a small change in PCT for a plant calculation (see Section 5.7.3, below).

5.6.2.2 Tie Plate Countercurrent Flow

TRAC-PF1/MOD1 calculations for Test 10, Phase B by LANL and Test 12, Run 14 by GRS showed insufficient agreement for tie-plate CCFL. A GRS calculation for Test 13 also showed insufficient agreement. In particular, TRAC failed to predict the changing liquid distribution throughout the system. It appears that this is indicative of the flow phenomena at the tie plate differing from the flow regimes that TRAC is based on. In this situation, the difference in flow regime occurs because of the material boundaries constraining the flow. This differs from the situation above the core simulator where sources (the injectors) cause the flow regime to deviate from the usual two-phase flow regimes. An appropriate CCFL model could alleviate the problem although flow regime models are situation-specific. A calculation of UPTF Test 20, a UPI test which had similar phenomena, performed with a preliminary version of TRAC-PF1/MOD2, was in reasonable agreement with data. Specifically, the overall (integrated) tie plate breakthrough flow and ECC delivery to the core were predictable. The calculation overpredicted the liquid level in the upper plenum and underpredicted loop mass flows.

5.6.2.3 Phenomena in Downcomer during End-of-Blowdown

UPTF Test 4 Phase A, was an integral test which investigated phenomena occurring near the end of blowdown. TRAC-PF1/MOD2 has special flow regime models for downcomer countercurrent flow and, unlike the core simulator injectors, these models adequately represent the physical situation. TRAC-PF1/MOD2 predicted the key observation that the lower plenum filled by the end of blowdown.

UPTF Tests 5, 6 and 7 complemented Test 4. Specifically, downcomer penetration and bypass were investigated as a function of steam and ECC flow rates. The tests showed that most ECC injected into the cold legs away from the broken cold leg penetrated to the lower plenum, even at high steam flow rates. Conversely, even at low steam flow rates much of the ECC injected into the loop nearest the broken cold leg went out the break. TRAC-PF1/MOD2 showed the same phenomena for penetration and bypass as the tests. Integrated penetration values were also in reasonable to excellent agreement (Table 5.6-2).

5.6.2.4 Phenomena in Downcomer during Reflood

Test 25 investigated entrainment from the downcomer out the break during reflood. The phenomena of interest cause a change in the driving head for reflood of about 0.01 MPa. The TRAC calculation did not calculate the downcomer to upper core differential pressure with sufficient precision to show this effect.

5.6.2.5 Flow Phenomena in Loops

UPTF Test 8 was designed to specifically investigate steam/ECC interactions in the vicinity of the ECC injection ports. When there is sufficient liquid to condense steam flowing through the loop, a liquid plug forms in the vicinity of the ECC port. A GRS calculation using TRAC-PF1/MOD1 version 13.0 correctly predicted plug formation and the magnitude of cold leg plug oscillations (Figure 5.6-1). It predicted the transition to stable stratified flow at too high an ECC flow rate. A GRS calculation for UPTF Test 9 using MOD1 version 13.0, showed similar agreement. A code error correction applied to MOD1 versions 13.3 and later, increased the ECC flow required for plugging to occur so that a GRS calculation using MOD1 version 14.3 failed to predict plugging. A LANL calculation of Test 8, Phase B using TRAC-PF1/MOD2 showed that MOD2 predicts plug formation, the frequency of the plug oscillations and the transition to stable stratified flow (Figure 5.6-2). However, it overpredicted the magnitude of the oscillations. An examination of UPTF Test 2 showed similar results. The calculation of UPTF Test 17 correctly predicted only stable stratified flow during LPCI. It appears that TRAC-PF1/MOD2 will correctly predict these phenomena in plant calculations while the final version of MOD1 will not.

5.6.2.6 Hot Leg Countercurrent Flow

UPTF Test 11 investigated countercurrent flow in a hot leg where liquid flowed from the steam generator simulator toward the vessel and steam flowed in the other direction. TRAC-PF1/MOD1 underpredicted the steam velocity for complete liquid flow reversal (Figure 5.6-3). Three stratified flow interfacial drag correlations were tested for possible inclusion in TRAC-PF1/MOD2. A correlation by Ohnuki proved best. It accurately predicted the point of complete flow turnaround but overpredicted the liquid flow at lower steam flow rates, as also shown in Figure 5.6-3.

5.6.2.7 Downcomer Injection and Vent Valve Test Phenomena

UPTF Test 21 was a test of downcomer penetration/bypass similar to Tests 5, 6 and 7 but with downcomer rather than cold leg ECC injection. ECC was injected into the downcomer at relatively high velocities where it impinged on the core barrel. This test had more bypass than seen in the cold leg injection tests. TRAC has the option of using interfacial shear models specifically for countercurrent downcomer flow as discussed previously for the cold leg injection tests. This model is appropriate for streams of liquid passing through steam. The standard interfacial shear package can also be used for downcomer flows (depending upon a change in the TRAC input for the vessel). Neither of these options yielded reasonable results for this test which appears to have a highly dispersed droplet flow unlike classical pipe flow regimes. The standard model package yielded better but still minimal agreement. Modeling this type of dispersed flow would require a special interfacial shear model.

UPTF Test 22, Phase A was a downcomer injection test in which the vent valves were free to open. This test covered both the end-of-blowdown/refill and reflood phases of a LOCA. Overall, the results of a TRAC-PF1/MOD2 version 5.3 calculation were in reasonable agreement with the test data. Specifically, TRAC predicted the amount of ECC swept into the intact loop cold legs and out the broken cold leg reasonably well. Also, TRAC correctly predicted the water levels in the downcomer (Figure 5.6-4) and lower plenum, and therefore the ECC penetration rate. As Figure 5.6-5 indicates, the collapsed water level in the core was slightly overpredicted but the reflood rate was well predicted. Finally, the upper plenum water level and upper plenum-to-downcomer differential pressure were also predicted with reasonable agreement.

UPTF Test 23, Phase B was a downcomer injection/vent valve test which covered only reflood conditions. A post-test analysis with MOD2 version 5.3 adequately predicted the amount of ECC entrained out the broken cold leg by the vent valve steam flow. As in the Test 22 analysis, most of the phenomena, including the upper plenum-to-downcomer differential pressure (Figure 5.6-6), were predicted with reasonable agreement to the test data. Also, the liquid levels in the core and downcomer were predicted reasonably well.

5.6.2.8 Accumulator Nitrogen Discharge

UPTF Test 27, Phase A simulated the nitrogen surge in US/JPWRs following the emptying of the accumulators. A TRAC-PF1/MOD2 calculation for UPTF Test 27, Phase A was in reasonable agreement with the test data. As shown in Figure 5.6-7, TRAC predicted the pressure trends in the upper plenum and downcomer during nitrogen discharge; however, the rate of condensation in the downcomer during the nitrogen injection period was slightly greater than indicated for the test. Also, broken cold leg flow resistance may have been too small. As a consequence, the downcomer pressure never exceeded the upper plenum pressure as seen in the test. Thus TRAC did not produce as large a liquid surge into the core as seen in the test.

5.6.3 Karlstein Facility TRAC Calculations

The Karlstein facility was used to test core simulator and core/upper plenum instrumentation systems for UPTF. The Karlstein facility included one simulated fuel assembly. TRAC-PF1/MOD1 was used by GRS to perform post-test analyses of selected Karlstein tests, particularly the tests with countercurrent flow conditions. The TRAC calculations reasonably predicted the upper CCFL point; i.e., the boundary where all upflow occurs. However, at reduced upflow, the TRAC calculations significantly overpredicted the liquid downflow because the calculation tended to "switch" from no downflow to total downflow rather than show a region of partial downflow. Finer axial nodalization in the tie plate region did not improve the predictions. These calculations led to the implementation in TRAC of an optional CCFL model which could be used in such situations.

5.6.4 Conclusions

The most apparent deficiency in modeling UPTF tests was the inability to adequately model the core simulator injectors and consequently the phenomena downstream of the core simulator. Because this deficiency is unique to UPTF modeling, it does not affect the modeling of PWRs or test facilities with a heated core (e.g., CCTF and SCTF). A more significant deficiency is that TRAC cannot model flows with liquid rising in the form of entrained droplets and simultaneously falling as films or rivulets in the same vicinity. This is a fundamental limitation of two field modeling. The consequences of this limitation with respect to steam binding will be discussed further in Section 5.7.3. Another deficiency is that TRAC underpredicts tie plate liquid downflow in countercurrent flow situations (e.g., upper plenum injection and hot leg injection). Although these deficiencies increase the uncertainty in LBLOCA and other system calculations, they do not prevent TRAC from calculating most of the major trends and phenomena expected.

Table 5.6-1

TRAC ANALYSES OF UPTF TESTS

Test Number (Run No. or Phase)	Description	Reference	TRAC Version	Overall Agreement	Parameters Predicted	Deficiencies	
						Overpredicted	Underpredicted
2	US/J PWR integral reflood	U-713 U-714	PF1/MOD1 v. 5.3	Insufficient in vessel, reasonable in cold legs	Plugging phenomena in cold legs	—	Carryover from UP to hot legs
4 (Phase A)	US/J PWR integral refill	U-711	PF1/MOD1 v. 5.3	Reasonable	Filling of lower plenum by end of blowdown	Break flow, depressurization rate	—
5 (Phase A)	Downcomer transient refill	U-711	PF1/MOD1 v. 5.3	Excellent	Bypass of ECC injected into the cold leg nearest the broken cold leg, penetration of ECC injected into cold legs away from the break	Break flow, mass storage in cold legs	—
6 (Run 133)	Downcomer countercurrent flow	E-611 U-711	PF1/MOD1 v. 12.5 PF1/MOD2 v. 5.3	Reasonable to excellent (v.5.3)	Total ECC penetration (v.5.3)	—	—
7 (Runs 200 & 201)	Downcomer countercurrent flow	U-711	PF1/MOD2 v. 5.3	Reasonable to excellent	Bypass of ECC injected into the cold leg nearest the broken cold leg, penetration of ECC injected into cold legs away from the break	—	—
8 (Phases A & B)	Cold/Hot leg flow pattern	G-641 U-712 U-714	PF1/MOD1 v. 13.0, 14.3 PF1/MOD2 v. 5.3	Reasonable (v. 13.0) Insufficient (v. 14.3) Reasonable (v. 5.3)	Water plug formation in cold leg (v. 13.0 and 5.3) magnitude of cold leg plug oscillations (v. 13.0) Frequency of cold leg plug oscillations (v. 5.3), transition to stable flow (v. 5.3)	ECC flow rate at transition to stratified flow (v. 13.0) Magnitude of oscillations (v. 5.3)	—
9 (Phase A)	Cold/Hot leg flow pattern	G-642	PF1/MOD1 v. 13.0	Reasonable	Formation and movement of plugs, cold leg temperatures	Condensation during hot leg ECC injection for water delivered to upper plenum	—

Table 5.6-1

TRAC ANALYSES OF UPTF TESTS

Page 2 of 3

Test Number (Run No. or Phase)	Description	Reference	TRAC Version	Overall Agreement	Parameters Predicted	Deficiencies	
						Overpredicted	Underpredicted
10 (Phase B)	Entrainment/ De-entrainment	U-709	PF1/MOD1 v. 14.3	Minimal with finely noded vessel, insufficient with course noding	Liquid accumulation in upper plenum during early phases of test with fine noding	Upper plenum water accumulation except at high steam and water injection rates	—
11	Hot leg countercurrent flow	U-708	PF1/MOD1 v. 14.3, MOD2 prelim	Reasonable	Complete liquid turnaround point (MOD2)	Liquid downflow at lower steam flows	Steam flow at complete turnaround (MOD 1)
12 (Run 014)	Tie plate countercurrent flow	G-644	PF1/MOD1 v. 12.5, 12.8, 14.4	Insufficient	Start of water downflow through tie plate	—	Net water downflow
13 (Run 071)	Tie plate countercurrent flow	G-645	PF1/MOD1 v. 12.5, 12.8, 14.3	Insufficient (v. 12.5, 12.8) Minimal (v. 14.3)	Start of water downflow through tie plate	—	Net water downflow
17 (Phase B)	US/J PWR integral Reflood	U-713 U-714	PF1/MOD2 v. 5.3	Insufficient in vessel, reasonable in cold legs	Stratified flow in cold legs	—	Carryover from UP to hot legs
20	Upper Plenum Injection	U-710	PF1/MOD2 prelim.	Reasonable	Tie-plate breakthrough flow	UP liquid level	Intact loop mass flow
21 (Phases A &B)	Downcomer injection	U-715	PF1/MOD2 v. 5.3	Minimal	—	Water storage in cold legs	ECC penetration
22 (Phase A)	Downcomer injection/ vent valves -- refill	U-715	PF1/MOD2 v. 5.3	Reasonable	Vessel liquid level during refill, bypass from injection port nearest broken cold leg, penetration below injection port away from break	Vent valve differential pressure during refill	Downcomer level during reflood
23 (Phase B)	Downcomer injection/ vent valves -- reflood	U-715	PF1/MOD2 v. 5.3	Reasonable	Downcomer level, differential pressure across vent valves	Core water level	Break flow

Table 5.6-1

TRAC ANALYSES OF UPTF TESTS

Page 3 of 3

Test Number (Run No. or Phase)	Description	Reference	TRAC Version	Overall Agreement	Parameters Predicted	Deficiencies	
						Overpredicted	Underpredicted
25 (Phases A & B)	Downcomer/Cold leg reflood	U-714	PF1/MOD2 v. 5.3 + error corr.	Reasonable	Plug formation in cold legs, transition to stable flow	Condensation heat transfer	---
27 (Phase A)	US/J PWR integral refill/reflood	U-716	PF1/MOD2 v. 5.3	Reasonable	Pressure trends in upper plenum and downcomer during nitrogen injection	Condensation in downcomer during nitrogen surge	Magnitude of core liquid level surge
29 (Phase B)	Entrainment/ De-entrainment	U-713	PF1/MOD2 v. 5.3	Insufficient	---	---	Carryover from upper plenum to hot legs

TABLE 5.6-2

COMPARISON OF VESSEL INVENTORY CHANGE IN
UPTF TESTS 4, 5, 6, AND 7 WITH TRAC-PF1/MOD2 CALCULATIONS

Test Number, Run Number	Integrated ECC Injection for Analysis Period (kg)	Vessel Inventory Change: Data Evaluation [1]		Vessel Inventory Change: MOD2 Calculation [3]	
		(kg)	Percent of ECC Injection [2]	(kg)	Percent of ECC Injection [2]
UPTF 4A	19794	17414	88	19605	99
UPTF 5A	27660	14482	52	15383	56
UPTF 6, Run 133	33790	16032	47	14473	43
UPTF 7, Run 200-I	38400	1814	5	2551	7
UPTF 7, Run 200-II	46880	18556	40	18723	40
UPTF 7, Run 201-I	57857	48596	84	48921	85

NOTES:

1. From the MPR data evaluation -- see Reference U-455, Table 5-1.

2. These numbers are not necessarily the percent of the ECC water that penetrated for the time period analyzed. Most of the water that penetrated came from ECC, but condensation and possible changes in inventory location may have contributed to the vessel inventory change.

3. From Reference U-711.
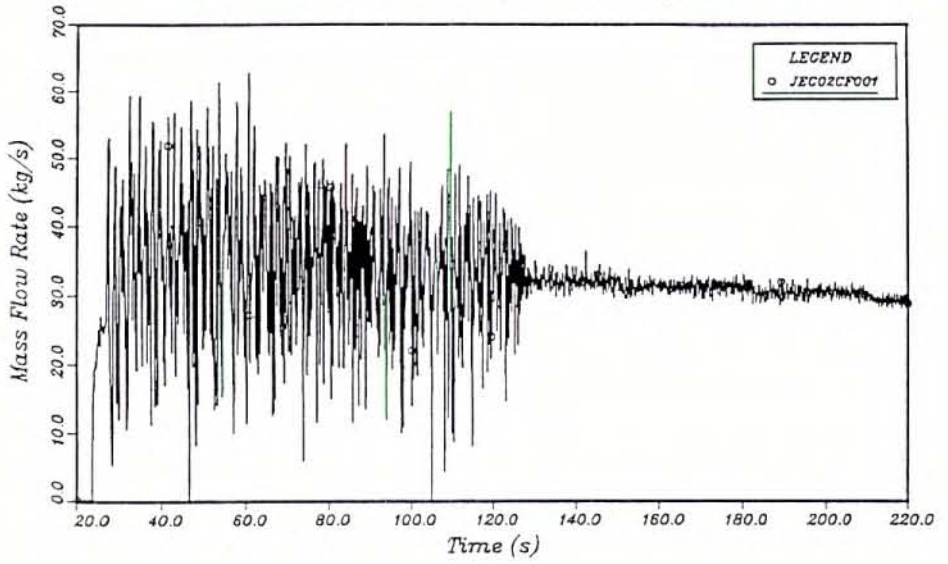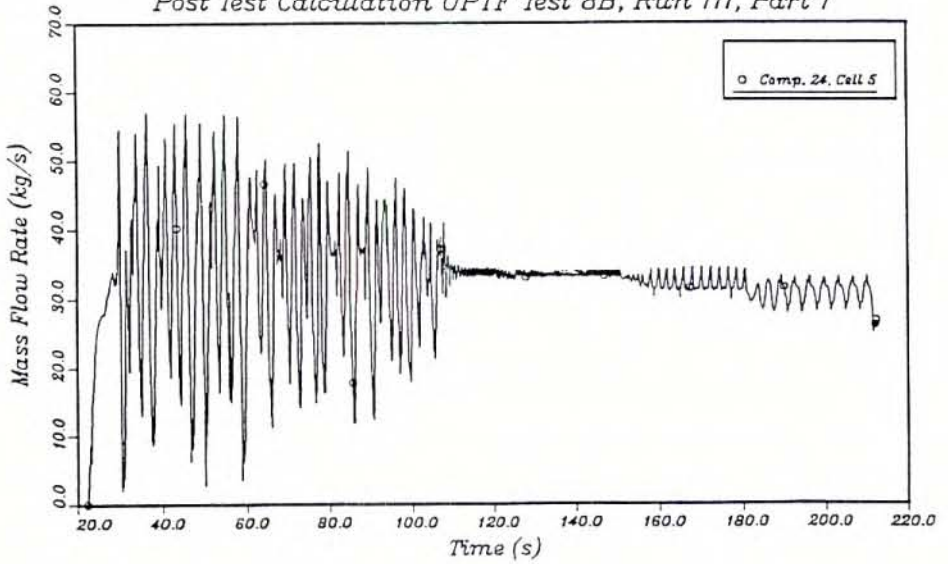
TRAC/DATA COMPARISON OF COLD LEG MASS FLOW
UPTF TEST 8B
FIGURE 5.6-1
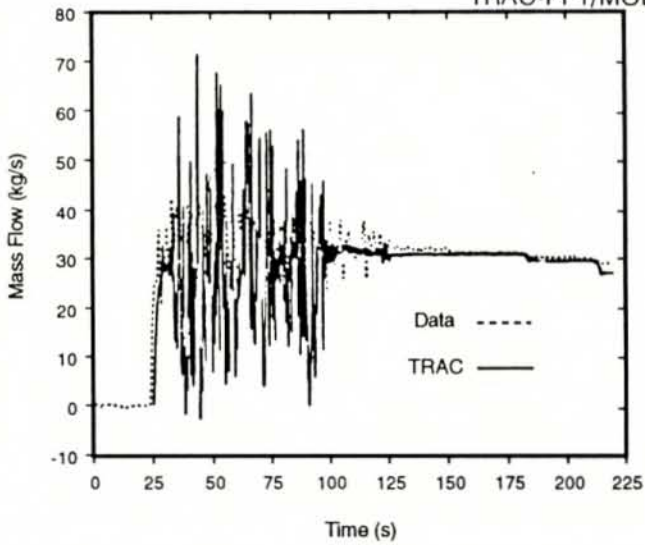
TRAC/DATA COMPARISON OF COLD LEG MASS FLOW
UPTF TEST 8B
FIGURE 5.6-2
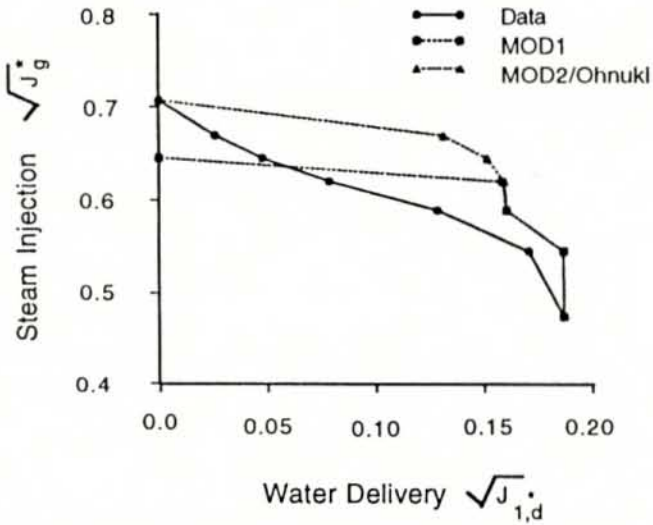
TRAC/DATA COMPARISON OF HOT LEG CCFL
UPTF TEST 11
FIGURE 5.6-3
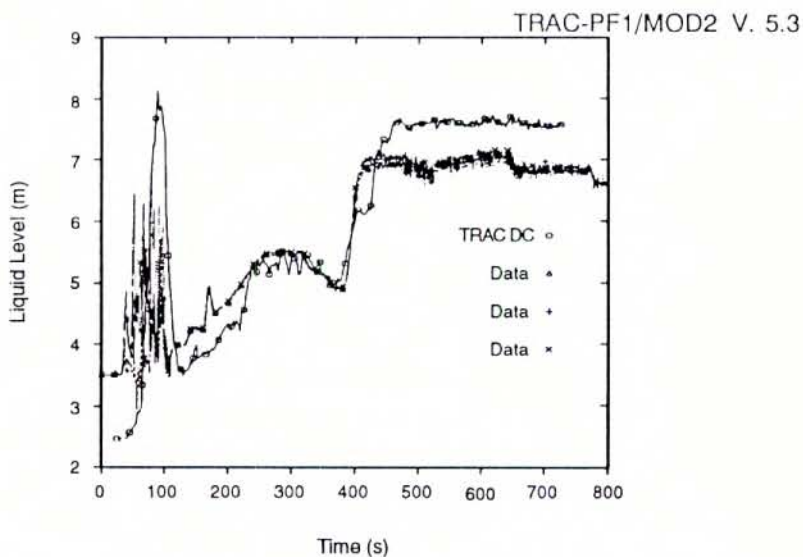
TRAC/DATA COMPARISON OF DOWNCOMER WATER LEVEL
UPTF TEST 22A
FIGURE 5.6-4
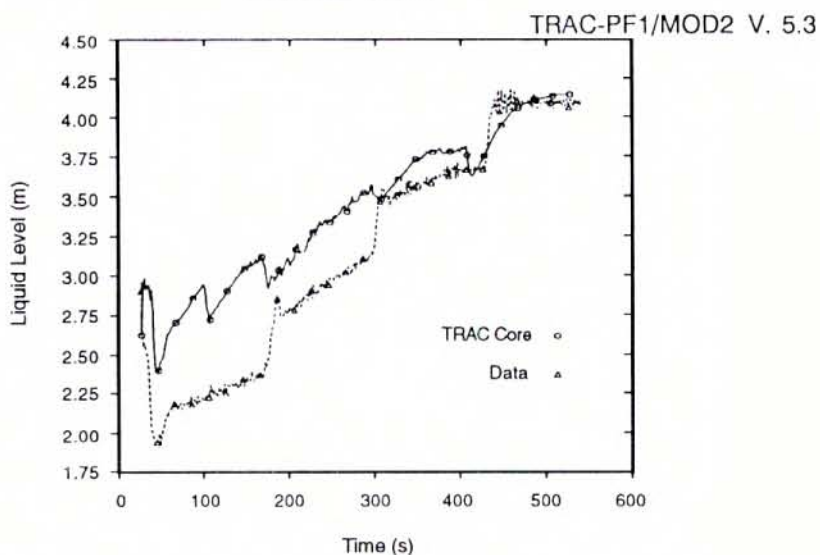
TRAC/DATA COMPARISON OF CORE WATER LEVEL
UPTF TEST 23B
FIGURE 5.6-5
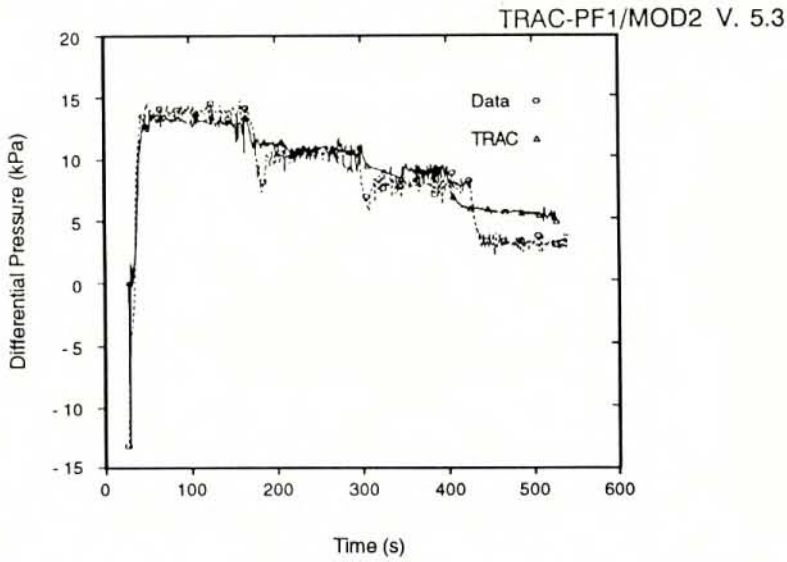
TRAC/DATA COMPARISON OF UPPER PLENUM-DOWNCOMER
DIFFERENTIAL PRESSURE
UPTF TEST 23B
FIGURE 5.6-6
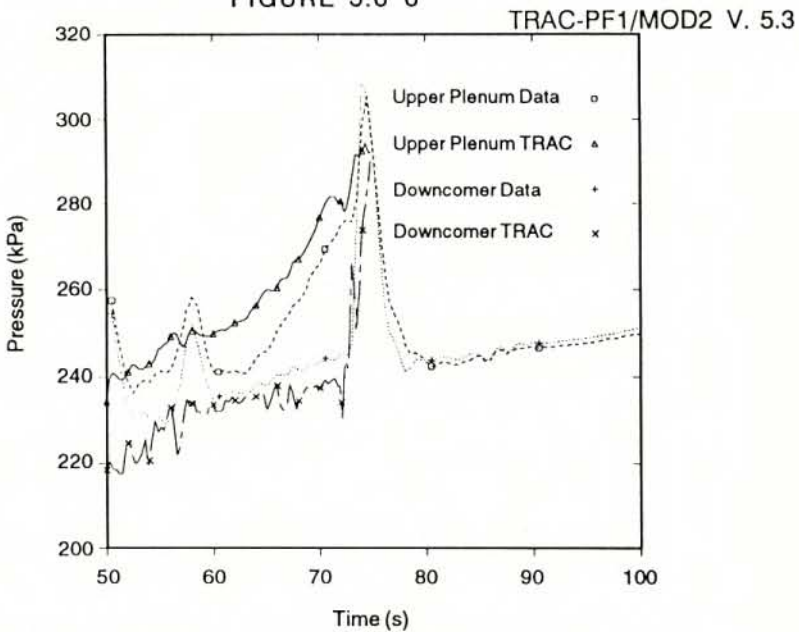
TRAC/DATA COMPARISON OF VESSEL PRESSURES
UPTF TEST 27A
FIGURE 5.6-7

5.7 TRAC PREDICTIVE CAPABILITY

The assessment calculations performed with released versions of TRAC have shown that this series of computer codes can calculate most of the phenomena associated with LBLOCAs. These assessments cover a wide range of separate effects and integral tests. Tests from the 2D/3D Program provided the largest body of test data for code assessment on LBLOCA phenomena. 2D/3D data are also significant for determining predictive capability in that data from the 2D/3D Program are at large-scale (1/1 for UPTF and 1/21 for CCTF and SCTF). Most integral data are at smaller scales. Assessment results have shown that TRAC-PF1/MOD1 can be used to calculate the key parameters, PCT in particular, that would be expected during PWR calculations involving similar phenomena. Key phenomena and trends can also be calculated. Some of the details of the phenomena, timing of events, and minor trends may not be calculated correctly. These have been highlighted in the previous discussions. The CSAU effort (Section 5.7.3) attempted to quantify these for TRAC-PF1/MOD1.

Since TRAC-PF1/MOD1 and TRAC-PF1/MOD2 are currently in use, assessment results for these two code releases are summarized below. Older code versions and the assessment calculations performed with them were important to the development of TRAC but are no longer of current interest.

5.7.1 TRAC-PF1/MOD1 Assessment Results Using 2D/3D Data

To assess a system simulation code such as TRAC, Reference U-681 defined three categories that provide a useful framework within which code performance can be assessed. The categories are: (1) the prediction of key parameters, (2) the prediction of key phenomena, and (3) the prediction of important trends.

Prediction of Key Parameters
The key parameter from the licensing perspective is PCT. The use of a single parameter such as PCT to reflect the overall degree to which code calculations and measurements agree should always be accompanied by a review of the predictions of underlying phenomena that contribute to the single parameter. TRAC-PF1/MOD1 has generally been able to predict PCT in SCTF and CCTF tests with at least reasonable agreement. Underlying phenomena are discussed below.

Prediction of Key Phenomena
Particular phenomena have been identified as being of interest because of their effect on determining PCT. These include, for example, core flooding rate, vessel inventory, and loop differential pressure. TRAC-PF1/MOD1 was consistently able to predict these key thermal-hydraulic phenomena in SCTF and CCTF tests with reasonable agreement. In CCTF UPI tests, MOD1 predicted the channeling effect, the asymmetric core reflood, the negative core-inlet flow, and breakthrough location. In SCTF

5.7-1

calculations, TRAC correctly predicted flow circulation within the core and tie plate breakthrough locations.

Prediction of Key Trends
One measure of code quality is the ability to accurately calculate test-to-test differences or trends resulting from the parametric variations of initial and boundary conditions. Generally, TRAC was able to predict trends in rod temperatures, flow patterns, and changes in flow and heat transfer caused by power distributions and other variations.

5.7.2 TRAC-PF1/MOD2 Assessment Results Using 2D/3D Data

TRAC-PF1/MOD2 shows results similar to those seen with TRAC-PF1/MOD1. The constitutive relations in MOD2 are significantly better in the sense that they were taken largely from recent literature and are more soundly based. The MOD1 constitutive package relied to a greater extent on models based on engineering judgment.

Assessment of TRAC-PF1/MOD2 is limited in comparison to the assessment set for TRAC-PF1/MOD1. Also, TRAC-PF1/MOD1 was used extensively for a period of years with regular releases of new versions containing error corrections and improvements while TRAC-PF1/MOD2 version 5.3 is the initial TRAC-PF1/MOD2 release. As the initial version, TRAC-PF1/MOD2 version 5.3 shows promise as a tool for PWR analyses. Additional assessment and possibly error corrections (new versions) may be necessary before TRAC-PF1/MOD2 can be used with confidence for PWR analyses.

Prediction of Key Parameters
TRAC-PF1/MOD2 shows similar performance to MOD1 in calculating PCT. One significant difference is that MOD1 had equations for the heat transfer above the quench front that were tuned to compensate for underprediction of liquid above the quench front. MOD2 uses equations that do not have this tuning. Consequently, MOD2 predictions for rod temperatures above the quench front are not as good as MOD1 predictions. This has only a small effect on the prediction of PCT.

Prediction of Key Phenomena
TRAC-PF1/MOD2 shows similar performance to MOD1 in calculating most of the phenomena that it has been assessed against. One improvement is that MOD2 does a better job of calculating the entrainment above the quench front.

Prediction of Key Trends
Although TRAC-PF1/MOD2 has not been assessed against a large number of tests with parametric variations as was TRAC-PF1/MOD1 against SCTF and CCTF tests, the similarity of the results obtained with MOD1 suggest that TRAC-PF1/MOD2 would similarly predict test-to-test trends.

5.7.3 Code Scaling, Applicability and Uncertainty (CSAU) Study

In an effort separate from the 2D/3D Program, the USNRC developed a methodology to evaluate thermal-hydraulic code scaling, applicability and uncertainty (Reference E-609). This methodology was demonstrated by applying it to the use of TRAC-PF1/MOD1 version 14.3 for a cold leg LBLOCA in a Westinghouse 4-loop PWR. Results are included here because: (1) The CSAU effort gave a quantitative estimate of the uncertainty of TRAC-PF1/MOD1 in calculating rod peak cladding temperatures, as opposed to the qualitative assessments discussed above; (2) the CSAU results provide a guide to the relative importance of phenomena in calculating the PCT; and (3) 2D/3D data were extensively utilized in quantifying the uncertainty of TRAC-PF1/MOD1.

Initially, LBLOCA phenomena were ranked for importance. Reference E-609 summarized the ranking: "The most important phenomena in each LBLOCA phase are summarized as follows. For blowdown, the fuel rod stored energy, break flow, and reactor coolant pump degradation have the highest rank. During refill, the highest ranked phenomena are cold leg and downcomer condensation (ECCS bypass related) and downcomer multidimensional flow. For reflood, the core reflood heat transfer,void generation, three-dimensional flow, entrainment and de-entrainment in the upper plenum and hot legs, steam binding, and the effect of noncondensible gases in the cold legs receive the highest rating."

The important phenomena were then compared with code models to determine which correlations in TRAC-PF1/MOD1 contain modeling uncertainties that might significantly affect calculations of PCT. These evaluations consisted of analytical calculations, review of code assessments and engineering judgments based on model evaluations. When it was determined that significant uncertainties existed, the parameters were ranged for use in code evaluation later in the procedure. Seven parameters were identified as needing further study in a ranging (bounding) process to evaluate associated uncertainties. These were: (1) break mass flow rate; (2) pump head and torque degradation; (3) stored energy (gap conductance, fuel rod peaking factor, fuel conductivity, convective heat transfer); (4) blowdown and reflood heat transfer (minimum rewetting temperature, convective heat transfer); (5) delivery and bypassing of ECC; (6) steam binding(core liquid entrainment to upper plenum and hot legs, boiling within U-tubes); and (7) noncondensible gases (partial pressure and dissolved nitrogen).

Data from the 2D/3D Program were used extensively in evaluating Items 4, 5 and 6. The ranging of break flow, pump performance, stored energy, and heat transfer was determined from data and applied to the plant calculations. Uncertainties for ECC bypass and steam binding were evaluated as biases with single values that were added to the uncertainties determined from the ranging calculations. The biases for late reflood PCT for steam binding and ECC bypass were respectively, 59 K and

-19 K, respectively. The negative sign indicates that the TRAC calculation produces a conservative result (i.e., higher calculated temperatures).

The final result of the CSAU project was a pair of numbers for mean PCT and PCT bound with the estimated uncertainties. These were a mean peak cladding temperature $\leq$ 962 K and 95th percentile peak cladding temperature $\leq$ 1129 K.

To summarize, the CSAU methodology was developed to evaluate code scaling, applicability and uncertainty for a particular transient in a particular plant. A demonstration of the methodology was done using TRAC-PF1/MOD1 version 14.3. It showed that TRAC was applicable to the LBLOCA evaluated, and produced an estimate of the uncertainties associated with the calculation of PCT. Although the CSAU process has not been done with TRAC-PF1/MOD2, LANL expects that the result would be similar. TRAC-PF1/MOD2 may be somewhat better in that known deficiencies in TRAC-PF1/MOD1 were addressed in the development of TRAC-PF1/MOD2.

5.8 CONCLUSIONS

The TRAC series of computer codes provided useful analysis support during the design phases of UPTF and SCTF. The TRAC code also provided useful information for specification of instrumentation and determination of initial and boundary conditions for CCTF, SCTF, and UPTF tests.

The TRAC series of computer codes were extensively assessed against data from the 2D/3D Program. Over the course of the program, results from the assessment calculations performed in the program were continually fed back to the TRAC developers and this contributed significantly to improve the quality of the code.

The assessment results from the 2D/3D Program provided an excellent technical basis for the development and validation of the TRAC code for the prediction of phenomena in full-size PWRs during the end-of-blowdown, refill, and reflood phases of an LBLOCA with cold leg, upper plenum, downcomer, or combined ECC injection system. TRAC has generally been able to calculate the important phenomena (e.g., rod temperature transient) observed in 2D/3D tests as well as experiments from other test programs. Therefore, TRAC is expected to be able to calculate these phenomena for a PWR LBLOCA.

Much of the analysis work performed in the 2D/3D Program utilized TRAC-PF1/MOD1. MOD1 is a mature, stable computer code with a large assessment base. It is suitable for a wide range of PWR analyses and can be used with confidence. TRAC-PF1/MOD2, which was released near the end of the 2D/3D Program, has several important improvements relative to MOD1; namely, improved numerics for the multidimensional "VESSEL" component, improved closure relationships, and new features for LWR safety analysis (e.g., the generalized heat structure). At the completion of the 2D/3D Program, it appears that MOD2 has not yet reached the level of maturity and stability of MOD1. Therefore, potential users will need to compare the benefits of the improvements in MOD2 against the maturity and stability of MOD1 when deciding which code version to use.

Section 6

ADVANCED INSTRUMENTATION

6.1 OVERALL INSTRUMENT DEVELOPMENT

The USNRC provided advanced instrumentation to CCTF, SCTF, and UPTF in support of the 2D/3D Program. Conventional instrumentation was supplied by each facility to measure temperature, pressure, differential pressure, water level and single phase flow rate (see Sections 3 and 4). The advanced instrumentation was applied in the three facilities to measure local two-phase flow parameters; e.g., void fraction, phase velocity, etc. The provision of the advanced instruments involved major efforts in the areas of development, design, testing, fabrication, installation, software, and documentation. Advanced instrumentation was provided primarily by Idaho National Engineering Laboratory (INEL) and Oak Ridge National Laboratory (ORNL). Selected hardware components and algorithms for calculating tie plate mass flow rate were supplied by FRG/Siemens. Some of the instrumentation provided to 2D/3D Program facilities was based on the experience from previous USNRC instrument development programs. Other instrumentation was developed specifically for the 2D/3D Program. There were ten major types of instruments provided to 2D/3D Program facilities, as shown below.

ORNL-Supplied Instrumentation

- Tie Plate Drag Sensors (Drag Bodies and Breakthrough Detectors)
- Purged Differential Pressure Measurement Systems
- Film and Impedance Probes (Flag Probes, Prong Probes, String Probes, Film Probes)

INEL-Supplied Instrumentation

- Turbine Meters
- Drag Discs
- Gamma Densitometers
- Liquid Level Detectors/Fluid Distribution Grids
- Spool Pieces
- Velocimeters
- Video Probes

Table 6.1-1 shows the number and location of instruments provided to each 2D/3D Program facility. In CCTF and SCTF where multiple cores were used, instruments were sometimes refurbished and sometimes provided new when replacement cores were installed (Table 6.1-1). See Sections 3.1 and 4.1 of this report and References U-801 and U-802 for a more detailed description of the locations of advanced instruments.

For each type of instrument and each facility as identified in Table 6.1-1, the following process was used in providing the instruments.

- A specification for the instrumentation was prepared.

- An instrument interface document was developed by the facility. (For example, Reference G-804.)

- A preliminary instrument design (including hardware, electronics, and software) was defined by the pertinent laboratory.

- Meetings were held to resolve the instrument design and facility interface issues.

- Instruments were fabricated and tested in accordance with the final design criteria and requirements.

- Instrument support items (software, documentation) were developed.

- Instruments were shipped to the facility or appropriate subassembly fabricator.

- Instruments were installed and checked out by facility and US-laboratory personnel.

- Instrument operation and maintenance were carried out by facility personnel. Laboratory personnel reviewed data from the first few actual tests to ensure proper instrument performance. Special problems were resolved using laboratory personnel when needed.

Each of the ten instrument types is discussed individually in Section 6.2. The discussion includes a brief description of the instrument and its applications, the instrument performance, and the value of the data in the 2D/3D Program. Reports describing instrument performance in selected facilities are provided in the following References: U-801 through U-813, J-802, U-401, U-412, U-414, U-421, U-431, and U-441.

TABLE 6.1-1

SUMMARY OF ADVANCED INSTRUMENTATION IN 2D/3D PROGRAM

Location and Instrument Type	Quantity Installed (Note 1)					
	CCTF-I	CCTF-II	SCTF-I	SCTF-II	SCTF-III	UPTF
UPPER PLENUM						
Purged DP	—	—	—	—	—	36
Turbine Meter	—	4	12	12(R)	—	6
Gamma Densitometer	—	—	4	4(R)	4(R)	—
LLD/FDG (Note 2)	3 x 17	11 x 10(N)	8 x 8	8 x 8(R)	8 x 8(R)	8 x 19 45 x 7
Impedance (Prong) Probe	—	4	8	4(R)	4(R)	—
Structure Film Probe	—	4	6	4(R)	—	—
Wall Film Probe	—	—	6	6(R)	3(R)	—
Video Probe	1	1(N)	1	1(R)	1(R)	3
END BOX						
Tie Plate Drag Body	—	—	—	—	4	36
Breakthrough Detector	—	—	—	—	2	94
Purged DP	—	—	—	—	—	9
Turbine Meter	—	8	—	—	8	42
Gamma Densitometer	—	—	5	5(R)	1(R)	—
LLD/FDG (Note 2)	Note 3	Note 3	Note 3	Note 3	Note 3	Note 3
Video Probe	—	—	1	1(R)	1(R)	—
CORE						
Gamma Densitometer	—	—	10	10(R)	10(R)	—
LLD/FDG (Note 2)	6 x 17	6 x 16(N)	4 x 20	4 x 20(N)	4 x 20(N)	2 x 19
Impedance (Flag) Probe	—	24	8	4(N)	4(N)	—
Rod Film Probe	—	—	6	6(N)	—	—
Wall Film Probe	—	—	8	8(R)	8(R)	—
LOWER PLENUM						
Turbine Meter	—	—	4	4(R)	4(R)	—
LLD/FDG (Note 2)	3 x 5	3 x 5(R)	—	—	—	—
Velocimeter	—	4	—	—	—	—

TABLE 6.1-1

SUMMARY OF ADVANCED INSTRUMENTATION IN 2D/3D PROGRAM

Location and Instrument Type	Quantity Installed (Note 1)					
	CCTF-I	CCTF-II	SCTF-I	SCTF-II	SCTF-III	UPTF
DOWNCOMER						
Turbine Meter	—	—	—	—	—	8
Drag Disk	4	2(R)	3	3(R)	3(R)	—
LLD/FDG (Note 2)	3 x 17	6 x 6 7 x 18	6 x 7	6 x 7(R)	6 x 7(R)	50 x 3 50 x 1
Impedance (String) Probe	—	—	3	3(R)	—	—
Video Probe	—	1	—	—	—	—
COLD LEGS						
Spool Piece Containing: Drag Screen, Turbine Meter, 3-Beam Gamma Densitometer, Thermocouple and Pressure/DP Sensors	4	4(R)	1	1(R)	1(R)	—
Pipe Flowmeter Containing: 4 Drag Disks, 3-Beam Gamma Densitometer, Thermocouple and Pressure Sensor	—	—	—	—	—	1
HOT LEGS						
Spool Piece (as described above under COLD LEGS)	4	4(R)	—	—	—	—
Spool Piece Contianing: 4 Drag Disks, 4 Gamma Densitometers, Thermocouples and Pressure Sensor	—	—	1	1(R)	1(R)	—
Pipe Flowmeter (as described above under COLD LEG)	—	—	—	—	—	4
Film Probe	—	4	—	—	—	—
Video Probe	—	1	—	—	—	—

TABLE 6.1-1

SUMMARY OF ADVANCED INSTRUMENTATION IN 2D/3D PROGRAM

Location and Instrument Type	Quantity Installed (Note 1)					
	CCTF-I	CCTF-II	SCTF-I	SCTF-II	SCTF-III	UPTF
VENT VALVES						
Transducer DP	---	---	---	---	---	5
Turbine Meter	---	2	---	---	---	5
String Probe	---	2	---	---	---	---
Vent Pipe Spool Piece Containing: Drag Screen, Turbine Meter, Thermocouple, and Pressure/DP sensors	---	---	1	1(R)	1(R)	---

NOTES: 1. On CCTF-II, SCTF-II and SCTF-III, (R) indicates refurbished and (N) indicates new instrument.

2. LLD/FDG quantity expressed as AxB, where A indicates the number of strands and B is the number of sensors per strand.

3. Some upper plenum LLD/FDG sensors extended into the end box region.

6.2 INSTRUMENT DESIGN, CALIBRATION, APPLICATION, AND EVALUATION

6.2.1 Tie Plate Drag Sensors

Description
Two types of tie plate drag sensors were developed by ORNL for use in the 2D/3D Program: tie plate drag bodies (DBs) and breakthrough detectors (BTDs). Both sensors use the same basic measurement approach of a strain-gaged support element holding a drag target located in the flow stream. In the DB, the drag target is cut from the tie plate and is supported in its normal position by the strain gage transducer (Figure 6.2-1). This approach was used to eliminate disruption of the flow pattern by the transducer. In the BTD, a small target was located below the tie plate, supported as a cantilever by the strain gage transducer (Figure 6.2-2). This approach provided a much less-expensive approach than the DB, but the BTD instrument sampled only a very local region of the flow (three tie plate holes) as opposed to the larger area (majority of a fuel assembly) sampled by a DB.

The strain gages used in DBs and BTDs were fully encapsulated in Inconel sheaths to protect them from the steam/water environment. Strain gages were welded to the transducers. Thermocouples were also welded to the transducers adjacent to strain gages so that temperature effects (apparent strain) on the measurements could be compensated for to optimize accuracy.

All DB and BTD instruments were mechanically, thermally, and thermal-shock tested to verify reliability. All instruments were individually force-calibrated and thermally-calibrated. Prototype instruments were subjected to extreme life-cycle mechanical, thermal, and thermal shock tests to ensure reliability of the design. Also, prototype instruments were calibrated in both single- and two-phase flow at ORNL. DB measurements were interpreted in conjunction with other measurements (turbine meter velocities and differential pressures) to obtain bi-directional mass flow rate at the tie plate. BTD measurements were correlated to downward liquid mass flow rate through the tie plate, and BTD data were used to determine "breakthrough" from the upper plenum to the core based on a pre-determined flow rate threshold.

Final design DB and BTD instruments were calibrated in conjunction with other tie plate instruments at FRG (Karlstein), using single- and two-phase flow. The algorithm to calculate tie plate flow rate in UPTF and SCTF-III was developed based on these calibration tests (Reference G-803). Also, the UPTF core simulator feedback system, which uses BTD measurements, was covered by these tests.

Application
DBs were used at 36 (out of 193) tie plate locations in UPTF and four (out of eight) tie plate locations in SCTF-III. BTDs were used at 94 tie plate locations in UPTF and two tie plate locations in SCTF-III. The measurement locations were evenly distributed across the top of the core in both facilities.

Evaluation
Reliability of DBs in UPTF was less than desired. DB transducer failures occurred at the rate of several per year. Defective transducers were replaced during UPTF outages in 1987 (15 DBs), 1988 (5 DBs), and 1989 (18 DBs) to help restore lost capability. At the end of the program 10 of 36 DBs were operational.

Extensive failure analyses were performed by ORNL and Siemens. Based on the results of the analyses, changes were made in the design and fabrication of DB transducers. These changes, however, did not solve the problems. The Siemens' investigation also identified the high pH environment as a contributing factor to the failures. (It should be noted that the primary system pH was increased to 10.5 after the instruments were designed.) A detailed discussion of the problems with UPTF DBs is in References U-801, G-807, and G-808.

Reliability of DBs in SCTF-III was excellent with no failed instruments. One of the four SCTF-III DBs was not installed properly; the drag target interfered with other structure and was not free to move. As a result, no valid data were obtained from this one instrument. BTD reliability was excellent in both UPTF and SCTF, with only four failed instruments in UPTF, which were replaced in an outage in 1987.

The data from DBs and BTDs were very useful in evaluating the test results. Specifically, these instruments provided the most direct and accurate indication of flow distribution at the top of the core. Accurate characterization of the highly nonuniform flow pattern at the core exit in tests simulating upper plenum injection and hot leg injection was facilitated by these instruments.

6.2.2 Purged Differential Pressure Measurement System

Description
A purged differential pressure (DP) measurement system covering 45 DP measurements was developed by ORNL for use in UPTF. This system was necessitated by the requirement to take local DP measurements at locations within the primary system. Hence, a conventional DP measurement approach using wall taps at the pressure boundary would not be adequate; instead, pressure tap lines had to be routed within the pressure boundary. Since internally routed lines are exposed to a wide range of conditions including superheated steam and subcooled water, the fluid density in the tap lines could be subject to substantial change, thus introducing

unacceptable errors in DP measurements. FRG (Siemens) designed and installed sophisticated tap routing to minimize heat transfer to the tap lines. The purged DP measurement system was designed to continuously purge DP lines with a small flow rate of liquid water, so that tap line density changes would be small (Reference U-923). The purged DP measurement system used conventional DP sensors mounted remotely from the vessel. Equipment to supply and control purge flow was a key part of the system. Figure 6.2-3 shows an overview of the system. Key considerations from the outset of the development of this system were the accuracy and frequency response of the measurements and the performance of the purge during UPTF system pressure transients. Extensive developmental testing was performed by ORNL to demonstrate acceptable performance of the DP system. All DP transducers used with the system were individually calibrated. Each "purge block" was also tested to demonstrate it provided the needed performance. Purged DPs with appropriate internal taps were calibrated in single- and two-phase flow at both ORNL and FRG (Karlstein). DP measurements were interpreted in conjunction with other measurements (DBs and turbine meters) to obtain mass flow rate at the tie plate.

Application
A purged DP measurement system was provided only to UPTF. A system capable of covering 45 DP measurements (nine across the tie plate and 36 from tie plate to top of upper plenum) was provided to UPTF by ORNL.

Evaluation
Reliability of the DP measurement system in UPTF was excellent. No significant problems occurred and reliable data were obtained from these instruments. The data from the DP measurements were very useful, particularly in determining upper plenum liquid inventory distribution and tie plate flow rate. These measurements were important to understand the phenomena occurring for the several different types of ECC systems tested. Further, in some cases tie plate DPs provided backup to tie plate drag bodies which had failed.

6.2.3 Film and Impedance Probes

Description
Film and impedance probes were developed by ORNL in a variety of configurations for use in the 2D/3D Program. All of the film and impedance probes work on the same basic principle; i.e., that the electrical properties (conductance, capacitance, etc.) between two electrodes within a test system change in accordance with the relative amounts of steam and water between the electrodes. Impedance probes were intended to determine void fraction in a flow stream and film probes were intended to determine film thickness on vertical surfaces. In both cases, determination of velocity by cross-correlation of signals from adjacent sensors was intended in some applications, but did not prove to be successful.

Three basic types of impedance probes were utilized (Figure 6.2-4): flag probes for making incore subchannel measurements, prong probes for making upper plenum measurements, and string probes for making downcomer and vent valve measurements. The main difference between probe types is the electrode shape. Three principal configurations of film probes were employed (Figure 6.2-5): rod-mounted probes for incore use, structure-mounted probes for upper plenum use, and wall-mounted probes for incore or upper plenum use. Because water conductivity significantly influences probe response, a "reference probe" (liquid conductivity sensor) was also used in each facility employing film and impedance probes.

The primary development efforts for film and impedance probes were: (1) development of suitable insulators (including brazing techniques) which could withstand the temperature, pressure and thermal shock requirements; (2) signal conditioning electronics; and (3) signal interpretation. A metal/ceramic (cermet) insulating material and a high temperature braze alloy and brazing technique were developed and extensively tested by ORNL; use of these materials provided reasonable reliability. Signal conditioning electronics were developed to measure small probe capacitance and conductance values in the pressure of large cable capacitances and conductances. All film and impedance probes were electrically calibrated both wet and dry; prototype probes were calibrated under controlled two-phase flow conditions to support signal interpretation. It was found that the flow regime between the probes had the most significant influence on signal interpretation.

Application
Film and impedance probes were employed in CCTF-II, SCTF-I, SCTF-II, and SCTF-III. The number of each type of instrument used in these facilities is identified in Table 6.1-1. In SCTF-II and SCTF-III, some instruments were refurbished from the previous core and others were provided new.

Evaluation
Film and impedance probe reliability was moderate. The majority of the ex-core sensors survived and provided data throughout the test series. However, incore sensors failed steadily throughout each test series so that at the end of a test series only a few, at most, were operating. This was attributed to the severe temperature and thermal shock conditions occurring in the core.

The film thickness and void fraction information gained from film and impedance probe data was mainly qualitative, because the data were not highly accurate. The measurement trends showed good overall agreement with global measurements such as core and upper plenum DP. The major benefits from these instruments are that they directly confirmed the presence of water throughout the core and upper plenum during reflood and that they directly detected the propensity of water to collect on unheated surfaces (films). No usable velocity data were obtained from the instruments, because of poor signal coherence between adjacent sensors.

6.2.4 Turbine Meters

Description

Probe-type and full-flow turbine meters had been successfully employed in ECC research programs prior to the 2D/3D Program and thus were natural candidates for obtaining data in 2D/3D. Full-flow turbine meters are discussed below under "Spool Pieces and Pipe Flowmeters," and the turbine probe instruments are discussed here.

Turbine probes were provided by INEL to several of the 2D/3D Program facilities. These instruments consist of a "stalk" which holds a "head" out in the region to be measured (Figure 6.2-6). The "head" has a flow bore containing a free-spinning turbine rotor. Magnetic or RF pickup coils located within the head sense the turbine blade passing and thus give an output signal frequency proportional to turbine rotational speed. A probe-type turbine is a free-field measurement; i.e., only a portion of the entire flow field is sampled.

The major design challenges in employing turbine probes are the turbine bearing performance and life, the survivability of pickup coils in the severe environment, and signal interpretation, particularly in two-phase flow applications. The development and significant use of sapphire bearings in turbine probes was accomplished in the 2D/3D Program, which provided good bearing performance. All turbine meters were tested under limiting temperature and pressure conditions to verify acceptable construction and all were calibrated in single-phase flow by directing flow through the turbine bore with a tube. Prototype turbine meters were subjected to severe thermal shock conditions to verify design adequacy and were calibrated in appropriate free-field configurations to support signal interpretation. Free-field calibration was performed at INEL, ORNL and FRG (Karlstein). Data from turbine meters used at the tie plate in UTPF and SCTF-III were interpreted in conjunction with other instruments (DB and DP) to determine tie plate mass flow rate.

Application

As shown in Table 6.1-1, probe-type turbine meters were employed in CCTF-II (upper plenum and vent valves); SCTF-I, II, and III (lower plenum, tie plate and upper plenum); and UPTF (downcomer, tie plate, vent valves, and upper plenum).

Evaluation

Turbine meter reliability was favorable, with most turbines surviving the duration of the test series and providing useful data. Several UPTF turbines failed during the three-year test cycle and replacements were installed during facility outages. Leakage through an internal quick-disconnect fitting was identified as the main cause of failures.

While the data from most turbine meters were very useful, the data from some turbine meters were not useful. The turbine meters in the UPTF downcomer provided detailed information on flow distribution, particularly during ECC penetration/bypass tests.

Regions of steam upflow and liquid downflow could be clearly identified. Tie plate turbine meters in UPTF and SCTF provided useful information on core exit flow distribution. Also, tie plate turbine meter measurements in UPTF and SCTF-III were used in calculating tie plate flow rates. The upper plenum turbine meters provided qualitative information. The lower plenum turbine meters in SCTF did not provide usable data because of electromagnetic interference. The vent valve turbine meters in UPTF did not provide useful information because of the highly non-uniform flow field around these instruments in the downcomer.

6.2.5 Drag Disks

Description
Drag disks had been successfully utilized on previous ECC research programs and were also employed in the 2D/3D Program. Probe-type drag disks are discussed here; full-flow drag disks (or drag screens) are discussed below under "Spool Pieces and Pipe Flowmeters."

Drag disks were provided by INEL to all of the 2D/3D Program test facilities (CCTF, SCTF, and UPTF). A typical drag disk is a flange-mounted device which has an arm protruding into the flow stream to be measured (Figure 6.2-7). A drag target is located at the end of the arm. In the original development of these instruments prior to the 2D/3D Program, the target was circular; hence the name "disk." In most 2D/3D applications a noncircular target was utilized. The arm containing the target is supported back in the flange region by a pivot and spring. Displacement of the arm about the pivot occurs when the drag target is loaded by flow forces. The displacement is measured by a linear variable differential transformer (LVDT). This output is proportional to the force on the target, which is proportional to the flow momentum flux.

A major challenge in employing drag disks in the 2D/3D Program was that a low measurement range was desired to be able to accurately measure the nominal flows associated with reflood, but a high survivability range was needed to ensure the instrument would tolerate high flows associated with end-of-blowdown. This was accomplished by incorporating a mechanical stop for the arm in the drag disk design. In this manner, the instrument could survive momentum fluxes over ten times its measurement range.

All drag disks were tested at limiting pressure and temperature conditions to ensure proper construction, and all were force-calibrated. Prototype drag disks were exposed to the full range of limiting environmental conditions to ensure proper design and were calibrated in single-phase flow to ensure that the measurement signals could be meaningfully interpreted.

Application

Drag disks were employed in the downcomer of CCTF and SCTF to measure liquid velocity during reflood. Drag disks were also employed in the hot leg of SCTF, and in the four hot legs and broken cold leg of UPTF. In these large-pipe applications, four drag disks were employed at a single pipe location and these instruments were interpreted in conjunction with gamma densitometer measurements at the same pipe location to determine mass flow rate. The large pipe applications are discussed more fully below under "Spool Pieces and Pipe Flowmeters."

Evaluation

A problem with failure of some of the drag targets was encountered in UPTF. Reference U-801 contains a more complete description of the problem. The failures were attributed to high transient loads resulting from water slugs. The targets were re-designed to make them smaller and stronger, with some sensitivity penalty. Also, selected drag disks were removed during tests which could potentially create slug conditions at the measurement location. When this approach was used, the problems were alleviated.

There were also some problems in UPTF with the external measurement parts (arm, spring, and set screws) which degraded some of the data but did not render the instruments non-operational.

In the CCTF and SCTF downcomers, velocities measured by the drag disks were near the low end of the drag disk range; i.e., several cm/sec. The drag disk measurements did not show any unusual results such as large spatial flow distributions. Other than this observation of low, relatively uniform flows, there were no major benefits derived from the downcomer drag disks.

The drag disks in the hot legs of SCTF and UPTF provided valuable data on the flow regime and flow rate at these locations, as discussed under "Spool Pieces and Pipe Flowmeters" below.

6.2.6   Gamma Densitometers

Description

Single- and multi-beam gamma densitometers had been successfully utilized in previous ECC research programs and were also employed in the 2D/3D Program. Single-beam gamma densitometers are discussed here; multi-beam gamma densitometers are discussed below under "Spool Pieces and Pipe Flowmeters."

Single-beam gamma densitometers were provided by INEL to SCTF for use in the core, end box, and upper plenum regions. The unique slab-shaped configuration of SCTF provided an ideal opportunity to obtain several gamma densitometer density

measurements in these regions. The gamma densitometer consists of a gamma ray source and detector located on opposite sides of the fluid volume to be measured (Figure 6.2-8). A collimated gamma beam passes from source to detector and is attenuated according to the fluid density in the intervening space. The measured gamma ray intensity at the detector is thus a measurement of fluid density.

The gamma densitometer was adapted to SCTF by using flange-mounted sources and detectors which attached directly on the vessel. In the core region, the beam collimator produced a narrow beam to pass through the small rod subchannel space.

Gamma densitometers were calibrated in-situ at the "wet" and "dry" states. Interpretation of two-phase measurements (densities between wet and dry) was done in accordance with theory as supported by calibrations performed at INEL.

Application
As shown in Table 6.1-1, 10 single-beam gamma densitometers were employed in the SCTF core region, five were used in the end box region, and four were used in the upper plenum. These instruments were used in all three cores of SCTF, except that four end box measurements were removed for SCTF-III because of other hardware modifications. Gamma densitometers were also used in conjunction with other instruments in the hot and cold legs of CCTF, SCTF and UPTF, as discussed under "Spool Pieces and Pipe Flowmeters."

Evaluation
The gamma densitometers performed acceptably in SCTF. One problem was encountered with some of the core densitometers during some tests, in which movement of the bundle rods during the tests obstructed the gamma beam. This problem, which could be readily detected, invalidated the associated data. The bundle movement was due to thermal effects and occurred most strongly on tests involving top injection with highly nonuniform core cooling.

Gamma densitometer data were very useful for determining two-dimensional density distribution in the core and upper plenum and for providing local measurements to supplement global DP inventory measurements. Gamma densitometer data could also be used in conjunction with end box turbine meter data to evaluate phase mass flow rates across the core. These evaluations showed a higher water presence at the outer edge of the core (Reference U-802).

6.2.7   Liquid Level Detectors and Fluid Distribution Grids

Description
Conductivity-type liquid level detectors (LLDs) had been successfully employed on previous ECC research programs and were also used in the 2D/3D Program. During 2D/3D, the fluid distribution grid (FDG) concept was developed and implemented,

which is basically a 2- or 3-dimensional array of LLDs. Also, optical-type sensors for use in LLDs/FDGs were developed and employed in 2D/3D.

An LLD/FDG sensor detects the presence or absence of water at a single location. Conductivity LLD sensors use the change in conductance between electrodes as an indicating signal, while optical LLD sensors use the reflection/refraction of light at a sapphire/fluid interface to detect presence or absence of water (Figure 6.2-9). Several sensors are arranged on a stalk to create an LLD, and several stalks are used in a volume (such as upper plenum, core, etc.) to create an FDG. The bi-stable outputs of an array of sensors can be displayed in an appropriate format to provide a "picture" of water/steam distribution in a test volume.

All LLD/FDG sensors were tested under limiting pressure and temperature conditions to ensure proper construction. Prototype LLD/FDG sensors were exposed to the limiting range of environmental conditions to ensure suitable design. All sensors were calibrated in-situ at known wet and dry conditions; the sensor electronics were then used to set the wet/dry bi-stable discrimination.

Application
LLD/FDG systems were used in upper plenum, core and downcomer regions in CCTF, SCTF, and UPTF. Optical LLD sensors were used in the upper plenum and downcomer regions of CCTF-II and throughout UPTF. Otherwise, conductivity sensors were utilized. As shown in Table 6.1-1, up to several hundred sensors were employed in each facility.

Evaluation
LLD/FDG systems performed acceptably in the 2D/3D facilities; there were a few failures of individual sensors as each test series progressed. Optical sensor degradation in UPTF was the result of surface corrosion due to the high pH environment (pH = 10.5). (It should be noted that the primary system pH was increased to 10.5 after the instruments were designed.) This was remedied during outage periods by polishing the probe surfaces and by increasing the light source intensity.

Data from LLD/FDG systems were qualitatively useful. The most meaningful data were obtained in situations where the two-phase flow was well-separated. This occurred most often in the downcomer. The flow regime in the core and upper plenum (and the downcomer in some cases) typically was well-mixed. Under these conditions, the LLD/FDG systems tended to give a biased reading toward "wet"; i.e., the individual probes were easily wetted by a small water presence but were not so easily unwetted. Accordingly, most sensors usually indicated wet shortly after the start of reflood.

6.2.8 Spool Pieces and Pipe Flowmeters

Description

A spool piece refers to a combination of instruments at a pipe location. Often these instruments are supplied as a completed, flanged pipe section; hence, the name "spool piece." At UPTF such instruments were separately supplied and mated to the facility pipes; the name "pipe flowmeter" was used to describe this arrangement. Regardless of name, the intent of using multiple instruments at a single pipe location is to obtain detailed information on two-phase flow.

Instrumented pipe spool pieces had been successfully employed in ECC research programs prior to the 2D/3D Program and were selected for use in 2D/3D at the outset of the program. A six-inch (150 mm) diameter spool piece containing a full-flow drag screen, full-flow turbine meter, 3-beam gamma densitometer, and pressure/temperature instrumentation (Figure 6.2-10) had already been developed at the outset of the 2D/3D Program. Similar spool pieces were supplied by INEL for the hot and cold legs of CCTF and the cold leg of SCTF. Large pipe configurations in the SCTF hot leg and UPTF loops necessitated developing a modified design since full flow drag screens and turbine meters were not feasible. In these cases an array of four drag disks (Section 6.2.5) and either three (UPTF) or four (SCTF) gamma densitometer beams (Section 6.2.6) along with pressure/temperature instrumentation provided the desired measurement (Figures 6.2-11 and 6.2-12).

The principal challenge in spool piece use is data interpretation in two-phase flow. The measurements from the combination of instruments need to be interpreted to determine flow regime, void fraction, phasic velocities and phasic densities. The six-inch spool pieces utilized the substantial base of two-phase testing and algorithm development that had occurred prior to the 2D/3D Program. All component instruments were of course calibrated as described in the preceding sections. Two-phase flow testing of the large SCTF hot leg spool piece was carried out by INEL to confirm data evaluation algorithms. UPTF pipe flowmeter data interpretation was based on algorithms adapted from other spool piece applications, supplemented by limited in-situ, single-phase calibration at UPTF.

Application

Eight nominally identical spool pieces were employed in the hot and cold legs of CCTF. A similar spool piece was used in the broken cold leg of SCTF, and a similar spool piece without the three-beam gamma densitometer was used in the vent pipe of SCTF. A single spool piece was provided for the large oval hot leg of SCTF. Five sets of instruments to provide five pipe flowmeters were supplied for the hot legs and broken cold leg of UPTF. All of this spool piece instrumentation was supplied by INEL.

Evaluation

Spool pieces and pipe flowmeters performed acceptably in 2D/3D Program facilities. Some problems occurred with the UPTF drag disks (which were corrected by modifying the drag paddles as discussed in Section 6.2.5) and with the UPTF gamma densitometer electronics (which were corrected by simplifying the electronics).

Data from the spool pieces provided useful information which would not have been obtainable without these instruments. In particular, the flow regime and water transport in the hot legs was a key result determined from these instruments. Stratified water layers and countercurrent flow in the SCTF and UPTF hot legs were directly measured with the spool pieces. Similar phenomena were not detected in the smaller CCTF hot legs, indicating an effect of scale. The spool piece data were used in the development and confirmation of appropriate correlations and theory to explain the behavior.

6.2.9 Velocimeters

Description

The velocimeter provided by INEL to the 2D/3D Program measures single-phase liquid velocity. The velocimeter consisted of a cooled plenum which was sufficiently instrumented to quantify the heat absorbed from the water flowing past the probe (Figure 6.2-13). Velocity was determined from the plenum and fluid temperatures and the heat transfer rate. The principle is that changes in water velocity change the convection heat transfer coefficient.

The limitation in applying this type of velocimeter is that the fluid velocity must be large enough to overcome free convection effects if it is to be measurable. Testing was carried out at INEL to investigate this limitation. Testing showed an instrument range down to 10 cm/sec was achievable with limited possibilities to obtain some information below 10 cm/sec.

Application

Velocimeters were supplied only to CCTF-II for use in the lower plenum. It was desired to obtain information on core inlet flow distribution during reflood, where velocities are nominally several cm/sec. Although the velocimeter was not ideally suited to this application, it came closer than any other developed instrument. As shown in Table 6.1-1, four velocimeters were supplied to CCTF-II.

Evaluation

Velocimeters functioned properly but provided essentially no usable output during CCTF-II reflood tests. The liquid velocity was below the instrument range and could not be measured.

6.2.10 Video Probes

Description

The intent of video probes was to allow two-phase flow in selected regions of test systems to be directly observed. The original instrument conceived to provide direct internal observation was the stereo lens system which is based on the rod lens concept. A stereo lens system was supplied to CCTF-I by LANL. This system did not achieve the desired performance. A video probe system supplied by INEL was used in other facilities. The video probe system consists of a borescope to convey the image to the outside of the vessel, light source, and video camera/recorder/monitor (Figure 6.2-14). Appropriate insulation and active cooling are also provided to protect the components. Optical deflectors and enlargers are also used to handle the image.

Video probes for 2D/3D Program test facilities were built and tested to demonstrate the environmental conditions could be tolerated. No flow testing was performed.

Application

Video probes were employed in the upper plenum of CCTF, SCTF, and UPTF. In UPTF these video probes viewed the regions of the hot leg nozzles. Video probes were also used in the SCTF end box and in the CCTF-II downcomer and hot leg. See Table 6.1-1.

Evaluation

In reflood tests, video probe images confirmed the flow pattern is well-mixed. In these cases, unfortunately, the visual depth of field drops to near zero so that detailed information about the flow is difficult to obtain. Thus, for reflood tests, video probes confirmed the presence of entrained water but did not provide detailed flow information. In the UPTF hot leg countercurrent flow test, the video probe provided a clear image of the stratified flow entering the upper plenum from the hot leg. This provided direct visual confirmation of the flow regime.

Strain gages

Transducer element

Thermocouple

Dummy fuel rods

Drag body

Control rods
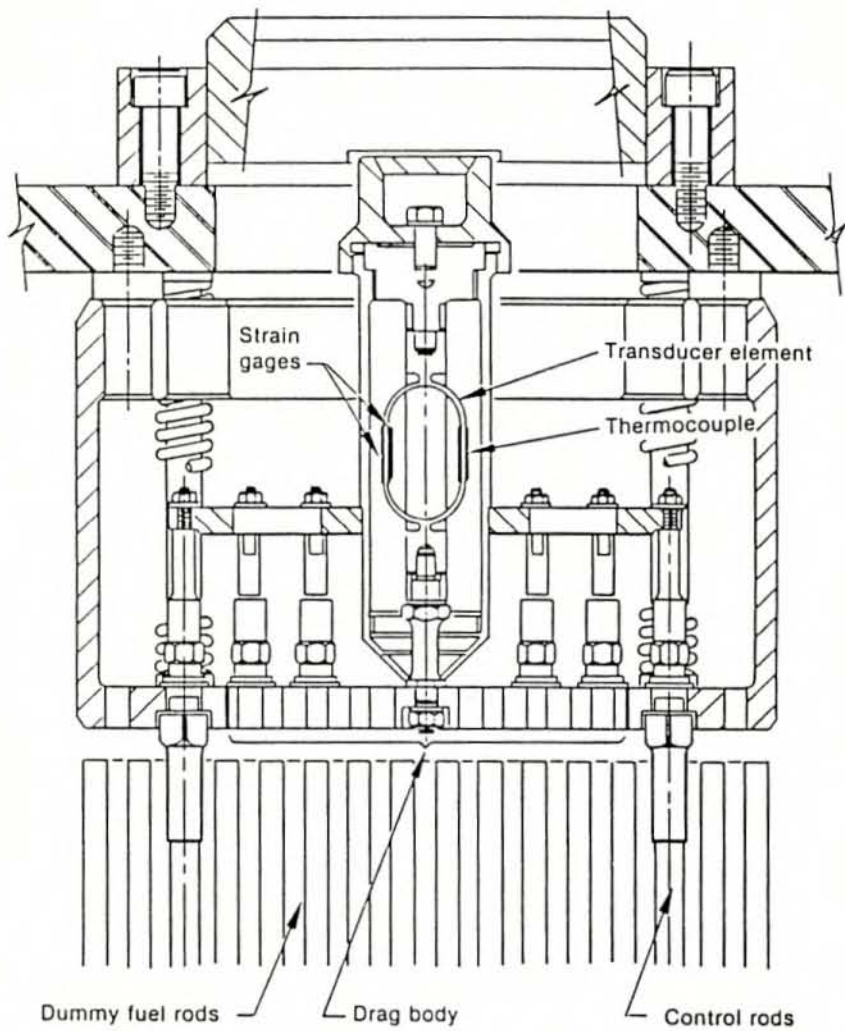
TIE PLATE DRAG BODY
FIGURE 6.2-1

Transducer Cables

Mounting base

Full Bridge Strain Gage

Flow

Housing

Target (senses flow through three tie plate holes)
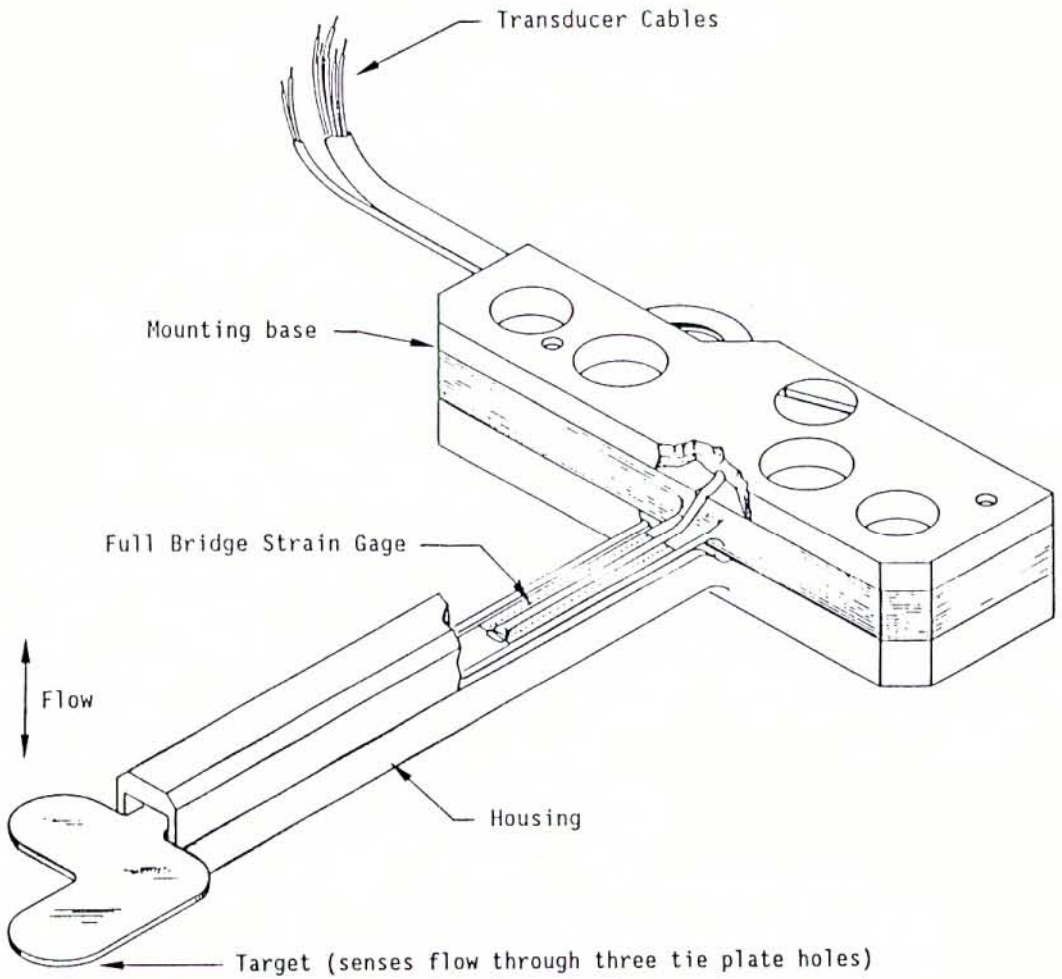
BREAKTHROUGH DETECTOR
FIGURE 6.2-2

EX-VESSEL

IN-VESSEL

DP TRANSDUCER

CONTROLLED
PURGE FLOW

TAPS

WATER, AIR AND
POWER SUPPLIES

D/P

PURGE
SUPPLY
SYSTEM

PRESSURE BOUNDARY
PENETRATION

TAP LINES
EXPOSED TO
IN-VESSEL
ENVIRONMENT

TAP LINES

VESSEL BOUNDARY
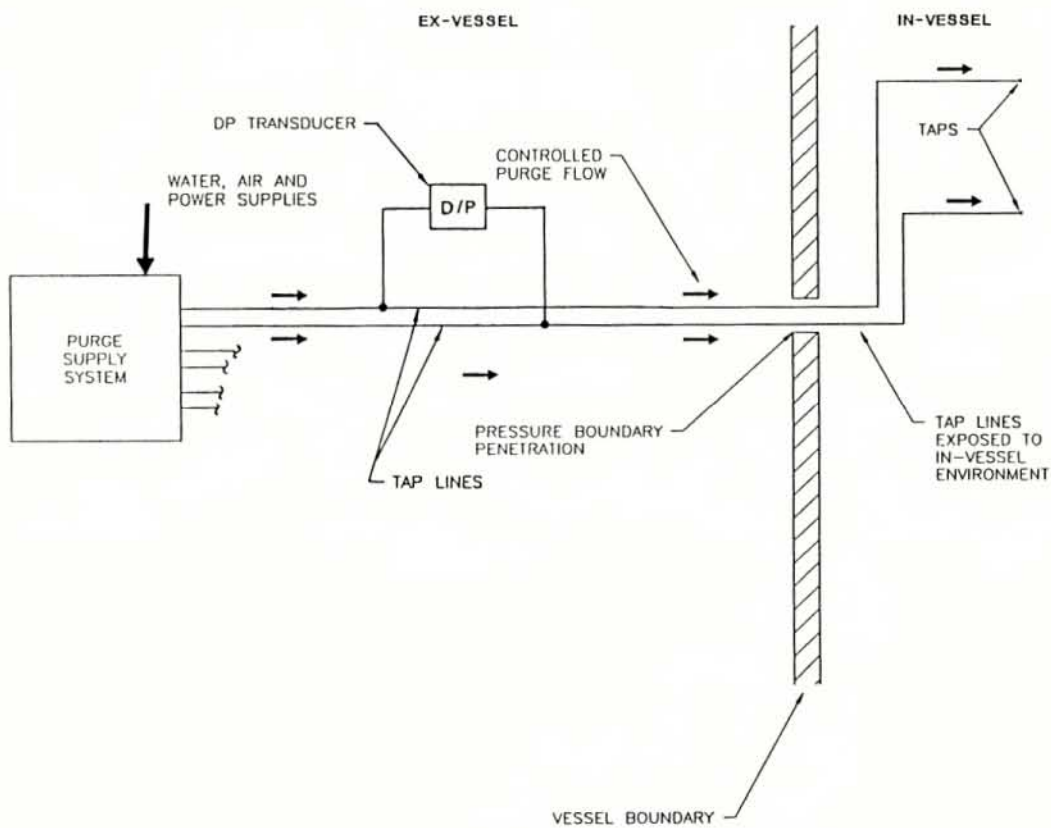
PURGED DP SYSTEM
FIGURE 6.2-3

≈ 80 mm

STRING PROBE
(VOID FRACTION)
ONLY

13.7 mm

UPPER
MEASURING
STATION

≅ 4 m

13.7 mm

≅ 2 m

UPPER STATION

LOWER
STATION

LOWER STATION

UPPER PLENUM
PRONG PROBE
(VOID FRACTION
ONLY)

IN-CORE FLAG PROBE
(VELOCITY AND VOID FR.)
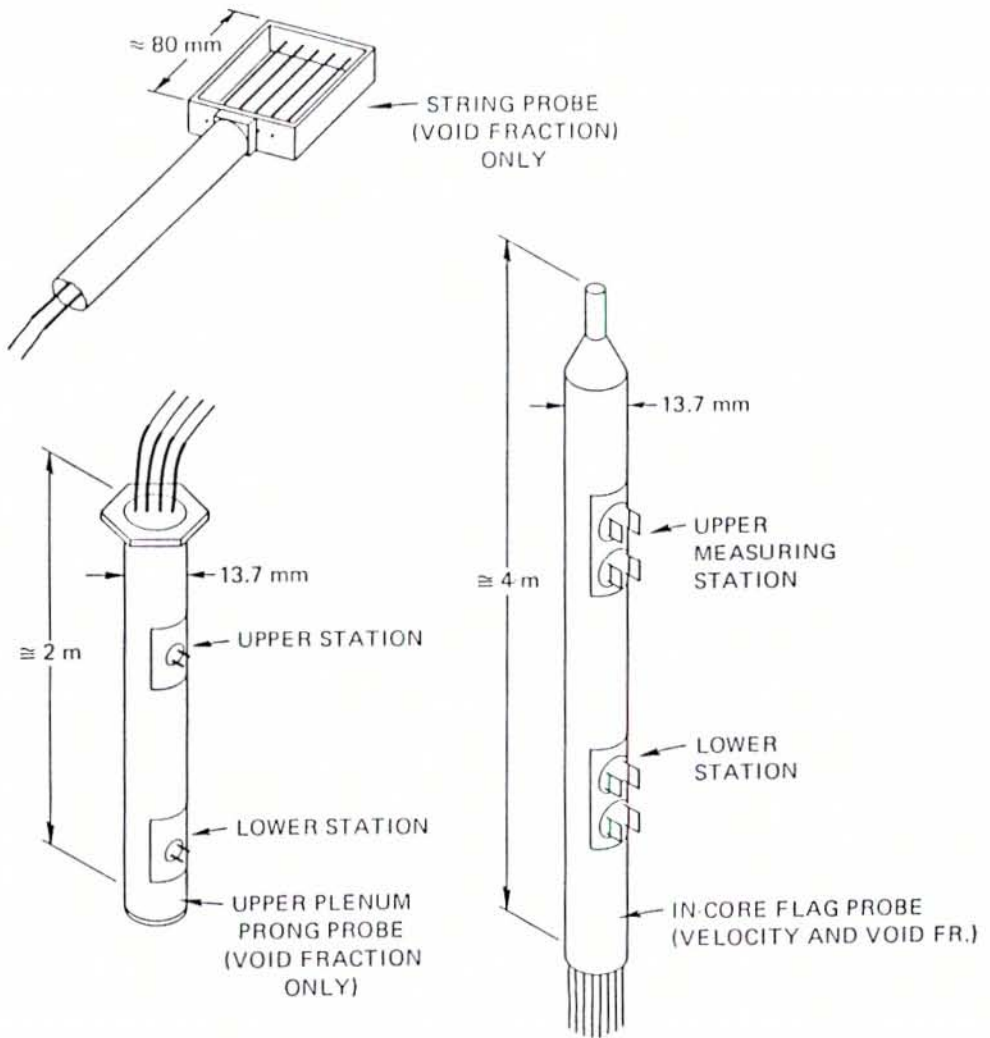
IMPEDANCE PROBES FOR 2D/3D PROGRAM
FIGURE 6.2-4
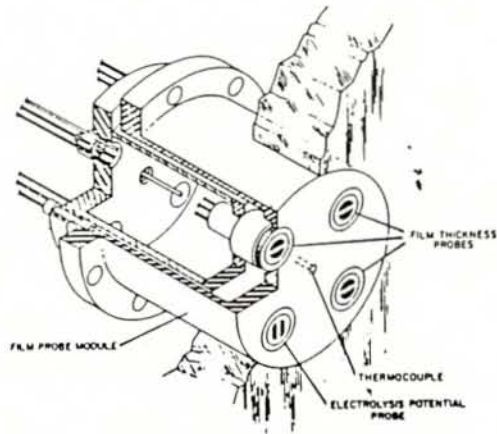
WALL FILM PROBE
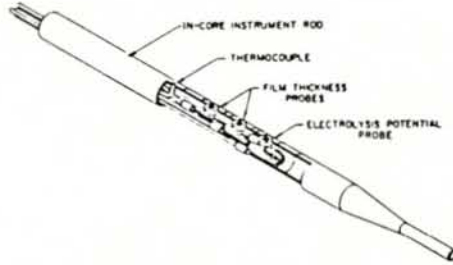
IN-CORE ROD FILM PROBE
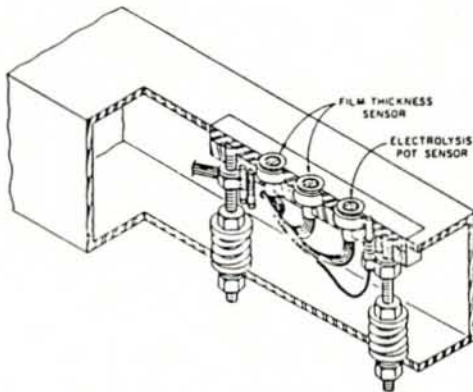
STRUCTURAL FILM PROBE

FILM PROBES FOR 2D/3D PROGRAM
FIGURE 6.2-5

TURBINE ROTOR,
SUPPORT AND BEARINGS

BORE

HEAD

SUPPORT STALK

TURBINE SENSING
COILS CONTAINED
IN HEAD

INSTRUMENT CABLES
ROUTED WITHIN
SUPPORT STALK

FLOW
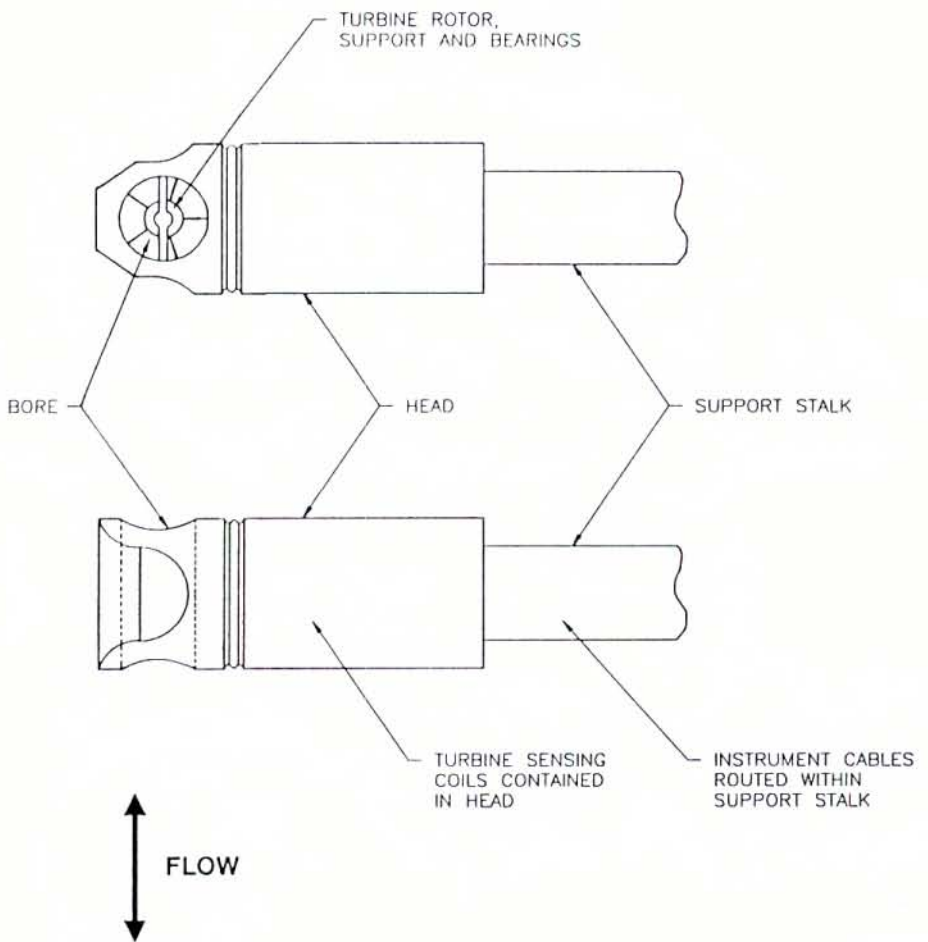
TURBINE PROBE
FIGURE 6.2-6
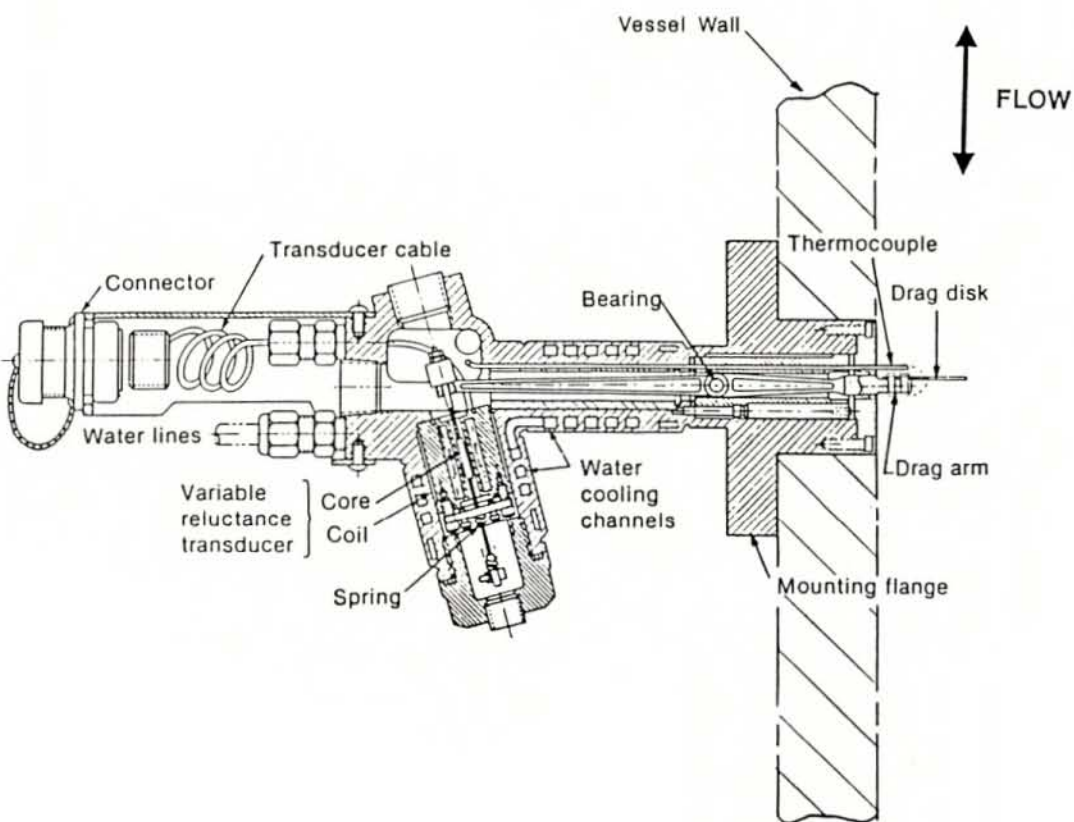
DRAG DISK ASSEMBLY
FIGURE 6.2-7

Detector

Vessel Wall

Source
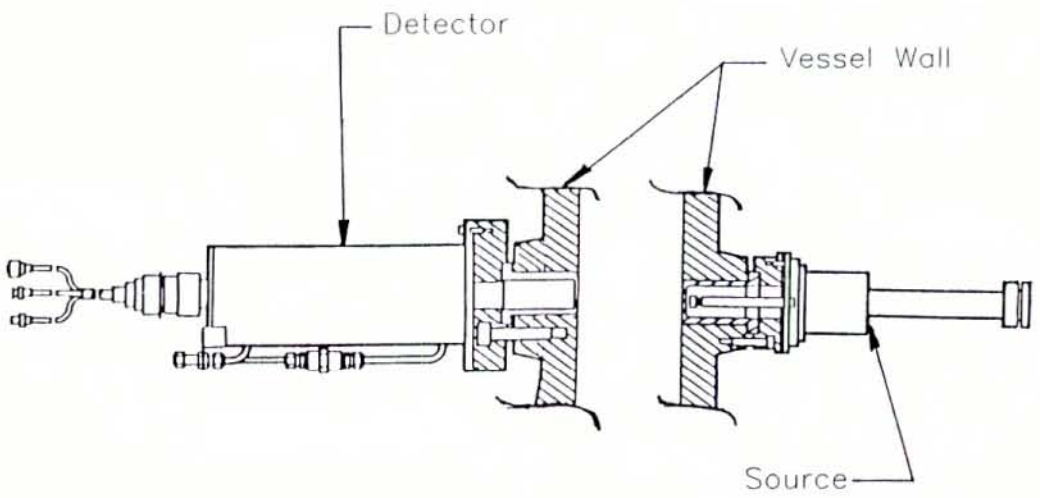
SINGLE BEAM GAMMA DENSITOMETER
FIGURE 6.2-8

Stainless steel-sheathed
cable 1.018 mm (0.040 in.)
diameter

Laser
weld

Two conductor

Inconel X-750

Ceramic
sleeve

Ceramic
seal

Single conductor

Moisture
seal
typical

Inconel X-750

CONDUCTIVITY SENSOR

Light
source

Transmitting fibers

Receiving fiber

Photo detector/
amplifier
combination
integrated
circuit

Fiber
guide

Probe
sapphire
window

Dry

Wet

OPTICAL SENSOR

LLD/FDG SENSORS USED IN 2D/3D PROGRAM
FIGURE 6.2-9
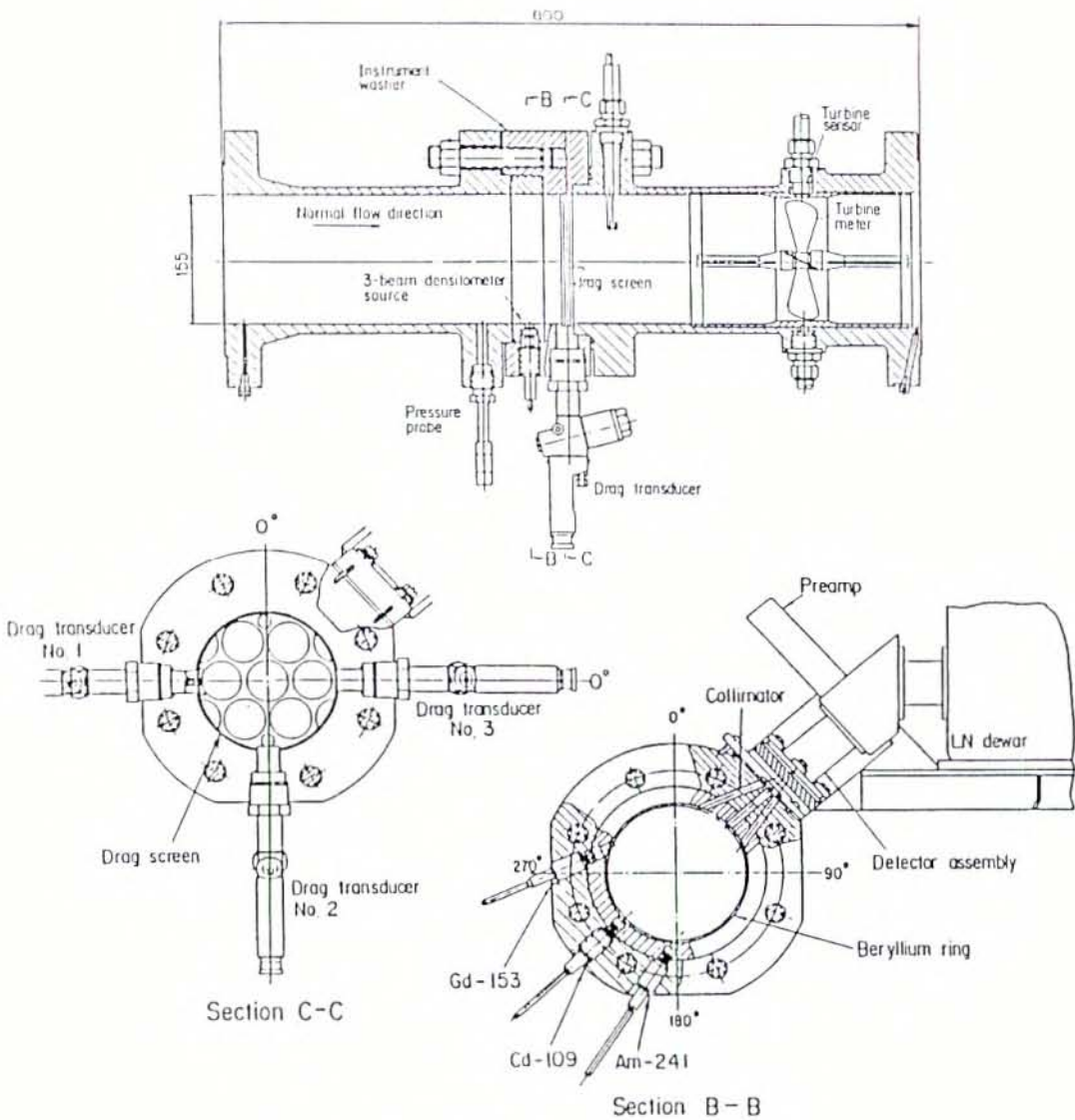
INSTRUMENTED SPOOL PIECE USED IN
CCTF HOT LEG/COLD LEG AND SCTF COLD LEG
FIGURE 6.2-10

Densitometer
beam No. 1

Pressure
probe

Region 1

Region 2

Densitometer
beam No. 2

Metal Temperature Probe

Densitometer
beam No. 3

Drag disk
transducer (4)

Region 3

Region 4

Densitometer
beam No. 4
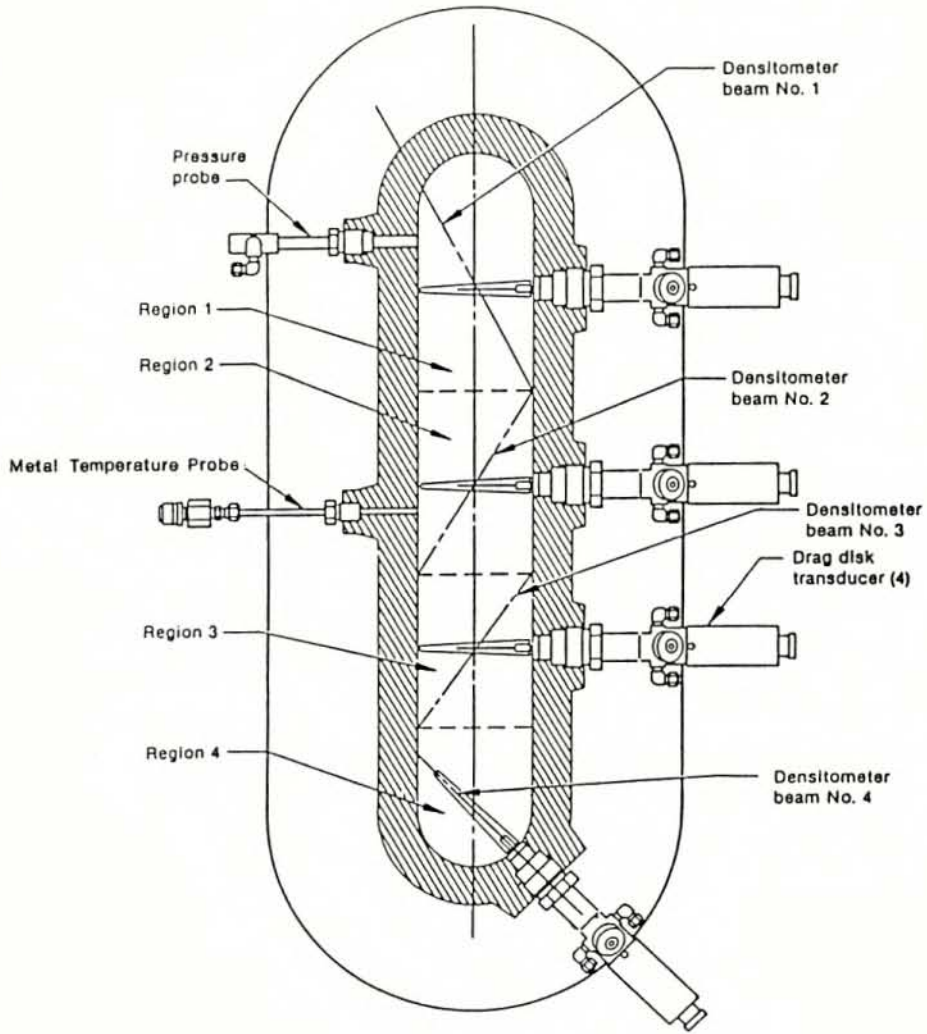
SSCF HOT LEG SPOOL PIECE
CROSS-SECTION
FIGURE 6.2-11

Drag Rake № 1
Thermocouple № 1

Source

59.7°
43.5°
19.2°

Drag Rake № 4
Thermocouple
№ 4

20°±2°

Pressure
Transducer
№ 1

6°±2°

Detector 3

Drag Rake № 2
Thermocouple
№ 2

Detector 2

TC

Detector 1
(beam 1)

60

The Thermocouple is attached
to the Drag Rake

Drag Rake № 3
Thermocouple № 3

Test Vessel

Pipe Flow Meter

5084 (Intact Loop)
5007 (Broken Loop)

350

Pipe Flow Meter

2610   350

DR GD
TC
PA

995

GD   DR;TC;PA

ECC

Pipe Flow Meter consists of:
1 Absolute Pressure Transducer (PA)
4 Fluid Thermocouples (TC, 1 recorded)
4 Drag Rakes (DR)
1 γ-Densitometer (3 Detectors, GD)

Note: Dimensions in mm

UPTF PIPE FLOW METER
FIGURE 6.2-12
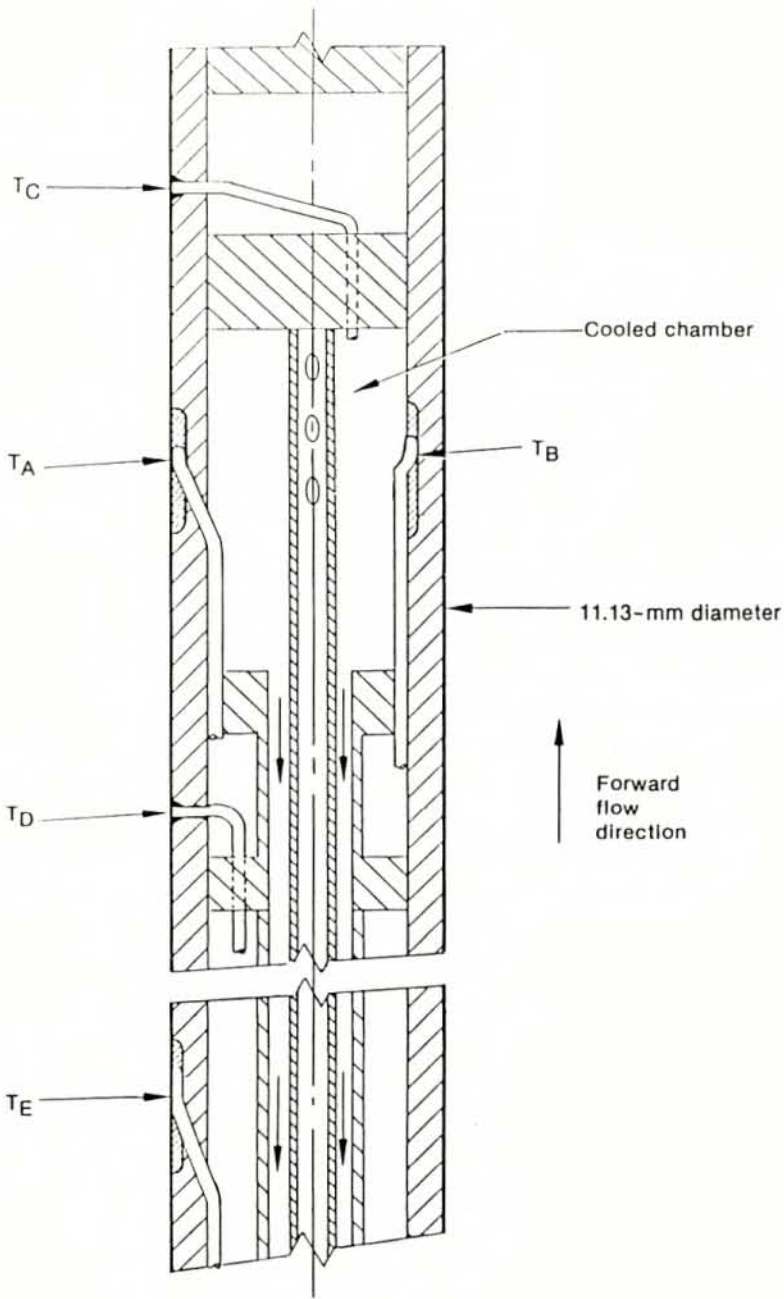
VELOCIMETER CROSS-SECTION
FIGURE 6.2-13
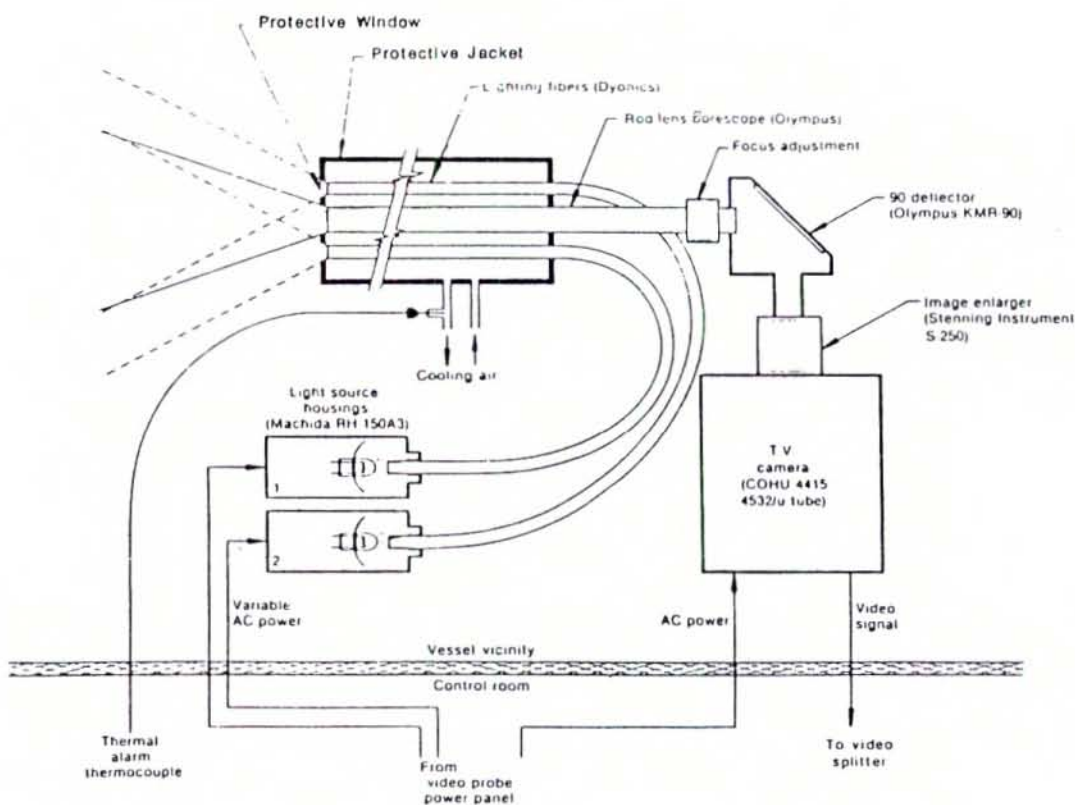
VIDEO PROBE ASSEMBLY
FIGURE 6.2-14

6.3 SUMMARY

A substantial quantity and variety of advanced instrumentation were utilized in CCTF, SCTF, and UPTF. Valuable data, both quantitative and qualitative, were obtained from these instruments. Some instruments performed well while others performed marginally. Instruments which provided valuable quantitative measurements and should be strongly considered for future two-phase flow applications include:

· Drag Bodies and Breakthrough Detectors

· Purged DP Measurement System

· Turbine Meters (when the flow is one-dimensional and calibration is in a realistic configuration)

· Drag discs

· Gamma densitometers

· Spool Pieces and Pipe Flowmeters

Instruments which provided mainly qualitative information and would need to be further developed before future applications include:

· Film and Impedance Probes

· Turbine Meters (in other than straightforward flow configurations)

· Liquid Level Detectors/Fluid Distribution Grid

· Velocimeters

· Video Probes

The experience from developing, designing, calibrating, interfacing, and testing these instruments is also a valuable product of the program. The following references provide extensive information in this regard: G-801 through G-806, J-801, J-802, U-821 through U-825, U-831 through U-834, U-841, U-842, U-846, U-847, U-851 through U-854, U-861, U-862, U-866 through U-868, U-871, U-872, U-876, U-921 through U-923, U-925, and U-934.

Section 7

SUMMARY AND CONCLUSIONS

The 2D/3D Program comprised 15 years of coordinated reactor safety research sponsored by BMFT, JAERI, and USNRC. The program investigated the thermal-hydraulic phenomena which occur in a PWR during a LOCA. Each country contributed significant effort to the program and all three countries shared the results. The contributions from each country are summarized below.

- Japan constructed and operated CCTF, a full-height, 1/21-scale model of an 1,100 MWe, four-loop PWR. Tests at the CCTF investigated system behavior during the refill and reflood phases of an LBLOCA for different types of ECC injection systems. A total of 58 tests were performed.

- Japan also constructed and operated SCTF, a full-height, full-radius, 1/21-scale model of a sector of an 1,100 MWe four-loop PWR. The SCTF test program studied two-dimensional behavior in the core during refill and reflood phases of an LBLOCA. The three test series performed within the 2D/3D Program included a total of 76 tests.

- FRG constructed and operated UPTF, a full-scale model of a 1,300 MWe, four-loop PWR. Tests at UPTF investigated multidimensional behavior of steam and water in the upper plenum, loops and downcomer during the end-of-blowdown, refill, and reflood phases of an LBLOCA. Selected SBLOCA phenomena were also investigated. The UPTF test program consisted of 30 tests comprising a total of 80 test runs.

- The US carried out an analysis program which assessed the predictive capability of the US-developed TRAC computer code against 2D/3D tests. The analysis program also provided analytical support during the design of UPTF and SCTF, and helped specify initial and boundary conditions for some tests. A total of 91 TRAC calculations were performed by the US as part of the 2D/3D Program. Selected TRAC calculations were also performed by other program participants.

- The US also developed and fabricated advanced instrumentation to measure local two-phase flow parameters (e.g., void fraction, phase velocity, etc.). Instruments were provided to all three test facilities. In addition, the US provided the data acquisition systems for UPTF.

The major results of the 2D/3D Program on PWR LOCA behavior are summarized below. While Sections 3 through 5 of this report discuss the results of the test programs and analyses separately, the following summary synthesizes the results from the three test facilities and applicable TRAC analyses by phenomena. The summary draws on a companion report, "Reactor Safety Issues Resolved by the 2D/3D Program," which discusses the program results by issue and shows how each issue has been resolved.

7.1 RESULTS RELATED TO ECC DELIVERY TO LOWER PLENUM DURING DEPRESSURIZATION

During the end-of-blowdown phase of an LBLOCA, steam and entrained water flow up the downcomer to escape out the break. This two-phase upflow may carry some or all of the ECC injected in cold legs and/or downcomer out the broken cold leg thereby preventing delivery to the lower plenum. This is referred to as ECC bypass.

In CCTF tests, ECC injected in the cold legs was completely carried out the break until depressurization was almost complete. However, in UPTF tests, delivery of ECC to the lower plenum was initiated earlier in the depressurization transient (i.e., at a higher system pressure) due to multidimensional flow phenomena not observed at CCTF or other small-scale facilities. Specifically, ECC injected in the cold legs away from the break tended to be delivered while ECC injected in the cold leg adjacent to the break was nearly completely bypassed.

ECC delivery behavior in tests with downcomer injection and open vent valves was similar to that in the cold leg injection tests. This was the result of two offsetting effects. First, downcomer injection promoted ECC bypass because the ECC was dispersed as the high velocity injection streams impinged on the core barrel. Separate effects tests with downcomer injection but without vent valves confirmed strong bypass throughout end-of-blowdown, although it appears nozzle configuration details may significantly influence the results. Second, when the vent valves were open, significant delivery of water from the nozzle away from the break occurred as a result of the flow through the vent valves changing the flow rate and flow pattern in the downcomer.

In tests with combined ECC injection, ECC injected in the hot legs flowed downward through the core providing core cooling during blowdown. Lower plenum refill was initiated during the end-of-blowdown by ECC injected into the hot legs. Shortly thereafter the ECC injected to the cold legs away from the break was delivered to the lower plenum, but the ECC injected to the cold leg adjacent to the break continued to be almost completely bypassed.

For all three ECC injection modes, refill overlapped with the end-of-blowdown and the lower plenum was filled to the bottom of the core barrel prior to the end of depressurization. This result shortens the portion of the refill phase where core cooling is very low and significant core heat up could occur.

7.2 RESULTS RELATED TO DOWNCOMER BEHAVIOR DURING REFLOOD

The reflood phase of an LBLOCA begins when the reactor vessel water level reaches the bottom of the core. This creates a seal between the core and downcomer and further ECC injection tends to fill the downcomer to near the cold leg elevation. Steam generated in the core flows out the top of the core to the upper plenum and toward the downcomer via the intact loops or the vent valves. Subcooled ECC condenses a portion of the steam. Steam not condensed by ECC flows circumferentially around the downcomer and out the break, potentially entraining water out the break and reducing the downcomer water level. The downcomer collapsed water level is further reduced by steam generation on hot downcomer walls.

In cold leg injection tests, downcomer behavior was markedly different during the accumulator and LPCI portions of reflood due to the difference in ECC injection rates. During accumulator injection, all of the intact loop steam flow was condensed by the high flow of ECC. Consequently, there was no steam flow out the broken cold leg and entrainment did not occur. Further, subcooled water was delivered to the downcomer and boiling on the downcomer walls was suppressed. As a result, the downcomer filled to the cold leg (i.e., spillover) elevation. However, during LPCI, the intact loop steam flow was only partially condensed and the ECC delivered to the downcomer was essentially saturated. The uncondensed steam entrained water from the downcomer out the break and reduced the downcomer water level. As the saturated water gradually replaced subcooled water in the downcomer, wall boiling created voiding in the downcomer. The combined level reduction due to entrainment and voiding was on the order of 1 m.

Analyses of counterpart CCTF and UPTF tests indicates that downcomer water entrainment and the attendant level reduction decreased at small-scale for full-height facilities where the vertical flow area is scaled by the scale factor. This is due to decreases in the steam velocity in the downcomer and at the broken cold leg nozzle at small-scale.

In UPTF tests with downcomer ECC injection and open vent valves, essentially all LPCI injected through the nozzle close to the break was swept out the break, even at low steam flows. However, ECC injected through the nozzle away from the break was delivered to the downcomer. The steam flow in the downcomer entrained water out the break and thereby reduced the downcomer water level. For tests with downcomer injection and vent valves, the downcomer water level reduction was comparable to that

in cold leg injection tests due to two offsetting effects. First, downcomer ECC injection promoted entrainment because the ECC flow was introduced into the downcomer at a higher elevation. Second, redistribution of steam in the downcomer due to the flow through the vent valves decreased water entrainment and the downcomer level reduction.

In combined injection tests, most of the steam generated in the core was condensed in the upper plenum and hot legs throughout reflood. Residual intact loop steam flow was condensed in the cold legs, and there was no steam flow in the downcomer to entrain water out the break. Also, the flow of highly subcooled ECC from the cold legs suppressed wall boiling in the downcomer. Consequently, there was no reduction in the downcomer water level during reflood.

In UPI tests, most of the steam flow out of the core was condensed in the upper plenum by LPCI. The intact loop steam flow was condensed in the cold legs by HPCI. Consequently, there was no steam flow around the downcomer and no entrainment out the break.

7.3 RESULTS RELATED TO TIE PLATE/UPPER PLENUM FLOW PHENOMENA

With combined injection or UPI, tie plate/upper plenum flow phenomena involve simultaneous two-phase upflow from the core and ECC downflow to the core. The ECC downflow occurs under countercurrent flow conditions at the tie plate. During end-of-blowdown/refill, ECC downflow occurs without hold-up because the upflow is negligible. During reflood, however, the two-phase upflow is significant and can potentially limit downflow.

In UPTF separate effects tests with ECC injection into the hot legs, flow phenomena at the tie plate and in the upper plenum were multidimensional. Specifically, water downflow through the tie plate occurred in discrete regions while two-phase upflow occurred over the remainder of the tie plate. The downflow regions were located in front of the hot legs with ECC injection. Water accumulation in the upper plenum was also multidimensional with greater accumulation over the downflow regions. Due to these multidimensional phenomena, water downflow was significantly greater than predicted by CCFL correlations for uniform flow conditions. For flow rates typical of reflood in combined injection PWRs, essentially all ECC delivered to the upper plenum flowed downward through the tie plate; i.e., downflow was not countercurrent flow limited. Most of the steam generated in the core was condensed by ECC injected in the hot legs and returned to the core with the water downflow. Measurements below the tie plate indicate that, even though the ECC was warmed by condensation, the water downflow was substantially subcooled.

In CCTF and UPTF tests with ECC injection directly into the upper plenum, water downflow through the tie plate occurred in a single region near the injection location and two-phase upflow from the core occurred outside the downflow region. Essentially all ECC injected in the upper plenum penetrated to the core. A significant portion of the steam flow was condensed in the upper plenum as the two-phase upflow and ECC injection mixed. For the single LPCI pump failure case, about half the steam was condensed. All steam was condensed for the no failure case. The condensate, as well as some of the water carried out the core, was returned to the core with the water downflow, which had small subcooling.

7.4 RESULTS RELATED TO UPPER PLENUM/HOT LEG DE-ENTRAINMENT

During reflood, steam generated in the core flows through the upper plenum and hot legs toward the break. Some of the water carried by the steam flow evaporates due to heat transfer from hot surfaces, principally the steam generator U-tubes. This additional steam flow inhibits core venting and can degrade core cooling. This is referred to as steam binding.

In CCTF and UPTF tests with cold leg injection, water carried out of the core de-entrained and accumulated upstream of the steam generator tube regions, principally in the upper plenum and steam generator inlet plena. This de-entrainment delayed carryover to tube regions by about 20 to 30 seconds, which was beneficial for core cooling. At large-scale, water accumulation and (in some cases) runback in the hot legs initiated after the delay, which reduced the amount of water carried to the steam generators. CCTF tests showed that essentially all water carried over to the tube regions was vaporized.

In tests with downcomer injection and vent valves, a substantial portion of the steam flowed from the upper plenum to the downcomer via the vent valves rather than the loops. The low loop steam flows reduced carryover to the steam generator tube regions. In fact, at low core steam flows, there was no carryover to the tube regions.

In tests with UPI or combined injection, most of the steam generated in the core was condensed in the upper plenum and hot legs. Consequently, loop steam flows were low and the effects of carryover to the steam generators on core reflood were not significant.

7.5 RESULTS RELATED TO STEAM/ECC INTERACTIONS IN THE LOOPS

During an LBLOCA, subcooled ECC injected into the loops interacts with the loop steam flows. The steam is partially or completely condensed by the ECC. The extent of condensation strongly affects the flow regime and delivery of ECC to the reactor vessel.

For high ECC injection rates into the cold legs where the condensation potential exceeded the steam flow, the loop steam flow was completely condensed resulting in formation of water plugs in the cold legs. The plugs oscillated upstream and downstream from the injection nozzle location. Consequently, delivery of ECC to the reactor vessel fluctuated. For low ECC injection rates typical of LPCI in US/J PWRs, the condensation potential was less than the steam flow and only a portion of the loop steam flow was condensed. The resultant flow regime was stratified cocurrent flow and ECC delivery to the downcomer was steady. With both plug flow and stratified flow essentially all ECC injected in the cold legs was delivered to the downcomer.

For hot leg ECC injection rates and loop steam flows typical of GPWRs with combined injection, the condensation potential of the ECC exceeded the steam flow and water plugs typically formed in the hot legs. In UPTF tests, the plugs grew toward the steam generator simulators as ECC accumulated in the hot legs. In some tests, steam was injected into the steam generator simulators when the plug front reached the tube regions to simulate vaporization by heat transfer from the secondary side. The plug was discharged into the upper plenum when either the hydrostatic head of the plug, or the pressure increase due to steam injection in the steam generator simulator exceeded the loop differential pressure. Therefore ECC delivery to the upper plenum fluctuated. For lower loop steam flows, stratified countercurrent flow occurred in the hot legs even though the condensation potential was greater than the steam flow. Analyses indicate that the momentum flux of the steam flow was too low to support plug formation. With stratified flow, water delivery to the upper plenum was steady. Regardless of the flow regime, essentially all ECC injected in the hot legs was delivered to the upper plenum.

7.6 RESULTS RELATED TO CORE THERMAL-HYDRAULIC BEHAVIOR

Core thermal-hydraulic behavior determines the fuel temperature history during an LBLOCA and is sensitive to the boundary conditions at the core created by ECC system effectiveness and overall system response. The core behavior was studied extensively in tests at CCTF and SCTF.

In tests with cold leg or downcomer ECC injection, the core heated up nearly adiabatically during the brief period after blowdown and before the lower plenum refilled to the bottom of the core. When the water level reached the core, extensive steam generation initiated. A quench front initiated and advanced steadily up the core. Some of the water flow into the core was entrained by steam flow and two-phase flow was quickly established over the entire core. The presence of water in the upper regions of the core provided good core cooling above the quench front. Parameter effects tests indicated that entrained water was evenly distributed across the core regardless of the initial power and temperature profiles in the core.

The core flooding rate was controlled by upper plenum-to-downcomer differential pressure and the downcomer driving head. In tests with vent valves, flow through the vent valves reduced the upper plenum-to-downcomer differential pressure. This resulted in an increase in the core flooding rate.

With combined injection, ECC injected in the hot legs flowed downward to the core in discrete regions. During end-of-blowdown, tests and analyses indicate core cooling was provided by two-phase flow through the core and water downflow from the upper plenum. Within the downflow regions, fuel rods were quenched by the flow of subcooled water. After blowdown and before the lower plenum refilled to the bottom of the core, fuel rods outside the downflow regions heated up while those in the downflow regions continued to be effectively cooled.

During reflood, hot leg ECC injection delivered to the lower plenum either flowed up the downcomer to the break or back into the core from the bottom. Outside the downflow regions, steam generation initiated at the bottom of the cores as water entered the core from the lower plenum. Water entrained by the steam flow was carried to the upper regions of the core and to the upper plenum. The presence of water above the quench front re-established core cooling throughout the core. Most of the steam vented out the top of the core was condensed in the upper plenum and hot legs by the hot leg ECC injection. The condensed steam, as well as water carried over to the upper plenum, was returned to the core with the water downflow; i.e., a recirculation flow path was established. Condensation of steam in the upper plenum and hot legs reduced the upper plenum pressure and resulted in a high core flooding rate. Consequently, the quench front advanced quickly up the core.

In CCTF tests with LPCI into the upper plenum, ECC flowed down to the core during refill and reflood. Downflow occurred only in a local region below the injection nozzles. During refill, the top portion of the core within the downflow region was cooled by the water downflow while the remainder of the core heated up essentially adiabatically. During reflood, core cooling by water downflow was limited to the upper elevations of the core within the downflow region. Cooling of the remainder of the core initiated as water which penetrated to the lower plenum flowed back into the core. Quench front propagation was mainly from the bottom up. Steam generated in the core entrained water to the upper regions of the core. The presence of water in the upper regions of the core re-established cooling throughout the core. The distribution of entrained water was uniform across the core.

Overall, core cooling was adequate for all ECC injection modes.

7.7 RESULTS RELATED TO ACCUMULATOR NITROGEN DISCHARGE

In some ECC systems, nitrogen is rapidly discharged into the primary system when the accumulators empty. The surge of nitrogen into the cold legs and downcomer suppresses steam condensation and pressurizes the downcomer. The increase in downcomer pressure forces water from the downcomer into the core. Increased steam generation in the core and the reduced downcomer water level subsequently lead to a water outsurge from the core, which removes the beneficial core cooling effect.

In a UPTF integral test which included simulation of accumulator nitrogen discharge, the high flow of nitrogen pressurized the downcomer resulting in a surge of water into the core. The core water level increased by 1.5 m; however, due to premature test termination, the peak level was not observed. While core heat transfer was not covered in the test, TRAC PWR analyses indicate the hottest parts of the core are quenched by the surge in core water level.

7.8 RESULTS RELATED TO SBLOCA PHENOMENA

In the reflux condenser mode of core cooling of an SBLOCA, steam generated in the core flows from the reactor vessel through the hot legs to the steam generators countercurrent to condensate flowing back from the steam generators to the upper plenum. UPTF test results indicated uninhibited water runback is expected during reflux condenser conditions of a PWR SBLOCA.

In certain SBLOCA scenarios ECC is injected into water-filled cold legs while the loops are stagnated. If mixing of the ECC and primary coolant is poor, the ECC can "stream" through the cold leg and into downcomer, and potentially cool local regions of the downcomer wall. In UPTF tests, ECC entering the downcomer was significantly warmed by mixing in the cold leg and the resultant plume of cooler water in the downcomer decayed quickly. These results suggest that ECC injection into water-filled cold legs does not cause severe local changes in fluid temperature at the vessel wall which could lead to pressurized thermal shock.

During an SBLOCA in which the core uncovers and heats up at elevated pressure, the high pressure injection system (HPIS) is the only available source of ECC. For PWRs with combined ECC injection, the HPIS injects ECC into the hot legs and delivery to the core is determined by the countercurrent flow limitation at the tie plate. In the UPTF test simulating these phenomena, water downflow through the tie plate was not inhibited by the steam upflow from the core and essentially all ECC injected in the hot legs was delivered to the core.

7.9 CONCLUSIONS

The 2D/3D Program demonstrated the effectiveness of existing ECC systems and quantified the margin associated with traditional, conservative evaluation approaches. Furthermore, the program developed insights into the controlling phenomena, including multidimensional effects, on emergency core cooling. Scaling effects on these phenomena were investigated and quantified.

Section 8

BIBLIOGRAPHY

This bibliography provides a comprehensive listing of reports prepared within the 2D/3D Program and references to supporting material generated outside the 2D/3D Program. Each document is assigned a four character code consisting of a letter and a three-digit number (i.e., A-###). The letter designates the origin of the document and the number indicates the type of document. These codes are defined below.

Letter Prefixes

G	Published by FRG within the 2D/3D Program
J	Published by Japan within the 2D/3D Program
U	Published by US within the 2D/3D Program
E	External to 2D/3D Program

Numbers

001 - 200	Data Reports
201 - 400	Quick Look Reports
401 - 600	Evaluation Reports
601 - 800	Code Analysis Reports
801 - 900	Advanced Instrumentation Reports
901 - 999	Papers, Presentations, and Correspondence

NOTICE: Data generated in the 2D/3D International Program are only for use by authorized users within the restrictions of the 2D/3D Program; consequently, distribution of reports which contain 2D/3D Program test data (i.e., many of the reports listed in this bibliography) is restricted.

REPORTS AND PAPERS PUBLISHED BY FRG WITHIN 2D/3D PROGRAM

DATA REPORTS

UPTF

G-001   2D/3D Program Upper Plenum Test Facility Experimental Data Report, "Test No. 1 Fluid-Fluid Mixing Test," prepared by KWU, R 515/87/09, April 1987.

G-002   2D/3D Program Upper Plenum Test Facility Experimental Data Report, "Test No. 2 US/J PWR Integral Test with Cold Leg ECC Injection," prepared by Siemens/KWU, U9 316/88/5, April 1988.

G-003   2D/3D Program Upper Plenum Test Facility Experimental Data Report, "Test No. 3 GPWR Integral Test 5/8 Combined ECC Injection," prepared by KWU, R 515/87/14, August 1987.

G-004   2D/3D Program Upper Plenum Test Facility Experimental Data Report, "Test No. 4 US/J PWR Integral Test With Cold Leg ECC Injection," prepared by Siemens/KWU, E314/90/004, April 1990.

G-005   2D/3D Program Upper Plenum Test Facility Experimental Data Report, "Test No. 5 Downcomer Separate Effect Test," prepared by KWU, R 515/87/16, September 1987.

G-006   2D/3D Program Upper Plenum Test Facility Experimental Data Report, "Test No. 6 Downcomer Countercurrent Flow Test," prepared by Siemens/KWU, U9 316/88/18, December 1988.

G-007   2D/3D Program Upper Plenum Test Facility Experimental Data Report, "Test No. 7 Downcomer Countercurrent Flow Test," prepared by Siemens/KWU, U9 316/89/14, 1989.

G-008   2D/3D Program Upper Plenum Test Facility Experimental Data Report, "Test No. 8 Cold/Hot Leg Flow Pattern Test," prepared by Siemens/KWU, U9 316/88/12, September 1988.

G-009   2D/3D Program Upper Plenum Test Facility Experimental Data Report, "Test No. 9 Cold/Hot Leg Flow Pattern Test," prepared by Siemens/KWU, U9 316/89/5, February 1989.

G-010   2D/3D Program Upper Plenum Test Facility Experimental Data Report, "Test No. 10 Tie Plate Countercurrent Flow Test," prepared by Siemens/KWU, U9 316/88/1, February 1988.

G-011   2D/3D Program Upper Plenum Test Facility Experimental Data Report, "Test No. 11 Countercurrent Flow in PWR Hot Leg Test," prepared by KWU, R 515/87/10, May 1987.

G-012   2D/3D Program Upper Plenum Test Facility Experimental Data Report, "Test No. 12 Tie Plate Countercurrent Flow Test," prepared by KWU, R 515/86/14, November 1986.

G-013   2D/3D Program Upper Plenum Test Facility Experimental Data Report, "Test No. 13 Tie Plate Countercurrent Flow Test," prepared by KWU, U9 316/87/21, November 1987.

G-014   2D/3D Program Upper Plenum Test Facility Experimental Data Report, "Test No. 14 GPWR Integral Test with 5/8 Combined ECC Injection," prepared by Siemens/KWU, E314/90/15, September 1990.

G-015   2D/3D Program Upper Plenum Test Facility Experimental Data Report, "Test No. 15 Tie Plate Countercurrent Flow Test," prepared by Siemens/KWU, U9 316/88/17, December 1988.

G-016   2D/3D Program Upper Plenum Test Facility Experimental Data Report, "Test No. 16 Tie Plate Countercurrent Flow Test," prepared by Siemens/KWU, E314/89/21, December 1989.

G-017   2D/3D Program Upper Plenum Test Facility Experimental Data Report, "Test No. 17 US/J-PWR Integral Test with Cold Leg ECC Injection," prepared by Siemens/KWU, E314/89/18, November 1989.

G-018   2D/3D Program Upper Plenum Test Facility Experimental Data Report, "Tests No. 18 GPWR Integral Test with 5/8 Combined ECC Injection," prepared by Siemens/KWU, U9 316/89/10, June 1989.

G-019   2D/3D Program Upper Plenum Test Facility Experimental Data Report, "Test No. 19 GPWR Integral Test with 5/8 Combined ECC Injection," prepared by Siemens/KWU, U9 316/89/16, 1989.

G-020   2D/3D Program Upper Plenum Test Facility Experimental Data Report, "Test No. 20 Upper Plenum Injection Simulation Test," prepared by Siemens/KWU, U9 316/88/08, June 1988.

G-021   2D/3D Program Upper Plenum Test Facility Experimental Data Report, "Test No. 21 Downcomer Injection Test," prepared by Siemens/KWU, E314/90/17, October 1990.

G-022   2D/3D Program Upper Plenum Test Facility Experimental Data Report, "Test No. 22 Downcomer Injection Test with Vent Valves," prepared by Siemens/KWU, E314/91/007, March 1991.

G-023   2D/3D Program Upper Plenum Test Facility Experimental Data Report, "Test No. 23 Downcomer Injection Test with Vent Valves," prepared by Siemens/KWU, E314/91/001, January 1991.

G-024   2D/3D Program Upper Plenum Test Facility Experimental Data Report, "Test No. 24 Integral Test with Vent Valves," prepared by Siemens/KWU, E314/90/21, November 1990.

G-025   2D/3D Program Upper Plenum Test Facility Experimental Data Report, "Test No. 25 Downcomer/Cold Leg Steam/Water Interaction Test," prepared by Siemens/KWU, E314/90/11, August 1990.

G-026   2D/3D Program Upper Plenum Test Facility Experimental Data Report, "Test No. 26 Hot Leg Flow Pattern Test," prepared by Siemens/KWU, E314/91/005, February 1991.

G-027   2D/3D Program Upper Plenum Test Facility Experimental Data Report, "Test No. 27 Integral Test with Cold Leg Injection," prepared by Siemens/KWU, E314/90/24, September 1990.

G-028   2D/3D Program Upper Plenum Test Facility Experimental Data Report, "Test No. 28 GPWR Integral Test with 7/8 Combined ECC Injection," prepared by Siemens/KWU, E314/90/07, July 1990.

G-029   2D/3D Program Upper Plenum Test Facility Experimental Data Report, "Test No. 29 Entrainment/De-entrainment Test," prepared by Siemens/KWU, E314/90/05, June 1990.

G-030   2D/3D Program Upper Plenum Test Facility Experimental Data Report, "Test No. 30 Tie Plate Countercurrent Flow Test H-P Injection," prepared by Siemens/KWU, U9 316/89/9, April 1989.

QUICK LOOK REPORTS

G-201   2D/3D Program Upper Plenum Test Facility Quick Look Report, "Test No.
         1 Fluid-Fluid Mixing Test," prepared by KWU, R 515/87/1, January 1987.

G-202   2D/3D Program Upper Plenum Test Facility Quick Look Report, "Test No.
         2 US/J PWR Integral Test with Cold Leg ECC Injection," prepared by
         Siemens/KWU, U9 316/88/2, March 1988.

G-203   2D/3D Program Upper Plenum Test Facility Quick Look Report, "Test No.
         3 GPWR Integral Test with 5/8 Combined ECC Injection," prepared by
         KWU, R 515/87/15, September 1987.

G-204   2D/3D Program Upper Plenum Test Facility Quick Look Report, "Test No.
         4 US/J PWR Integral Test with Cold Leg ECC Injection," prepared by
         Siemens/KWU, E314/90/06, July 1990.

G-205   2D/3D Program Upper Plenum Test Facility Quick Look Report, "Test No.
         5 Downcomer Separate Effect Test," prepared by KWU, U9 316/87/17,
         October 1987.

G-206   2D/3D Program Upper Plenum Test Facility Quick Look Report, "Test No.
         6 Downcomer Countercurrent Flow Test," prepared by Siemens/KWU,
         U9 316/89/2, March 1989.

G-207   2D/3D Program Upper Plenum Test Facility Quick Look Report, "Test No.
         7 Downcomer Countercurrent Flow Test," prepared by Siemens/KWU,
         E314/90/003, March 1990.

G-208   2D/3D Program Upper Plenum Test Facility Quick Look Report, "Test No.
         8 Cold/Hot Leg Flow Pattern Test," prepared by Siemens/KWU,
         U9 316/88/11, September 1988.

G-209   2D/3D Program Upper Plenum Test Facility Quick Look Report, "Test No.
         9 Cold/Hot Leg Flow Pattern Test," prepared by Siemens/KWU,
         U9 316/89/6, March 1989.

G-210   2D/3D Program Upper Plenum Test Facility Quick Look Report, "Test No.
         10 Tie Plate Countercurrent Flow Test," prepared by Siemens/KWU,
         U9 316/88/3, 1988.

G-211   2D/3D Program Upper Plenum Test Facility Quick Look Report, "Test No. 11 Countercurrent Flow in PWR Hot Leg Test," prepared by KWU, R 515/87/08, March 1987.

G-212   2D/3D Program Upper Plenum Test Facility Quick Look Report, "Test No. 12 Tie Plate Countercurrent Flow Test," prepared by KWU, R 515/86/13, October 1986.

G-213   2D/3D Program Upper Plenum Test Facility Quick Look Report, "Test No. 13 Tie Plate Countercurrent Flow Test," prepared by KWU, U9 316/87/22, December 1987.

G-214   2D/3D Program Upper Plenum Test Facility Quick Look Report, "Test No. 14 GPWR Integral Test with 5/8 Combined ECC Injection," prepared by Siemens/KWU, E314/90/14, September 1990.

G-215   2D/3D Program Upper Plenum Test Facility Quick Look Report, "Test No. 15 Tie Plate Countercurrent Flow Test," prepared by Siemens/KWU, U9 316/89/01, February 1989.

G-216   2D/3D Program Upper Plenum Test Facility Quick Look Report, "Test No. 16 Tie Plate Countercurrent Flow Test," prepared by Siemens/KWU, E314/89/22, December 1989.

G-217   2D/3D Program Upper Plenum Test Facility Quick Look Report, "Test No. 17 US/J PWR Integral Test with Cold Leg ECC Injection," prepared by Siemens/KWU, E314/89/20, December 1989.

G-218   2D/3D Program Upper Plenum Test Facility Quick Look Report, "Test No. 18 GPWR Integral Test with 5/8 Combined ECC Injection," prepared by Siemens/KWU, U9 316/89/11, June 1989.

G-219   2D/3D Program Upper Plenum Test Facility Quick Look Report, "Test No. 19 GPWR Integral Test with 5/8 Combined ECC Injection," prepared by Siemens/KWU, U9 316/89/16, October 1989.

G-220   2D/3D Program Upper Plenum Test Facility Quick Look Report, "Test No. 20 Upper Plenum Injection Simulation Test," prepared by Siemens/KWU, U9 316/88/07, June 1988.

G-221   2D/3D Program Upper Plenum Test Facility Quick Look Report, "Test No. 21 Downcomer Injection Test," prepared by Siemens/KWU, E314/90/16, September 1990.

G-222   2D/3D Program Upper Plenum Test Facility Quick Look Report, "Test No. 22 Downcomer Injection Test with Vent Valves," prepared by Siemens/KWU, E314/91/008, March 1991.

G-223   2D/3D Program Upper Plenum Test Facility Quick Look Report, "Test No. 23 Downcomer Injection Test with Vent Valves," prepared by Siemens/KWU, E314/90/25, December 1990.

G-224   2D/3D Program Upper Plenum Test Facility Quick Look Report, "Test No. 24 Integral Test with Vent Valves," prepared by Siemens/KWU, E314/90/22, September 1990.

G-225   2D/3D Program Upper Plenum Test Facility Quick Look Report, "Test No. 25 Downcomer/Cold Leg Steam/Water Interaction Test," prepared by Siemens/KWU, E314/90/13, September 1990.

G-226   2D/3D Program Upper Plenum Test Facility Quick Look Report, "Test No. 26 Hot Leg Flow Pattern Test," prepared by Siemens/KWU, E314/91/003, February 1991.

G-227   2D/3D Program Upper Plenum Test Facility Quick Look Report, "Test No. 27 US/J PWR Integral Test with Cold Leg ECC Injection," prepared by Siemens/KWU, E314/90/26, December 1990.

G-228   2D/3D Program Upper Plenum Test Facility Quick Look Report, "Test No. 28 GPWR Integral Test with 7/8 Combined ECC Injection," prepared by Siemens/KWU, E314/90/08, September 1990.

G-229   2D/3D Program Upper Plenum Test Facility Quick Look Report, "Test No. 29 Entrainment/De-entrainment Test," prepared by Siemens/KWU, E314/90/19, November 1990.

G-230   2D/3D Program Upper Plenum Test Facility Quick Look Report, "Test No. 30 Tie Plate Countercurrent Flow Test HP-Injection," prepared by Siemens/KWU, E314/89/22, December 1989.

EVALUATION REPORTS

SCTF

G-401   Pointner, W., "Empirical Equation for the Entrainment in SCTF-III," Gesellschaft fuer Reaktorsicherheit, GRS-A-1404, January 1988.

UPTF

G-411   UPTF Summary Report (to be published).

G-412   2D/3D Program Upper Plenum Test Facility, "UPTF: Program and System Description," prepared by Siemens/KWU, U9 414/88/023, November 1988.

G-413   2D/3D Program Upper Plenum Test Facility, "Work Report: UPTF Test Instrumentation," prepared by KWU, R 515/85/23, September 1985.

G-414   Gehrmann, R., "Input to Test Objectives and Conditions for the UPTF Vent Valve Test No. 24 (Integral Test)," ASEA-Brown Boveri, ABB Technical Report No. GBRA 012023, June 6, 1989.

G-415   Glaeser, H., "Downcomer and Upper Tie Plate Countercurrent Flow in the Upper Plenum Test Facility," Gesellschaft fuer Reaktorsicherheit, GRS-A-1726, November 1990.

CODE ANALYSIS REPORTS

Karlstein Tests

G-601   Glaeser, H., and Schertel, H., "Analyses Der Karlstein-Dampf-Wasser-Gegenstromungsexperimente Mit TRAC-PF1 (11.1)," Gesellschaft fuer Reaktorsicherheit, GRS-A-1179, January 1986.

G-602   Glaeser, H., "Analysis of the Karlstein Saturated Water Tests on Steam-Water-Countercurrent Flow Using the Computer Code TRAC-PF1 (11.1, 12.5)," Gesellschaft fuer Reaktorsicherheit, GRS-A-1249, July 1986.

CCTF Tests

G-611   Krey, L.,"Post Test Calculation of CCTF Test C2-20, Run 80 with the Code System ATHLET/FLUT No. 8A," Technischer Ueberwachungs-Verein Bayern e.V., Muenchen, October 1991.

SCTF Tests

G-621   Schwarz, S., "SCTF Vent Valve Test S3-17 (Run 721) BBR Coupling Test Comparison to the TRAC Reactor Analysis," Gesellschaft fuer Reaktorsicherheit, GRS-A-1471, July 1988.

G-622   Thiele, T.H., "Post Test Calculation of SCTF S3-11 (715) using FLUT No. 6A," Pitscheider Report No. 9027, April 1990.

UPTF Tests -- Pre-test Conditioning Calculations

G-631   Schwarz, S., "UPTF - Konditionierungsrechung Für ABB Vent Valve Tests Datensatz, Erfahrung und Endergebnis," Gesellschaft fuer Reaktorsicherheit, GRS-A-1621, October 1989.

UPTF Test -- Post-test Analyses

G-641   Riegel, B., "Post Test Calculation of UPTF Test 8 with the Advanced Computer Code TRAC-PF1/MOD1," Gesellschaft fuer Reaktorsicherheit, GRS-A-1666, May 1990.

G-642   Riegel, B., "Post Test Calculation of UPTF Test 9 with the Advanced Computer Code TRAC-PF1/MOD1," Gesellschaft fuer Reaktorsicherheit, GRS-A-1738, December 1990.

G-643   Sonnenburg, H.G., "Analysis of UPTF 11 (Hot Leg CCF) with a Full-Range Drift Flux Model," Gesellschaft fuer Reaktorsicherheit, GRS-A-1681, June 1990.

G-644   Glaeser, H., "Post Test Calculations of UPTF Test 12 with the Advanced Computer Code TRAC-PF1/MOD1," Gesellschaft fuer Reaktorsicherheit, GRS-A-1727, November 1990.

G-645   Glaeser, H., "Post Test Calculation of UPTF Test 13 with the Advanced Computer Code TRAC-PF1/MOD1," Gesellschaft fuer Reaktorsicherheit, GRS-A-1728, November 1990.

G-646   Sonnenburg, H.G., "Analysis of UPTF - Test 26 Run 230 by ATHLET Code with Full-Range Drift Flux Model," Gesellschaft fuer Reaktorsicherheit, GRS-A-1723, October 1990.

G-647   Hora, A., and Teschendorff, V., "Post Test Calculation of UPTF Test 5B with the Computer Code FLUT," Gesellschaft fuer Reaktorsicherheit, GRS-A-1798, June 1991.

G-648   Gasteiger, H., "Post Test Calculation of UPTF Test 18 with the Code System ATHLET/FLUT," Teschnischer Ueberwachungs-Verein Bayern e.V., Muenchen, June 1991.

G-649   Thiele, T.H., "Post Test Calculation of UTPF Test No. 20 using Code System ATHLET/MOD 1.0-Cycle C," Pitscheider Report No. 9058, December 18, 1990.

G-650   Thiele, T.H., "Post Test Calculation of UPTF Test 29A using Code System ATHLET-FLUT, Version No. 8," Pitscheider Report No. 9055, November 13, 1990.

GPWR Analyses

G-661   Riegel, B., "Calculation of a Double Ended Break in the Cold Leg of the Primary Coolant Loop of a German Pressurized Water Reactor with a 5/8 Emergency Cooling Injection (Calculated with TRAC-PF1/MOD1 (Version 12.5))," Gesellschaft fuer Reaktorsicherheit, GRS-A-1322, February 1987.

G-662   Schwarz,S., "GPWR Analysis with TRAC PF1/MOD1 Version 12.5 BBR Type Reactor, 200% Cold Leg Pump Discharge Break EM-Conditions," Gesellschaft fuer Reaktorsicherheit, GRS-A-1403, January 1988.

G-663   Hrubisko, M., "Calculation of a Double Ended Break in the Hot Leg of the Primary Coolant Loop of a German Pressurized Water Reactor with a 5/8 Emergency Coolant Injection (Calculated with TRAC-PF1/MOD1 Version 12.5)," Gesellschaft fuer Reaktorsicherheit, GRS-A-1771, April 1991.

G-664   Gasteiger, H., "Calculation of a Double Ended Break in the Cold Leg of the Primary Coolant Loop of a German Pressurized Water Reactor (GPWR) with the Code System ATHLET/FLUT," Technischer Ueberwachungs-Verein Bayern e.V., Muechen, December 1990.

ADVANCED INSTRUMENTATION REPORTS

G-801   Mewes, D., Laake, H.J., and Spatz, R., "Fluid Dynamic Effects in the Area of the Tie Plate and the Spacer of the Fuel Elements Installed in Pressurized Water Reactors," Institute for Process Technology, University of Hanover, March 1985.

G-802   "Calibration of the UPTF Tie Plate Flow Module with 'Advanced Instrumentation' and Investigation of the Function from the Core Simulator Feed Back Control System with Break-Thru-Detectors," prepared by KWU, R 917/86/002, April 1986.

G-803   Hampel, G., et. al., "Final Report on the 'Advanced Instrumentation' Study-2D/3D Project," Battelle-Frankfurt Institute, BF-R-64.525.2.

G-804   "UPTF-Instrumentation Control Document," Revision 1, prepared by KWU, April 1984.

G-805   Emmerling R., "Proposal for UPTF Tie-plate Mass Flow Algorithm," KWU/R152, May 1984.

G-806   Emmerling, R., "Computer Program for the Determination of Steam/Water Mass Flow Rates through the Tie Plate," KWU, R15-85-e1021, December 1985.

G-807   Gaul, H.P., "Status of UPTF Advanced Instrumentation and Systems Failure Time History," KWU Work-Report R515/86/10, July 30, 1986.

G-808   Gaul, H.P., and Hein, K.H., "UPTF Experiment: US Advanced Instrumentation und Datenerfassungsanlage; Zusammenfassung der bearbeiteten Probleme fuer den Zeitraum- Februar 1985 - Januar 1986," Arbeits-Bericht R515/86/6, March 5, 1986.

G-809   Gaul, H.P., and Wandzilak, L., "Ueberpruefung des PFM Algorithmus mit Dummy Daten und Versuchsrechnungen," Arbeits-Bericht U9 316/88/16, September 27, 1988.

G-810   Gaul, H.P., and Schulz, N., Beschreibung der beim UPTF Pipe Flow Meter aufgetretenen Hardwareprobleme und durchgefuehrte Modifikationen an der Hardware," Arbeits-Bericht U9 316/88/10, June 20, 1988.

PAPERS, PRESENTATIONS, AND CORRESPONDENCE

Papers - Data Evaluation

G-901   Kroening, H., Hawighorst, A., and Mayinger, F., "The Influence of Flow Restrictions on the Countercurrent Flow Behavior in the Fuel-Element Top Nozzle Area," European Two-phase Flow Group Meeting, Paris-La-Defence, June 2-4, 1982.

G-902   Weiss, P., Sawitzki, M., and Winkler, F., "UPTF, a Full-scale PWR Loss-of-Coolant Accident Experiment Program," Atomkernenergie Kerntechnik Vol. 49 (1986), No. 1/2.

G-903   Hertlein, P.J., and Weiss, P.A., "UPTF Test Results - First Downcomer CCF Test," Proceedings of the Fifteenth Water Reactor Safety Information Meeting, October 26-29, 1987, NUREG/CP-0091, Volume 4, pp. 533-547.

G-904   Weiss, P.A., "UPTF Experiment - Principal Experimental Results to be used for Improved LB LOCA Understanding," Proceedings of the Sixteenth Water Reactor Safety Research Information Meeting, October 24-28, 1988, NUREG/CP-0097, Volume 4, pp. 543-555.

G-905   Weiss, P., Watzinger, H., and Hertlein, R., "UPTF Experiment - A Synopsis of Full-Scale Test Results," presented at The Third International Topical Meeting on Nuclear Power Plant Thermal-Hydraulics and Operations, Seoul, Korea, November 14-17, 1988.

G-906   Glaeser, H., "Analysis of Downcomer and Tie Plate Countercurrent Flow in the Upper Plenum Test Facility (UPTF)," presented at the Fourth International Topical Meeting on Nuclear Reactor Thermal-Hydraulics, Karlsruhe, FRG, October 10-13, 1989.

G-907   Liebert, J., and Weiss, P., "UPTF-Experiment - Effect of Full-Scale Geometry on Countercurrent Flow Behaviors in PWR Downcomer," presented at the Fourth International Topical Meeting on Nuclear Reactor Thermal-Hydraulics, Karlsruhe, FRG, October 10-13, 1989.

G-908   Weiss, P., "UPTF-Experiment - Principal Full-Scale Test Results for Enhanced Knowledge of Large Break LOCA Scenarios in PWRs," presented at the Fourth International Topical Meeting on Nuclear Reactor Thermal-Hydraulics, Karlsruhe, FRG, October 10-13, 1989.

G-909   Winkler, F., and Krebs, W., "Impact of 2D/3D Project on LOCA Licensing Analysis and Reactor Safety of PWRs," presented at the Fourth International Topical Meeting on Nuclear Reactor Thermal-Hydraulics, Karlsruhe, FRG, October 10-13, 1989.

G-910   Weiss, P., "UPTF-Experiment - Full-Scale Test on Large Break LOCA Thermal-Hydraulic Scenarios in PWR: Status & Findings," Proceedings of the Seventeenth Water Reactor Safety Research Information Meeting, October 22-25, 1989.

G-911   Emmerling, R., and Weiss, P., "UPTF-Experiment - Analysis of Flow Pattern in Pipes of Large Diameter with Subcooled Water Injection," presented at the European Two-Phase Flow Group Meeting, Paris, France, May 29-June 1, 1989.

8-12

G-912   "PWRs with Cold Leg or Combined ECC Injection -- Synopsis of Test Results," Handout G-2 from 2D/3D Coordination Meeting, Tokai-Mura, Japan, May 21-25, 1990.

G-913   Weiss, P.A., and Hertlein, R.J., "UPTF Test Results: First Three Separate Effects Tests," Nuclear Engineering and Design, Vol. 108, No. 1/2, pp. 249-263 (1988).

G-914   Weiss, P., Watzinger, H., and Hertlein, R., "UPTF Experiment: A Synopsis of Full Scale Test Results," Nuclear Engineering and Design, Vol. 122, No. 1, pp. 219-234 (1990). (Also see G-905.)

G-915   Glaeser, H., "Downcomer and Tie Plate Countercurrent Flow in the Upper Plenum Test Facility (UPTF)," Nuclear Engineering and Design, Vol. 133, pp. 259-283 (1992).

Papers - Code Analysis

G-921   Puetter, B., "50% Cold Leg Break in KWU Plant," presented at 2D/3D Coordination Meeting, Mannheim, FRG, June 18, 1985.

G-922   Plank, H., "Analyses of a Double-Ended Cold Leg Break of a 1300 MW KWU-PWR with TRAC-PF1/MOD1 (12.5)," presented at 2D/3D Analysis Meeting, Erlangen, FRG, June 5-13, 1986.

G-923   Riegel, B., Plank, H., Liesch, K., "Multidimensional Representation of GPWR Primary System in 200% LOCA Calculation," Proceedings of the Fourteenth Water Reactor Safety Information Meeting, October 27-30, 1986, NUREG/CP-0082, Volume 4, pp. 499-521.

G-924   Sonnenburg, H.G., "Analysis of UPTF Test 11 (Hot Leg CCF) with Full-Range Drift-Flux Model," Proceedings of the Fifteenth Water Reactor Safety Information Meeting, October 26-29, 1987, NUREG/CP-0091, Volume 4, pp. 585-607.

G-925   Hertlein, R., and Herr, W., "A New Model for Countercurrent Flow in the Upper Part of a PWR Core," presented at the Fourth International Topical Meeting on Nuclear Reactor Thermal-Hydraulics, Karlsruhe, FRG, October 10-13, 1989.

REPORTS AND PAPERS PUBLISHED BY JAERI WITHIN 2D/3D PROGRAM

DATA REPORTS

CCTF Core-I

J-001   "Data Report on Large Scale Reflood Test-1 -- CCTF Shakedown Test C1-SH1 (Run 005)," prepared by Japan Atomic Energy Research Institute, JAERI-Memo-8795, February 1980.

J-002   "Data Report on Large Scale Reflood Test-2 -- CCTF Shakedown Test C1-SH2 (Run 006)," prepared by Japan Atomic Energy Research Institute, JAERI-Memo-8797, February 1980

J-003   "Data Report on Large Scale Reflood Test-3 -- CCTF Shakedown Test C1-SH3 (Run 007)," prepared by Japan Atomic Energy Research Institute, JAERI-Memo-8931, June 1980.

J-004   "Data Report on Large Scale Reflood Test-4 -- CCTF Shakedown Test C1-SH4 (Run 008)," prepared by Japan Atomic Energy Research Institute, JAERI-Memo-8932, June 1980.

J-005   "Data Report on Large Scale Reflood Test-5 -- CCTF Shakedown Test C1-SH5 (Run 009)," prepared by Japan Atomic Energy Research Institute, JAERI-Memo-8933, June 1980.

J-006   "Data Report on Large Scale Reflood Test-10 -- CCTF C1-1 (Run 010)," prepared by Japan Atomic Energy Research Institute, JAERI-Memo-9997, March 1982.

J-007   "Data Report on Large Scale Reflood Test-11 -- CCTF Test C1-2 (Run 011)," prepared by Japan Atomic Energy Research Institute, JAERI-Memo-57-156, July 1982.

J-008   "Data Report on Large Scale Reflood Test-12 -- CCTF Test C1-3 (Run 012)," prepared by Japan Atomic Energy Research Institute, JAERI-Memo-57-175, July 1982.

J-009   "Data Report on Large Scale Reflood Test-13 -- CCTF Test C1-4 (Run 013)," prepared by Japan Atomic Energy Research Institute, JAERI-Memo-57-210, August 1982.

J-010   "Data Report on Large Scale Reflood Test-14 -- CCTF Test C1-5 (Run 014)," prepared by Japan Atomic Energy Research Institute, JAERI-Memo-57-214, August 1982.

J-011   "Data Report on Large Scale Reflood Test-15 -- CCTF Test C1-6 (Run 015)," prepared by Japan Atomic Energy Research Institute, JAERI-Memo-57-239, September 1982.

J-012   "Data Report on Large Scale Reflood Test-19 -- CCTF Test C1-7 (Run 016)," prepared by Japan Atomic Energy Research Institute, JAERI-Memo-57-343, November 1982.

J-013   "Data Report on Large Scale Reflood Test-20 -- CCTF Test C1-8 (Run 017)," prepared by Japan Atomic Energy Research Institute, JAERI-Memo-57-349, November 1982.

J-014   "Data Report on Large Scale Reflood Test-27 -- CCTF Test C1-9 (Run 018)," prepared by Japan Atomic Energy Research Institute, JAERI-Memo-57-373, July 1982.

J-015   "Data Report on Large Scale Reflood Test-36 -- CCTF Test C1-10 (Run 019)," prepared by Japan Atomic Energy Research Institute, JAERI-Memo-58-063, March 1983.

J-016   "Data Report on Large Scale Reflood Test-37 -- CCTF Test C1-11 (Run 020)," prepared by Japan Atomic Energy Research Institute, JAERI-Memo-58-064, March 1983.

J-017   "Data Report on Large Scale Reflood Test-38 -- CCTF Test C1-12 (Run 021)," prepared by Japan Atomic Energy Research Institute, JAERI-Memo-58-065, March 1983.

J-018   "Data Report on Large Scale Reflood Test-53 -- CCTF Test C1-13 (Run 022)," prepared by Japan Atomic Energy Research Institute, JAERI-Memo-59-031, February 1984.

J-019   "Data Report on Large Scale Reflood Test-54 -- CCTF Test C1-14 (Run 023)," prepared by Japan Atomic Energy Research Institute, JAERI-Memo-59-032, February 1984.

J-020   "Data Report on Large Scale Reflood Test 55 -- CCTF Test C1-15 (Run 024)," prepared by Japan Atomic Energy Research Institute, JAERI-Memo-59-033, February 1984.

J-021   "Data Report on Large Scale Reflood Test-56 -- CCTF Test C1-16 (Run 025)," prepared by Japan Atomic Energy Research Institute, JAERI-Memo-59-034, February 1984.

J-022   "Data Report on Large Scale Reflood Test-57 -- CCTF Test C1-17 (Run 036)," prepared by Japan Atomic Energy Research Institute, JAERI-Memo-59-035, February 1984.

J-023   "Data Report on Large Scale Reflood Test-58 -- CCTF Test C1-18 (Run 037)," prepared by Japan Atomic Energy Research Institute, JAERI-Memo-59-036, February 1984.

J-024   "Data Report on Large Scale Reflood Test-59 -- CCTF Test C1-19 (Run 038)," prepared by Japan Atomic Energy Research Institute, JAERI-Memo-59-037, February 1984.

J-025   "Data Report on Large Scale Reflood Test-60 -- CCTF Test C1-20 (Run 039)," prepared by Japan Atomic Energy Research Institute, JAERI-Memo-59-038, February 1984.

J-026   "Data Report on Large Scale Reflood Test-61 -- CCTF Test C1-21 (Run 040)," prepared by Japan Atomic Energy Research Institute, JAERI-Memo-59-039, February 1984.

J-027   "Data of CCTF Test C1-11 (Run 20), C1-19 (Run 38), and C1-20 (Run 039): Spool Piece Data," prepared by Japan Atomic Energy Research Institute, January 17, 1983.

J-028   "Data Report on Large Scale Reflood Test-62 -- CCTF Test C1-22 (Run 041)," prepared by Japan Atomic Energy Research Institute, JAERI-Memo-59-040, March 1984.

CCTF Core-II

J-041   "Data Report on Large Scale Reflood Test-40 -- CCTF Core-II Test C2-AC1 (Run 051)," prepared by Japan Atomic Energy Research Institute, JAERI-Memo-58-150 May 1983.

J-042   "Data Report on Large Scale Reflood Test-41 -- CCTF Core-II Test C2-AC2 (Run 052)," prepared by Japan Atomic Energy Research Institute, JAERI-Memo-58-154, May 1983.

J-043   "Data Report on Large Scale Reflood Test-42 -- CCTF Core-II Shakedown Test C2-SH1 (Run 053)," prepared by Japan Atomic Energy Research Institute, JAERI-Memo-58-166, May 1983.

J-044   "Data Report on Large Scale Reflood Test-43 -- CCTF Core-II Shakedown Test C2-SH2 (Run 054)," prepared by Japan Atomic Energy Research Institute, JAERI-Memo-58-155, May 1983.

J-045   "Data Report on Large Scale Reflood Test-44 -- CCTF Test C2-1 (Run 055)," prepared by Japan Atomic Energy Research Institute, JAERI-Memo-58-156, May 1983.

J-046   "Data Report on Large Scale Reflood Test-45 -- CCTF Core-II Test C2-2 (Run 056)," prepared by Japan Atomic Energy Research Institute, JAERI-Memo-58-157, May 1983.

J-047   "Data Report on Large Scale Reflood Test-77 -- CCTF Core-II Test C2-AA1 (Run 057)," prepared by Japan Atomic Energy Research Institute, JAERI-Memo-59-445, February 1985.

J-048   "Data Report on Large Scale Reflood Test-78 -- CCTF Core-II Test C2-AA2 (Run 058)," prepared by Japan Atomic Energy Research Institute, JAERI-Memo-59-446, February 1985.

J-049   "Data Report on Large Scale Reflood Test-79 -- CCTF Core-II Test C2-AS1 (Run 059)," prepared by Japan Atomic Energy Research Institute, JAERI-Memo-59-447, February 1985.

J-050   "Data Report on Large Scale Reflood Test-80 -- CCTF Core-II Test C2-AS2 (Run 060)," prepared by Japan Atomic Energy Research Institute, JAERI-Memo-59-448, February 1985.

J-051   "Data Report on Large Scale Reflood Test-81 -- CCTF Core-II Test C2-3 (Run 061)," prepared by Japan Atomic Energy Research Institute, JAERI-Memo-59-449, February 1985.

J-052   "Data Report on Large Scale Reflood Test-82 -- CCTF Core-II Test C2-4 (Run 062)," prepared by Japan Atomic Energy Research Institute, JAERI-Memo-59-450, February 1985.

J-053   "Data Report on Large Scale Reflood Test-83 -- CCTF Core-II Test C2-5 (Run 063)," prepared by Japan Atomic Energy Research Institute, JAERI-Memo-59-451, February 1985.

J-054   "Data Report on Large Scale Reflood Test-84 -- CCTF Core-II Test C2-6 (Run 064)," prepared by Japan Atomic Energy Research Institute, JAERI-Memo-59-452, February 1985.

J-055   "Data Report on Large Scale Reflood Test-85 -- CCTF Core-II Test C2-7 (Run 065)," prepared by Japan Atomic Energy Research Institute, JAERI-Memo-59-467, February 1985.

J-056   "Data Report on Large Scale Reflood Test-86 -- CCTF Core-II Test C2-8 (Run 067)," prepared by Japan Atomic Energy Research Institute, JAERI-Memo-59-453, February 1985.

J-057   "Data Report on Large Scale Reflood Test-87 -- CCTF Core-II Test C2-9 (Run 068)," prepared by Japan Atomic Energy Research Institute, JAERI-Memo-59-454, February 1985.

J-058   "Data Report on Large Scale Reflood Test-88 -- CCTF Core-II Test C2-10 (Run 069)," prepared by Japan Atomic Energy Research Institute, JAERI-Memo-59-455, February 1985.

J-059   "Data Report on Large Scale Reflood Test-89 -- CCTF Core-II Test C2-11 (Run 070)," prepared by Japan Atomic Energy Research Institute, JAERI-Memo-60-011, February 1985.

J-060   "Data Report on Large Scale Reflood Test-95 -- CCTF Core-II Test C2-12 (Run 071)," prepared by Japan Atomic Energy Research Institute, JAERI-Memo-60-172, July 1985.

J-061   "Data Report on Large Scale Reflood Test-96 -- CCTF Core-II Test C2-13 (Run 072)," prepared by Japan Atomic Energy Research Institute, JAERI-Memo-60-157, July 1985.

J-062   "Data Report on Large Scale Reflood Test-97 -- CCTF Core-II Test C2-14 (Run 074)," prepared by Japan Atomic Energy Research Institute, JAERI-Memo-60-173, July 1985.

J-063   "Data Report on Large Scale Reflood Test-98 -- CCTF Core-II Test C2-15 (Run 075)," prepared by Japan Atomic Energy Research Institute, JAERI-Memo-60-191, August 1985.

J-064   "Data Report on Large Scale Reflood Test-99 -- CCTF Core-II Test C2-16 (Run 076)," prepared by Japan Atomic Energy Research Institute, JAERI-Memo-60-158, February 1985.

J-065   "Data Report on Large Scale Reflood Test-100 -- CCTF Core-II Test C2-17 (Run 077)," prepared by Japan Atomic Energy Research Institute, JAERI-Memo-61-143, April 1986.

J-066   "Data Report on Large Scale Reflood Test-101 -- CCTF Core-II Test C2-18 (Run 078)," prepared by Japan Atomic Energy Research Institute, JAERI-Memo-60-223, August 1985.

J-067   "Data Report on Large Scale Reflood Test-128 -- CCTF Core-II Test C2-19 (Run 079)," prepared by Japan Atomic Energy Research Institute, JAERI-Memo-63-081, March 1988.

J-068   "Data Report on Large Scale Reflood Test-129 -- CCTF Core-II Test C2-20 (Run 080)," prepared by Japan Atomic Energy Research Institute, JAERI-Memo-63-082, March 1988.

J-069   "Data Report on Large Scale Reflood Test-130 -- CCTF Core-II Test C2-21 (Run 081)," prepared by Japan Atomic Energy Research Institute, JAERI-Memo-63-083, March 1988.

J-070   "Data Report on Major Experimental Results from CCTF Tests," prepared by Japan Atomic Energy Research Institute, JAERI-Memo-01-014.

SCTF Core-I

J-081   "Data Report on Large Scale Reflood Test-6 -- SCTF Test S1-SH1 (Run 505)," prepared by Japan Atomic Energy Research Institute, JAERI-Memo-9939, February 1982.

J-082   "Data Report on Large Scale Reflood Test-7 -- SCTF Test S1-SH2 (Run 506)," prepared by Japan Atomic Energy Research Institute, JAERI-Memo-9975, March 1982.

J-083   "Data Report on Large Scale Reflood Test-8 -- SCTF Test S1-01 (Run 507)," prepared by Japan Atomic Energy Research Institute, JAERI-Memo-9976, March 1982.

J-084   "Data Report on Large Scale Reflood Test-9 -- SCTF Test S1-02 (Run 508)," prepared by Japan Atomic Energy Research Institute, JAERI-Memo-9977, March 1982.

J-085   "Data Report on Large Scale Reflood Test-16 -- SCTF Test S1-03 (Run 509)," prepared by Japan Atomic Energy Research Institute, JAERI-Memo-57-318, November 1982.

J-086   "Data Report on Large Scale Reflood Test-17 -- SCTF Test S1-04 (Run 510)," prepared by Japan Atomic Energy Research Institute, JAERI-Memo-57-319, November 1982.

J-087   "Data Report on Large Scale Reflood Test-18 -- SCTF Test S1-05 (Run 511)," prepared by Japan Atomic Energy Research Institute, JAERI-Memo-57-320, November 1982.

J-088   "Data Report on Large Scale Reflood Test-21 -- SCTF Test S1-06 (Run 512)," prepared by Japan Atomic Energy Research Institute, JAERI-Memo-57-350, November 1982.

J-089   "Data Report on Large Scale Reflood Test-22 -- SCTF Test S1-07 (Run 513)," prepared by Japan Atomic Energy Research Institute, JAERI-Memo-57-351, November 1982.

J-090   "Data Report on Large Scale Reflood Test-23 -- SCTF Test S1-08 (Run 514)," prepared by Japan Atomic Energy Research Institute, JAERI-Memo-57-354, November 1982.

J-091   "Data Report on Large Scale Reflood Test-24 -- SCTF Test S1-09 (Run 515)," prepared by Japan Atomic Energy Research Institute, JAERI-Memo-57-355, November 1982.

J-092   "Data Report on Large Scale Reflood Test-25 -- SCTF Test S1-10 (Run 516)," prepared by Japan Atomic Energy Research Institute, JAERI-Memo-57-365, December 1982.

J-093   "Data Report on Large Scale Reflood Test-26 -- SCTF Test S1-11 (Run 517)," prepared by Japan Atomic Energy Research Institute, JAERI-Memo-57-372, December 1982.

J-094   "Data Report on Large Scale Reflood Test-28 -- SCTF Test S1-12 (Run 518)," prepared by Japan Atomic Energy Research Institute, JAERI-Memo-57-380, December 1982.

J-095   "Data Report on Large Scale Reflood Test-33 -- SCTF Test S1-13 (Run 519)," prepared by Japan Atomic Energy Research Institute, JAERI-Memo-57-401, December 1982.

J-096   "Data Report on Large Scale Reflood Test-29 -- SCTF Test S1-14 (Run 520)," prepared by Japan Atomic Energy Research Institute, JAERI-Memo-57-381, December 1982.

J-097   "Data Report on Large Scale Reflood Test-30 -- SCTF Test S1-15 (Run 521)," prepared by Japan Atomic Energy Research Institute, JAERI-Memo-57-382, December 1982.

J-098   "Data Report on Large Scale Reflood Test-31 -- SCTF Test S1-16 (Run 522)," prepared by Japan Atomic Energy Research Institute, JAERI-Memo-57-384, December 1982.

J-099   "Data Report on Large Scale Reflood Test-32 -- SCTF Test S1-17 (Run 523)," prepared by Japan Atomic Energy Research Institute, JAERI-Memo-57-385, December 1982.

J-100   "Data Report on Large Scale Reflood Test-34 -- SCTF Test S1-18 (Run 524)," prepared by Japan Atomic Energy Research Institute, JAERI-Memo-57-402, December 1982.

J-101   "Data Report on Large Scale Reflood Test-35 -- SCTF Test S1-19 (Run 525)," prepared by Japan Atomic Energy Research Institute, JAERI-Memo-57-403, December 1982.

J-102   "Data Report on Large Scale Reflood Test-46 -- SCTF Test S1-SH3 (Run 528)," prepared by Japan Atomic Energy Research Institute, JAERI-Memo-58-296, September 1983.

J-103   "Data Report on Large Scale Reflood Test-47 -- SCTF Test S1-SH4 (Run 529)," prepared by Japan Atomic Energy Research Institute, JAERI-Memo-58-297, September 1983.

J-104   "Data Report on Large Scale Reflood Test-48 -- SCTF Test S1-20   (Run 530)," prepared by Japan Atomic Energy Research Institute, JAERI-Memo-58-298, September 1983.

J-105   "Data Report on Large Scale Reflood Test-49 -- SCTF Test S1-21 (Run 531)," prepared by Japan Atomic Energy Research Institute, JAERI-Memo-58-311, September 1983.

J-106   "Data Report on Large Scale Reflood Test-50 -- SCTF Test S1-22   (Run 532)," prepared by Japan Atomic Energy Research Institute, JAERI-Memo-58-299, September 1983.

J-107   "Data Report on Large Scale Reflood Test-51 -- SCTF Test S1-23   (Run 536)," prepared by Japan Atomic Energy Research Institute, JAERI-Memo-58-300, September 1983.

J-108 "Data Report on Large Scale Reflood Test-52 -- SCTF Test S1-24   (Run 537)," prepared by Japan Atomic Energy Research Institute, JAERI-Memo-58-301, September 1983.

SCTF Core-II

J-121 "Data Report on Large Scale Reflood Test-63 -- SCTF Test S2-AC1 (Run 601)," prepared by Japan Atomic Energy Research Institute, JAERI-Memo-59-280, September 1984.

J-122 "Data Report on Large Scale Reflood Test-64 -- SCTF Test S2-AC2 (Run 602)," prepared by Japan Atomic Energy Research Institute, JAERI-Memo-59-281, September 1984.

J-123 "Data Report on Large Scale Reflood Test-65 -- SCTF Test S2-AC3 (Run 603)," prepared by Japan Atomic Energy Research Institute, JAERI-Memo-59-286, September 1984.

J-124 "Data Report on Large Scale Reflood Test-66 -- SCTF Test S2-SHI (Run 604)," prepared by Japan Atomic Energy Research Institute, JAERI-Memo-59-282, September 1984.

J-125 "Data Report on Large Scale Reflood Test-67 -- SCTF Test S2-SH2 (Run 605)," prepared by Japan Atomic Energy Research Institute, JAERI-Memo-59-287, September 1984.

J-126 "Data Report on Large Scale Reflood Test-68 -- SCTF Test S2-01 (Run 606)," prepared by Japan Atomic Energy Research Institute, JAERI-Memo-59-288, September 1984.

J-127 "Data Report on Large Scale Reflood Test-69 -- SCTF Test S2-02 (Run 607)," prepared by Japan Atomic Energy Research Institute, JAERI-Memo-59-283, September 1984.

J-128 "Data Report on Large Scale Reflood Test-70 -- SCTF Test S2-03   (Run 608)," prepared by Japan Atomic Energy Research Institute, JAERI-Memo-59-432, January 1985.

J-129 "Data Report on Large Scale Reflood Test-71 -- SCTF Test S2-04   (Run 609)," prepared by Japan Atomic Energy Research Institute, JAERI-Memo-59-433, January 1985.

J-130   "Data Report on Large Scale Reflood Test-72 -- SCTF Test S2-05 (Run 610)," prepared by Japan Atomic Energy Research Institute, JAERI-Memo-59-434, February 1985.

J-131   "Data Report on Large Scale Reflood Test-73 -- SCTF Test S2-06 (Run 611)," prepared by Japan Atomic Energy Research Institute, JAERI-Memo-59-435, February 1985.

J-132   "Data Report on Large Scale Reflood Test-74 -- SCTF Test S2-07 (Run 612)," prepared by Japan Atomic Energy Research Institute, JAERI-Memo-59-436, February 1985.

J-133   "Data Report on Large Scale Reflood Test-75 -- SCTF Test S2-08 (Run 613)," prepared by Japan Atomic Energy Research Institute, JAERI-Memo-59-437, February 1985.

J-134   "Data Report on Large Scale Reflood Test-76 -- SCTF Test S2-09 (Run 614)," prepared by Japan Atomic Energy Research Institute, JAERI-Memo-59-438, February 1985.

J-135   "Data Report on Large Scale Reflood Test-90 -- SCTF Test S2-10   (Run 615)," prepared by Japan Atomic Energy Research Institute, JAERI-Memo-60-110, May 1985.

J-136   "Data Report on Large Scale Reflood Test-91 -- SCTF Test S2-11   (Run 616)," prepared by Japan Atomic Energy Research Institute, JAERI-Memo-60-111, May 1985.

J-137   "Data Report on Large Scale Reflood Test-92 -- SCTF Test S2-12 (Run 617)," prepared by Japan Atomic Energy Research Institute, JAERI-Memo-60-112, May 1985.

J-138   "Data Report on Large Scale Reflood Test-93 -- SCTF Test S2-13 (Run 618)," prepared by Japan Atomic Energy Research Institute, JAERI-Memo-60-113, May 1985.

J-139   "Data Report on Large Scale Reflood Test-94 - SCTF Test S2-14 (Run 619)," prepared by Japan Atomic Energy Research Institute, JAERI-Memo-60-114, May 1985.

J-140   "Data Report on Large Scale Reflood Test-99 -- SCTF Test S2-15 (Run 620)," prepared by Japan Atomic Energy Research Institute, JAERI-Memo-60-258, October 1985.

J-141   "Data Report on Large Scale Reflood Test-100 -- SCTF Test S2-16 (Run 621)," prepared by Japan Atomic Energy Research Institute, JAERI-Memo-60-259, October 1985.

J-142   "Data Report on Large Scale Reflood Test-101 -- SCTF Test S2-17 (Run 622)," prepared by Japan Atomic Energy Research Institute, JAERI-Memo-60-260, October 1985.

J-143   "Data Report on Large Scale Reflood Test-102 -- SCTF Test S2-18 (Run 623)," prepared by Japan Atomic Energy Research Institute, JAERI-Memo-60-268, October 1985.

J-144   "Data Report on Large Scale Reflood Test-103 -- SCTF Test S2-19 (Run 624)," prepared by Japan Atomic Energy Research Institute, JAERI-Memo-60-269, October 1985.

J-145   "Data Report on Large Scale Reflood Test-104 -- SCTF Test S2-21 (Run 626)," prepared by Japan Atomic Energy Research Institute, JAERI-Memo-60-270, October 1985.

SCTF Core-III

J-151   "Data Report on Large Scale Reflood Test-105 -- SCTF Test S3-SHI (Run 703)," prepared by Japan Atomic Energy Research Institute, JAERI-Memo-62-115, March 1987.

J-152   "Data Report on Large Scale Reflood Test-106 -- SCTF Test S3-SH2 (Run 704)," prepared by Japan Atomic Energy Research Institute, JAERI-Memo-62-116, March 1987.

J-153   "Data Report on Large Scale Reflood Test-107 -- SCTF Test S3-01 (Run 705)," prepared by Japan Atomic Energy Research Institute, JAERI-Memo-62-117, March 1987.

J-154   "Data Report on Large Scale Reflood Test-108 -- SCTF Test S3-02 (Run 706)," prepared by Japan Atomic Energy Research Institute, JAERI-Memo-62-118, March 1987.

J-155   "Data Report on Large Scale Reflood Test-109 -- SCTF Test S3-03   (Run 707)," prepared by Japan Atomic Energy Research Institute, JAERI-Memo-62-119, March 1987.

J-156   "Data Report on Large Scale Reflood Test-110 -- SCTF Test S3-04 (Run 708)," prepared by Japan Atomic Energy Research Institute, JAERI-Memo-62-120, March 1987.

J-157   "Data Report on Large Scale Reflood Test-111 -- SCTF Test S3-05 (Run 709)," prepared by Japan Atomic Energy Research Institute, JAERI-Memo-62-121, March 1987.

J-158   "Data Report on Large Scale Reflood Test-112 -- SCTF Test S3-06 (Run 710)," prepared by Japan Atomic Energy Research Institute, JAERI-Memo-62-122, March 1987.

J-159   "Data Report on Large Scale Reflood Test-113 -- SCTF Test S3-07 (Run 711)," prepared by Japan Atomic Energy Research Institute, JAERI-Memo-62-123, March 1987.

J-160   "Data Report on Large Scale Reflood Test-114 -- SCTF Test S3-08 (Run 712)," prepared by Japan Atomic Energy Research Institute, JAERI-Memo-62-124, March 1987.

J-161   "Data Report on Large Scale Reflood Test-115 -- SCTF Test S3-09 (Run 713)," prepared by Japan Atomic Energy Research Institute, JAERI-Memo-62-125, March 1987.

J-162   "Data Report on Large Scale Reflood Test-116 -- SCTF Test S3-10 (Run 714)," prepared by Japan Atomic Energy Research Institute, JAERI-Memo-62-126, March 1987.

J-163   "Data Report on Large Scale Reflood Test-117 -- SCTF Test S3-11   (Run 715)," prepared by Japan Atomic Energy Research Institute, JAERI-Memo-63-076, March 1988.

J-164   "Data Report on Large Scale Reflood Test-118 -- SCTF Test S3-12   (Run 716)," prepared by Japan Atomic Energy Research Institute, JAERI-Memo-63-233, June 1988.

J-165   "Data Report on Large Scale Reflood Test-119 -- SCTF Test S3-13 (Run 717)," prepared by Japan Atomic Energy Research Institute, JAERI-Memo-63-077, March 1988.

J-166   "Data Report on Large Scale Reflood Test-120 -- SCTF Test S3-14 (Run 718)," prepared by Japan Atomic Energy Research Institute, JAERI-Memo-62-335, September 1987.

J-167   "Data Report on Large Scale Reflood Test-121 -- SCTF Test S3-15 (Run 719)," prepared by Japan Atomic Energy Research Institute, JAERI-Memo-62-330, September 1987.

J-168   "Data Report on Large Scale Reflood Test-122 -- SCTF Test S3-16 (Run 720)," prepared by Japan Atomic Energy Research Institute, JAERI-Memo-63-078, March 1988.

J-169   "Data Report on Large Scale Reflood Test-123 -- SCTF Test S3-17 (Run 721)," prepared by Japan Atomic Energy Research Institute, JAERI-Memo-63-079, March 1988.

J-170   "Data Report on Large Scale Reflood Test-124 -- SCTF Test S3-18 (Run 722)," prepared by Japan Atomic Energy Research Institute, JAERI-Memo-63-234, June 1988.

J-171   "Data Report on Large Scale Reflood Test-126 -- SCTF Test S3-20 (Run 724)," prepared by Japan Atomic Energy Research Institute, JAERI-Memo-63-080, March 1988.

J-172   "Data Report on Large Scale Reflood Test-127 -- SCTF Test S3-21 (Run 725)," prepared by Japan Atomic Energy Research Institute, JAERI-Memo-01-397, November 1989.

J-173   "Data Report on Large Scale Reflood Test-128 -- SCTF Test S3-22 (Run 726)," prepared by Japan Atomic Energy Research Institute, JAERI-Memo-01-065, March 1989.

QUICK LOOK REPORTS

CCTF Core-I

J-201   "Quick Look Report on Large Scale Reflood Test, Shakedown Test 1--CCTF Test C1-SH1 (Run 005)," prepared by Japan Atomic Energy Research Institute, JAERI-Memo-8641, January 1979.

J-202   "Quick Look Report on Large Scale Reflood Test, Shakedown Test 3--CCTF Test C1-SH3 (Run 007)," prepared by Japan Atomic Energy Research Institute, JAERI-Memo-8930, June 1980.

J-203   "Quick Look Report on Large Scale Reflood Test, Shakedown Test 4--CCTF Test C1-SH4 (Run 008)," prepared by Japan Atomic Energy Research Institute, JAERI-Memo-9149, October 1980.

J-204   "Quick Look Report on Large Scale Reflood Test-1 -- CCTF Test C1-1 (Run 010)," prepared by Japan Atomic Energy Research Institute, JAERI-Memo-8453, August, 1979.

J-205   "Quick Look Report on Large Scale Reflood Test-2 -- CCTF Test C1-2 (Run 011)," prepared by Japan Atomic Energy Research Institute, JAERI-Memo-8530, October 1979.

J-206   "Quick Look Report on Large Scale Reflood Test-3 -- CCTF Test C1-3 (Run 012)," prepared by Japan Atomic Energy Research Institute, JAERI-Memo-8538, November 1979.

J-207   "Quick Look Report on Large Scale Reflood Test-4 -- CCTF Test C1-4 (Run 013)," prepared by Japan Atomic Energy Research Institute, JAERI-Memo-8685, February 1980.

J-208   "Quick Look Report on Large Scale Reflood Test-5 -- CCTF Test C1-5 (Run 014)," prepared by Japan Atomic Energy Research Institute, JAERI-Memo-8696, February 1980.

J-209   "Quick Look Report on Large Scale Reflood Test-6 -- CCTF Test C1-6 (Run 015)," prepared by Japan Atomic Energy Research Institute, JAERI-Memo-8990, July 1980.

J-210   "Quick Look Report on Large Scale Reflood Test-7 -- CCTF Test C1-7 (Run 016)," prepared by Japan Atomic Energy Research Institute, JAERI-Memo-8991, July 1980.

J-211   "Quick Look Report on Large Scale Reflood Test-8 -- CCTF Test C1-8 (Run 017)," prepared by Japan Atomic Energy Research Institute, JAERI-Memo-8992, July 1980.

J-212   "Quick Look Report on Large Scale Reflood Test-9 -- CCTF Test C1-9 (Run 018)," prepared by Japan Atomic Energy Research Institute, JAERI-Memo-9125, September 1980.

J-213   "Quick Look Report on Large Scale Reflood Test-10 -- CCTF Test C1-10 (Run 019)," prepared by Japan Atomic Energy Research Institute, JAERI-Memo-9207, November 1980.

J-214   "Quick Look Report on Large Scale Reflood Test-11 -- CCTF Test C1-11 (Run 020)," prepared by Japan Atomic Energy Research Institute, JAERI-Memo-9208, November 1980.

J-215   "Quick Look Report on Large Scale Reflood Test-12 -- CCTF Test C1-12 (Run 021)," prepared by Japan Atomic Energy Research Institute, JAERI-Memo-9270, January 1981.

J-216   "Quick Look Report on Large Scale Reflood Test-13 -- CCTF Test C1-13 (Run 022)," prepared by Japan Atomic Energy Research Institute, JAERI-Memo-9282, January 1981.

J-217   "Quick Look Report on Large Scale Reflood Test-14 -- CCTF Test C1-14 (Run 023)," prepared by Japan Atomic Energy Research Institute, JAERI-Memo-9305, February 1981.

J-218   "Quick Look Report on Large Scale Reflood Test-15 -- CCTF Test C1-15 (Run 024)," prepared by Japan Atomic Energy Research Institute, JAERI-Memo-9329, February 1981.

J-219   "Quick Look Report on Large Scale Reflood Test-16 -- CCTF Test C1-16 (Run 025)," prepared by Japan Atomic Energy Research Institute, JAERI-Memo-9349, March 1981.

J-220   "Quick Look Report on Large Scale Reflood Test-18 -- CCTF Test C1-17 (Run 036)," prepared by Japan Atomic Energy Research Institute, JAERI-Memo-9712, October 1981.

J-221   "Quick Look Report on Large Scale Reflood Test-19 -- CCTF Test C1-18 (Run 037)," prepared by Japan Atomic Energy Research Institute, JAERI-Memo-9713, October 1981.

J-222   "Quick Look Report on Large Scale Reflood Test-23 -- CCTF Test C1-19 (Run 038)," prepared by Japan Atomic Energy Research Institute, JAERI-Memo- 9767, November 1981.

J-223   "Quick Look Report on Large Scale Reflood Test-24 -- CCTF Test C1-20 (Run 039)," prepared by Japan Atomic Energy Research Institute, JAERI-Memo-9768, November 1981.

J-224   "Quick Look Report on Large Scale Reflood Test-29 -- CCTF Test C1-21 (Run 040)," prepared by Japan Atomic Energy Research Institute, JAERI-Memo-9903, January 1982.

J-225   "Quick Look Report on Large Scale Reflood Test-30 -- CCTF Test C1-22 (Run 041)," prepared by Japan Atomic Energy Research Institute, JAERI Memo 9904, February 1982.

CCTF Core-II

J-241   "Quick Look Report on Large Scale Core-II Reflood Test, First Shakedown
         Test C2-SH1 (Run 53)," prepared by Japan Atomic Energy Research
         Institute, JAERI-Memo-57-397, December 1982.

J-242   "Quick Look Report on CCTF Core-II Reflood Test, Second Shakedown
         Test, C2-SH2 (Run 54)," prepared by Japan Atomic Energy Research
         Institute, JAERI-Memo-57-391, December 1982.

J-243   "Quick Look Report on CCTF Core-II Reflood Test C2-1 (Run 55),"
         prepared by Japan Atomic Energy Research Institute, JAERI-Memo-57-392,
         December 1982.

J-244   "Quick Look Report on CCTF Core-II Reflood Test C2-2 (Run 56),"
         prepared by Japan Atomic Energy Research Institute, JAERI-Memo-57-393,
         December 1982.

J-245   "Quick Look Report on CCTF Core-II Reflood Test C2-AA1 (Run 57) --
         Investigation of the Reflood Phenomena Under Upper Plenum Injection
         Condition," prepared by Japan Atomic Energy Research Institute, JAERI-
         Memo-58-415, November, 1983.

J-246   "Quick Look Report on CCTF Core-II Reflood Test C2-AA2 (Run 58) --
         Investigation of Downcomer Injection Effects," prepared by Japan Atomic
         Energy Research Institute, JAERI-Memo-58-386, October 1983.

J-247   "Quick Look Report on CCTF Core-II Reflood Test, C2-AS1 (Run 59) --
         Investigation on the Reflood Phenomena Under Upper Plenum Injection
         Condition," prepared by Japan Atomic Energy Research Institute, JAERI-
         Memo-58-416, November 1983.

J-248   "Quick Look Report on CCTF Core-II Reflood Test C2-AS2 (Run 60) --
         Effect of Vent Valve Type ECCS.1," prepared by Japan Atomic Energy
         Research Institute, JAERI-Memo-58-459, January 1984.

J-249   "Quick Look Report on CCTF Core-II Reflood Test C2-3 (Run 61) --
         Investigation of Initial Downcomer Water Accumulation Rate Effects,"
         prepared by Japan Atomic Energy Research Institute, JAERI-Memo-58-460,
         January 1984.

J-250   "Quick Look Report on CCTF Core-II Reflood Test C2-4 (Run 62) --
         Investigation of Reproducibility," prepared by Japan Atomic Energy
         Research Institute, JAERI-Memo-58-479, January 1984.

J-251   "Quick Look Report on CCTF Core-II Reflood Test, C2-5 (Run 63) -- Investigation of the Reflood Phenomena Under Low Power Condition," prepared by Japan Atomic Energy Research Institute, JAERI-Memo-59-046, February 1984.

J-252   "Quick Look Report on CCTF Core-II Reflood Test, C2-6 (Run 64) -- Effect of Radial Power Profile," prepared by Japan Atomic Energy Research Institute, JAERI-Memo-59-012, February 1984.

J-253   "Quick Look Report on CCTF Core-II Reflood Test, C2-7 (Run 65) -- Calibration Test," prepared by Japan Atomic Energy Research Institute, JAERI-Memo-59-047, February 1984.

J-254   "Quick Look Report on CCTF Core-II Reflood Test, C2-8 (Run 67) --Effect of Systems Pressure," prepared by Japan Atomic Energy Research Institute, JAERI-Memo-59-028, February 1984.

J-255   "Quick Look Report on CCTF Core-II Reflood Test C2-9 (Run 68) -- Effect of LPCI Flow Rate," prepared by Japan Atomic Energy Research Institute, JAERI-Memo-59-048, February 1984.

J-256   "Quick Look Report on CCTF Core-II Reflood Test C2-10 (Run 69) -- Effect of Vent Valve Type ECCS 2," prepared by Japan Atomic Energy Research Institute, JAERI-Memo-59-029, February 1984.

J-257   "Quick Look Report on CCTF Core-II Reflood Test C2-11 (Run 70) -- Investigation of the End-of-Bypass and Refill Phenomena Under the Condition of Loop Isolations," prepared by Japan Atomic Energy Research Institute, JAERI Memo-59-013, February 1984.

J-258   "Quick Look Report on CCTF Core-II Reflood Test C2-12 (Run 71) -- Best Estimate Reflood Experiment," prepared by Japan Atomic Energy Research Institute, JAERI Memo-59-326, October 1984.

J-259   "Quick Look Report on CCTF Core-II Reflood Test, C2-13 (Run 72) -- Investigation of the Reflood Phenomena for No LPCI Pump Failure Simulation Upper Plenum Injection Test," prepared by Japan Atomic Energy Research Institute, JAERI-Memo-59-416, January 1985.

J-260   "Quick Look Report on CCTF Core-II Reflood Test C2-14 (Run 74) -- Investigation of the Refill Phenomena and Its Effect on the Reflooding Behavior," prepared by Japan Atomic Energy Research Institute, JAERI-Memo-59-352, October 1984.

J-261   "Quick Look Report on CCTF Core-II Reflood Test C2-15 (Run 75) --
         Investigation of FLECHT-SET Coupling Test Results," prepared by Japan
         Atomic Energy Research Institute, JAERI-Memo-60-255, September 1985.

J-262   "Quick Look Report on CCTF Core-II Reflood Test C2-16 (Run 76) -- Effect
         of Asymmetric Upper Plenum Injection on Reflood Phenomena," prepared
         by Japan Atomic Energy Research Institute, JAERI-Memo-60-142, June
         1985.

J-263   "Quick Look Report on CCTF Core-II Reflood Test C2-17 (Run 77) --
         Investigation of the Refill Phenomena with Core Reversal Steam Flow,"
         prepared by Japan Atomic Energy Research Institute, JAERI- Memo-61-
         136, May 1986.

J-264   "Quick Look Report on CCTF Core-II Reflood Test C2-18 (Run 78) -- Best
         Estimated Refill/Reflood Upper Plenum Injection Test," prepared by Japan
         Atomic Energy Research Institute, JAERI-Memo-60-372, December 1985.

SCTF Core-I

J-281   "Quick Look Report on Large Scale Reflood Test-17 -- SCTF Test S1-SH1
         (Run 505)," prepared by Japan Atomic Energy Research Institute, JAERI-
         Memo-9702, September 1981.

J-282   "Quick Look Report on Large Scale Reflood Test-20 -- SCTF Test S1-SH2
         (Run 506)," prepared by Japan Atomic Energy Research Institute, JAERI-
         Memo-9732, October 1981.

J-283   "Quick Look Report on Large Scale Reflood Test-22 -- SCTF Test S1-02
         (Run 508)," prepared by Japan Atomic Energy Research Institute, JAERI-
         Memo-9734, November 1981.

J-284   "Quick Look Report on Large Scale Reflood Test-25 -- SCTF Test S1-03
         (Run 509)," prepared by Japan Atomic Energy Research Institute, JAERI-
         Memo-9803, November 1981.

J-285   "Quick Look Report on Large Scale Reflood Test-26 -- SCTF Test S1-04
         (Run 510), prepared by Japan Atomic Energy Research Institute, JAERI-
         Memo-9804, November 1981.

J-286   "Quick Look Report on Large Scale Reflood Test-27 -- SCTF Test S1-05
         (Run 511)," prepared by Japan Atomic Energy Research Institute, JAERI-
         Memo-9805, November 1981.

J-287   "Quick Look Report on Large Scale Reflood Test-28 -- SCTF Test S1-06 (Run 512)," prepared by Japan Atomic Energy Research Institute, JAERI-Memo-9806, November 1981.

J-288   "Quick Look Report on Large Scale Reflood Test-31 -- SCTF Test S1-07 (Run 513)," prepared by Japan Atomic Energy Research Institute, JAERI-Memo-57-176, July 1982.

J-289   "Quick Look Report on Large Scale Reflood Test-32 -- SCTF Test S1-08 (Run 514)," prepared by Japan Atomic Energy Research Institute, JAERI-Memo-57-177, July 1982.

J-290   "Quick Look Report on Large Scale Reflood Test-33 -- SCTF Test S1-09 (Run 515)," prepared by Japan Atomic Energy Research Institute, JAERI-Memo-57-178, July 1982.

J-291   "Quick Look Report on Large Scale Reflood Test 34 -- SCTF Test S1-10 (Run 516)," prepared by Japan Atomic Energy Research Institute, JAERI-Memo-57-179, July 1982.

J-292   "Quick Look Report on Large Scale Reflood Test-35 -- SCTF Test S1-11 (Run 517)," prepared by Japan Atomic Energy Research Institute, JAERI-Memo-57-180, July 1982.

EVALUATION REPORTS

CCTF Core-I

J-401   "Evaluation Report on CCTF Core-I Reflood Test C1-SH5 (Run 009) -- Investigation of the PKL Coupling Test," prepared by Japan Atomic Energy Research Institute, JAERI-Memo-9965, February 1982.

J-402   "Evaluation Report on CCTF Core-I Reflood Test C1-1 (Run 010) -- Investigation of the Loop Flow Resistance Effect," prepared by Japan Atomic Energy Research Institute, JAERI-Memo-9966, February 1982 (publicly released as JAERI-M-83-140, September 1983).

J-403   "Evaluation Report on CCTF Core-I Reflood Tests C1-2 (Run 11) and C1-11 (Run 20) -- Reproducibility Test," prepared by Japan Atomic Energy Research Institute, JAERI-Memo-57-048, March 1982.

J-404   "Evaluation Report on CCTF Core-I Reflood Tests C1-2 (Run 11) and C1-11 (Run 20) -- Effect of the Installment of the Baffle Plates in the Control Rod Guide Tubes and the Spool Piece in the Primary Loops," prepared by Japan Atomic Energy Research Institute, JAERI-M-83-094, June 1983.

J-405   "Evaluation Report on CCTF Core-I Reflood Tests C1-2 (Run 11) and C1-3 (Run 12) -- Effects of Initial Downcomer Wall Temperature on System Behavior of a PWR during Reflood Phase of a Loss-Of-Coolant Accident," prepared by Japan Atomic Energy Research Institute, JAERI-Memo-9925, January 1982.

J-406   "Evaluation Report on CCTF Core-I Reflood Tests C1-2 (Run 11) and C1-3 (Run 12) -- Effects of Initial Superheat of the Downcomer Wall," prepared by Japan Atomic Energy Research Institute, JAERI-M-83-090, June 1983.

J-407   "Evaluation Report on CCTF Core-I Reflood Test C1-4 (Run 13) and C1-15 (Run 24) -- Investigation of the Refill Simulation and the Nitrogen Injection Effects," prepared by Japan Atomic Energy Research Institute, JAERI-Memo-9967, February 1982 (publicly released as JAERI-M-83-121, August 1983).

J-408   "Evaluation Report on CCTF Core-I Reflood Test C1-5 (Run 14) -- Overall System Thermo-Hydrodynamic Behavior Observed in the Base Case Test," prepared by Japan Atomic Energy Research Institute, JAERI-Memo-57-051, March, 1982 (publicly released as JAERI-M-83-207, February 1983).

J-409   "Evaluation Report on CCTF Core-I Reflood Tests C1-5 (Run 14), C1-10 (Run 19) and C1-12 (Run 21) -- Effects of Containment Pressure on System Behaviors During Reflood Phase of a LOCA," prepared by Japan Atomic Energy Research Institute, JAERI-Memo-57-013, February 1982 (publicly released as JAERI-M-83-091, June 1983).

J-410   "Evaluation Report on CCTF Core-I Reflood Tests C1-5 (Run 14), C1-17 (Run 36) and C1-20 (Run 39) -- Core Thermo-Hydrodynamics and Thermally Multidimensional Effects On It," prepared by Japan Atomic Energy Research Institute, JAERI-Memo-57-052, March 1982.

J-411   "Evaluation Report on CCTF Core-I Reflood Tests C1-6 (Run 15), C1-9 (Run 18), C1-11 (Run 20) and C1-13 (Run 22) -- Effects of ECC Water Injection Rate," prepared by Japan Atomic Energy Research Institute, JAERI-Memo-57-018, March 1982 (publicly released as JAERI-M-83-044).

J-412   "Evaluation Report on CCTF Core-I Reflood Tests C1-7 (Run 16) and C1-14 (Run 23) -- Effects of Initial Clad Temperature," prepared by Japan Atomic Energy Research Institute, JAERI-Memo-9953, February 1982 (publicly released as JAERI-M-83-026).

J-413   "Evaluation Report on CCTF Core-I Reflood Tests C1-18 (Run 37) and C1-8 (Run 17) -- Investigation of the Effect of Water Remaining in the Loop Seal Section on Reflood Behavior," prepared by Japan Atomic Energy Research Institute, JAERI-Memo-9996, February 1982 (publicly released as JAERI-M-83-115, July 1983).

J-414   "Evaluation Report on CCTF Core-I Reflood Tests C1-16 (Run 25), C1-21 (Run 40) and C1-22 (Run 41) -- Comparison of the FLECHT-SET Test Results With The FLECHT Coupling Test Results," prepared by Japan Atomic Energy Research Institute, JAERI-Memo-57-014, March 1982 (publicly released as JAERI-M-83-065, May 1983).

J-415   "Evaluation Report on CCTF Core-I Reflood Tests C1-17 (Run 36) and C1-20 (Run 39)," prepared by Japan Atomic Energy Research Institute, JAERI-M-83-028, February 1983.

J-416   "Evaluation Report on CCTF Core-I Reflood Test C1-19 (Run 38) -- Experimental Assessment of the Evaluation Model For the Safety Analysis on the Reflood Phase of a PWR LOCA," prepared by Japan Atomic Energy Research Institute, JAERI-Memo-57-053, March, 1982 (publicly released as JAERI-M-83-029, February 1983).

J-417   "Development of the Model for the Mass Balance Calculation of the CCTF Test -- The Estimation of the Core Inlet Mass Flow Rate," prepared by Japan Atomic Energy Research Institute, JAERI-Memo-9936, January 1982.

J-418   "Analysis Report on CCTF Core-I Reflood Tests," prepared by Japan Atomic Energy Research Institute, JAERI-Memo-57-057, March 1982.

J-419   "Large Scale Reflood Test With Cylindrical Core Test Facility (CCTF) -- Core-I FY 1979 Tests," prepared by Japan Atomic Energy Research Institute, JAERI-Memo-82-002, March 1982.

J-420   "CCTF Core-I Test Results," prepared by Japan Atomic Energy Research Institute, JAERI-M-82-073, July 1982.

J-421   "Findings in CCTF Core-I Test," prepared by Japan Atomic Energy Research Institute, JAERI-Memo-58-050, February 1983.

J-422   "Results of Downcomer CCFL Experiment," prepared by Japan Atomic Energy Research Institute, JAERI-Memo-59-245, August 1984.

CCTF Core-II

J-441   "Evaluation of CCTF Core-II Acceptance Test-1 (Run 051)," prepared by Japan Atomic Energy Research Institute, JAERI-Memo-57-275, October 1982.

J-442   "Evaluation Report on CCTF Core-II Reflood Tests C2-AC1 (Run 51) and C2-4 (Run 62) -- Effect of Initial Clad Temperature," prepared by Japan Atomic Energy Research Institute, JAERI-M-84-026, February 1984.

J-443   "Evaluation of CCTF Core-II Acceptance Test 2 (Run 052)," prepared by Japan Atomic Energy Research Institute, JAERI-Memo-57-375, November 1982.

J-444   "Evaluation of CCTF Core-II Second Acceptance Test C2-AC2 (Run 052) -- Investigation of Difference in Reflooding Behaviors Between Core-I and Core-II Facilities," prepared by Japan Atomic Energy Research Institute, JAERI-M-84-036, March 1984.

J-445   "Evaluation Report on CCTF Core-II Reflood Test Second Shakedown Test C2-SH2 (Run 54) -- Effect of Core Supplied Power on Reflood Phenomena," prepared by Japan Atomic Energy Research Institute, JAERI-M-85-025, March 1985.

J-446   "Evaluation Report on CCTF Core-II Reflood Test C2-AA2 (Run 58) -- Investigation of Downcomer Injection Effects," prepared by Japan Atomic Energy Research Institute, JAERI-M-89-227, January 1990.

J-447   "Evaluation Report on CCTF Core-II Reflood Test C2-3 (Run 61) -- Investigation of Initial Downcomer Water Accumulation Velocity Effects," prepared by Japan Atomic Energy Research Institute, JAERI-M-86-185, January 1987.

J-448   "Evaluation Report on CCTF Core-II Reflood Test C2-4 (Run 62) -- Investigation of Reproducibility," prepared by Japan Atomic Energy Research Institute, JAERI-M-85-026, March 1985.

J-449   "Evaluation Report on CCTF Core-II Reflood Test C2-6 (Run 64) -- Effect of Radial Power Profile," prepared by Japan Atomic Energy Research Institute, JAERI-M-85-027, March 1985.

J-450   "Evaluation Report on CCTF Core-II Reflood Test C2-8 (Run 67) -- Effect System Pressure," prepared by Japan Atomic Energy Research Institute, JAERI-M-87-001, January 1987.

J-451   "Evaluation Report on CCTF Core-II Reflood Test C2-9 (Run 68) -- Effect of LPCI Flow Rate," prepared by Japan Atomic Energy Research Institute, JAERI-M-87-002, February 1987.

J-452   "Evaluation Report on CCTF Core-II Reflood Test C2-16 (Run 76) -- Effect of Asymmetric Upper Plenum Injection on Reflood Phenomena," prepared by Japan Atomic Energy Research, JAERI-M-87-051, March 1987.

J-453   "Evaluation Report on CCTF Core-II Reflood Test C2-18 (Run 78) --Best Estimate Refill/Reflood Upper Plenum Injection Test," prepared by Japan Atomic Energy Research Institute, JAERI-M-87-052, March 1987.

J-454   "Evaluation Report on CCTF Core-II Reflood Test C2-19 (Run 79) -- Combined Injection Mode Under EM Condition," prepared by Japan Atomic Energy Research Institute, JAERI-Memo-62-334, September 1987.

J-455   Pointner, W., "Study on Effects of Combined Injection (EM Conditions) on Reflood Phenomena (Test C2-19/Run 79)," Japan Atomic Energy Research Institute, JAERI-Memo-62-294, August 1987.

J-456   "Evaluation Report on CCTF Core-II Reflood Tests C2-20 (Run 80) and C2-21 (Run 81) -- BE Condition & Effect of Hot Leg ECC Flow Rate Under Combined Injection Mode," prepared by Japan Atomic Energy Research Institute, JAERI-Memo-63-267, July 1988.

J-457   "Analysis Report on Large Scale Reflood Tests with Cylindrical Core Test Facility -- Tests in FY 1983," prepared by Japan Atomic Energy Research Institute, JAERI-Memo-60-108.

J-458   "Analysis Report on Large Scale Reflood Tests with Cylindrical Core Test Facility -- Tests in FY 1984," prepared by Japan Atomic Energy Research Institute, JAERI-Memo-60-403.

J-459   "Analysis Report on CCTF Reflood Test," prepared by Japan Atomic Energy Research Institute, JAERI-Memo-61-059.

SCTF Core-I

J-481   "Design of Slab Core Test Facility (SCTF) in Large Scale Reflood Test
         Program. Part I: Core-I," prepared by Japan Atomic Energy Research
         Institute, JAERI-Memo-9701, September 1981 (publicly released as JAERI-
         M-83-080, June 1983).

J-482   "System Pressure Effects on Reflooding Phenomena Observed in the SCTF
         Core-I Forced Flooding Effects," prepared by Japan Atomic Energy
         Research Institute, JAERI-Memo-9729, October 1981 (publicly released as
         JAERI-M-83-079, June 1983).

J-483   "Dispersed Flow and Corresponding Phenomena in SCTF Observed with
         High-Speed Camera," prepared by Japan Atomic Energy Research
         Institute, JAERI-M-9971, February 1982.

J-484   "Effects of Core Inlet Water Subcooling on Reflooding Phenomena
         Under Forced Flooding in SCTF Core-I Tests," prepared by Japan Atomic
         Energy Research Institute, JAERI-Memo-9972, February 1982 (publicly
         released as JAERI-M-83-122, August 1983).

J-485   "Effect of Upper Plenum Water Accumulation on Reflooding Phenomena
         Under Forced Flooding in SCTF Core-I Tests," prepared by Japan Atomic
         Energy Research Institute, JAERI-Memo-9973, February 1982 (publicly
         released as JAERI-M-83-114, July 1983).

J-486   "SCTF Core-I Tests Results: System Pressure Effects on Reflooding
         Phenomena," prepared by Japan Atomic Energy Research Institute, JAERI-
         M-82-075, July 1982.

J-487   "Examination of Repeatability in Reflood Phenomena Under Forced
         Flooding in SCTF Core-I Tests," prepared by Japan Atomic Energy
         Research Institute, JAERI-Memo-57-251, September 1982 (publicly released
         as JAERI-M-083-237, January 1984).

J-488   "Core Thermal Behavior Under Forced Feed Flooding in SCTF Core-I
         Tests," prepared by Japan Atomic Energy Research Institute, JAERI-Memo-
         57-270, October 1982.

J-489   "Heat Transfer Enhancement Due to Chimney Effect in Reflood Phase,"
         prepared by Japan Atomic Energy Research Institute, JAERI-Memo-57-297,
         October 1982.

J-490   "Effect of LPCI Water Injection Rate on Carryover Characteristics During Reflood," prepared by Japan Atomic Energy Research Institute, JAERI-Memo-58-035, February 1983.

J-491   "Droplets Flow and Heat Transfer at Top Region of Core In Reflood Phase," prepared by Japan Atomic Energy Research Institute, JAERI-M-83-022, February 1983.

J-492   "Evaluation of Cross Flow Velocity Across Rod Bundles During Reflood Phase in SCTF Core-I Forced Feed Flooding Tests," prepared by Japan Atomic Energy Research Institute, JAERI-Memo-58-443, December 1983.

J-493   "Effects of Upper Plenum Injection on Thermo-Hydrodynamic Behavior Under Refill and Reflood Phases of a PWR-LOCA," prepared by Japan Atomic Energy Research Institute, JAERI-Memo-59-052, February 1984 (publicly released as JAERI-M-84-221, December 1984).

J-494   "Cold Leg Injection Reflood Test Results in the SCTF Core-I Under Constant System Pressure," prepared by Japan Atomic Energy Research Institute, JAERI-Memo-59-053, February 1984 (publicly released as JAERI-M-90-129, August 1990).

J-495   "Characteristics of Lower Plenum Injection Reflood Tests in SCTF Core-I," prepared by Japan Atomic Energy Research Institute, JAERI-Memo-59-051, March 1984 (publicly released as JAERI-M-84-223, December 1984).

J-496   "Examination of Refill Simulation Test Results in SCTF Core-I," prepared by Japan Atomic Energy Research Institute, JAERI-Memo-60-098, April 1985.

J-497   "Effects of Core Inlet Water Mass Flow Rate on Reflooding Phenomena in the Forced Feed SCTF Core-I Tests," prepared by Japan Atomic Energy Research Institute, JAERI-Memo-61-024, February 1986 (publicly released as JAERI-M-88-166, September 1988).

J-498   "Effects of Radial Core Power Profile on Core Thermo-Hydraulic Behavior during Reflood Phase in SCTF Core-I Forced Feed Tests," prepared by Japan Atomic Energy Research Institute, JAERI-M-91-093, June 1991.

SCTF Core-II

J-521   "Design of Slab Core Test Facility (SCTF) in Large Scale Reflood Test
         Program, Part II: Core-II," prepared by Japan Atomic Energy Research
         Institute, JAERI-Memo-59-396, December 1984.

J-522   "Effects of Radial Power Profile on Two-Dimensional Thermal-Hydraulic
         Behavior in Core in SCTF Core-II Cold Leg Injection Tests," prepared by
         Japan Atomic Energy Research Institute, JAERI-Memo-59-415, January
         1985.

J-523   "Study on ECC Injection Modes in Reflood Tests with SCTF Core-II
         Comparison between Gravity and Forced Feeds," prepared by Japan
         Atomic Energy Research Institute, JAERI-Memo-61-115, March 1985
         (publicly released as JAERI-M-91-001, February 1991).

J-524   "Development of SCTF Cold Leg Injection Test Method for Eliminating U-
         Tube Oscillation During the Initial Period," prepared by Japan Atomic
         Energy Research Institute, JAERI-Memo-60-145, June 1984 (publicly
         released as JAERI-M-90-107, July 1990).

J-525   "Two Dimensional Thermal-Hydraulic Behavior in Core in SCTF Core-II Cold
         Leg Injection Tests (Radial Power Profile Test Results)," prepared by Japan
         Atomic Energy Research Institute, JAERI-M-85-106, July 1985.

J-526   "Evaluation of SCTF Core-II Tests with Upward Steam Flow and Upper
         Plenum Water Injection," prepared by Japan Atomic Energy Research
         Institute, JAERI-Memo-60-287, October 1985.

J-527   "Data Reduction and Analysis Procedures in SCTF Core-II," prepared by
         Japan Atomic Energy Research Institute, JAERI-Memo-60-393, January
         1986.

J-528   "Two-Dimensional Thermal-Hydraulic Behavior in Core in SCTF Core-II
         Forced Feed Reflood Tests (Effects of Radial Power and Temperature
         Distributions)," prepared by Japan Atomic Energy Research Institute,
         JAERI, Memo-60-395, January 1986 (publicly released as JAERI-M-86-195,
         January 1987).

J-529   "Comparison of Facility Characteristics Between SCTF Core-I and Core-II,"
         prepared by Japan Atomic Energy Research Institute, JAERI-Memo-61-018,
         February 1986 (publicly released as JAERI-M-90-130, August 1990).

J-530   "Large Scale Reflood Test Results with Slab Core Test Facility (SCTF): Core-II Tests in FY 1984," prepared by Japan Atomic Energy Research Institute, JAERI-Memo-61-058.

J-531   "Reflood Behavior at Low Initial Clad Temperature in Slab Core Test Facility Core-II," prepared by Japan Atomic Energy Research Institute, JAERI-Memo-61-066, March, 1986 (publicly released as JAERI-M-90-106, July 1990).

J-532   "Analysis of SCTF/CCTF Counterpart Test Results," prepared by Japan Atomic Energy Research Institute, JAERI-Memo-61-114, March 1986 (publicly released as JAERI-M-90-083, June 1990).

J-533   "Effects of System Pressure on Two-Dimensional Thermal-Hydraulic Behavior in Core in SCTF Core-II Reflood Tests." prepared by Japan Atomic Energy Research Institute, JAERI-Memo-61-265, August 1986.

J-534   "Evaluation Report on SCTF Core-II Test S2-19 (Effect of LPCI Flow Rate on Core Thermal Hydraulic Behavior During Reflood in a PWR)," prepared by Japan Atomic Energy Research Institute, JAERI-Memo-01-078, March 1989.

J-535   "Evaluation Report on SCTF Core-II Test S2-08 (Effect of Core Inlet Subcooling on Thermal-Hydraulic Behavior Including Two-Dimensional Behavior in Pressure Vessel during Reflood in a PWR)," prepared by Japan Atomic Energy Research Institute, JAERI-Memo-01-058, March 1989 (publicly released as JAERI-M-90-236, January 1991).

J-536   "Analysis Report on SCTF Core-I and II Reflood Test," prepared by Japan Atomic Energy Research Institute, JAERI-Memo-01-348.

J-537   "Evaluation Report on SCTF Core-II Test S2-19 (Quantitative Evaluation of Relation Between Degree of Heat Transfer Enhancement Due to Radial Power Distribution and Amount of Increase of Upward Liquid Flow Rate During Reflood in PWR-LOCA)," prepared by Japan Atomic Energy Research Institute, JAERI-M-91-033, March 1991.

SCTF Core-III

J-551   "Design of Slab Core Test Facility (SCTF) in Large Scale Reflood Test Program, Part III: Core-III," prepared by Japan Atomic Energy Research Institute, JAERI-Memo-62-110, March 1987.

J-552   "Analysis Report on Large Scale Reflood Tests with Core-III of the Slab Core Test Facility -- Test in FY 1985," prepared by Japan Atomic Energy Research Institute, JAERI-Memo-61-197.

J-553   "Evaluation Report on SCTF Core-III Test S3-SH1 (Overall Thermal-Hydraulic Characteristics Under Combined Injection Mode for German-Type PWR)," prepared by Japan Atomic Energy Research Institute, JAERI-Memo-62-093, March 1987.

J-554   "Evaluation Report on SCTF Core-III Test S3-06 (Effect of Radial Power Distribution on Thermal-Hydraulic Characteristics Under Combined Injection Mode German PWR)," prepared by Japan Atomic Energy Research Institute, JAERI-Memo-62-111, March 1987 (publicly released as JAERI-M-88-213, October 1988).

J-555   Pointner, W., "Method for the Determination of the Steam Injection Rates to the UPTF Core Simulator for SCTF/UPTF Coupling Tests," Japan Atomic Energy Research Institute, JAERI-Memo-62-293, August 1987.

J-556   "Analysis Report on Large Scale Reflood Tests with Core-III of Slab Core Test Facility -- Test in FY 1986," prepared by Japan Atomic Energy Research Institute, JAERI-Memo-62-295.

J-557   Pointner, W., "System Behavior for the Refill/Reflood Phase During a Combined Injection Test With Conditions in SCTF and CCTF -- Comparison between SCTF Test S3-11 (Run 715) and CCTF Test C2-20 (Run 80)," Japan Atomic Energy Research Institute, JAERI-Memo-62-296, August 1987.

J-558   "Evaluation Report on SCTF Core-III Tests S3-14, S3-15 and S3-16 (Effect of Radial Power Profile Shape on Two Dimensional Thermal Hydraulic Behavior)," prepared by Japan Atomic Energy Research Institute, JAERI-Memo-62-329, September 1987 (publicly released as JAERI-M-88-060, March 1988).

J-559   "Evaluation Report on SCTF-III Test S3-SH2 (Observed Reflood Phenomena in S3-SH2 Test Under Combined Injection Mode for German Type PWR)," prepared by Japan Atomic Energy Research Institute, JAERI-Memo-62-344, October 1987.

J-560   Pointner, W., "Empirical Core Model for CCTF and SCTF," Japan Atomic Energy Research Institute, JAERI-Memo-63-068, March 1988.

J-561   "Evaluation Report on SCTF Core-III Tests S3-7 and S3-8 (Investigation of Tie Plate Water Temperature Distribution Effects on Water Break-through and Core Cooling During Reflooding)," prepared by Japan Atomic Energy Research Institute, JAERI-Memo-63-070, March 1988 (publicly released as JAERI-M-90-035, March 1990).

J-562   "Evaluation Report on SCTF-III Test S3-12 (Observed Reflood Phenomena in Test S3-12 Under Combined Injection Mode for German-Type PWR," prepared by Japan Atomic Energy Research Institute, JAERI-Memo-63-071, March 1988.

J-563   "Evaluation Report on SCTF-III Test S3-13 (Observed Reflood Phenomena in Test S3-13 Under Combined Injection Mode For German-Type PWR)," prepared by Japan Atomic Energy Research Institute, JAERI-Memo-63-072, March 1988.

J-564   "Evaluation Report on the SCTF-III Test S3-18 (Observed Reflood Phenomena in Test S3-18 Under Combined Injection Mode for German-Type PWR)," prepared by Japan Atomic Energy Research Institute, JAERI-Memo-63-073, March 1988.

J-565   "Evaluation Report on SCTF Core-III Test S3-20 (Investigation of Water Break Through and Core Cooling Behaviors Under Intermittent ECC Water Delivery," prepared by Japan Atomic Energy Research Institute, JAERI-Memo-63-074, March 1988 (publicly released as JAERI-M-90-080, May 1990).

J-566   "Evaluation Report on SCTF Core-III Test S3-01 (Effect of Water Sealing at Bottom of Downcomer on Thermal-Hydraulic Behavior in Pressure Vessel in a PWR with Combined Injection Type ECCS)," prepared by Japan Atomic Energy Research Institute, JAERI-Memo-63-230, June 1988.

J-567   "Evaluation Report on SCTF Core-III Test S3-02 (Effect of Water Temperature Falling Into Core on Core Thermal-Hydraulic Behavior in a PWR With Combined Injection Type ECCS)," prepared by Japan Atomic Energy Research Institute, JAERI, Memo-63-231, June 1988.

J-568   "Evaluation Report on SCTF Core-III Test S3-17 (Investigation of Thermo-Hydrodynamic Behavior During Reflood Phase of LOCA in a PWR with Vent Valves)," prepared by Japan Atomic Energy Research Institute, JAERI-Memo-63-232, June 1988 (publicly released as JAERI-M-90-036, March 1990).

J-569   "Evaluation Report on SCTF Core-III Test S3-SH1 (Effect of Hot Leg Injection on Core Thermal-Hydraulics With Combined Injection Type ECCS)," prepared by Japan Atomic Energy Research Institute, JAERI-M-88-125, July 1988.

J-570   "Evaluation Report on SCTF-III Test S3-3, S3-4 and S3-5 Countercurrent Flow Limitation Phenomenon in Full-Radius Core," prepared by Japan Atomic Energy Research Institute, JAERI-Memo-01-028, January 1989.

J-571   "Study on Flow Circulation Phenomena in Pressure Vessel During Reflood Phase of PWR with Combined-Injection Type ECCS Under Cold-Leg-Large-Break LOCA," prepared by Japan Atomic Energy Research Institute, JAERI-Memo-01-015, February 1989.

J-572   "Evaluation Report on SCTF Core-III Test S3-22 (Investigation of Water Break-through and Core Cooling Behaviors under Alternate ECC Water Delivery from Hot Legs to Upper Plenum during Reflooding in PWRs with Combined-Injection Type ECCS," prepared by Japan Atomic Energy Institute, JAERI-Memo-01-077 (publicly released as JAERI-M-91-104, July 1991).u

J-573   "Evaluation Report on SCTF-III Test S3-10: Reflood Phenomena Under Best Estimate Conditions," prepared by Japan Atomic Energy Research Institute, JAERI-Memo-01-086, March 1989.

J-574   "Experimental Study on In-Core Reflood Behavior Under Combined Injection of ECC Water," prepared by Japan Atomic Energy Research Institute, JAERI-Memo-63-467, January 1989.

J-575   "Evaluation Report on SCTF Core-III Test S3-9: Investigation of Reflooding Behavior Under An Evaluation Model Condition in PWRs with Cold-Leg-Injection-Type ECCS," prepared by Japan Atomic Energy Research Institute, JAERI-Memo-01-251, July 1989 (publicly released as JAERI-M-90-046).

J-576   "Evaluation Report on SCTF-III Test S3-11: Observed Reflood Phenomena Under BE Condition of Combined ECC Injection Mode For German Type PWR," prepared by Japan Atomic Energy Research Institute, JAERI-Memo-01-263, August 1989.

J-577   "Evaluation Report on SCTF-III Test S3-21: Observed Reflood Phenomena in Test S3-21 Under Combined ECC Injection Mode," prepared by Japan Atomic Energy Research Institute, JAERI-Memo-02-069, March 1990.

J-578   "Evaluation Report on SCTF Core-III Test S3-9 (Investigation of CCTF Coupling Test Results Under An Evaluation Model Condition in PWRs With Cold-Leg-Injection-Type ECCS)," prepared by Japan Atomic Energy Research Institute, JAERI-M-90-046, March 1990.

Other JAERI Facilities

J-581   "Evaluation of the Pressure Difference across the Core during PWR-LOCA Reflood Phase," prepared by Japan Atomic Energy Research Institute, JAERI-M-8168, March 1979.

J-582   "Experimental Results of the Effective Water Head in Downcomer during Reflood Phase of a PWR LOCA," prepared by Japan Atomic Energy Research Institute, JAERI-M-8978, August 1980.

J-583   "Preliminary Analysis of the Effect of the Grid Spacers on the Reflood Heat Transfer," prepared by Japan Atomic Energy Research Institute, JAERI-M-9992, February 1982.

J-584   "Quench Model for Lower Temperature than Thermo-Hydrodynamic Maximum Liquid Superheat," prepared by Japan Atomic Energy Research Institute, JAERI-M-10000, March 1982.

J-585   "The Characteristics of Cross Flow in a Rod Bundle," prepared by Japan Atomic Energy Research Institute, JAERI-M-82-003, March 1982.

J-586   "Study of the Thermo-Hydrodynamic Phenomena in the Nuclear Core during Reflood Phase," prepared by Japan Atomic Energy Research Institute, JAERI-M-83-032, March 1983.

J-587   "Report on Reflood Experiment of Grid Spacer Effect," prepared by Japan Atomic Energy Research Institute, JAERI-M-84-131, July 1984.

J-588   "Thermal-Hydraulic Evaluation Study of the Effectiveness of Emergency Core Cooling System for Light Water Reactors," prepared by Japan Atomic Energy Research Institute, JAERI-M-85-122, August 1985.

J-589   "Cross Flow Resistance in Air-Water Two-Phase Flow in Rod Bundle," prepared by Japan Atomic Energy Research Institute, JAERI-M-86-184, January 1987.

J-590   "Study on Thermo-Hydraulic Behavior during Reflood Phase of a PWR-LOCA," prepared by Japan Atomic Energy Research Institute, JAERI-M-88-262, January 1989.

J-591   "Estimation of Shear Stress in Counter-Current Gas-Liquid Annular Two-Phase Flow," prepared by Japan Atomic Energy Research Institute, JAERI-M-90-215, January 1991.

CODE ANALYSIS REPORTS

CCTF

J-601   "Assessment of TRAC-PD2 Reflood Core Thermal-Hydraulic Model by CCTF Test C1-16," prepared by Japan Atomic Energy Research Institute, JAERI-M-82-166, November 1982.

J-602   "Assessment of Core Thermo-Hydrodynamic Models of REFLA-1D with CCTF Data," prepared by Japan Atomic Energy Research Institute, JAERI-M-83-103, June 1983.

J-603   "Analysis of TRAC-PD2 Prediction for the Cylindrical Core Test Facility Evaluation-Model Test C1-19 (Run 38)," prepared by Japan Atomic Energy Research Institute, JAERI-M-84-041, March 1979.

J-604   "Assessment of TRAC-PF1 Predictive Capability for the Thermal-Hydraulic Behaviors along a Primary Loop during the Reflood Phase of a PWR-LOCA," prepared by Japan Atomic Energy Research Institute, JAERI-M-84-042, March 1984.

J-605 "Assessment of REFLA Local Power Effect Model with CCTF Data," prepared by Japan Atomic Energy Research Institute, JAERI-M-84-246, February 1985.

J-606 "Analysis of TRAC-PF1 Calculated Core Heat Transfer for CCTF Test C1-5 (Run 14)," prepared by Japan Atomic Energy Research Institute, JAERI-M-85-117, August 1985.

J-607 "Assessment of TRAC-PF1/MOD1 Code for Cylindrical Core Test Facility Base Case Test C2-4," prepared by Japan Atomic Energy Research Institute, JAERI-Memo-01-007, February 1989.

J-608 Pointner, W., "Comparison Between a TRAC GPWR Calculation and a CCTF Test With Combined Injection and EM Boundary Conditions for the Reflood Phase of a German PWR-LOCA," Japan Atomic Energy Research Institute, JAERI-Memo-62-292, August 1987.

J-609 "Assessment of TRAC-PF1/MOD1 Code for Core Thermal Hydraulic Behavior during Reflood with CCTF and SCTF Data," prepared by Japan Atomic Energy Research Institute, JAERI-Memo-01-009, February 1989.

SCTF

J-611 "Computer Codes HeatT and HeatQ for Heat Transfer Analysis in SCTF," prepared by Japan Atomic Energy Research Institute, JAERI-Memo-9867, January 1982.

J-612 "Comparison Between SCTF Tests S1-SH2, S1-01, S1-02, and S1-04 and the TRAC Post-Test Predictions," prepared by Japan Atomic Energy Research Institute, JAERI-Memo-58-339, September 1983.

J-613 "COBRA/TRAC Analysis of Two-Dimensional Thermal-Hydraulic Behavior in SCTF Reflood Tests," prepared by Japan Atomic Energy Research Institute, JAERI-Memo-60-219, August, 1985 (publicly released as JAERI-M-86-196, January 1987).

J-614 "Predictability of REFLA Core Model for SCTF Data," prepared by Japan Atomic Energy Research Institute, JAERI-87-163, October 1987.

J-615 "Assessment of TRAC-PF1/MOD1 Code for Thermal Hydraulic Behavior Including Two-Dimensional Behavior In Pressure Vessel During Reflood in Slab Core Test Facility," prepared by Japan Atomic Energy Research Institute, JAERI-Memo-01-006, February 1989.

Other

J-621   "REFLA-1D/MODE 1: A Computer Program for Reflood Thermo-Hydrodynamic Analysis during PWR-LOCA User's Manual," prepared by Japan Atomic Energy Research Institute, JAERI-M-9286, January 1981.

J-622   "REFLAP/REFLA (Mod 0): A System Reflooding Analysis Computer Program," prepared by Japan Atomic Energy Research Institute, JAERI-M-9397, March 1981.

J-623   "One-dimensional System Analysis Code for Reflood Phase during LOCA," prepared by Japan Atomic Energy Research Institute, JAERI-M-9780, November 1981.

J-624   "Improvement of Core Mass Balance Calculation in REFLA-1D/MODE1," prepared by Japan Atomic Energy Research Institute, JAERI-M-82-099, August 1982.

J-625   "Investigation of Reflood Models by Coupling REFLA-1D and Multi-loop System Model," prepared by Japan Atomic Energy Research Institute, JAERI-M-83-147, September 1983.

J-626   "REFLA-1D/MODE3: A Computer Code for Reflood Thermo-Hydrodynamic Analysis during PWR-LOCA. User's Manual," prepared by Japan Atomic Energy Research Institute, JAERI-M-84-243, February 1985.

J-627   "Updating of Best Evaluation Codes Fiscal Year 1984 Work Report," prepared by Japan Atomic Energy Research Institute, JAERI-Memo-60-394, December 1985.

J-628   "User's Manual of the REFLA-1D/MODE4 Reflood Thermo-Hydrodynamic Analysis Code: Incorporation of Local Power Effect Model and Fuel Temperature Profile Effect Model into REFLA-1D," prepared by Japan Atomic Energy Research Institute, JAERI-M-85-210, January 1986.

J-629   "Assessment of TRAC-PF1/MOD1 for Countercurrent, Annular and Stratified Flows," prepared by Japan Atomic Energy Research Institute, JAERI-M-85-219, January 1986 (this is the public release of a LANL 2D/3D Technical Note -- see U-704).

J-630   "Improvement of TRAC-PF1 Code with JAERI's Reflood Model of REFLA-1D Code, prepared by Japan Atomic Energy Research Institute, JAERI-Memo-02-009 February 1990.

J-631   "Implementation of an Implicit Method Into Heat Conduction Calculation of TRAC-PF1/MOD1 Code," prepared by Japan Atomic Energy Research Institute, JAERI-Memo-01-008, February 1989 (publicly released as JAERI-M-90-122, August 1990).

ADVANCED INSTRUMENTATION REPORTS

J-801   "Data Processing of Advanced Two-Phase Flow Instrumentation In Slab Core Test Facility (SCTF) Core-I," prepared by Japan Atomic Energy Research Institute, JAERI-Memo-9802, November 1981.

J-802   "Evaluation of Advanced Two-Phase Flow Instrumentation In SCTF Core-I," prepared by Japan Atomic Energy Research Institute, JAERI-Memo-57-206, August 1982 (publicly released as JAERI-M-84-065, March 1984).

PAPERS, PRESENTATIONS, AND CORRESPONDENCE

Papers - Data Evaluation

J-901   Murao, Y., Sudo, Y., and Iguchi, T., "Topics on Hydrodynamic Models of PWR Reflood Phenomena," presented at the Japan - US Seminar on Two-Phase Flow Dynamics, Kobe, Japan, July 31 - August 3, 1979.

J-902   Sudo, Y., "Estimation of Average Void Fraction in Vertical Two-Phase Flow Channel Under Low Liquid Velocity," Journal of Nuclear Science & Technology, Vol. 17, No. 1 (January 1980).

J-903   Sudo, U., "Film Boiling Heat Transfer during Reflood Phase in Postulated PWR Loss-of-Coolant Accident," Journal of Nuclear Science and Technology, Vol. 17, No. 7, pp. 516-530 (July 1980).

J-904   Murao, Y., Sudoh, T., and Sugimoto, J., "Experimental and Analytical Modeling of the Reflood-Phase during PWR-LOCA," presented at the Nineteenth National Heat Transfer Conference, Orlando, FL, USA, July 27-30, 1980.

J-905   Hirano, K., Murao, Y.,"Large Scale Reflood Test," Nippon Genshiryoku Gakkai-Shi, Vol. 22, No. 10, pp. 681-686 (October 1980).

J-906   Murao, Y., and Sugimoto, J., "Correlation of Heat Transfer Coefficient for Saturated Film Boiling During Reflood Phase Prior to Quenching," Journal of Nuclear Science and Technology, Vol. 18, No. 4, pp. 275-284 (April 1981).

J-907   Sudo, Y., and Akimoto, H., "Downcomer Effective Water Head during Reflood in Postulated PWR LOCA," Journal of Nuclear Science and Technolgy, Vol. 19, No. 1 (January 1982).

J-908   Osakabe, M., and Adachi, H., "Characteristic of Two-Phase Slanting Flow in Rod Bundle," Journal of Nuclear Science and Technology, Vol. 19, No. 6, pp. 504-506 (June 1982).

J-909   Okubo, T., and Murao, Y., "Effects of ECC Water Injection Rate on Reflood Phase during LOCA," Journal of Nuclear Science and Technology, Vol. 19, No. 7, pp. 593-595 (July 1982).

J-910   Murao, Y., and Iguchi, T., "Experimental Modeling of Core Hydrodynamics during Reflood Phase of LOCA," Journal of Nuclear Science and Technology, Vol. 19, No. 8, pp. 613-627, (August 1982).

J-911   Murao, Y., Akimoto, H., Sudoh, T., and Okubo, T., "Experimental Study of System Behavior during Reflood Phase of PWR-LOCA using CCTF," Journal of Nuclear Science and Technology, Vol. 19, No. 9, pp. 705-719 (September 1982).

J-912   Murao, Y., Sudoh, T., Iguchi, T., et al, "Findings in CCTF Core-I Test," Proceedings of the Tenth Water Reactor Safety Information Meeting, October 12-15, 1982, NUREG/CP-0041, Vol. 1, pp. 275-286.

J-913   Adachi, H., Sudo, Y., Sobajima, M., et al, "SCTF Core-I Reflood Test Results," presented at the Tenth Water Reactor Safety Information Meeting, October 12-15, 1982, NUREG/CP-0041, Vol. 1, pp. 287-306.

J-914   Sobajima, M., and Ohnuki, A., "Carryover Characteristic during Reflood Process in Large Scale Separate Effects Tests," Nuclear Engineering and Design, Vol. 74, No. 2, pp. 165-171 (February 1983).

J-915   Ohnuki, A., and Sobajima, M., "Mass Effluent Rate Out of Core during Reflood," Journal of Nuclear Science and Technology, Vol. 20, No. 3, pp. 267-269 (March 1983).

J-916   Sudo, Y., and Osakabe, M., "Effects of Partial Flow Blockage on Core Heat Transfer in Forced-Feed Reflood Tests," Journal of Nuclear Science and Technology, Vol. 20, No. 4, pp. 322-332 (April 1983).

J-917   Iguchi, T., and Murao, Y., "Water Accumulation Phenomena in Upper Plenum during Reflood Phase of PWR-LOCA by Using CCTF Data," *Journal of Nuclear Science and Technology*, Vol. 20, No. 6, pp. 453-466 (June 1983).

J-918   Osakabe, M., and Sudo, Y., "Heat Transfer Calculation of Simulated Heater Rods throughout Reflood Phase in Postulated PWR-LOCA Experiments," *Journal of Nuclear Science and Technology*, Vol. 20, No. 7, pp. 559-570 (July 1983).

J-919   Abe, Y., Sudo, Y., and Osakabe, M., "Experimental Study of Upper Core Quench in PWR Reflood Phase," *Journal of Nuclear Science and Technology*, Vol. 20, No. 7, pp. 571-583 (July 1983).

J-920   Sugimoto, J., and Murao, Y., "Experimental Study of Effect of Initial Clad Temperature on Reflood Phenomena during PWR-LOCA," *Journal of Nuclear Science and Technology*, Vol. 20, No. 8, pp. 645-657 (August 1983).

J-921   Iguchi, T., Okubo, T., and Murao, Y., "Visual Study of Flow Behavior in Upper Plenum during Simulated Reflood Phase of PWR-LOCA," *Journal of Nuclear Science and Technology*, Vol. 20, No. 8, pp. 698-700 (August 1983).

J-922   Sudo, Y., and Ohnuki, A., "Mechanism of Falling Water Limitation in Two-Phase Counter Flow through Single Hole Vertical Channel," *Nippon Kikai Gakkai Ronbunshu*, B. Hen, Vol. 49, No. 444, pp. 1685-1694 (August 1983).

J-923   Iwamura, T., Osakabe, M., and Sudo, Y., "Effects of Radial Core Power Profile on Core Thermo-Hydraulic Behavior during Reflood Phase in PWR-LOCAs," *Journal of Nuclear Science and Technology*, Vol. 20, No. 9, pp. 743-751 (September 1983).

J-924   Adachi, H., Sobajima, M., Iwamura, T., et al, "SCTF Core-I Reflood Test Results," Proceedings of the Eleventh Water Reactor Safety Research Information Meeting, October 14-24, 1983, NUREG/CP-0048, Vol. 2, pp. 277-296.

J-925   Murao, Y., Iguchi, T., Sugimoto, J., et al, "Status of CCTF Test Program," Proceedings of the Eleventh Water Reactor Safety Research Information Meeting, October 14-24, 1983, NUREG/CP-0048, Vol. 2, pp. 257-276.

J-926   Sudo, Y., "Parameter Effects on Downcomer Penetration of ECC Water in PWR-LOCA," Journal of Nuclear Science and Technology, Vol. 21, No. 1, pp. 32-41 (January 1984).

J-927   Osakabe, M., and Sudo, Y., "Analysis of Saturated Film Boiling Heat Transfer in Reflood Phase of PWR-LOCA: Turbulent Boundary Layer Model," Journal of Nuclear Science and Technology, Vol. 21, No. 2, pp. 115-125 (February 1984).

J-928   Sugimoto, J., and Murao, Y., "Effect of Grid Spacers on Reflood Heat Transfer in PWR-LOCA," Journal of Nuclear Science and Technology, Vol. 21, No. 2, pp. 103-114 (February 1984).

J-929   Akimoto, H., Iguchi, T., and Murao, Y., "Pressure Drop Through Broken Cold Leg during Reflood Phase of Loss-of-Coolant Accident of Pressurized Water Reactor," Journal of Nuclear Science and Technology, Vol. 21, No. 6, pp. 450-465 (June 1984).

J-930   Murao, Y., "Quench Front Movement during Reflood Phase," Proceedings of the First International Workshop on Fundamental Aspects of Post-Dryout Heat Transfer, April 2-4, 1984, Salt Lake City, UT, USA, NUREG/CP-0060, pp. 103-117.

J-931   Sudo, Y., and Ohnuki, A., "Mechanism of Falling Water Limitation under Counter-Current Flow through a Vertical Flow Path," Bull, JSME, Vol. 27, No. 226, pp. 708-715 (April 1984).

J-932   Murao, Y., Adachi, H., and Iguchi, T., "Status of CCTF/SCTF Test Program," Proceedings of the Twelfth Water Reactor Safety Research Information Meeting, October 23-26, 1984, NUREG/CP-0058, Vol. 2, pp. 342-372.

J-933   Murao, T., Iguchi, T., Okabe, K., et al, "Results of CCTF Upper Plenum Injection Tests," Proceedings of the Twelfth Water Reactor Safety Research Information Meeting, October 23-26, 1984, NUREG/CP-0058, Vol. 2, pp. 306-341.

J-934   Okabe, K., and Murao, Y., "Swelling Model of Two-Phase Mixture in Lower Plenum at End of Blowdown Phase of PWR-LOCA," Journal of Nuclear Science and Technology, Vol. 21, No. 12, pp. 919-930 (December 1984).

J-935   Okubo, T., and Murao, Y., "Experimental Study of ECC Water Injection Rate Effects on Reflood Phase of PWR-LOCA," Journal of Nuclear Science and Technology, Vol. 22, No. 2, pp. 93-108 (February 1985).

J-936   Akimoto, H., Tanaka, Y., Kozawa, Y., et al., "Oscillatory Flows Induced by Direct Contact Condensation of Flowing Steam with Injected Water," Journal of Nuclear Science and Technology, Vol. 22, 1985, pp. 269-283 (April 1985).

J-937   Sobajima, M., and Adachi, H., "Coolability Study on Two-Bundle Scale Flow Blockage in the Reflood Process," Nuclear Engineering and Design, Vol. 86, No. 3, pp. 345-355 (June 1985).

J-938   Iwamura, T., and Adachi, H., "Initial Thermal-Hydraulic Behaviors under Simultaneous ECC Water Injection into Cold Leg and Upper Plenum in a PWR LOCA," Journal of Nuclear Science and Technology, Vol. 22, No. 6, pp. 451-460 (June 1985).

J-939   Akimoto, H., Iguchi, T., and Murao, Y., "Core Radial Power Profile Effect on System and Core Cooling Behavior during Reflood Phase of PWR-LOCA with CCTF Data," Journal of Nuclear Science and Technology, Vol. 22, No. 7, pp. 538-550 (July 1985).

J-940   Iguchi, T., and Murao, Y., "Experimental Study on Reflood Behavior in PWR with Upper Plenum Injection Type ECCS by Using CCTF," Journal of Nuclear Science and Technology, Vol. 22, No. 8, pp. 637-652 (August 1985).

J-941   Sobajima, M., "Experimental Modeling of Steam-Water Countercurrent Flow Limit for Perforated Plates," Journal of Nuclear Science and Technology, Vol. 22, No. 9, pp. 723-732, (September 1985).

J-942   Murao, Y., Iguchi, T., Sugimoto, J., et al, "Results of CCTF Tests," Proceedings of the Thirteenth Water Reactor Safety Research Information Meeting, October 22-25, 1985, NUREG/CP-0072, Vol. 4, pp. 289-314.

J-943   Iwamura, T., Sobajima, M., Adachi, H., et al, "Results of SCTF Reflood Tests," Proceedings of the Thirteenth Water Reactor Safety Research Information Meeting, October 22-25, 1985, NUREG/CP-0072, Vol. 4, pp. 315-330.

J-944   Sugimoto, J., Okubo, T., and Murao, Y., "Heat Transfer Enhancement due to Water Accumulation near Grid Spacers during Reflood," Proceedings of the Third International Topical Meeting on Reactor Thermal Hydraulics, Newport, RI, USA, October 15-18, 1985.

J-945   Murao, Y., Fujiki, K., and Akimoto, H., "Experimental Assessment of Evaluation Model for Safety Analysis on Reflood Phase of PWR-LOCA," Journal of Nuclear Science and Technology, Vol. 22, No. 11, pp. 890-902 (November 1985).

J-946   Iwamura, T., Adachi, H., and Sobajima, M., "Experimental Study of Two-Dimensional Thermal-Hydraulic Behavior in Core during Reflood Phase of PWR LOCA," Journal of Nuclear Science and Technolgoy, Vol. 23, No. 2, pp. 123-135 (February 1986).

J-947   Ohnuki, A., "Experimental Study of Countercurrent Two-Phase Flow in Horizontal Tube Connected to Inclined Riser," Journal of Nuclear Science and Technology, Vol. 23, No. 3, pp. 219-232 (March 1986).

J-948   Adachi, H., Iwamura, T., Ohnuki, A., et al, "Recent Study on Two-Dimensional Thermal-Hydraulic Behavior in PWR Core During the Reflood Phase of LOCA with the Slab Core Test Facility (SCTF)," Proceedings of the Second International Topical Meeting on Nuclear Power Plant Thermal Hydraulics and Operations, Tokyo, Japan, April 15-17, 1986.

J-949   Sobajima, M., Adachi, H., Iwamura, T., and Ohnuki, A., "Two Dimensional Fall Back Flow and Core Cooling in the Slab Core Test Facility (SCTF)," Proceedings of the Second International Topical Meeting on Nuclear Power Plant Thermal Hydraulics and Operations, Tokyo, Japan, April 15-17, 1986.

J-950   Iguchi, T., Murao, Y., Akimoto, H., et al, "Assessment of Current Safety Evaluation Analysis on the Reflood Phase during a LOCA in a PWR with the Cold Leg Injection Type ECCS: 1) System Behavior, and 2) Thermal-hydraulic Behavior in the Core," Proceedings of the Second International Topical Meeting on Nuclear Power Plant Thermal Hydraulics and Operations, Tokyo, Japan, April 15-17, 1986.

J-951   Abe, Y., Sobajima, M. and Murao, Y., "Experimental Study of Effects of Upward Steam Flow Rate on Quench Propagation by Falling Water Film," Journal of Nuclear Science and Technology, Vol. 23, No. 5, pp. 415-432 (May 1986).

J-952   Iwamura, T., Adachi, H., and Sobajima, M., "Air-Water Two-Phase Cross Flow Resistance in Rod Bundle," Journal of Nuclear Science and Technology, Vol. 23, No. 7, pp. 658-660 (July 1986).

J-953   Iwamura, T., Adachi, H., Sobajima, M. et al, "Heat Transfer Enhancement in SCTF Tests," Proceedings of the Fourteenth Water Reactor Safety Research Information Meeting, October 27-31, 1986, NUREG/CP-0082, Vol. 4, pp. 429-444.

J-954   Iguchi, T., Murao, T., Sugimoto, J., et al, "Summary of CCTF Test Results," Proceedings of the Fourteenth Water Reactor Safety Research Information Meeting, October 27-31, 1986, NUREG/CP-0082, Vol. 4, pp. 387-406.

J-955   Akimoto, H., Iguchi, T., and Murao, Y., "System Pressure Effect on System and Core Cooling Behavior during Reflood Phase of PWR LOCA," Journal of Nuclear Science and Technology, Vol. 24, No. 4, pp. 276-288 (April 1987).

J-956   Ohnuki, A., and Adachi, H., "Limitation of Countercurrent Gas-Liquid Flow in a Horizontal Flow Path Connected to an Inclined Flow Path: Prediction of Gas Velocity on Initiation of Liquid Penetration," Nippon Kikai Gakkai Ronbunshu, B. Hen, Vol. 53, No. 490, pp. 1685-1690 (June 1987).

J-957   Okubo, T., Iguchi, T., and Murao, Y., "Experimental Study of Initial Downcomer Water Accumulation Velocity Effects on Reflood Phase of PWR-LOCA," Journal of Nuclear Science and Technology, Vol. 24, No. 7, pp. 573-579 (July 1987).

J-958   Ohnuki, A., Adachi, H., and Murao, Y., "Scale Effects on Countercurrent Gas-Liquid Flow in Horizontal Tube Connected to Inclined Riser," Proceedings from ANS National Heat Transfer Conference, Pittsburgh, PA, USA, August 9-12, 1987. (Also see J-966.)

J-959   Adachi, H., Iguchi, T., Iwamura, T., et al, "Multi-dimensional Effect Found in SCTF Reflood Tests for US/J PWR," Proceedings of the Fifteenth Water Reactor Safety Information Research Meeting, October 26-30, 1987, NUREG/CP-0091, Vol. 4, pp. 549-558.

J-960   Murao, Y., Iguchi, T., Sugimoto, J., et al, "Reflooding Phenomena of German PWR Estimated from CCTF (Cylindrical Core Test Facility), SCTF (Slab Core Test Facility), and UPTF (Upper Plenum Test Facility) Results," Proceedings of the Fifteenth Water Reactor Safety Research Information Meeting, October 26-30, 1987, Vol. 4 Addenda.

J-961   Okabe, K., and Murao, Y., "Hydrodynamics of ECC Water Bypass and Refill of Lower Plenum at PWR-LOCA," Journal of Nuclear Science and Technology, Vol. 24, No. 10, pp. 785-797 (October 1987).

J-962   Iguchi, T., and Murao, Y., "Effect of Decay Heat Level on Reflood Phenomena during PWR-LOCA," Journal of Nuclear Science and Technology, Vol. 24, No. 10, pp. 821-831 (October 1987).

J-963   Iguchi, T., Murao, Y., Akimoto, H., et al, "Assessment of Current Safety Evaluation Analysis on Reflood Behavior during PWR-LOCA by Using CCTF Data," Journal of Nuclear Science and Technology, Vol. 24, No. 11, pp. 887-896 (November 1987).

J-964   Akimoto, H., Iguchi, T., and Murao, Y., "Effect of Pressure Drop through Broken Cold Leg on Thermal Hydraulic Behavior during Reflood Phase of PWR-LOCA," Journal of Nuclear Science and Technology, Vol. 25, No. 1, pp. 45-55 (January 1988).

J-965   Iguchi, T., and Murao, Y., "Effect of Asymmetric Upper Plenum Injection on Reflood Behavior," Journal of Nuclear Science and Technology, Vol. 25, No. 4, pp. 350-358 (April 1988).

J-966   Ohnuki, A., Adachi, H., and Murao, Y., "Scale Effects on Countercurrent Gas-Liquid Flow in a Horizontal Tube Connected to an Inclined Riser," Nuclear Engineering and Design, Vol. 107. No. 3, pp. 283-294 (May 1988). (Also see J-958.)

J-967   Iguchi, T., Iwamura, T., Akimoto, H., et al, "SCTF-III Test Plan and Recent SCTF-III Test Results," Nuclear Engineering and Design, Vol. 108, No. 1/2, pp. 241-247 (June 1988).

J-968   Iguchi, T., Murao, Y., and Sugimoto, J., "Summary of CCTF Test Results - - Assessment of Current Safety Evaluation Analysis on Reflood Behavior during a LOCA in a PWR with Cold-Leg-Injection-Type ECCS," Nuclear Engineering and Design, Vol. 108, No. 1/2, pp. 233-239 (June 1988).

J-969   Iguchi, T., Okubo, T., and Murao, Y., "Effect of Loop Seal on Reflood Phenomena in PWR," Journal of Nuclear Science and Technology, Vol. 25, No. 6, pp. 520-527 (June 1988).

J-970   Iguchi, T., Adachi, H., Sugimoto, J., et al, "Recent Results of Analytical Study on SCTF-III Tests for Reflood Phenomena of PWR with Combined-Injection-Type ECCS under Cold-Leg-Large-Break LOCA," Proceedings of the Sixteenth Water Reactor Safety Research Information Meeting, October 24-27, 1988, NUREG/CP-0097, Vol. 4, pp. 557-581.

J-971   Iwamura, T., Iguchi, T., Adachi, H., and Murao, Y., "Quantitative Evaluation of Heat Transfer Enhancement due to Radial Power Distribution during Reflood Phase of PWR-LOCA," Journal of Nuclear Science and Technology, Vol. 26, No. 4, pp. 428-440 (April 1989).

J-972   Murao, Y., Iguchi, T., Adachi, H., et al, "Multi-Dimensional Thermal-Hydraulics in Pressure Vessel during Reflood Phase of a PWR-LOCA," Proceedings of the Fourth International Topical Meeting on Nuclear Reactor Thermal-Hydraulics (NURETH-4), Karlsruhe, FRG, October 1989.

J-973   Okubo, T., Iguchi, T., and Murao, Y., "Experimental Study of Reflooding Behavior in PWRs under Downcomer Injection," Journal of Nuclear Science and Technology, Vol. 27, No. 1, pp. 30-44 (January 1990).

J-974   Ohnuki, A., Akimoto, H., and Murao, Y., "Effect of Liquid Flow Rate on Film Boiling Heat Transfer during Reflood in Rod Bundle," Journal of Nuclear Science and Technology, Vol. 27, No. 6, pp. 535-546 (June 1990).

Papers - Code Analysis

J-981   Murao, Y., "Analytical Study of Thermo-Hydrodynamic Behavior of Reflood-Phase during LOCA," Journal of Nuclear Science and Technology, Vol. 16, No. 11, pp. 802-817 (November 1979).

J-982   Murao, Y., Sugimoto, J., Okubo, T., et al, "Reflood Code Development Work in JAERI," Proceedings of the Eleventh Water Reactor Safety Research Information Meeting, October 11-24, 1983, NUREG/CP-0048, Vol. 1, pp. 137-149.

J-983   Murao, Y., "Reflood Analysis Code REFLA," Proceedings of the First International Workshop on Fundamental Aspects of Post-Dryout Heat Transfer, Salt Lake City, UT, USA, April 2-4, 1984, NUREG/CP-0060, pp. 56-67.

J-984 Okubo, T., and Murao, Y., "Assessment of Core Thermo-Hydrodynamic Models of REFLA-1D Code with CCTF Data for Reflood Phase of PWR-LOCA," Journal of Nuclear Science and Technology, Vol. 22, No. 12, pp. 983-994 (December 1985).

J-985 Akimoto, H., "Analysis of TRAC-PF1 Calculated Core Heat Transfer for CCTF Test C1-5 (Run 14)," Nuclear Engineering and Design, Vol. 88, pp. 215-227 (1985).

J-986 Sugimoto, J., Sudoh, T., and Murao, Y., "Analytical Study of Thermal Response Similarity between Simulated Fuel Rods and Nuclear Fuel Rods during Reflood Phase of PWR-LOCA," Journal of Nuclear Science and Technology, Vol. 23, No. 4, pp. 315-325 (April 1986).

J-987 Murao, Y., Iguchi, T., Adachi, H., et al, "Development of Reflood Model at JAERI," Proceedings of the Fourteenth Water Reactor Safety Research Information Meeting, October 27-31, 1986, NUREG/CP-0082, Vol. 4, pp. 445-458.

J-988 Akimoto, H., Iwamura, T., Ohnuki, A., et al, "Status of J-TRAC Code Development," Proceedings of the Fourteenth Water Reactor Safety Research Information Meeting, October 27-31, 1986, NUREG/CP-0082, Vol. 5, pp. 381-394.

J-989 Iguchi, T., Murao, Y., and Akimoto, H., "Assessment of Core Radial Profile Effect Model for REFLA Code by Using CCTF Data," Journal of Nuclear Science and Technology, Vol. 24, No. 7, pp. 536-546 (July 1987).

J-990 Murao, Y., "Status of Development of Thermal-Hydraulic Reactor Transient Analysis Code J-TRAC and Future Plan," Proceedings of the Fourth Seminar on Software Development in Nuclear Energy Research," Tokai, Ibaraki, Japan, September 9-10, 1987, JAERI-M-87-199, pp. 18-48.

J-991 Murao, Y., and Hojo, T., "Numerical Simulation of Reflooding Behavior in Tight-Lattice Rod Bundles," Nuclear Technology Vol. 80, No. 1, pp. 83-92 (January 1988).

J-992 Hojo, T., Iguchi, T., and Murao, Y., "Application of REFLA Core Model to Safety Evaluation Code," Journal of Nuclear Science and Technology, Vol. 25, No. 2, pp. 190-197 (February 1988).

J-993   Murao, Y., "Status of ICAP Activities in Japan," Proceedings of the Sixteenth Water Reactor Safety Research Information Meeting, October 24-27, 1988, NUREG/CP-0097, Vol. 4, pp. 199-218.

J-994   Akimoto, J., Ohnuki, A., Kikuta, M., et al, "Assessment of J-TRAC Code with CCTF/SCTF Test Data," Proceedings of the Sixteenth Water Reactor Safety Research Information Meeting, October 24-27, 1988, NUREG/CP-0097, Vol. 4, pp. 583-606.

J-995   Okubo, T., Sugimoto, J., Iguchi, T., and Murao, Y., "Developmental Assessment of REFLA-1DS Code with Data from CCTF Tests for Reflood Phase of LOCA in PWRs with Cold-Leg-Injection Type ECCS," Proceedings of the Fourth International Topical Meeting on Nuclear Reactor Thermal Hydraulics (NURETH-4), Karlsruhe, FRG, October 10-13, 1989, Vol. 1, pp. 190-195.

J-996   Murao, Y., Akimoto, H., Iguchi, T., et al, "Code Improvements Based on Results from the 2D/3D and ICAP Activities," Proceedings of the Seventeenth Water Reactor Safety Research Information Meeting, October 23-25, 1989, NUREG/CP-0105, Vol. 3, pp. 159-186.

J-997   Asaka, H., Murao, Y., and Kukita, Y., "Assessment of TRAC-PF1 Condensation Heat Transfer Model for Analysis of ECC Water Injection Transients," Journal of Nuclear Science and Technology, Vol. 26, No. 11, pp. 1045-1057 (November 1989).

REPORTS AND PAPERS PUBLISHED BY US WITHIN 2D/3D PROGRAM

EVALUATION REPORTS

CCTF Core-I

U-401   "Research Information Report on the Results of the Core-I Test Series at the Japan Atomic Energy Research Institute Cylindrical Core Test Facility," prepared by MPR Associates, MPR-863, Revision 1, October 1985.

CCTF Core-II

U-411   "Literature Survey of Emergency Core Cooling Tests Related to Upper Plenum Injection," prepared by MPR Associates, Revision 1, December 18, 1985.

U-412   "CCTF-II Research Information Report for Tests Related to Upper Plenum Injection (UPI)," prepared by MPR Associates, MPR-933, March 1987.

U-413   "Evaluation of Thermal Hydraulic Behavior in the CCTF-II Best Estimate Reflood Test," prepared by MPR Associates, Revision 1, April 20, 1987.

U-414   "Research Information Report for the Cylindrical Core Test Facility (CCTF) Core-II Test Series (Excluding Tests Involving Upper Plenum Injection)," prepared by MPR Associates, MPR-934, April 1988.

SCTF Core-I

U-421   "Research Information Report on the Results of the Core-I Test Series at the Japan Atomic Energy Research Institute Slab Core Test Facility," prepared by MPR Associates, MPR-918, April 1988.

SCTF Core-II

U-431   "Research Information Report on the Slab Core Test Facility (SCTF) Core-II Test Series," prepared by MPR Associates, MPR-1115, July 1989.

SCTF Core-III

U-441   "Research Information Report on the Slab Core Test Facility (SCTF) Core-III
          Test Series," prepared by MPR Associates, MPR-1263, September 1992.

UPTF

U-451   "Upper Plenum Injection (UPI) of Emergency Core Coolant (ECC) --
          Previous Tests and Analyses, and Capabilities of the Upper Plenum Test
          Facility (UPTF) to Perform UPI Tests," prepared by MPR Associates,
          September 13, 1985.

U-452   "Summary of Results from the UPTF Hot Leg Separate Effects Test,
          Comparison to Scaled Tests and Application to U.S. Pressurized Water
          Reactors," prepared by MPR Associates, MPR-1024, Revision 1,
          December 1987.

U-453   "Evaluation of the UPTF Entrainment/De-entrainment Test," Revision 1,
          prepared by MPR Associates, April 1, 1988.

U-454   "Summary of Results from the UPTF Upper Plenum Injection (UPI) Separate
          Effects Test, Comparison to Previous Scaled Tests and Application to U.S.
          Pressurized Water Reactors," prepared jointly by MPR Associates and
          Siemens (UB KWU) December 1988.

U-455   "Summary of Results from the UPTF Downcomer Separate Effects Tests,
          Comparison to Previous Scaled Tests and Application to U.S. Pressurized
          Water Reactors," prepared by MPR Associates, MPR-1163, July 1990.

U-456   "Summary of Results from the UPTF Carryover/Steam Binding Separate
          Effects Tests, Comparison to Previous Scaled Tests and Application to U.S.
          Pressurized Water Reactors," prepared by MPR Associates, MPR-1213,
          October 1990.

U-457   Theofanous, T.G., and Yan, H., "A Unified Interpretation of One- Fifth to Full
          Scale Thermal Mixing Experiments Related to Pressurized Thermal Shock,"
          University of California at Santa Barbara, NUREG/CR-5677, April 1991.

U-458   "Summary of Results from the UPTF Cold Leg Flow Regime Separate
          Effects Tests, Comparison to Previous Scaled Tests and Application to U.S.
          Pressurized Water Reactors," prepared by MPR Associates, MPR-1208,
          October 1992.

U-459   "Evaluation of Accumulator Nitrogen Discharge During a PWR Large Break LOCA," prepared by MPR Associates, MPR-1331, September 1992.

U-460   "Summary of Results from the UPTF Downcomer Injection/Vent Valve Separate Effects Tests, Comparison to Previous Scaled Tests and Application to U.S. Pressurized Water Reactors," prepared by MPR Associates, MPR-1329, September 1992.

CODE ANALYSIS REPORTS

CCTF Core-I

U-601   Motley, F., "Research Information Report Results From TRAC Analysis Of Cylindrical Core Test Facility Core-I Test Series," Los Alamos National Laboratory, LA-2D/3D-TN-86-10, July 1986.

U-602   Okubo, T., and Fujita, R.K., "Summary of Analysis of TRAC-PD2 Post Test Calculations for CCTF Core-I Parametric Effects Test," Los Alamos National Laboratory, LA-2D/3D-TN-82-5, February 1982.

U-603   Ireland, J.R., "Cylindrical Core Test Facility (CCTF) Posttest Sensitivity Analysis of Test C1-1 (Run 10) Using TRAC-PD2," Los Alamos National Laboratory, LA-UR-80-1999, July 1980.

U-604   Motley, F., "TRAC Analysis of CCTF Base Case C1-5 (Run 14) with a Multidimensional Model," Los Alamos National Laboratory, LA-2D/3D-TN-81-29, September 1981.

U-605   Okubo, T., "Analysis of a TRAC-PD2 Post-test Calculation of CCTF Test C1-5 (Run 14)," Los Alamos National Laboratory, LA-2D/3D-TN-81-26, October 1981.

U-606   Fujita, R.K., "TRAC-PD2 Post-Test Analysis of CCTF Test C1-5 (Run 14)," Los Alamos National Laboratory, LA-2D/3D-TN-81-27, October 1981.

U-607   Okubo, T., "An Analysis of a TRAC-PD2 Post-Test Calculation of CCTF Test C1-6 (Run 15)," Los Alamos National Laboratory, LA-2D/3D-TN-81-34, October 1981.

U-608   Okubo, T., "An Analysis of a TRAC-PD2 Code Calculation for CCTF Test C1-6 (Run 15)," Los Alamos National Laboratory, LA-2D/3D-TN-82-8, March 1982.

U-609   Fujita, R.K., "TRAC-PD2 Post Test Analysis of CCTF Test C1-10 (Run 19),"
          Los Alamos National Laboratory, LA-2D/3D-TN-81-30, October 1981.

U-610   Brown, T., and Williams, K.A., "TRAC-PD2 Post Test Analysis of CCTF Test
          C1-11 (Run 20)," Los Alamos National Laboratory, LA-2D/3D-TN-81-11,
          January 1981.

U-611   Fujita, R.K., "Analysis of CCTF Core-I Test C1-11 (Run 20)," Los Alamos
          National Laboratory, LA-2D/3D-TN-81-13, April 1981.

U-612   Fujita, R.K., "TRAC-PD2 Post Test Analysis of CCTF Test C1-12 (Run 21),"
          Los Alamos National Laboratory, LA-2D/3D-TN-81-31, October 1981.

U-613   Sugimoto, J., "TRAC-PD2 Reflood Code Assessment for CCTF Test C1-16,"
          Los Alamos National Laboratory, LA-2D/3D-TN-81-9, February 1981.

U-614   Motley, F., "TRAC-PD2 Post Test Analysis of the CCTF Evaluation Model
          Test C1-19 (Run 38)," Los Alamos National Laboratory, LA-2D/3D-TN-82-7,
          March 1982.

U-615   Akimoto, H., "Analysis of TRAC-PD2 and CCTF Results for the Cylindrical
          Core Test Facility Evaluation Model Test C1-19 (Run 38)," Los Alamos
          National Laboratory, LA-2D/3D-TN-82-9, September 1982.

U-616   Motley, F., "TRAC-PD2 Analysis of CCTF Multidimensional Test 11 (C1-20,
          Run 39)," Los Alamos National Laboratory, LA-2D/3D-TN-81-28, October
          1981.

U-617   Fujita, R.K., "Data Analysis of CCTF Core-I Base Case and Selected
          Parametric Effects Tests," Los Alamos National Laboratory, LA-2D/3D-TN-
          81-16, April 1981.

U-618   Williams, K.A., "Double Blind Pretest Prediction of the CCTF Core-I
          Evaluation Model Test Using TRAC-PD2," Los Alamos National Laboratory
          LA-2D/3D-TN-81-12, March 1981.

CCTF Core-II

U-621   Crowley, C.J., Cappiello, M.W., and Boyack, B.E., "Summary Report of TRAC-PF1 Assessment Against the CCTF Core-II Data," Los Alamos National Laboratory, LA-CP-89-17, February 1989.

U-622   Cappiello, M.W., Stumpf, H.J., and Boyack, B.E., "CCTF Core-II Upper Plenum Injection Summary," Los Alamos National Laboratory, LA-2D/3D-TN-86-16, March 1987.

U-623   Kotas, J.F., "TRAC-PF1 Calculation of CCTF Core-II Acceptance Test-1 (C2-AC1, Run 51)," Los Alamos National Laboratory, LA-2D/3D-TN-83-10, September 1983.

U-624   Motley, F., "TRAC-PF1 Calculation of CCTF Core-II Base Case (C2-SH1, Run 53)," prepared by Los Alamos National Laboratory, LA-2D/3D-TN-83-12, September 1983.

U-625   Crowley, C.J. and Rothe, P.H., "TRAC-PF1 Calculation of CCTF Core-II Reflood Test 54 (C2-SH2)," Los Alamos National Laboratory, LA-2D/3D-TN-86-2, March 1986.

U-626   Boyack, B.E., "TRAC-PF1/MOD1 Analysis of CCTF UPI Test C2-AA1 (Run 57)," Los Alamos National Laboratory, LA-2D/3D-TN-86-6, April 1986.

U-627   Roberts, M., "TRAC-PF1/MOD1 Upper Plenum Nodalization Studies of CCTF UPI Test C2-AA1 (Run 57)," Los Alamos National Laboratory, LA-2D/3D-TN-86-14, March 1986.

U-628   Siebe, D.A. and Boyer, B., "The Analysis of CCTF Run 58 with TRAC PF1/MOD1," Los Alamos National Laboratory, LA-2D/3D-TN-86-19.

U-629   Cappiello, M., "CCTF Run 59 TRAC-PF1/MOD1 Analysis," Los Alamos National Laboratory, LA-2D/3D-TN-85-1, January 1985.

U-630   Kotas, J.F., "The Effect of the Radial Power Upon the Reflood Phase of a Loss-of-Coolant Accident: A TRAC Analysis of CCTF Test C2-5 (Run 63) and CCTF Test C2-6 (Run 64)," Los Alamos National Laboratory, LA-2D/3D-TN-84-6, September 1984.

U-631   Slater, C.E., "TRAC-PF1 Calculation of CCTF Core-II Reflood Test C2-10 (Run 69)," Los Alamos National Laboratory, LA-2D/3D-TN-85-7, September 1984.

U-632   Crowley, C.J., Fanning, M.W., and Rothe, P.H., "TRAC-PF1 Calculation of CCTF Core-II Refill Test 70," Los Alamos National Laboratory, LA-2D/3D-TN-85-14, December 1985.

U-633   Stumpf, H.J. and Wiilcutt, G.J., "CCTF Run 71 TRAC-PF1/MOD1 Analysis," Los Alamos National Laboratory, LA-2D/3D-TN-86-8, May 1986.

U-634   Cappiello, M.W., "TRAC-PF1/MOD1 Analysis of CCTF No-Failure UPI Test C2-13 (Run-72)," Los Alamos National Laboratory, LA-2D/3D-TN-86-7, July 1986.

U-635   Crowley, C.J. and Rothe, P.H., "TRAC-PF1 Calculation of CCTF Core-II Reflood Test 75 (C2-15)," Los Alamos National Laboratory, LA-2D/3D-TN-86-1, April 1986.

U-636   Stumpf, H.J., "CCTF Run 76 TRAC-PF1/MOD1 Analysis," Los Alamos National Laboratory, LA-2D/3D-TN-86-6, April 1986.

U-637   Stumpf, H.J., "CCTF Run 78 TRAC-PF1/MOD1 Analysis," Los Alamos National Laboratory, LA-2D/3D-TN-86-5, May 1986.

U-638   Cappiello, M.W., "TRAC-PF1/MOD1 Analysis of CCTF Combined Injection Test Run 79," Los Alamos National Laboratory, LA-2D/3D-TN-86-20.

SCTF Core-I

U-641   Williams, K.A., "Research Information Report on the TRAC Analysis and Experimental Results of the Core-I Test Series at the Japan Atomic Energy Research Institute Slab Core Test Facility," prepared by Los Alamos National Laboratory, LA-CP-88-52, March 1988.

U-642   Smith, S., "SCTF Steam Supply Design Analysis with TRAC," Los Alamos National Laboratory, NUREG/CR-1946, May 1981.

U-643   Smith, S., "A Parametric Study of the Effect of Material Properties on the Calculated Rod Heatup Rate for the SCTF," Los Alamos National Laboratory, LA-2D/3D-TN-81-21, June 1981.

U-644   Smith, S., "Revision of the TRAC Calculational Model for the SCTF," Los Alamos National Laboratory, LA-2D/3D-TN-81-17, October 1981.

U-645   Smith, S., "TRAC Analysis of the SCTF High Pressure Shakedown Test: Run 506," Los Alamos National Laboratory, LA-2D/3D-TN-81-22, October 1981.

U-646   Smith, S., "TRAC Analysis of the SCTF Base Case Test Run 507," Los Alamos National Laboratory, LA-2D/3D-TN-81-23, October 1981.

U-647   Smith, S., "TRAC Analysis of the SCTF Low Pressure Test: Run 508," Los Alamos National Laboratory, LA-2D/3D-TN-81-24, October 1981.

U-648   Smith, S., "TRAC Analysis of the SCTF High Subcooling Test: Run 510," Los Alamos National Laboratory, LA-2D/3D-TN-81-25, December 1981.

U-649   Fujita, R.K., "TRAC-PD2 Analysis of SCTF Power-Effects Tests," Los Alamos National Laboratory, LA-2D/3D-TN-82-3, March 1982.

U-650   Fujita, R.K., "TRAC-PD2 Analysis of SCTF Peak Core Power-Effects Tests," Los Alamos National Laboratory, LA-2D/3D-TN-82-5, March 1982.

U-651   Sudo, Y., "Analysis of TRAC and SCTF Results for System Pressure Effects Tests Under Forced Flooding: Runs 506, 507 and 508," Los Alamos National Laboratory, NUREG/CR-2622 (LA-2D/3D-TN-81-33; LA-9258-MS) March 1982.

U-652   Smith, S., "TRAC Analysis of the SCTF Forced Flooding ECC Injection Rate Tests: Runs 507, 511 and 515," Los Alamos National Laboratory, LA-2D/3D-TN-82-04, September 1982.

U-653   Smith, S., "Analysis of the SCTF FLECHT Counterpart Test Using TRAC-PF1," Los Alamos National Laboratory, LA-2D/3D-TN-83-02, January 1983.

U-654   Gilbert, J.S. and Williams, K.A., "Rod Bundle Cross-Flow Study," Los Alamos National Laboratory, LA-2D/3D-TN-83-13, September 1983.

U-655   Osakabe, M., Gilbert, J.S., and Fujita, R.K., "TRAC-PD2 Analysis of Radial Core Pressure Loss During Reflood for Test S1-08," Los Alamos National Laboratory, LA-2D/3D-TN-83-16, December 1983.

U-656   Lin, J.C., "TRAC-PF1 Calculation of SCTF Core-I Combined Injection Test: Run 529," Los Alamos National Laboratory, LA-2D/3D-TN-84-7, November 1984.

SCTF Core-II

U-661   Shire, P.R., Gilbert, J.S., and Lin, J.C., "SCTF Core-II TRAC-PF1/MOD1 Analysis Summary," Los Alamos National Laboratory, LA-CP-89-113, May 1, 1989.

U-662   Gilbert, J.S., "TRAC-PF1/MOD1 Calculation of SCTF Core-II Test S2-SH1 (Run 604)," Los Alamos National Laboratory, LA-2D/3D-TN-85-6, March 1985.

U-663   Shire, P.R. and Boyack, B.E, "Upper-Plenum Studies of SCTF Run 605," Los Alamos National Laboratory, LA-2D/3D-TN-86-15, August 1986.

U-664   Shire, P.R., "TRAC-PF1/MOD1 Re-Analysis of SCTF Core-II Test S2-SH2 (Run 605)," Los Alamos National Laboratory, LA-CP-87-103, December 1986.

U-665   Lin, J.C., "TRAC-PF1/MOD1 Calculation of SCTF Core-II Supply Test S2-03 (Run 608)," Los Alamos National Laboratory, LA-2D/3D-TN-85-13, July 1985.

U-666   Abe, Y., Lin, J.C., and Gilbert, J., "TRAC-PF1/MOD1 Calculation of SCTF Core-II Steam Supply Test S2-05 (Run 610)," Los Alamos National Laboratory, LA-2D/3D-TN-85-9, July 1985.

U-667   Gilbert, J.S., "TRAC-PF1/MOD1 Calculation of SCTF Core-II Test S2-06 (Run 611)," Los Alamos National Laboratory, LA-2D/3D-TN-86-9, March 1986.

U-668   Lin, J.C., "TRAC-PF1/MOD1 Calculation of SCTF Core-II FLECHT-SET Coupling Test S2-08 (Run 613)," Los Alamos National Laboratory, LA-2D/3D-TN-85-2, February 1985.

U-669   Gilbert, J.S., "TRAC-PF1/MOD1 Calculation of SCTF Core-II Test S2-09 (Run 614)," Los Alamos National Laboratory, LA-2D/3D-TN-85-4, March 1985.

U-670   Gilbert, J.S., "TRAC-PF1/MOD1 Calculation of SCTF Core-II Test S2-12 (Run 617)," Los Alamos National Laboratory, LA-2D/3D-TN-86-13, March 1987.

SCTF Core-III

U-681   Boyack, B.E., Shire, P.R., and Harmony, S.C., "TRAC-PF1/MOD1 Code Assessment Summary Report for SCTF Core-III," by Los Alamos National Laboratory, LA-CP-90-71, February 1990.

U-682   Gilbert, J.S., "TRAC-PF1/MOD1 Calculation of Operational Study No. 1," Los Alamos National Laboratory, LA-CP-87-112.

U-683   Harmony, S.C. and Boyack, B.E., "A Posttest Analysis of SCTF Run 703 Using TRAC-PF1/MOD1," Los Alamos National Laboratory, (to be issued).

U-684   Mascheroni, P.L. and Boyack, B.E., A Posttest Analysis of SCTF Run 704 Using TRAC-PF1/MOD1," Los Alamos National Laboratory, LA-CP-88-131, June 1988.

U-685   Harmony, S.C., "TRAC-PF1/MOD1 Analysis of SCTF Test S3-5 (Run 709)," Los Alamos National Laboratory, (to be issued).

U-686   Shire, P.R., "TRAC-PF1/MOD1 Analysis of SCTF Core-III Test S3-9 (Run 713)," Los Alamos National Laboratory, LA-CP-88-11, January 1988.

U-687   Harmony, S.C. and Boyack, B.E., "A Posttest Analysis of SCTF Run 714 Using TRAC-PF1/MOD1," Los Alamos National Laboratory, LA-CP-88-234, September 1988.

U-688   Boyack, B.E., "A Posttest Assessment of TRAC-PF1/MOD1 and TRAC-PF1/MOD2 Using SCTF Core-III Run 719 (Test S3-15)," Los Alamos National Laboratory, LA-CP-90-27, January 1990.

U-689   Rhee, G., "A Posttest Analysis of SCTF Run 720 Using TRAC-PF1/MOD1," Los Alamos National Laboratory, (to be issued).

UPTF

U-701   Cappiello, M.W., "TRAC-PF1 Calculations of a UPTF Intact Loop during ECC Injection," Los Alamos National Laboratory, LA-2D/3D-TN-81-20, May 1981.

U-702   Cappiello, M. "GPWR and UPTF Intact Loop Calculations -- Assessment of UPTF Alternative Loop Configurations," Los Alamos National Laboratory, LA-2D/3D-TN-82-2, January 1982.

U-703   Cappiello, M. "An Analysis of the UPTF Base Case with TRAC-PF1/MOD1," Los Alamos National Laboratory, LA-2D/3D-TN-85-8, July 1985.

U-704   Ohnuki, A. and Cappiello, M.W., "Assessment of TRAC-PF1/MOD1 for Countercurrent-Annular and Stratified Flows," Los Alamos National Laboratory, LA-2D/3D-TN-85-3, September 1985 (publicly released as a JAERI-M Report -- see J-629).

U-705   Dotson, P., "UPTF Downcomer Pretest Analysis," Los Alamos National Laboratory, LA-2D/3D-TN-85-10, October 1985.

U-706   Dotson, P., "Small-Break LOCA TRAC Pretest Calculation," Los Alamos National Laboratory, LA-2D/3D-TN-86-4, December 1986.

U-707   Hedstrom, J., and Cappiello, M.W., "Results of a Pretest Analysis of the UPTF US/Japanese Integral Test," Los Alamos National Laboratory, LA-2D/3D-TN-86-17, March 1987.

U-708   Cappiello, M., "Posttest Analysis of the Upper Plenum Test Facility Small-Break Loss-of-Coolant Accident Test with TRAC-PF1/MOD1 and MOD2," Los Alamos National Laboratory, LA-CP-88-154, July 1988.

U-709   Stumpf, H.J., "Posttest Analysis of UPTF Test 10B Using TRAC-PF1/MOD1," Los Alamos National Laboratory, LA-CP-90-1, January 1990.

U-710   Shire, P.R., "TRAC-PF1/MOD2 Analysis of UPTF Test 20 Upper Plenum Injection in a Two-Loop PWR," Los Alamos National Laboratory, LA-CP-90-2, January 1990.

U-711   Siebe, D.A., and Stumpf, H.J., "Posttest Analysis of the Upper Plenum Test Facility Downcomer Separate Effects Tests with TRAC- PF1/MOD2," Los Alamos National Laboratory, LA-CP-90-299, July 1990.

U-712   Stumpf, H.J., "Posttest Analysis of UPTF Test 08 Using TRAC-PF1/MOD2," Los Alamos National Laboratory, LA-CP-90-373, September 6, 1990.

U-713   Siebe, D.A., and Stumpf, H.J., "Assessment of the Ability of TRAC-PF1/MOD1 and TRAC-PF1/MOD2 to Predict Phenomena Related to Steam Binding," Los Alamos National Laboratory, LA-CP-92-79, March 1992.

U-714   Mullen, E. M., Stumpf, H. J. and Siebe, D. A., "Summary of Cold-Leg Flow Phenomena Observed in UPTF and CCTF Tests and TRAC Posttest Analyses," Los Alamos National Laboratory, LA-CP-91-332, September 1991.

U-715   Mullen, E.M., Stumpf, H.J., and Siebe, D.A., "Summary of Downcomer Injection Phenomena for UPTF and TRAC Post-test Analysis," Los Alamos National Laboratory, LA-CP-92-188, May 1992.

U-716   Siebe, D.A., and Stumpf, H.J., "An Assessment of TRAC-PF1/MOD2 against Data from the Upper Plenum Test Facility for Accumulator Nitrogen Surge," Los Alamos National Laboratory, LA-CP-92-408, November 1992.

US/J PWRs

U-721   Ireland, J. and Liles, D., "A TRAC-PD2 Analysis of a Large-Break Loss-of-Coolant Accident in a Reference US PWR," Los Alamos National Laboratory, LA-2D/3D-TN-81-10, March 1981.

U-722   Fujita, R.K., Motely, F., and Williams, K.A., "TRAC-PF1 Analysis of a Best-Estimate Large-Break LOCA in Westinghouse PWR with Four Loops and 17 x 17 Fuel," Los Alamos National Laboratory, LA-2D/3D-TN-83-4, September 1983.

U-723   Spore, J.W. and Cappiello, M.W., "TRAC-PF1/MOD1 Analysis of a 200% Cold-Leg Break in a US/Japanese PWR with Four Loops and 15x15 Fuel," Los Alamos National Laboratory, LA-2D/3D-TN-85-11, November 1985.

U-724   Coddington, P. and Motely, F., "TRAC-PF1/MOD1 Analysis of a Minimum Safeguards Large Break Loss-of-Coolant Accident in a 4-Loop PWR with 17 x 17 Fuel," Los Alamos National Laboratory, LA-2D/3D-TN-86-3, August 1986.

U-725   Gido, R.G. and Cappiello, M.W., "TRAC-PF1/MOD1 Analysis of a 200% Cold-Leg Break in a Babcock & Wilcox Lowered Loop Plant," Los Alamos National Laboratory, LA-2D/3D-TN-86-12, October 1986.

U-726   Shire, P.R and Spore, J.W., "TRAC-PF1/MOD1 Analysis of a Minimum Safeguards Large-Break LOCA in a US/Japanese PWR with Four Loops and 15 x 15 Fuel," Los Alamos National Laboratory, LA-CP-87-61, April 1987.

U-727   Gruen, G.E. and Fisher, J.E., "TRAC PF1/MOD1 US/Japanese PWR Conservative LOCA Prediction," EGG Idaho, NUREG/CR-4965 (EGG-2513), November 1987.

GPWRs

U-741   Motley, F. and Cappiello, M., "TRAC-PD2 Hot Leg Sensitivity Study," Los Alamos National Laboratory, LA-2D/3D-TN-81-1, February 1981.

U-742   Motley, F., "Review of the TRAC Calculated GPWR Upper Plenum/Core Flow Conditions to Aid in the Design of UPTF," Los Alamos National Laboratory, LA-2D/3D-TN-81-19, May 1981.

U-743   Motley, F., and Williams K.A., "TRAC-PD2 Calculation of a Double-Ended Cold-Leg Break in a Reference German PWR," Los Alamos National Laboratory, LA-2D/3D-TN-81-32, January 1981.

U-744   Motley, F., "TRAC-PF1 Calculation of a Reference German PWR at the Initiation of ECC Injection," Los Alamos National Laboratory, LA-2D/3D-TN-81-8, February 1981.

U-745   Cappiello, M.W., "TRAC-PF1 Sensitivity Studies of a GPWR Intact Loop During ECC Injection," Los Alamos National Laboratory, LA-2D/3D-TN-81-18, May 1981.

U-746   Cappiello, M.W., and Hrubisko, M., "GPWR-1982 TRAC-PF1 Input Deck Description," Los Alamos National Laboratory, LA-2D/3D-TN-82-10, December 1982.

U-747   Cappiello, M.W., "GPWR-1982 TRAC-PF1 Base Case Results," Los Alamos National Laboratory, LA-2D/3D-TN-83-6, February 1983.

U-748   Cappiello, M.W., and Vojtek, I., "TRAC-PF1 Analysis of a 200% Hot Leg Break in a German PWR," Los Alamos National Laboratory, LA-2D/3D-TN-83-8, August 1983.

ADVANCED INSTRUMENTATION REPORTS

<u>Evaluation of Instrument Performance</u>

U-801   "Program Plan for Correction of US Instrument Degradation or Failure in the Upper Plenum Test Facility (UPTF) in the Federal Republic of Germany," prepared by the Nuclear Regulatory Commission, NUREG-1284, July 1987.

U-802   "Insights Derived from USNRC Advanced Instrumentation in CCTF and SCTF," prepared by MPR Associates, MPR-1035, December 1987.

U-803   Fullmer, K.S., "Review of INEL SCTF Instrumentation," EGG Idaho, EGG-3D-6370, November 1983.

U-804   Fullmer, K.S., "Review of INEL CCTF Instrumentation," EGG Idaho, EGG-3D-6544, April 1984.

U-805   Fullmer, K.S., "Review of INEL CCTF-II Instrumentation," EGG Idaho, EGG-3D-6981, September 1985.

U-806   Fullmer, K.S., "Review of INEL SCTF Core-II Instrumentation," EGG Idaho, EGG-3D-6982, September 1985.

U-807   Hardy, J.E. and Herskovitz, M.B., "Assessment of the Adequacy of ORNL Instrumentation in Reflood Test Facilities," Oak Ridge National Laboratory, NUREG/CR-3651, (ORNL/TM-9067), April 1985.

U-808   Hardy, J.E., et.al., "ORNL Instrumentation Performance for Slab Core Test Facility (SCTF) - Core 1 Reflood Test Facility," Oak Ridge National Laboratory, NUREG/CR-3286 (ORNL/TM-8762), November 1983.

U-809   "ORNL Instrumentation Performance for Slab Core Test Facility Runs 604, 608 and 613," prepared by Oak Ridge National Laboratory, ORNL/NRC/LTR-85/19, June 1985.

U-810   "Performance of ORNL Instrumentation in Cylindrical Core Test Facility - Core-II (CCTF-II) for Runs 075, 076 and 079," prepared by Oak Ridge National Laboratory, ORNL/NRC/LTR-85/18, June 1985.

U-811   Morgan, K.A., "SCTF I Uncertainty Analysis," EGG Idaho, EGG-CAAD-5398, September 1981.

8-71

U-812   Morgan, K.A., "CCTF I Uncertainty Analysis," EGG Idaho, EGG-CAAD-5704, December 1981.

U-813   Lassahn, G.D., "BMFT UPTF Advanced Instrumentation Uncertainty Analysis Report," EGG Idaho, EGG-3D-6751, February 1985.

Instrument Interpretation in Two-Phase Flow

U-821   "Review and Evaluation of ORNL Instrument Development Loop Data and Formulation of a Mass Flow Rate Calculation Scheme," prepared by MPR Associates, March 1983.

U-822   "A Study of Special Effects Around a Tie Plate Turbine Meter in Two-Phase Upflow," prepared by MPR Associates, MPR-826, June 1984.

U-823   "Evaluation of a Steady State Mass Flow Rate Calculation Method Using ORNL Instrument Development Loop Transient Data," prepared by MPR Associates, MPR-859, January 1985.

U-824   Hardy, J.E., "Mass Flow Measurements Under PWR Reflood Conditions in a Downcomer and at a Core Barrel Vent Valve Location," Oak Ridge National Laboratory, NUREG/CR-2710 (ORNL/TM-8331), 1982.

U-825   Thomas, D.G. and Combs, S.K., "Measurement of Two-Phase Flow at the Core/Upper Plenum Interface for a PWR Geometry Under Simulated Reflood Conditions, Oak Ridge National Laboratory, NUREG/CR-3138 (ORNL/TM-8204), 1983.

U-826   Lassahn, G.D., "Mass Flow Estimation Using Subroutines DRPOF4 and EMDOT4," EGG Idaho, EGG-3D-6305, July 1983.

Film and Impedance Probes

U-831   Eads, B.G., et.al., "Advanced Instrumentation for Reflood Studies Program Quarterly Progress Report (October-December 1977)," Oak Ridge National Laboratory, ORNL/NUREG/TM-202, 1977.

U-832   Moorhead, A.J., et.al., "Fabrication of Sensors for High-Temperature Steam Instrumentation Systems," Oak Ridge National Laboratory, NUREG/CR-1359 (ORNL/NUREG-65), 1980.

U-833   Hardy, J.E., et.al., "Transient Testing of an In-core Impedance Flow Sensor in a 9-Rod Heated Bundle," Oak Ridge National Laboratory, ORNL/NUREG/TM-389, 1981

U-834   Hardy, J.E and Hylton, J.O., "Electrical Impedance String Probes for Two-Phase Void and Velocity Measurements," Oak Ridge National Laboratory, ORNL/NUREG/TM-8172, 1982.

Turbine Meters

U-841   "CCTF-II Operation and Maintenance Manual - Turbine Flowmeter Measurement System," Measurements Incorporated OM-236-1, July 1981.

U-842   Jensen, M.F., "Turbine Flowmeter System Tests," EGG Idaho, EGG-3D-5372, March 1981.

Drag Discs

U-846   "CCTF Operation and Maintenance Manual-Instrumented Spool Piece and Downcomer Drag Disk Flow Measurement Systems," prepared by EGG Idaho, EGG-3D-5105, March 1980.

U-847   "UPTF Drag Disk Transducer Test Report," EGG Idaho, EGG-3D-6980, July 1985.

Gamma Densitometers

U-851   "SCTF Operation and Maintenance Manual Single-Beam Density Measurement Systems," prepared by EGG Idaho, EGG-3D-5179, January 1981.

U-852   Rohrdanz, R.F., "Prototype Test Report for the SCTF Single Beam Density Measuring Systems," EGG Idaho, EGG-3D-5457, June 1981.

U-853   Grimesey, R.A. and Tomberlin, T.A., "Radiation Shielding Calculations for UPTF Gammaray Densitometer," EGG Idaho, EGG-PHYS-6201, March 1983.

U-854   Menkhaus, D.E., "BMFT UPTF Densitometer System Test Report," EGG Idaho, EGG-RTH-7075, November 1985.

Liquid Level Detectors/Fluid Distribution Grid

U-861   "CCTF Operation and Maintenance Manual -- Conductivity Liquid Level Measurement System (CLLMS)," EGG Idaho, EGG-3D-5046, December 1979.

U-862   "Optical Liquid-Level Detector Two-Phase Flow Test Report," EGG Idaho, EGG-3D-4523, May 1981.

Spool Pieces and Pipe Flowmeters

U-866   "SCTF Operation and Maintenance Manual -- Cold Leg and Vent Pipe Instrumented Spool Pieces and Downcomer Drag Disk Flow Measurement Systems," prepared by EGG Idaho, EGG-3D-5177, March 1981.

U-867   "SCTF Operation and Maintenance Manual -- Hot Leg Spool Piece Flow Measurement System," prepared by EGG Idaho, EGG-3D-5178, March 1981.

U-868   Cornell, J.A., "Two-Phase Flow Testing of SCTF Hot Leg Spool Piece Data Analysis Report," EGG Idaho, EGG-3D-5416, April 1981.

Velocimeters

U-871   "CCTF-II Operation and Maintenance Manual -- Cooled Velocimeter Flow Measurement System," prepared by EGG Idaho, EGG-3D-5809, April 1982.

U-872   Menkhaus, D.E., "CCTF-II Cooled Velocimeter Probe Performance Test Report," EGG Idaho, EGG-3D-5511, December 1981.

Video Probes

U-876   "CCTF-II Operation and Maintenance Manual -- Video Probe Systems," prepared by EGG Idaho, EGG-3D-5772, April 1982.

PAPERS, PRESENTATIONS, AND CORRESPONDENCE

Papers - Data Evaluation

U-901   Zuber, N., "Proposed UPTF Thermal Mixing Experiments," presented at the
         2D/3D Coordination Meeting, Mannheim, FRG, June 1985.

U-902   Theofanous, T.G., Iyer, K., Nourbakhsh, H.P., and Shabana, E., "Scaling of
         Thermal Mixing Phenomena from 1/5 to Full-Scale Test Facilities,"
         Proceedings of the Fourteenth Water Reactor Safety Information Meeting,
         October 27 - 31, 1986, Vol. 4, pp. 363-386.

U-903   Naff, S.A., "UPTF-Experiment Core Simulator Entrainment/De-entrainment
         Test 10C," Handout G-5 from 2D/3D Coordination Meeting, Mannheim,
         FRG, May 1987.

U-904   Damerell, P.S., Ehrich, N.E., and Wolfe, K.A., "Use of Full-Scale UPTF Data
         to Evaluate Scaling of Downcomer (ECC Bypass) and Hot Leg Two-Phase
         Flow Phenomena," Proceedings of the Fifteenth Water Reactor Safety
         Research Information Meeting, October 26-29, 1987, NUREG/CP-0091,
         Vol. 4, pp. 143-165.

U-905   Rhee, G., Damerell, P., and Simons, J., "Use of 2D/3D Data to Scale Up
         Liquid Carryover/De-entrainment (Steam Binding) Behavior to a PWR,"
         Proceedings of the Sixteenth Water Reactor Safety Research Information
         Meeting, October 24-27, 1988, NUREG/CP-0097, Vol, 4, pp. 485-509.

U-906   Russell, A., Damerell, P., Ahrens, G., and Weiss, P., "UPTF Upper Plenum
         Injection (UPI) Test Results and Application to PWR," Proceedings of the
         Sixteenth Water Reactor Safety Research Information Meeting, October 24-
         27, 1988, NUREG/CP-0097, Vol. 4, pp. 511-531.

Papers - Code Analysis

U-911   Coddington, P., "The Effect of Accumulator Nitrogen on the Reflood of a
         PWR Core during a Large Break LOCA," presented at the IAEA Specialists
         Meeting on Fuel Behavior under Accident Conditions and Acceptance
         Criteria, Warsaw, Poland, September 30 - October 4, 1985.

Papers - Instrumentation

U-921   Eads, G.B., et al., "Development of In-Vessel Reflood Instrumentation at ORNL," Meeting of the Japanese Nuclear Society, Osaka, Japan, March 26-28, 1979.

U-922   Combs, S.K., and Hardy, J.E., "An Experimental Investigation of Flow Monitoring Instrument in the Upper Plenum of an Air-Water Reflood Test Facility," Symposium on Polyphase Flow and Transport Technology, ASME Centennial Meeting, San Francisco, CA, August 12-15, 1980.

U-923   Zabriskie, W.L., et al., "Instrumentation Development for Low Range, Long Line Differential Pressure Measurements," ISA Transactions, Vol. 20, No. 4, pp. 61-75 (1981).

U-924   Hardy, J.E., and Hylton, J.O., "Electrical Impedance String Probes for Two-Phase Void and Velocity Measurements," International Journal of Multiphase Flow, October 1984.

U-925   Hardy, J.E., et al., "Measurement of Two-Phase Flow Momentum with Force Transducers," presented at International Symposium on Gas-Liquid Two-Phase Flows, ASME Winter Annual Meeting, Dallas, Texas, November 1990, CONF-901109-1.

Correspondence

U-931   "US Input to Definition of Test Objectives and Conditions for UPTF Fluid-Fluid Mixing Test (Test No. 1 in Matrix and Sequence)," enclosure to MPR letter from P. Damerell to L. Shotkin (USNRC), February 14, 1986.

U-932   "US Input to Definition of Test Objectives and Conditions for the Third UPTF Cold Leg Injection Integral Test No. 27," enclosure to MPR letter from P. Damerell to G. Rhee (USNRC), February 3, 1989.

REPORTS AND PAPERS EXTERNAL TO 2D/3D PROGRAM

DATA REPORTS

ECC Delivery Depressurization

E-001   Crowley, C.J., et al., "1/5 Scale Countercurrent Flow Data Presentation and Discussion," Creare, NUREG/CR-2106 (Creare TN-333), November 1981.

E-002   Crowley C.,J., et al., "Downcomer Effects in a 1/15 Scale PWR Geometry - Experimental Data Report," Creare, NUREG-0281, May 1977.

E-003   Crowley, C.J., and Sam, R.G., "Experimental Data Report for Flashing Transients," Creare, NUREG/CR-2060 (Creare TN-330), February 1982.

E-004   Cudnik, R.A., et al., "Topical Report on Penetration Behavior in a 1/15 Scale Model of a Four-Loop Pressurized Water Reactor," Battelle Columbus Labs, BMI-NUREG-1973, June 1977.

Upper Plenum Injection

E-011   "Experimental Data Report for Semiscale Mod-1 Tests S-05-6 and S-05-7 (Alternate ECC Injection Tests)," prepared by EGG Idaho, TREE-NUREG-1055, June 1977.

Hot Leg Countercurrent Flow/Reflux Condenser Mode

E-021   "Experiment Data Report for Semiscale Mod-2A Natural Circulation Tests S-NC-2B, S-NC-3 and S-NC-4B," prepared by EGG Idaho, NUREG/CR-2454, December 1981

E-022   "Experiment Data Report for Semiscale Mod-2A Natural Circulation Tests S-NC-5 and S-NC-6," prepared by EGG Idaho, NUREG/CR-2501, January 1982.

E-023   "Experimental Operating Specification, Natural Circulation Test Series, Semiscale Mod-2A," prepared by EGG Idaho, EGG-SEMI-5427, April 1981.

Accumulator Nitrogen Discharge

E-031   Denham, M.K., and Dore, P., "ISP-25 Boundary Conditions and Experimental Procedure for ACHILLES Run A1B105," AEEW, SESD Note 495, September 1988.

EVALUATION REPORTS

General

E-401   "Compendium of ECCS Research for Realistic LOCA Analysis," NUREG-1230, December 1988.

ECC Delivery during Depressurization

E-411   Beckner, W.D. et al., "Analysis of ECC Bypass Data," USNRC, NUREG-0573, July 1979.

E-412   Beckner, W.D., et al., "PWR Lower Plenum Refill Research Results," USNRC Research Information Letter No. 128, December 8, 1981.

E-413   "A Preliminary Study of Annulus ECC Flow Oscillations," Creare, NP-839, Research Project 347-1, August 1978.

E-414   Crowley, C.J., et al., "An Evaluation of ECC Penetration Using Two Scaling Parameters," Creare, Creare TN-233, September 1976.

E-415   Rothe, P.H., "Technical Summary Attachment to ECC Bypass RIL Volume I: Review of Findings," Creare, NUREG/CR-0885, Vol. 1 (Creare TN-296, Vol. 1), July 1979.

E-416   Crowley, C.J., Wei, S., Murrary, J.G., Rothe, P.H., and McKenna, S.A., "Technical Summary Attachment to ECC Bypass RIL Volume II: Technical Appendices," Creare, NUREG/CR-0885, Vol. 2 (Creare TN-296, Vol. 2), July 1979.

E-417   Crowley, C.J., and Sam, R.G., "Experimental Facility and Preliminary Results for Flashing Transients at 1/5 Scale," Creare, Creare TM-707, July 1980.

E-418   Crowley, C.J., Wei, S. and Rothe, P.H., "Analysis of Flashing Transient Effects During Refill," Creare, NUREG/CR-1765, March 1981.

E-419   Crowley, C.J., "Summary of Refill Effects Studies with Flashing and ECC Interactions," Creare, NUREG/CR-2058, November 1981.

E-420   Carbiener, W.A., et al., "Steam-Water Mixing an System Hydrodynamics Program; Task 4; Quarterly Progress Report; January 1, 1977 - March 31, 1977," Battelle Columbus Labs, BMI-NUREG-1972, May 1977.

E-421   Segev, A. and Collier, R.P., "Development of a Mechanistic Model for ECC Penetration in a PWR Downcomer," Battelle Columbus Labs, NUREG/CR-1426, June 1980.

E-422   Segev, A. and Collier, R.P., "Application of Battelle's Mechanistic Model to Lower Plenum Refill," Battelle Columbus Labs, NUREG/CR-2030, March 1981.

Loop Behavior

E-431   Brodrick, J.R., Burchill, W.E., and Lowe, P.A., "1/5 Scale Intact Loop Post-LOCA Steam Relief Tests," Combustion Engineering, CENPD-63, Revision 1, March 1973.

E-432   Burchill, W.E., Lowe, P.A., and Brodrick, J.R., "Steam-Water Mixing Test Program Task D: Formal Report for Task B and Final Report for the Steam Relief Phases of the Test Program," Combustion Engineering, AEC-COO-2244-1 (CENPD-101), October 1973.

E-433   Rothe, P.H., Wallis, G.B., and Thrall, D.E., "Cold Leg Flow Oscillations," Creare Inc., EPRI NP-282, November 1976.

E-434   Crowley, C.J., Sam, R.G. and Rothe, P.H., "Summary Report: Hot Leg ECC Flow Reversal Experiments," Creare R & D, Creare TM-870, 1982.

E-435   Lilly, G.P., Stephens, A.G. and Hochreiter, L.E., "Mixing of Emergency Core Cooling Water with Steam: 1/14 Scale Testing Phase," Westinghouse Electric Corporation, WCAP-8307 (EPRI Program 294-2), January 1975.

E-436   Lilly, G.P. and Hochreiter, L.E., "Mixing of Emergency Core Cooling Water with Steam: 1/3 Scale Test and Summary," Westinghouse Electric Corporation, WCAP-8423 (EPRI Program 294-2), June 1975.

Fluid/Fluid Mixing

E-441   Theofanous, T., et. al, "Decay of Buoyancy Driven Stratified Layers with Application to PTS," Purdue University, NUREG/CR-3700, February 1984.

Core Thermal-Hydraulic Behavior

E-451   Bruestle, H.R., et. al., "Thermal-Hydraulic Analysis of the Semiscale Mod-1 Reflood Test Series (Gravity Feed Tests)," Idaho National Engineering Laboratory, TREE-NUREG-1010, January 1977.

E-452   Cadek, F.F., et. al., "PWR FLECHT Final Report Supplement," Westinghouse Electric Corporation, WCAP-7931, October 1972.

E-453   Catton, I., and Toman, W.I., "Multidimensional Thermal-Hydraulic Reflood Phenomena in a 1692-Rod Slab Core," EPRI-NP-2392, 1982.

E-454   Conway, C.E., et. al., "PWR FLECHT Separate Effects and Systems Effects Test (SEASET), Program Plan," Westinghouse Electric Corporation, WCAP-9183, November 1977.

E-455   DeJarlais, G. and Ishii, M., "Inverted Annular Flow Experimental Study," Argonne National Laboratory, NUREG/CR-4277.

E-456   Addobo, C., Piplies, L. and Riebold, W. L., "LOBI-MOD 2:   Facility Description and Specification for OECD-CNI International Standard Problem No. 18 (ISP-18): Volume 1 - Geometrical Configuration of the Test Facility," CEC Communication No. 4010, July 1983.

E-457   Erbacher, F. J., Neitzel, H. J., and Wiehr, K., "Cladding Deformation and Emergency Core Cooling of a Pressurized Water Reactor in a LOCA," Summary Description of the REBEKA Program, KfK-4781, August 1990.

E-458   Kremin, H., et. al., "Transientenuntersuchungen in der PKL-Anlage (PKL III A) Abschlussbericht, Band 2: Beschreibung der Versuchsanlage," Siemens/KWU, U9 414/89/018, September 1989.

E-459   Arrieta, L. and Yadigaroglu, G., "Analytical Model for Bottom Reflooding Heat Transfer in Light Water Reactors (The UCFLOOD Code)", University of California, EPRI NP-756, August 1978.

E-460   "LOBI-MOD2: Research Program A Final Report," CEC Communication No. 4333, October 1990.

E-461   "Wiehr, K., "REBEKA-Buendelversuche: Untersuchungen zur Wechselwirkung zwischen aufblaehenden Zirkaloy-Huellen und einsetzender Notkuehlung," Abschlussbericht, KfK-4407, May 1988.

Upper Plenum Injection

E-465   Barathan, D., et. al., "An Investigation of the Distribution and Entrainment
         of ECC Water Injection into the Upper Plenum," Thayer School of
         Engineering, Dartmouth College, NUREG/CR-1078, January 1980.

Tie Plate Countercurrent Flow

E-471   Jones, D.D., "Subcooled Countercurrent Flow Limiting Characteristics of the
         Upper Region of a BWR Fuel Bundle," General Electric Company, Nuclear
         Systems Products Division, NEDG-NUREG-23549, 1977.

Steam Binding

E-481   Howard, R.C. and Hochreiter, L.E., "PWR FLECHT SEASET Steam
         Generator Separate Effects Task Data Analysis and Evaluation Report:
         NRC/EPRI/Westinghouse Report No. 9," Westinghouse Electric
         Corporation, NUREG/ CR-1534 (EPRI NP-1461; WCAP-9724),
         February 1982.

Hot Leg Countercurrent Flow/Reflux Condenser Mode

E-491   Krolewski, S.M., "Flooding Limits in a Simulated Nuclear Reactor Hot Leg,"
         Massachusetts Institute of Technology, Submission as Part of Requirement
         for a B.Sc., 1980.

E-492   "PWR FLECHT-SEASET Systems Effects, Natural Circulation and Reflux
         Condensation," prepared by Westinghouse Electric Corporation,
         NUREG/CR-3654 (EPRI NP-3497; WCAP-10415), August 1984.

E-493   Richter, H.J., Wallis, G.B., Carter, K.H. and Murphy, S.L., "Deentrainment
         and Countercurrent Air-water Flow in a Model PWR Hot Leg," Thayer
         School of Engineering, September 1978.

E-494   "ROSA-IV Large Scale Test Facility (LSTF) System Description,"
         JAERI-M 84-237, January 1985.

E-495   Wallis, G.B., "Flooding in Stratified Gas-Liquid Flow," Dartmouth College
         Report No. 27327-9, August 1970.

E-496   Zuber, N., "Problems in Modeling of Small Break LOCA," US Nuclear
         Regulatory Commission, NUREG-0724, October 1980.

<u>Vent Valves</u>

E-501   "Ueberstromvorrichtungen, Funktionssicherheit in der ersten Blowdown-Phase," FE-report Nr. 902-J 32 A (83), BMFT Research Program 150 376.

<u>PWRs</u>

E-511   Combustion Engineering System 80 Preliminary Safety Analysis Report (CESSAR), Docket STN-50-470.

E-512   Trojan Nuclear Plant Final Safety Analysis Report, Docket 50344-38.

E-513   Crystal River Unit 3 Final Safety Analysis Report, Docket 50-302.

E-514   Genkai Nuclear Plant Units 3 and 4 Final Safety Analysis Report.

E-515   Tomari Nuclear Plant Units 1 and 2 Safety Analysis Report.

CODE ANALYSIS REPORTS

<u>General</u>

E-601   Taylor, D.D., Shamway, R.W., and Singer, G.L., "TRAC-BD1/MOD1: An Advanced Best Estimate Computer Program for Boiling Water Reactor Transient Analysis," EG&G Idaho, NUREG/CR-3633 (EGG-2294), April 1984.

E-602   Boyack, B.E., Stumpf, H.J. and Lime, J.F., "TRAC User's Guide," Los Alamos National Laboratory, NUREG/CR-4442 (LA-10590-M), November 1985.

E-603   "TRAC-PF1/MOD1: An Advanced Best-Estimate Computer Program for Pressurized Water Reactor Thermal-Hydraulic Analysis," Los Alamos National Laboratory, NUREG/CR-3858, July 1986.

E-604   "TRAC-PF1/MOD1 Correlations and Models," prepared by Los Alamos National Laboratory, NUREG/CR-5069 (LA-11208-MS), December 1988.

E-605   "TRAC-PF1/MOD2 Code Manual: User's Guide," prepared by Los Alamos National Laboratory, NUREG/CR-5673, Vol. 2, July 1992.

E-606   "TRAC-PF1/MOD2 Code Manual: Theory," prepared by Los Alamos National Laboratory, NUREG/CR-5673, Vol. 1, (to be published).

E-607   "TRAC-PF1/MOD2 Code Manual: Programmer's Guide," prepared by Los Alamos National Laboratory, NUREG/CR-5673, Vol. 3, July 1992.

E-608   "TRAC-PF1/MOD2 Code Manual: Developmental Assessments," prepared by Los Alamos National Laboratory, NUREG/CR-5673, Vol. 4, (to be published).

E-609   "Quantifying Reactor Safety Margins: Application of Code Scaling, Applicability, and Uncertainty Evaluation Methodology to a Large-Break, Loss-of-Coolant," Idaho National Engineering Laboratory, NUREG/CR-5249, December 1989.

ECC Delivery During Depressurization

E-611   Rohatgi, U.S., et al., "Bias in Peak Clad Temperature Predictions Due to Uncertainties in Modeling of ECC Bypass and Dissolved Non-condensible Gas Phenomena," Brookhaven National Laboratory, NUREG/CR-5254, September 1990.

Hot Leg Countercurrent Flow/Reflux Condenser Mode

E-621   Dillistone, M.J., "Analysis of the UPTF Separate Effects Test 11 (Steam-Water Countercurrent Flow in the Broken Loop Hot Leg) Using RELAP5/MOD2," Winfrith Technology Centre, AEEW-M2555, August 1989 (also published as NUREG/IA-0071, June 1992).

E-622   Thompson, S.L. and Kmetyk, L.N., "RELAP5 Assessment: PKL Natural Circulation Tests," Sandia National Laboratories, NUREG/CR-3100 (SAND82-2902), January 1983.

PAPERS, PRESENTATIONS, AND CORRESPONDENCE

ECC Delivery During Depressurization

E-901   Alb, G.P., and Chambre, P.L., "Correlations for the Penetration of ECC Water in a Model of a PWR Downcomer Annulus," Nuclear Engineering and Design, 53, pp. 237-248 (1979).

E-902   Bankoff, S.G. and Lee, S.C., "A Brief Review of Countercurrent Flooding Models Applicable to PWR Geometries," Nuclear Safety, 26, 139-152 (1985).

E-903   Segev, A.; Flanigan, L.J.; Kurth, R.E. and Collier, R.P., "Countercurrent Steam Condensation and its Application to ECC Penetration," presented at the 19th National Heat Transfer Conference, Orlando, Florida, July 1980.

E-904   Simpson, H.C. and Rooney, D.H., "Further Studies of Non-Equilibrium During Refilling a PWR," University of Strathclyde Glasgow, Scotland, UK, presented at European Two-Phase Flow Group Meeting, Zurich, Switzerland, June 1983.

Loop Behavior

E-911   Aoki, S., Inoue, A., Kozawa, Y., and Akimoto, H., "Direct Contact Condensation of Flowing Steam onto Injected Water," Proceedings of the Sixth International Heat and Mass Transfer Conference, Toronto, Ontario August 1978, Volume 6, pp. 107-112.

E-912   Aya, L. and Nariai, H., "Threshold of Pressure and Fluid Oscillations Induced by Injection of Subcooled Water into Steam Flow in Horizontal Pipe," Proceedings of ASME-JSME Thermal Engineering Joint Conference, Vol. 3, pp. 417-424, 1983.

E-913   Block, J.A., "Condensation-Driven Fluid Motions," International Journal of Multiphase Flow, Volume 6, pp. 113-129 (1980).

E-914   Daly, B.J. and Harlow, F.H., "A Model of Countercurrent Steam-Water Flow in Large Horizontal Pipes," Nuclear Science and Engineering, Vol. 77, pp. 273-284 (1981).

E-915   Nariai, H. and Aya, I., "Fluid and Pressure Oscillations Occurring at Direct Contact Condensation of Steam Flow with Cold Water," Nuclear Engineering and Design, Vol. 95, pp. 35-45 (1986).

E-916   Rothe, P.H.; Wallis, G.B. and Block J.A., "Cold Leg ECC Flow Oscillations," presented at Symposium on Thermal and Hydraulic Aspects of Nuclear Reactor Safety, Vol. 1: Light Water Reactors, pp. 133-150, 1977.

Fluid/Fluid Mixing

E-921   Iyer, K., Gherson, P. and Theofanous, T.G., "Purdue's One-half Scale HPI Mixing Test Program," Proceedings of the Second Nuclear Thermal-Hydraulics Meeting of the Annual ANS Meeting, New Orleans, LA, USA, June 3 - 7, 1984, pp. 859 - 861.

E-922   Iyer, K. and Theofanous, T.G., "Decay of Buoyancy Driven Stratified Layers with Applications to PTS: Reactor Predictions," Proceedings from the National Heat Transfer Conference, Denver, CO, USA, August 4 - 7, 1985.

E-923   Iyer, K. and Theofanous, T.G., "Flooding-Limited Thermal Mixing: The Case of High-Fr Injection," presented at the Third International Topical Meeting on Reactor Thermal Hydraulics, Newport, RI, USA, October 15 - 18, 1985.

E-925   Theofanous, T. and Iyer, K., "Mixing Phenomena of Interest to SBLOCA's," presented at Specialists Meeting on Small-break LOCA Analyses in LWRs, Pisa, Italy, June 23-27, 1985.

E-926   Theofanous, T.G. and Nourbakhsh, "PWR Downcomer Fluid Temperature Transients due to High Pressure Injection at Stagnated Loop Flow," Proceedings of the Joint NRC/ANS Meeting on Basic Thermal Hydraulic Mechanisms in LWR Analysis, September 14 - 15, 1982, Bethesda, MD, USA, NUREG/CP-0043, pp. 583 - 612.

Tie Plate Countercurrent Flow

E-931   Bankoff, S.G., Tankin, R.S., Yuen, M.C. and Hsieh, C.L., "Countercurrent Flow of Air/Water and Steam/Water through a Horizontal Perforated Plate," International Journal of Heat Mass Transfer, Vol. 24, No. 8, pp. 1381-1395 (1981).

E-932   Dilber, I. and Bankoff, S.G., "Countercurrent Flow Limits for Steam and Cold Water through a Horizontal Perforated Plate with Vertical Jet Injection," International Journal of Heat Mass Transfer, Vol. 28, No. 12, pp. 2382-2385 (1985).

E-933   Kutateladze, S.S., "Elements of the Hydrodynamics of Gas-Liquid Systems, Fluid Mechanics," Soviet Research, Vol. 1, No. 4 (1972).

E-934   Naitoh, M., Chino, K. and Kawabe, R., "Restrictive Effect of Ascending Steam on Falling Water during Top Spray Emergency Core Cooling," Journal of Nuclear Science and Technology, Vol. 15, No. 11, pp. 806-815 (November 1978).

Hot Leg Countercurrent Flow/Reflux Condenser Mode

E-941   Gardner, G.C., "Flooded Countercurrent Two-Phase Flow in Horizontal Tubes and Channels," International Journal of Multiphase Flow, Vol. 9, No. 4, pp. 367-382 (1983).

E-942   Larson, T.K., et. al., "Scaling Criteria and an Assessment of Semiscale Mod-3 Scaling for Small-Break Loss-of-Coolant Transients," presented at the Joint NRC/ANS Meeting on Basic Thermal-Hydraulic Mechanisms in LWR Analysis, Bethesda, MD, September 14-15, 1982.

E-943   Mandl, R.M. and Weiss, P.A., "PKL Tests on Energy Transfer Mechanisms during Small-Break LOCAs," <u>Nuclear Safety</u>, Vol. 23, No. 2 (March-April 1982).

E-944   Tasaka, K., et. al., "The Results of 5% Small-Break LOCA Tests and Natural Circulation Tests at the ROSA-IV LSTF," Proceedings of the Fourteenth Water Reactor Safety Research Information Meeting, October 27-31, 1986, NUREG/CP-0082, Vol. 4, pp. 177-197.

Section 9

ABBREVIATIONS AND ACRONYMS

ABB	-	ASEA Brown Boveri
ACC	-	Accumulators
ATHLET	-	Code for Analysis of Thermal-Hydraulics of Leaks and Transients
B&W	-	Babcock & Wilcox
BBR	-	Brown Boveri Reaktor (now ASEA Brown Boveri)
BCL	-	Broken Cold Leg
BE	-	Best-estimate
BMFT	-	Bundesministerium fuer Forschung und Technologie (Federal Ministry for Research and Technology)
BOCREC	-	Bottom of Core Recovery
BTD	-	Breakthrough Detector
CCFL	-	Countercurrent Flow Limitation
CCTF	-	Cylindrical Core Test Facility
CE	-	Combustion Engineering (now ABB-CE)
CI	-	Combined Injection
CL	-	Cold Leg
CLI	-	Cold Leg Injection
CS	-	Core Simulator (UPTF)

CSAU	-	Code Scaling, Applicability, and Uncertainty Study
DAS	-	Data Acquisition System
DB	-	Drag Body
DC	-	Downcomer
DCI	-	Downcomer Injection
DP	-	Differential Pressure
ECC	-	Emergency Core Coolant
ECCS	-	Emergency Core Coolant System or Emergency Core Cooling System
EM	-	Evaluation Model
EOB	-	End-of-Blowdown
FASS	-	Fast Automatic Shutdown System (UPTF)
FDG	-	Fluid Distribution Grid
FLECHT-SEASET	-	Full-length Emergency Cooling Heat Transfer Separate Effects and Systems Effects Test
FRG	-	Federal Republic of Germany
GKM	-	Grosskraftwerk Mannheim
GPWR	-	German Pressurized Water Reactor
GRS	-	Gesellschaft fuer Anlagen- und Reaktorsicherheit (Company for Plant and Reactor Safety); formerly Gesellschaft fuer Reaktorsicherheit (Company for Reactor Safety)
HL	-	Hot Leg
HLI	-	Hot Leg Injection
HPCI	-	High Pressure Coolant Injection

HPI	-	High Pressure Injection
HPIS	-	High Pressure Injection System
HPSI	-	High Pressure Safety Injection
IDL	-	Instrument Development Loop
INEL	-	Idaho National Engineering Laboratory
J	-	Japan
JAERI	-	Japan Atomic Energy Research Institute
KWU	-	Kraftwerk Union (now a division of Siemens)
LANL	-	Los Alamos National Laboratory
LBLOCA	-	Large Break Loss-of-Coolant Accident
LLD	-	Liquid Level Detector
LOBI	-	Loop of Blowdown Investigation
LOCA	-	Loss-of-Coolant Accident
LOFT	-	Loss of Fluid Test
LPCI	-	Low Pressure Coolant Injection
LPI	-	Low Pressure Injection
LPIS	-	Low Pressure Injection System
MK	-	Muehlheim Kaerlich PWR
MPR	-	MPR Associates
ORNL	-	Oak Ridge National Laboratory
PCT	-	Peak Cladding Temperature
PKL	-	Primarkreislaufe (Primary Coolant Loop - KWU Test Facility)

PTS	-	Pressurized Thermal Shock
PWR	-	Pressurized Water Reactor
REFLA	-	Reflood Analysis (Code)
RELAP	-	Reactor Leak and Analysis Program (Code)
ROSA	-	Rig of Safety Assessment
SBLOCA	-	Small Break Loss-of-Coolant Accident
SCTF	-	Slab Core Test Facility
SG	-	Steam Generator
SGIP	-	Steam Generator Simulator Inlet Plena
SGS	-	Steam Generator Simulator
SGTR	-	Steam Generator Simulator Tube Regions
TRAC	-	Transient Reactor Analysis Code
TUM	-	Technische Universitaet Muenchen (Technical University of Munich)
TV	-	Test Vessel
UCSP	-	Upper Core Support Plate
UK	-	United Kingdom
UP	-	Upper Plenum
UPI	-	Upper Plenum Injection
UPTF	-	Upper Plenum Test Facility
US	-	United States
USNRC	-	United States Nuclear Regulatory Commission
VV	-	Vent Valve

W	-	Westinghouse Electric Corporation
W/S	-	Ratio of Core Simulator Water and Steam Injection Rates (UPTF)